Electric potential gradient and current during steady precipitation

Kevin M. Daily

ELECTRIC POTENTIAL GRADIENT AND CURRENT DURING STEADY PRECIPITATION

by

KEVIN M. DAILY B.Sc.

Presented in Candidature for the Degree of Doctor of Philosophy, in the University of Durham

November, 1973.

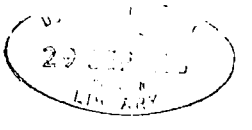

ABSTRACT

An outdoor site adjoining Durham Observatory was instrumented to measure the atmospheric potential gradient and precipitation current at the ground during periods of steady,quiet precipitation. A system was constructed to automatically record these quantities and to present the data in a form suitable for input to a computer.

Examination of most periods of quiet precipitation between January and June 1972 shows that rain is usually positively charged,with the potential gradient being negative,while during snow these signs are reversed.There is nearly always significant correlation between the two electrical quantities,with during rain variations in potential gradient most often leading those in precipitation current by several minutes;during snow the precipitation current leads by a similar amount.These two effects correspond to the so-called "inverse relation" and "mirror-image effect" often quoted in previous work.

These results are shown to be consistent with the precipitation charge being due to two charging processes,one acting on solid precipitation within the cloud,and the second occurring during the melting of snow to rain.Examination of aerological data shows that the time lags between corresponding variations of the electrical quantities can be explained during rain by the effects of the wind shear between the cloud and the ground on the falling precipitation.

The different electrical behaviour of a few periods of precipitation can be explained by the effects of a slow-moving cloud where electrical development is taking place,rather than by a passing cloud with constant electrical activity.

Comparison of periods of quiet precipitation with "disturbed" periods,when the electrical activity is much greater,suggests that the transition to disturbed precipitation occurs when the rate of electrical sign reversals exceeds 2 per hour and the precipitation rate exceeds 1·0 mm $hr.^{-1}$ The connection between the degrees of electrical and meteorological activity agrees with the suggestion that the electrical activity reflects the degree of atmospheric stability within the cloud.

CONTENTS

CHAPTER 1

The Study of Quiet Precipitation Electrification

1.1 Introduction

Cloud and precipitation electrification is studied to discover the nature of charge separation and transfer in the cloud and the free atmosphere, and how these processes are related to the prevailing meteorological conditions. Cloud electrification is most evident, of course, in the thundercloud, where the electrical and accompanying meteorological effects can constitute one of the most violent and hazardous of weather phenomena.

Unfortunately, the thunderstorm is a difficult subject of study, and so a precise knowledge of the processes leading to the intense charging of the thundercloud has yet to be obtained. Continuous, non-stormy precipitation offers much steadier conditions in which cloud electrification can be studied, but has received much less attention despite its more frequent occurrence in many parts of the world. While the electrical effects associated with such precipitation are considerably smaller in magnitude than those observed in the thundercloud, knowledge of the electrical processes in "quiet" precipitation may give an indication of possible processes in the thundercloud, more particularly in its earlier stages of development. Also there is increasing evidence that, in most types of cloud,

electrical processes may be an important factor in the growth and release of precipitation.

The observation that quiet precipitation carries down charge to the Earth's surface means that it makes a contribution to the transfer of charge between the atmosphere and the Earth's surface, and influences the maintenance of the Earth's charge. While the charge transferred during a thunderstorm is considerably greater, the more frequent occurrence of quiet precipitation over much larger areas of the Earth's surface may lead to a significant transfer of charge by this means.

Throughout the present work, the description "quiet" will be reserved for periods of continuous precipitation where violent or frequent variations in electrical activity are absent, and the magnitude of the activity is small. Continuous precipitation which cannot be described as "quiet" will be termed "disturbed".

1.2 Observations of quiet precipitation electricity

1.2.1 Early observations

ELSTER and GEITEL (1888) and SIMPSON(1909) were among the earliest workers to find that the atmospheric potential gradient is different in steady precipitation from that in fair-weather conditions, and often of opposite sign. Thus steady rain was found to produce excesses of positive charge, with the potential gradient generally being negative. SCRASE (1938) and CHALMERS and LITTLE(1940) quoted cases of positive rain charge and negative potential gradient continuing for long periods. The observation that the precipitation

charge and potential gradient are of opposite sign has been termed the "inverse relation", although strictly this would mean they were inversely proportional.

1.2.2 The electrification of quiet rain

During periods of steady, quiet rain, potential gradient values rarely exceed 1500 Vm^{-1} in magnitude, while the precipitation current density has values typically of up to 30 pAm^{-2} although higher currents of up to 100 pAm^{-2} are sometimes observed. By comparison, in heavy showers or storms, currents of up to 10 000 pAm^{-2} have been measured, with potential gradients at the earth's surface of 10 000 Vm^{-1} or more.

The total vertical current density during steady rain, including the atmospheric conduction current and any effects of splashing, has been found by CHALMERS(1956) to be usually positive downwards, that is of the same sign as the precipitation current. Since the potential gradient was usually negative at the time, the precipitation current appears to be the predominant current.

SIMPSON (1949) found that not only did the rain current and potential gradient usually have opposite signs, but that when conditions were not changing violently any change in sign occurred nearly simultaneously for both records. This was termed the "mirror-image" effect, because time variations of the rain current and potential gradient appeared as mirror images of each other, about either the zero line or one parallel to it. Later work, such as that of RAMSAY and

CHALMERS (1960), showed that appreciable time differences of up to several minutes could exist between corresponding features on records exhibiting the mirror-image effect. The effect was then most noticeable for one or other record shifted by this time difference (Fig.1.1). Both the potential gradient and precipitation current have been seen to lead the other on different occasions; there is evidence, however, that the potential gradient leads more often during rain.

1.2.3 The electrification of quiet snow

Observations during quiet snow have been much fewer in number, but SIMPSON (1949) reported an overall negative charge on snow and a positive potential gradient. CHALMERS (1956) confirmed this, finding an average precipitation current density of - 3.5 pAm^{-2} during steady snow compared with + 3.8 pAm^{-2} during steady rain. The presence of blowing or wet snow usually produces different results. REITER (1965) found similar results for steady snowfall.

The mirror image effect has been observed during snow, but usually with the precipitation current variations leading (RAMSAY and CHALMERS, 1960).

1.3 Charging processes in steady precipitation

1.3.1 The location of charging processes

The observed charging of both rain and snow may be due to processes operating in or below the cloud, or at the ground. CHALMERS (1956), however, argued that in the case of snow, separation of charge must occur in the cloud, whether or not

FIG. 1.1 An example of the "mirror-image" effect

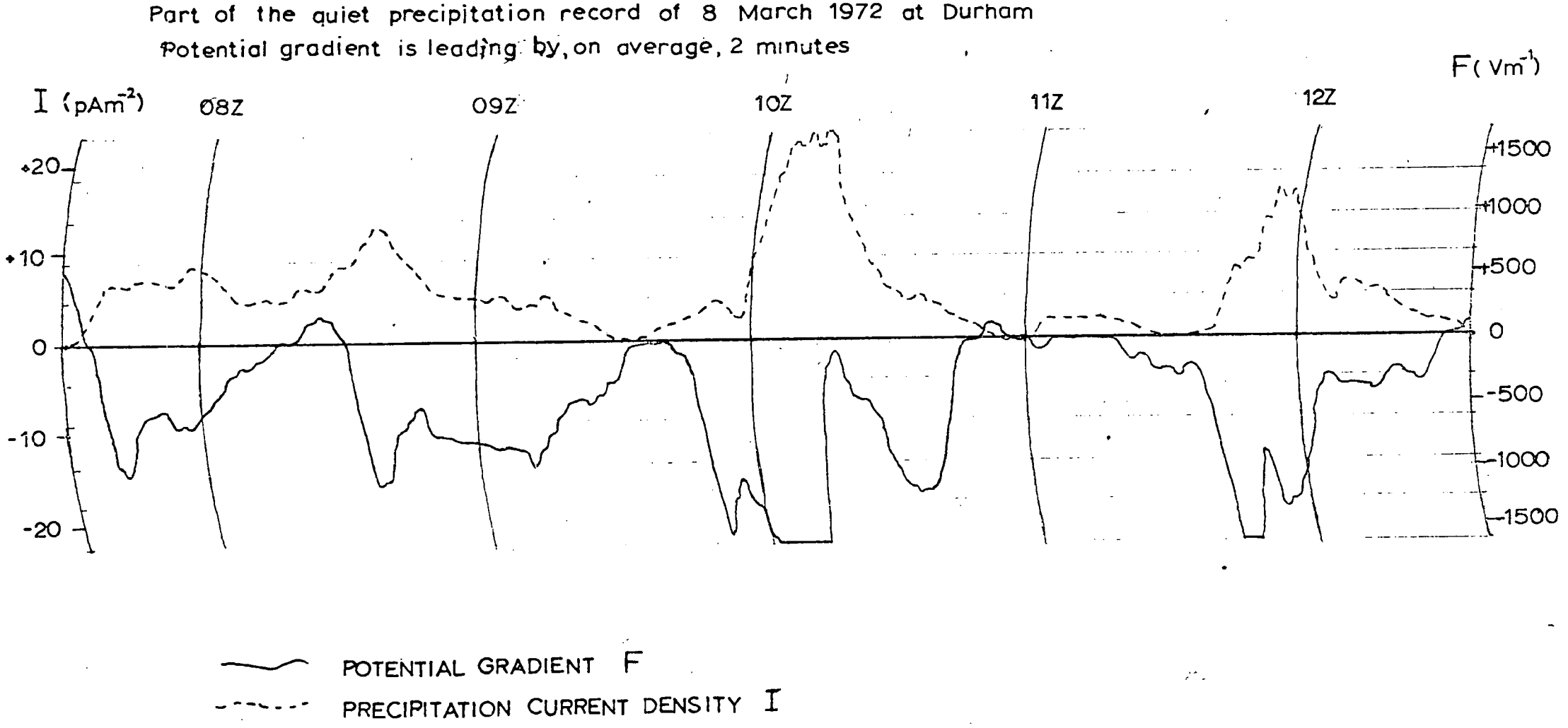

there is charge separation close to the ground. This conclusion is supported by measurements on individual snowflakes, which show them to be charged long before they reach the ground.

Chalmers further argued that most precipitation which reaches the ground as rain will have been in the solid state during part of its time in the cloud. Any charge separation process in the cloud will then operate whether the precipitation reaches the ground as rain or snow, and so a second charging process is required in the case of rain, which reverses the sign of the original precipitation charge. This second process must be of greater magnitude and of opposite sign to the process in the cloud, and operate at or below the melting level.

1.3.2 "Influence" theories of charge separation

Early theories of cloud electrification were mostly of the "influence" type, involving the selective capture of ions by precipitation falling in a vertical potential gradient. ELSTER and GEITEL (1913) proposed that raindrops would become polarized in a positive potential gradient, such as exists in fair-weather conditions, so that cloud droplets rebounding from the bottom of the falling raindrop would carry away positive charge, leaving the drop with a negative charge. The falling drops, in carrying their negative charges towards the cloud base would enhance the existing potential gradient in the cloud. This theory was later extended to the case of falling ice crystals by CHALMERS (1947).

WILSON (1929) proposed that, under certain conditions, an electrically polarized raindrop would acquire a net charge by a process of selective ion capture. A drop falling through

a positive potential gradient more rapidly than the positive ions, for example, would acquire a negative charge which then tends to increase the existing potential gradient. A mathematical theory of the process has been developed by WHIPPLE and CHALMERS (1944), and confirmed experimentally by ABBAS and LATHAM (1967).

1.3.3 Electrification associated with the freezing and melting of water.

It has been suggested by CHALMERS (1956) that because at least two charging processes, of opposite direction and magnitude are involved in continuous rain, they might be converse processes, one being a freezing process and the other a melting process. A possible freezing process could be that suggested by WORKMAN and REYNOLDS (1950), in which the partial glazing of supercooled water droplets on falling ice particles results in positive charges being thrown off on the fragments of the water droplets, with a negative charge remaining on the ice. The charges would be separated due to the gravitational separation of the ice particles and the water droplets.

MASON (1953) put forward a theory similar to that of Workman and Reynolds, but involving the riming of cloud droplets on falling ice particles. Positive charge was ejected into the air as ions, rather than on fragments of water splashing off. LATHAM and MASON (1961) modified the theory, with the positive charge being carried off on small ice splinters ejected during the freezing of the droplets.

Electrical charging during the melting of ice was found by DINGER and GUNN (1946), who passed a light current of air

over melting ice, producing positive charge in the melt water and negative charge in the air. MAGONO and KIKUCHI (1963, 1965) melted freely falling natural snow crystals and also found positive charging to result. The separation of charge was found by IRIBARNE and MASON (1967) to result from the bursting of air bubbles released from the ice during melting. The amount of charge appeared to be sensitive to the presence of impurities in the ice, the rate of melting, and the original rate of freezing of the ice specimen. DRAKE (1968) however, found that the effects of impurities were different in a well-ventilated specimen.

1.3.4 Ice impact electrification

Charge separation connected with the impact of ice crystals was first suggested by SIMPSON (1919) to account for large positive potential gradients observed by him in blizzards. SIMPSON and SCRASE (1937) suggested that the impact of ice crystals would lead to a negative charge on the ice fragments and a positive charge, in the form of ions, in the air. Generally, however, observational evidence about charge separation by ice impact has shown little agreement.

Later work, such as that of LATHAM (1963), has explained ice impact charging in terms of thermoelectric effects produced by temperature gradients in the ice particles.

1.3.5 Electrification produced by the rupture of water drops

Separation of charge produced by the disruption of water drops was noted by LENARD (1892), who found that the spray from the base of a waterfall was positively charged, while the mists of small droplets had an overall negative charge. SIMPSON (1909) established that the breaking of drops in a strong vertical air current also produced strong positive charging of the large fragments, with the surrounding air having an excess of negative ionic charge. Later work, such as that of CHAPMAN (1952), has indicated that the charge generated depends on the violence of the disruption of the drop.

SMITH (1955) attempted to explain the observed behaviour of the potential gradient and precipitation current at the ground in terms of charging due to the splashing of raindrops at the ground, which would be expected to give a negative charge to the air and a positive charge to the splashed water.

The break-up of large, freely-falling water drops in still air has been found by MATTHEWS and MASON (1964) to produce electrification, particularly in a large potential gradients. The break-up of large unstable drops formed from melted snowflakes may thus produce electrification.

1.3.6 Processes relevant to quiet precipitation

The few observations which have been made of the charge distribution in nimbostratus clouds producing steady precipitation (see Sec.2.2) indicate that charging occurs mostly in the 0° C to -12° C region, where liquid and solid particles most probably coexist. The riming of cloud droplets on

falling ice particles would be most likely to occur in this region; processes involving glazing are likely to be important only at lower temperatures.

CHALMERS (1967), however, pointed out that ice impact theories lead to the expectation of much larger effects in the very turbulent cumulo-nimbus cloud than the quiet nimbo-stratus cloud, as is indeed observed. Ice impact charging is certainly possible in the region of the cloud where charging is observed to be greatest; it is also possible, though, at higher levels.

Electrification almost certainly occurs on melting, with the Dinger - Gunn process being the most likely mechanism. Break-up of water drops could cause charging, however, if snowflakes melted to produce large, unstable, water drops which subsequently disintegrate.

Ion capture processes operating beneath the cloud are unlikely to be important, as these processes appear to be at least an order of magnitude too small to produce the observed electrification. In the absence of high potential gradients or heavy rain, splashing at the ground is also unlikely to be of importance (ADKINS, 1959).

1.4 Charge transfer in the atmosphere

It has been postulated by many workers that the Earth can be considered as the inner electrode of a giant spherical condenser, the outer electrode being the "electrosphere", a highly ionized and conducting region of the atmosphere extending upwards from an altitude of about 50 km. The potential of the electrosphere, estimated at 2.9×10^5 V,

is maintained despite the transfer of charge by various processes between the Earth and the electrosphere.

The overall positive charge brought to the Earth by the fair-weather conduction current and precipitation tends to discharge the condenser, and so it must be balanced by an upward transfer of positive charge by other processes, such as point discharge or lightning currents. WORMELL (1930) measured the transfer of charge to a portion of the Earth's surface by all means and found that the charge brought down by precipitation was a significant factor. His estimates of the total charge transferred by the various currents are shown in Table 1.1, together with later ones given by MASON (1971). Much of the precipitation charge may have been transferred during quiet rain; while the precipitation currents from shower and thunder clouds are often larger, the more frequent occurrence of sign reversals reduces the net charge transferred by such precipitation.

TABLE 1.1 ELECTRICAL BALANCE SHEET FOR A PORTION OF THE EARTH'S SURFACE (FROM MASON, 1971)

	Wormell (1930) C km^{-2} $Year^{-1}$	Later estimates C km^{-2} $Year^{-1}$
Fine weather current	+60	+120
Precipitation	+30	+30
Lightning discharges	-20	-20
Point discharge	-100	-170
Total	-30	-40

CHAPTER 2

The Physical and Electrical Characteristics of Quiet Precipitation.

2.1 The origin of quiet precipitation

2.1.1 The formation of clouds giving quiet precipitation

Electrically quiet precipitation generally falls from extensive stratiform clouds which are much less unstable than shower or thunder clouds and produce precipitation which is steadier and of much longer duration. In temperate latitudes, the conditions necessary for the formation of such stratiform clouds, namely the gradual ascent of a deep and extensive layer of moist warm air, are usually found in the frontal systems associated with depressions.

The air motions relative to a typical mid-latitude frontal depression, as given by BROWNING (1971), are shown in Fig.2.1. Formation of precipitation occurs within a well-defined tongue of warm air which flows ahead of the cold front before ascending above the warm front. Because of the narrowness of this flow, it has been sometimes termed the "warm conveyor belt". Large scale ascent within the warm conveyor belt is typically of the order of 10 ms^{-1}, but can be modified by weak, small-scale convection generated where the upper air overruns the warm ascending air. The ascent of the warm conveyor belt becomes most uniform ahead of the surface warm front, typically a distance of about 100 km marking the transition from convective to uniform ascent.

FIG. 2.1 The Large Scale Air Flow at a Frontal System

(From Browning, 1971)

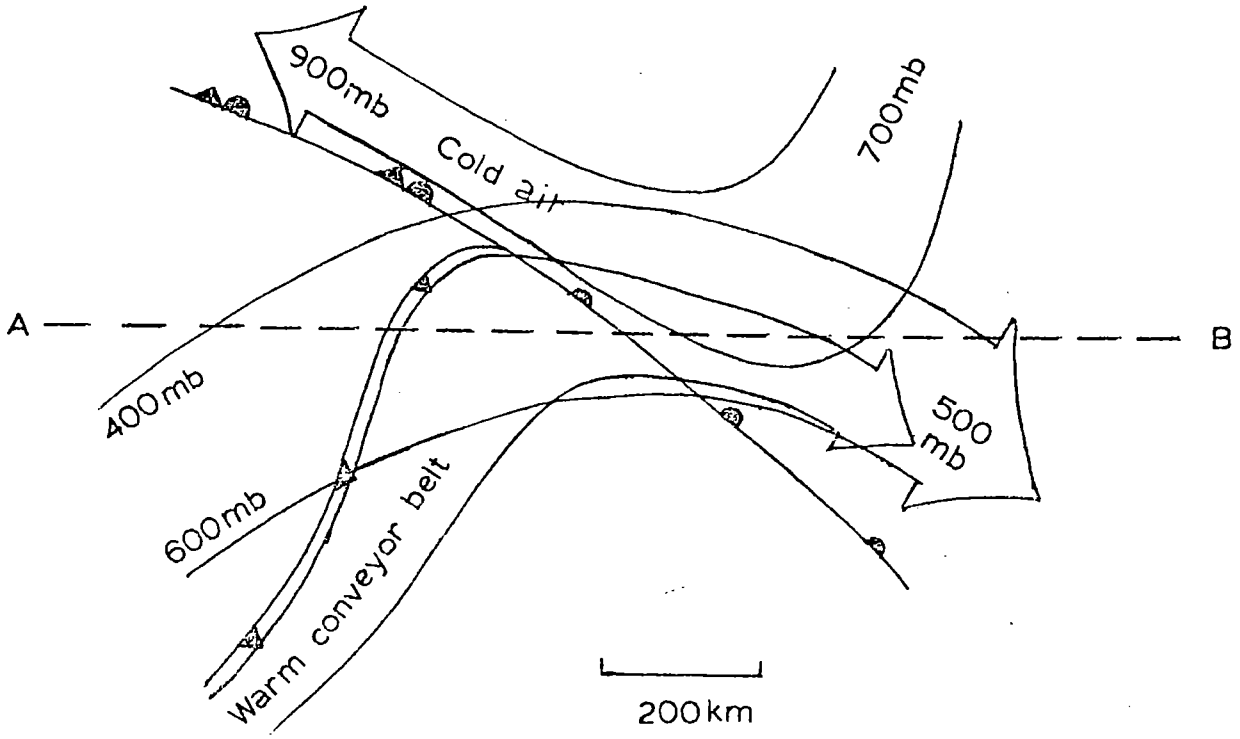

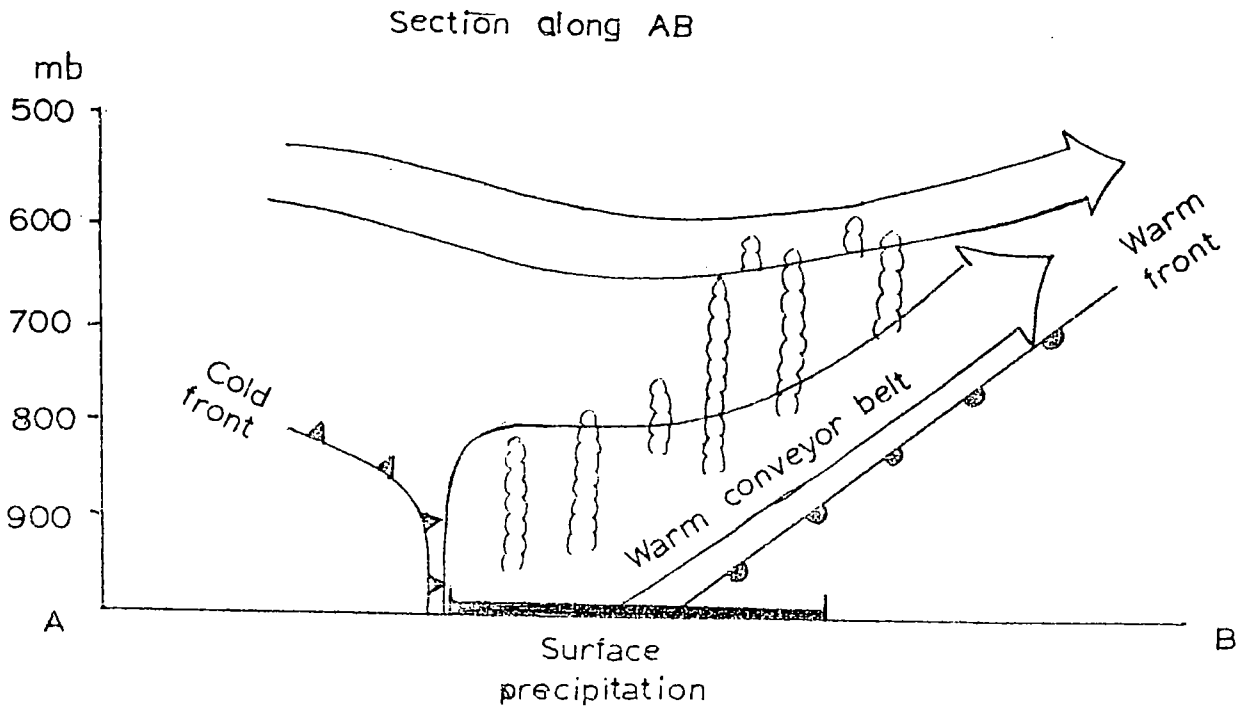

2.1.2 The large-scale pattern of precipitation

The general extent of the area of precipitation associated with a typical mid-latitude depression is shown in Fig. 2.2. A large area of precipitation, resulting from the region of uniform ascent above the warm front, occurs ahead of the surface warm front and extends along the surface occluded front. Bands of enhanced precipitation are sometimes found roughly parallel to the front, separated by about 200 km, but otherwise there are few significant large scale features of the area of precipitation.

2.1.3 The meso-scale pattern of precipitation

Clusters of individual convective cells producing regions of enhanced precipitation, or "meso-scale precipitation areas", can be arranged in bands inside the overall region of precipitation (Fig.2.2). These bands, a few tens of kilometres across, take two forms. In the warm sector they run roughly parallel to the warm conveyor belt and may be at a large angle to the surface warm front. Ahead of the surface warm front, the bands tend to run parallel to it, appearing to originate at the front and to then travel away from it.

A detailed analysis of an actual frontal system by BROWNING and HARROLD (1969) showed that the warm sector bands appeared to have orographic origins, giving swaths of heavy rain in certain geographical locations as they passed.

2.1.4 The vertical structure of a warm frontal system

The vertical air motions at a typical frontal system are shown in Figs. 2.3 and 2.4. These are detailed time - height

FIG. 2.2 The Meso-scale Patterns within the Warm Conveyor Belt

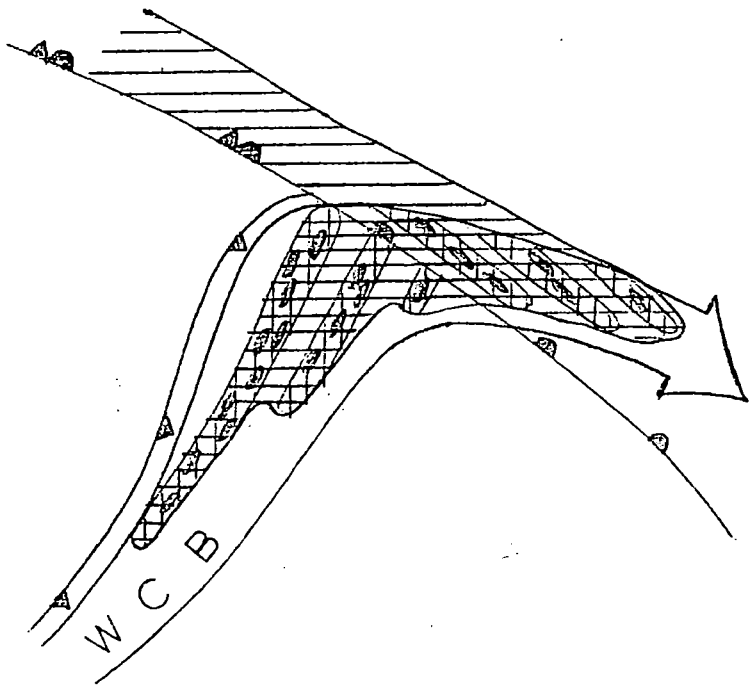

200 km.

Region of precipitation

Heavier precipitation

Meso-scale precipitation area

W C B Warm conveyor belt

FIG. 2.3 Time-height section showing transverse circulation at a warm front passing Pershore, Worcestershire

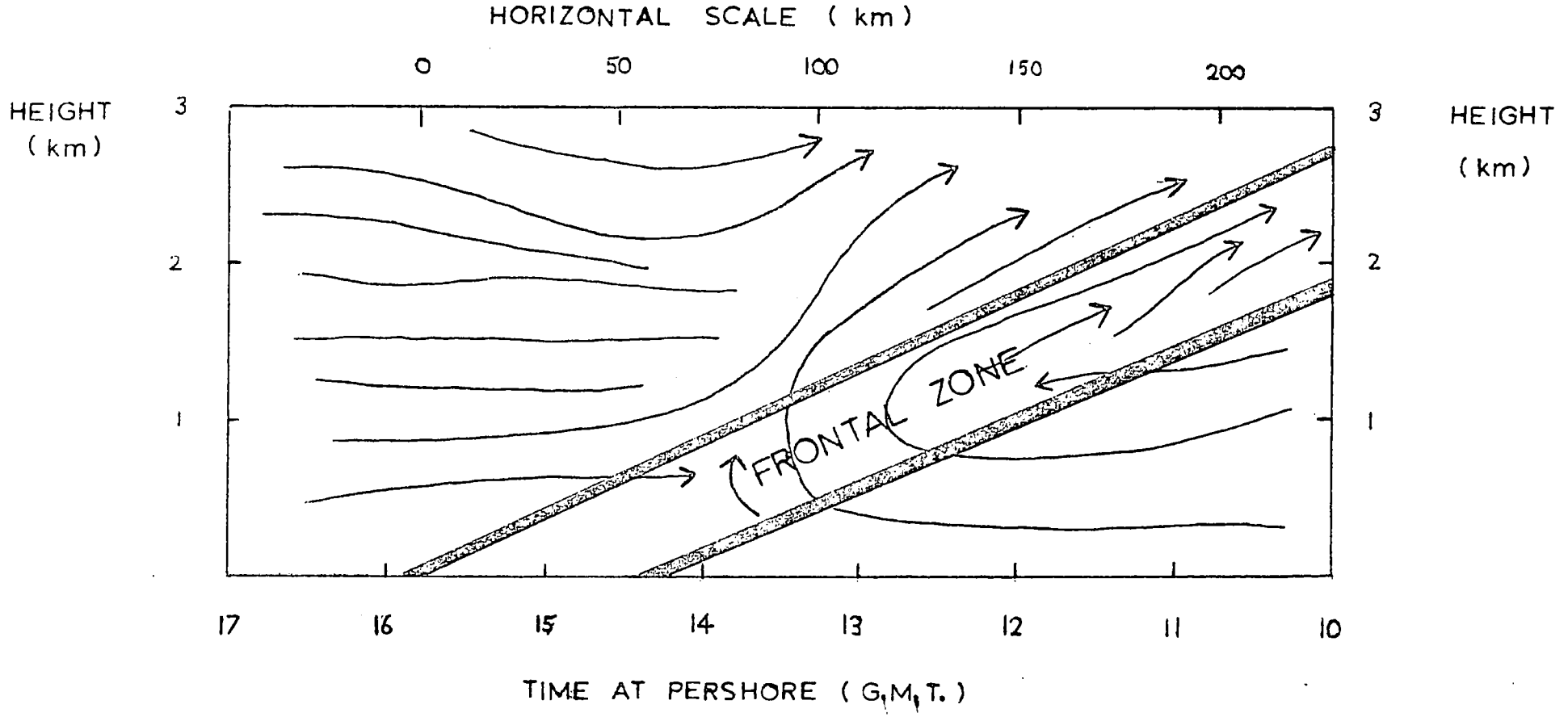

FIG. 2.4 Time-height section showing vertical air velocity at a warm front passing Pershore, Worcestershire

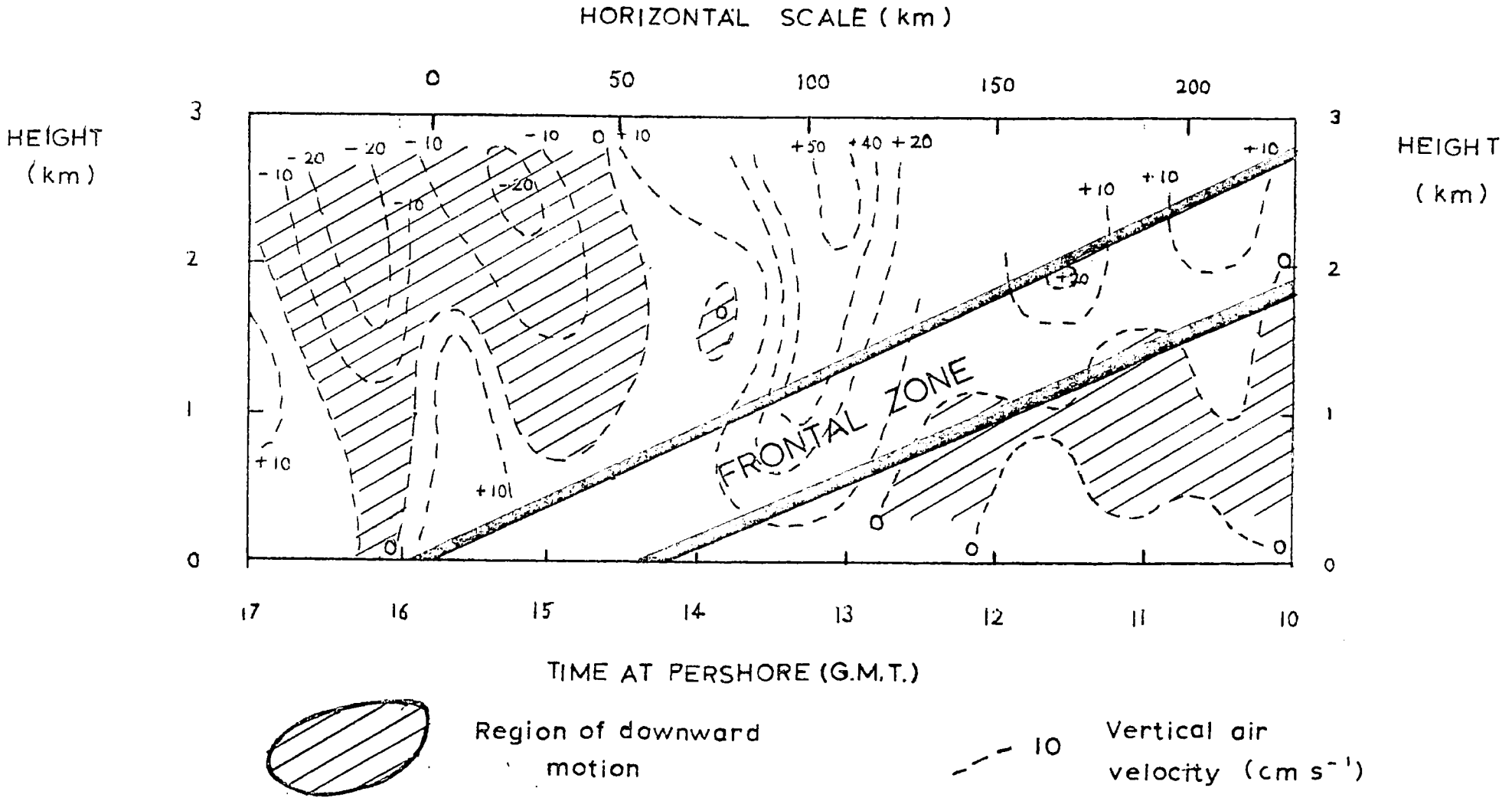

sections through an actual warm front, as given by BROWNING and HARROLD (1969); they show downward motion beneath the warm frontal surface, and the upward motion of the "conveyor belt" above the surface.

As the frontal system moves past an observer on the ground, light precipitation generally falls first from a layer of altostratus cloud with a base at about 3 km. Heavier, steady precipitation follows from nimbostratus cloud at about 1 - 3 km, beneath which may be layers of stratocumulus and stratus cloud down to a few hundred metres altitude. The total duration of precipitation can vary from an hour to 12 hours or more.

2.1.5 Aircraft observations of precipitating layer clouds

A number of aircraft investigations of precipitating layer clouds are summarised by MASON (1971), who concludes that in middle latitudes, although rain may occasionally fall from non-freezing clouds, it is usually produced from clouds which extend above the $0^{\circ}C$ level. In general, clouds need bases warmer than $-5^{\circ}C$ and a thickness greater than 1 km to produce continuous precipitation; for moderate rates the thickness is 2 km or more.

Precipitation at the ground is thus unlikely when the cloud base is greater than about 1 km above the melting level, and STEWART (1964) deduced from his observations that a cloud base higher than 1 km above the ground is unlikely to produce snow at the ground, due to evaporation of the crystals during fall.

The cloud top can extend to temperatures below $-20^{\circ}C$, some workers finding this in over half the clouds observed.

Clouds producing snow at the ground are always observed to have tops colder than -12°C.

Ice crystals are found in such clouds, with supercooled droplets in the lower parts, particularly at temperatures between 0°C and -4°C. However, precipitation is observed in a few cases when a cloud is entirely at temperatures above 0°C, or when no ice crystals are detected; the formation of rain in such cases is almost certainly due to coalescence of droplets.

Precipitation rates measured in the cloud often show a considerable increase at the lower levels. It has thus been suggested that the majority of the rain received at the ground must have come from the lowest levels of frontal clouds, with ice crystals from higher levels "seeding" the region just above the melting layer.

2.1.6 Radar observations of precipitating layer clouds

Radar displays of the precipitation areas associated with warm fronts usually show few features in the horizontal structure, the echoes usually being widespread and diffuse. Vertical cross-sections, however, usually show a narrow band of intense echo in the vicinity of the melting level, caused by enhanced reflection by melting snowflakes.

Above the melting level, the snow echoes often have considerable pattern, with strong echoes descending through the region to merge with the melting band and subsequently appearing at the ground as periods of increased rainfall. These regions of enhanced echo, termed "upper bands" by BOWEN (1951), often appear to originate in compact generating cells

at a height of 3 or 4 km and with dimensions of the order of 1 km. LANGLEBEN (1956) found generating cells tending to form in line arrays. Streaks of precipitation fall from these cells, becoming distorted in the wind shear to form the almost horizontal upper bands. LANGLEBEN (1954) has deduced from the behaviour of the pattern that the streaks are formed of snowflakes rather than crystals, which must have been aggregated at temperatures perhaps as low as -20°C.

Below the melting region, the precipitation shows little large scale pattern, but the more powerful radar used in recent years can show a cellular structure on the smaller scale; for instance HARROLD and BROWNING (1969) observed structure of horizontal dimensions about 1.5 km, travelling at the speed of the wind at the melting layer. Larger scale fluctuations on the scale of the meso-scale precipitation areas have been found by ATLAS et al (1969).

2.1.7 The process of formation of the precipitation

In middle latitudes, precipitating layer clouds nearly always extend well above the 0°C level, and so the initiation of precipitation is generally considered to be due to the Bergeron process of ice crystal growth.

BERGERON (1935) concluded that the release of precipitation was due to the appearance of a few ice crystals among a much larger population of supercooled water droplets in the regions of the cloud where the temperature is below -10°C. The ice crystals, probably formed by the occasional freezing of droplets, grow rapidly at the expense of the water droplets

due to the difference in the saturation vapour pressure between water and ice at the same temperature. In such mixed clouds, a state of approximate water saturation represents a supersaturation with respect to ice of, for example, 10% at $-10^{\circ}C$.

MASON (1952) showed that condensation or coalescence of water droplets cannot be the main process in layer clouds having the usually observed values of water content and updraught. Thus it appears that, in such cases, precipitation is due to the growth of ice crystals in the regions of cloud below $0^{\circ}C$; subsequently aggregation of crystals produces snowflakes.

2.2 The electrical structure of quiet precipitation

Direct electrical observations of steady, quiet precipitation and the clouds producing it are comparatively few. The most extensive investigations have probably been those of REITER (1965, 1968) and IMYANITOV and CHUBARINA (1965), which are summarised below.

2.2.1 The work of Reiter

The results quoted by Reiter are based on synoptic observations made over a number of years at a network of stations in a high mountain area. The stations range in altitude from 675 m to 3000 m, and have small horizontal separations.

Records of potential gradient and precipitation current generally show the inverse relation and mirror-image effects at all altitudes during steady precipitation; as usual, the precipitation current is positive during rain and negative during snow. However light precipitation from altostratus,

either in the form of rain or snow, usually results in both potential gradient and precipitation current being negative.

Reiter's most important conclusions concern the effects of the melting level and the degree of atmospheric stability on the electrication of the precipitation. In the former case, he finds that reversal of the signs of potential gradient and precipitation current occurs across the melting layer ($0^{o}C$ to $2^{o}C$ layer), both for simultaneous observations above and below the layer and for when the melting layer rises or falls past a single station. Reiter concludes that the melting layer is an electrically bipolar layer, the existence and structure of which is independent of its location inside or below the cloud, or its altitude.

The effect of the melting level is evident in Fig.2.5, where the percentage frequency of positive potential gradient is plotted against atmospheric temperature; the change from mostly positive to mostly negative values occurs exactly inside the melting layer.

Reiter found that the above conclusions applied only when stable stratification existed in the cloud space, and consequently atmospheric turbulence was at a minimum. This was indicated electrically by the average frequency of sign reversals of potential gradient being less than 1.5 per hour (Fig.2.6). He suggests that the electrical pattern of turbulence reflects the meteorological pattern, the observed decrease in electrical turbulence with altitude tending to support this idea. No melting layer effect is discernible in unstable conditions.

FIG 2.5 Frequency of positive potential gradient (E_+) and number of sign reversals per hour (S_h) of potential gradient as functions of temperature. (Quiet precipitation) From Reiter (1965)

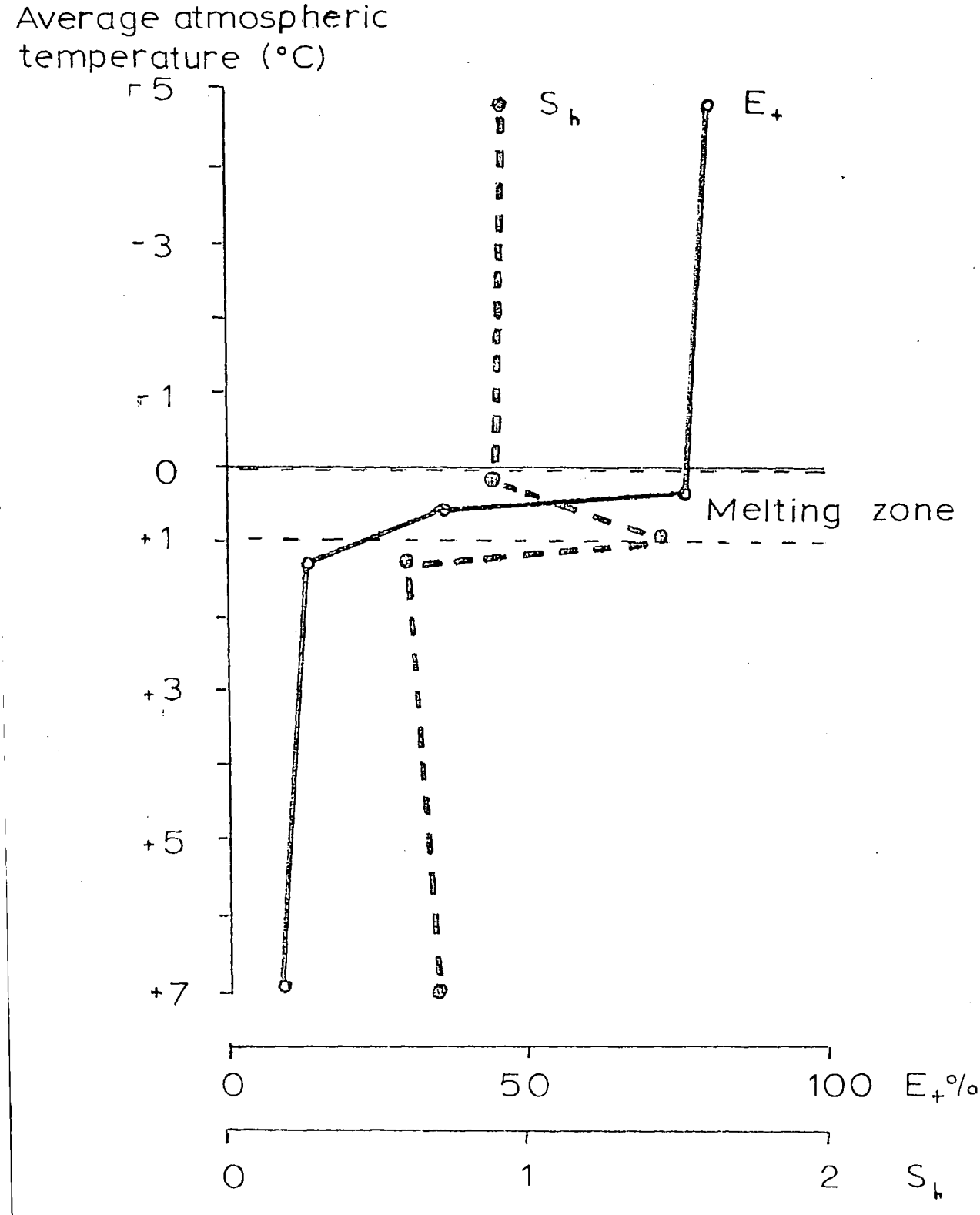

FIG. 2.6 Number of sign reversals per hour (S_h) of potential gradient as function of stability in atmospheric 500 - 700 mb layer.
From Reiter (1965)

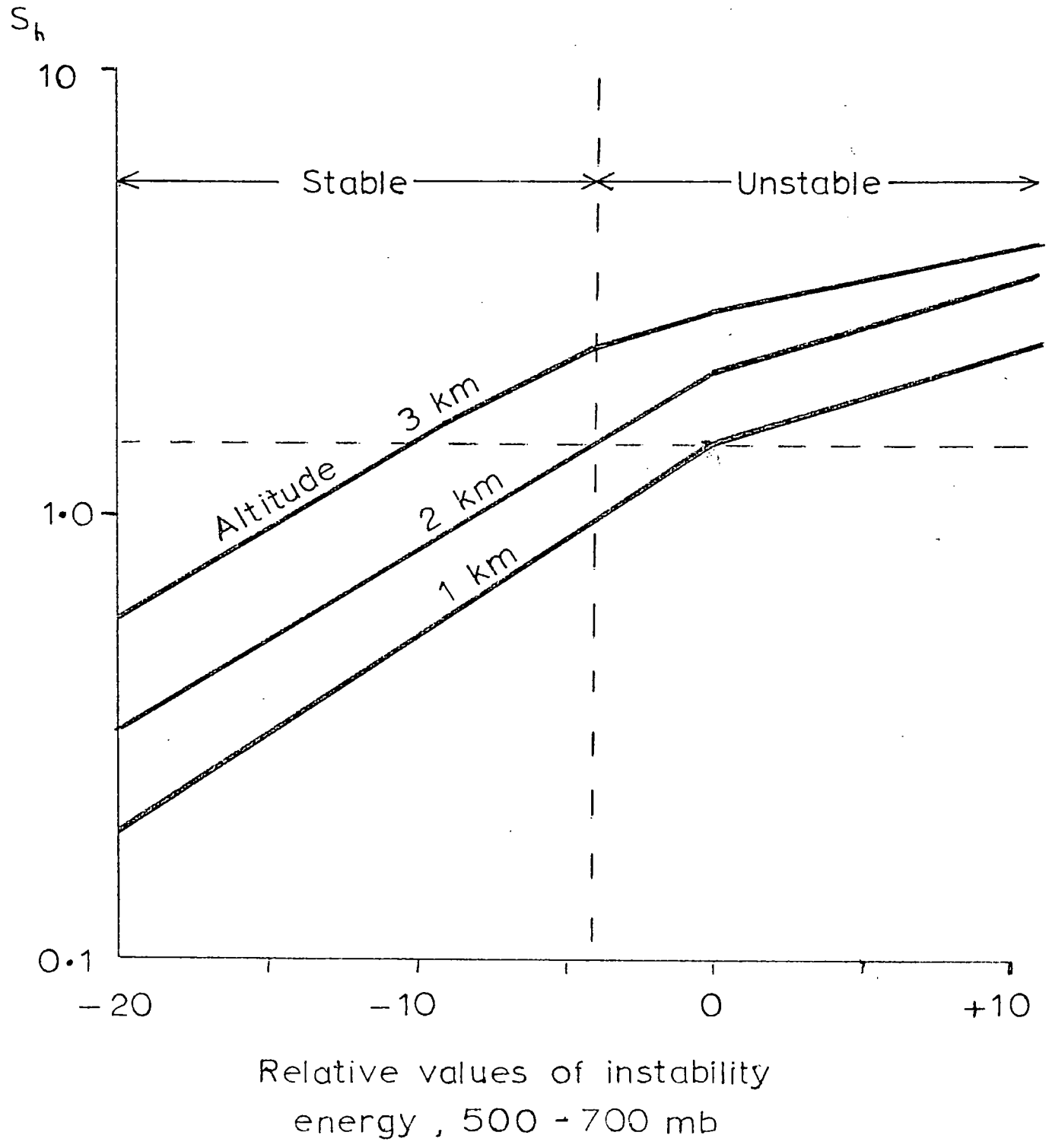

2.2.2 The work of Imyanitov and Chubarina

These workers report the results of systematic aircraft soundings of nimbostratus clouds made between 1958 and 1963 at middle latitudes in the Soviet Union. From the measured profiles of potential gradient, the charge distributions in and below the cloud were also deduced, assuming that conditions were uniform horizontally.

Their observations show that nimbostratus clouds are polarized, whether they produce rain or snow at the ground and whether or not they are "mixed", i.e. contain both solid and liquid precipitation. The cloud can be polarized either positively, with a positive upper charge and a negative lower charge, or negatively. All the various combinations of cloud type and polarization were found, with the two signs of polarization being nearly equally probable for "mixed" clouds.

Typical generalised profiles of potential gradient in nimbostratus clouds are shown in Fig. 2.7, together with the deduced charge distributions. These generalised profiles were obtained by reducing the measured cloud thickness in each case to a normalised value before averaging the potential gradient values. The mean values of charge found in this way for each type of cloud are given in Table 2.1.

Imyanitov and Chubarina deduce that the main region of charge separation in mixed clouds occurs in the $0^{o}C$ to $-10^{o}C$ or $-12^{o}C$ regions, indicating the probable role of melting and freezing processes of electrification. However the potential gradients and charges found in warm clouds were often comparable, which indicates the possibly considerable role of drop charging by processes not associated with phase transformations. They

FIG. 2.7 Potential gradient and charge distribution in a polarized nimbostratus cloud. (adapted from Imyanitov & Chubarina, 1967)

(a) Negatively polarized snow cloud

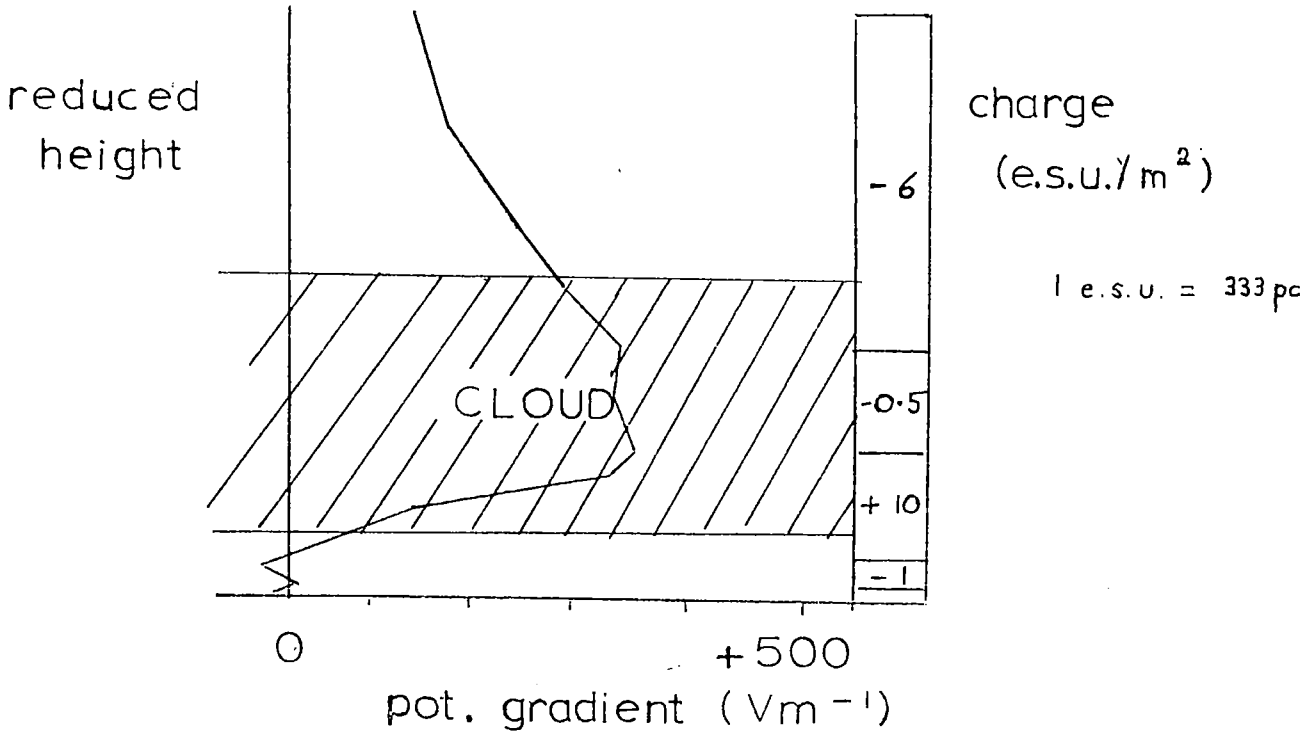

(b) Positively polarized "mixed" cloud

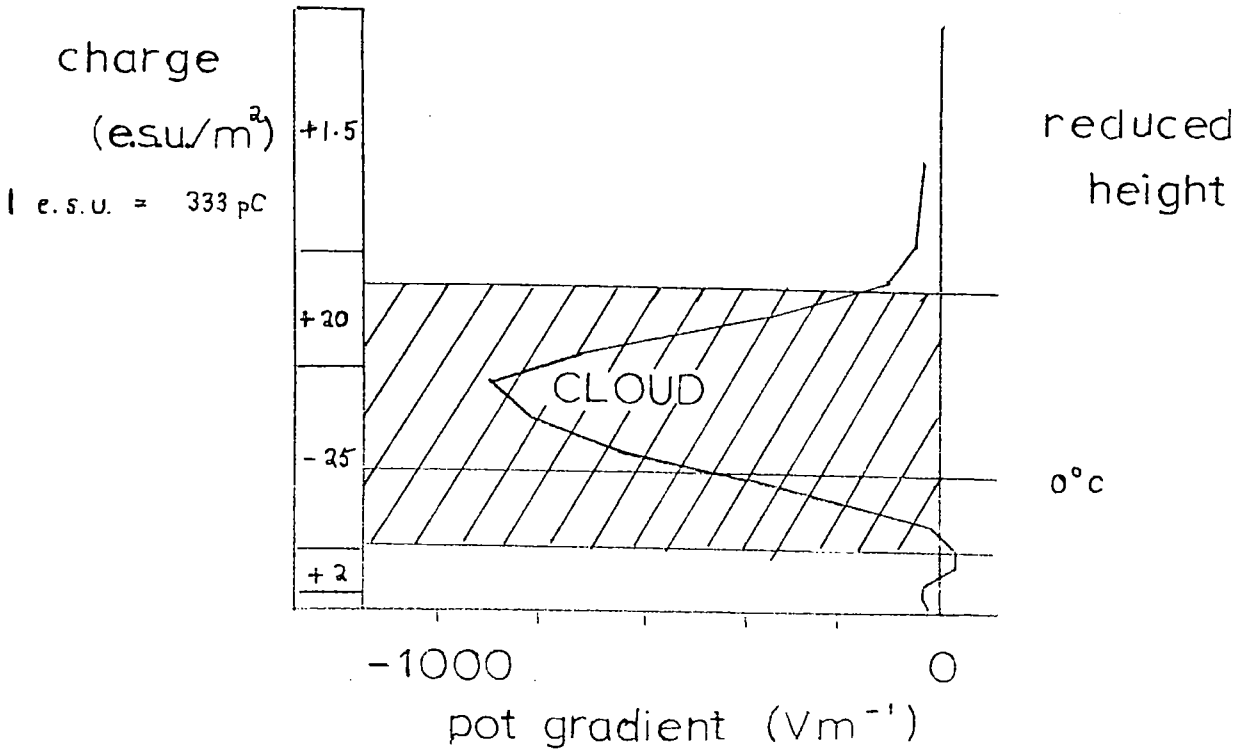

Table 2.1 Average cloud characteristics (as measured by Imyanitov and Chubarina, 1967)

CLOUD TYPE	CLOUD CHARGE ($pC m^{-2}$)			DENSITY OF CURRENT CHARGING CLOUD ($pA m^{-2}$)	
	UPPER	LOWER	BELOW	BENEATH CLOUD	WITHIN CLOUD
(a) Positively polarised					
Mixed	+6700	-8300	+700	12	30
Warm	+3800	-5300	+300	16	35
Snow	+2000	-1700	-200		
(b) Negatively polarised					
Mixed	-11300	+9300	+700		
Warm	-3300	+4000	-100		
Snow	-2000	+3300	-300		

attribute the inverse relation as observed at the ground to the falling precipitation charging the cloud oppositely; this results in the fall of charged precipitation in a potential gradient of opposite sign.

2.2.3 The conclusions of Chalmers

From their systematic observations of potential gradient below, in and above precipitating clouds, Imyanitov and Chubarina also deduced generalised height distributions of potential between the ground and the ionosphere for the various types of cloud. Their results give support to the conclusions of CHALMERS (1958) concerning the probable height distributions of potential for snow and rain clouds.

As mentioned in Chapter 1, CHALMERS (1956) argued that most or all quiet precipitation must have been in the solid state during part of its time in the cloud, so that if there is a process of charge separation connected with solid precipitation in the cloud, this will operate in all cases, whether the precipitation reaches the ground as snow or whether it first melts. To account for the observed electrification of snow by a single process, it must be one that brings negative charge downwards. A second process of opposite sign and greater magnitude must operate at or below the melting level in the case of rain.

The observed electrification could be accounted for differently if the precipitation leaves the cloud uncharged and obtains its charge close to the ground. Different processes could operate for rain and snow, producing different signs of charge.

CHALMERS (1958) presents height distributions of potential for rain and snow clouds, based on these arguments. These are shown in Fig.2.8, together with some of Imyanitov and Chubarina's experimental profiles. In the case of snow, CHALMERS (1956) deduced qualitatively that charge separation must occur in the cloud whether or not it occurred near the ground. He argued that charging of snow at the ground will lead to the cloud base having a negative potential with respect to the ground and the cloud top a positive potential; this means that a charge separation must also occur in the cloud whether or not it was first postulated. The consequent variation of potential with height is shown as curve 1 in Fig. 2.8(a).

Such an argument was not possible in the case of the "mixed" rain cloud, and so two height profiles of potential are possible; these are shown in Fig. 2.8(b), one representing charge separation in the cloud only (curve 3) and one representing charging at the ground (curve 4).

Also shown in the two figures are the appropriate generalised experimental curves of Imyanitov and Chubarina. In the case of snow clouds (curve 2) the profiles agree quite well, while for "mixed" rain clouds the experimental curve agrees most closely with the one for charge separation in the cloud. They also support the surprising conclusion that the potential of the cloud top depends on whether the precipitation reaches the ground as rain or snow.

2.3 The relationship between potential gradient and precipitation current.

2.3.1 The inverse relation

Observations of quiet precipitation electrification have

FIG. 2.8 Potential distribution in nimbostratus clouds

(a) Snow cloud

① Chalmers' theoretical curve for charging within the cloud
② Imyanitov's experimental curve

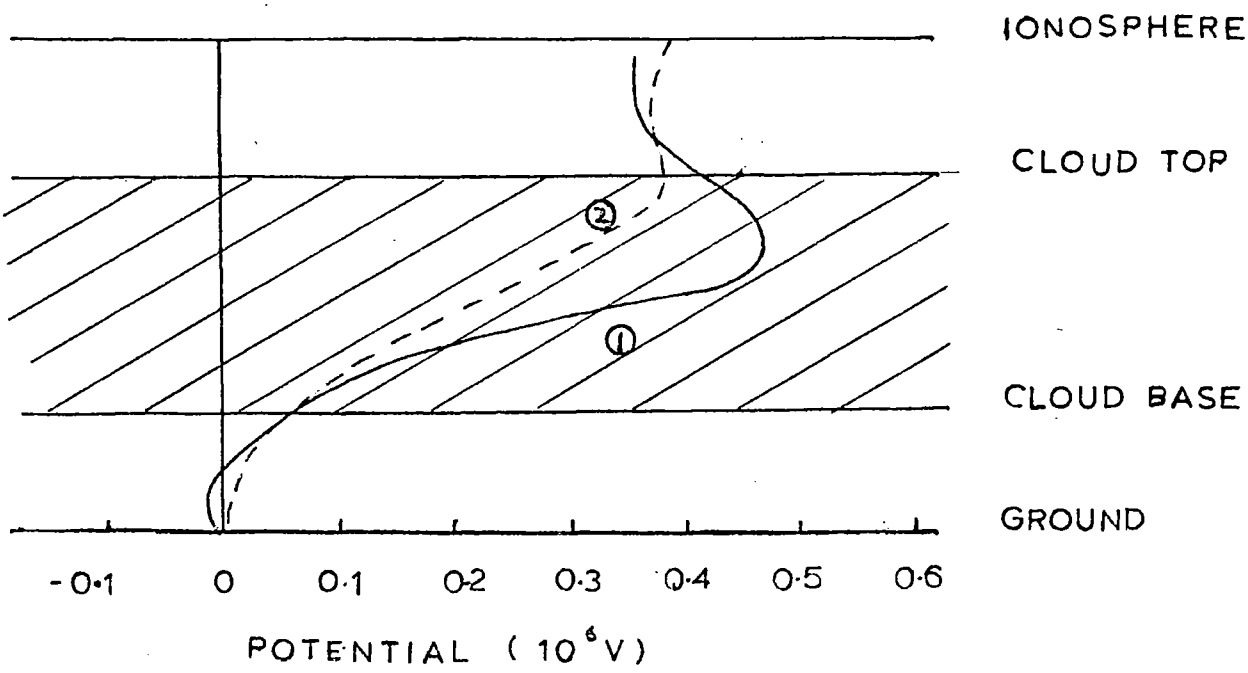

(b) Rain cloud

③④ Chalmer's theoretical curves
⑤ Imyanitov's experimental curve

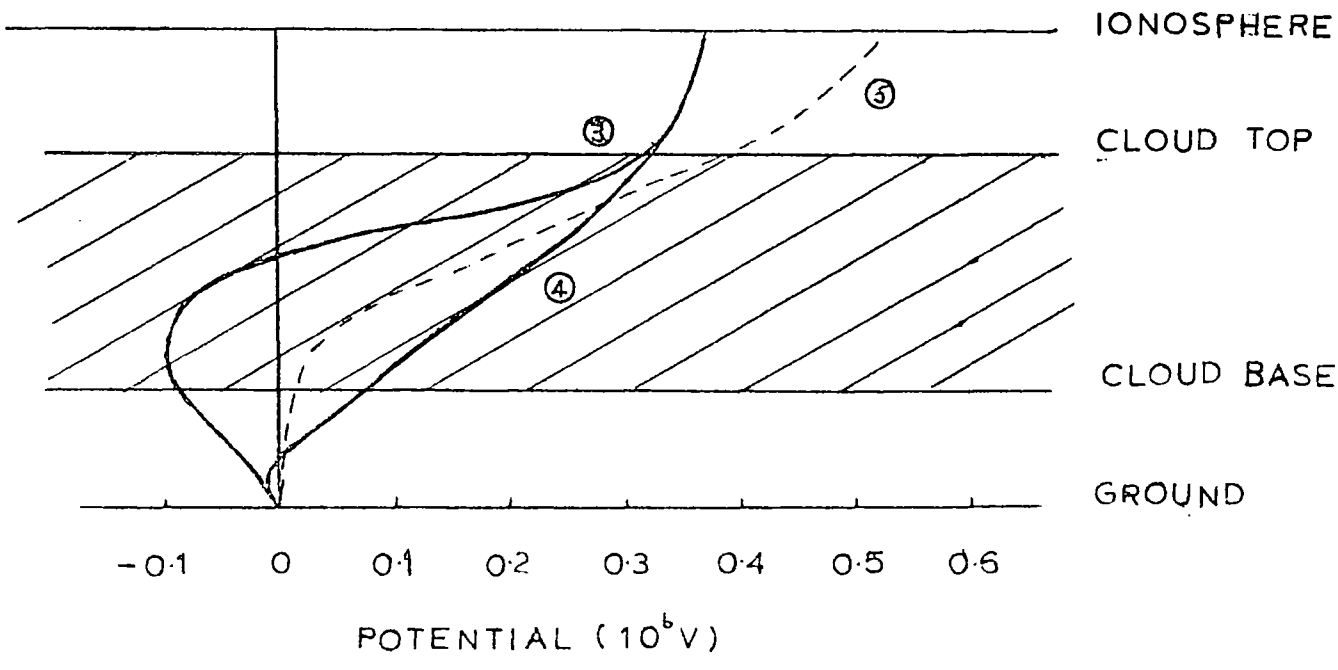

led several workers to express the relationship between potential gradient and precipitation current in a form such as:

$$I = - a (F - C) \qquad (2.1)$$

where I is the precipitation or total current density, F the potential gradient, and a and C constants. Evidently a must be positive for the inverse relation to apply. The inverse relation can thus be treated as a statistical one, the values of a and C being found statistically from observations of I and F.

SIMPSON (1949) suggested that the constant C might represent the normal fair-weather potential gradient, having obtained the expression for the charge q per unit volume of rain:

$$q = - 4.8 \times 10^{-8} (F - 400)$$

where q is in Cm^{-3} and F in Vm^{-1}. The value of C was thus 400 Vm^{-1}. REITER (1965) also found the current to depend on (F - C), finding a value of 40 Vm^{-1} for C, which agreed well with the local fair-weather potential gradient. Similarly CHALMERS (1956) measured the total current K to the Earth during rain, and obtained the relationship

$$K = - 1.18 \times 10^{-14} (F - 150)$$

where K is in Am^{-2}.

CHALMERS (1956) gave a general explanation of the inverse relation by considering some process giving a charge of one sign to the precipitation, while the opposite charge remained in the cloud. The observations of the electrical structure of quiet precipitation clouds outlined in the previous section support this idea. Chalmers also concluded that, when there is no point discharge, the precipitation current will be larger than the other currents such as the conduction current, and so

the potential gradient can be considered as being a consequence of the charging of the precipitation.

2.3.2 The mirror-image effect

CHALMERS (1965) extended the ideas mentioned above to discuss qualitatively how the mirror-image effect might arise during quiet precipitation. If there is a primary process in the cloud which separates charge, then changes in potential gradient and precipitation current at the ground will be due to one of three causes. A region of cloud in which the charge separation is more or less intense may pass over the observer, the cloud itself being in a steady state; a change with time of the intensity of the charge separation may occur in a stationary cloud; or a combination of the two cases may occur.

In the first case, assuming the potential gradient is sufficiently low so that point discharge cannot occur, the likely electrical behaviour at the ground of the precipitation is shown in Fig. 2.9. As the portion of cloud in which there is more intense negative charging passes over the observer, Chalmers considers there should be sufficient charge in the cloud to give a negative potential gradient at the ground, despite the positive space charge of the precipitation. The effect of wind shear between the cloud and the ground will be to delay the arrival of the precipitation at the ground until after the portion of cloud in which it originated has passed. When the precipitation does arrive, a minimum of negative potential gradient will result (or a maximum of positive gradient); thus the peak in potential gradient appears to lead the peak in precipitation current.

As, for example, will be seen in Chapter 7, wind shear

Fig. 2.9 Electrical Behaviour of Approaching Cloud
(from ~~Reiter~~ Chalmers, 1965)

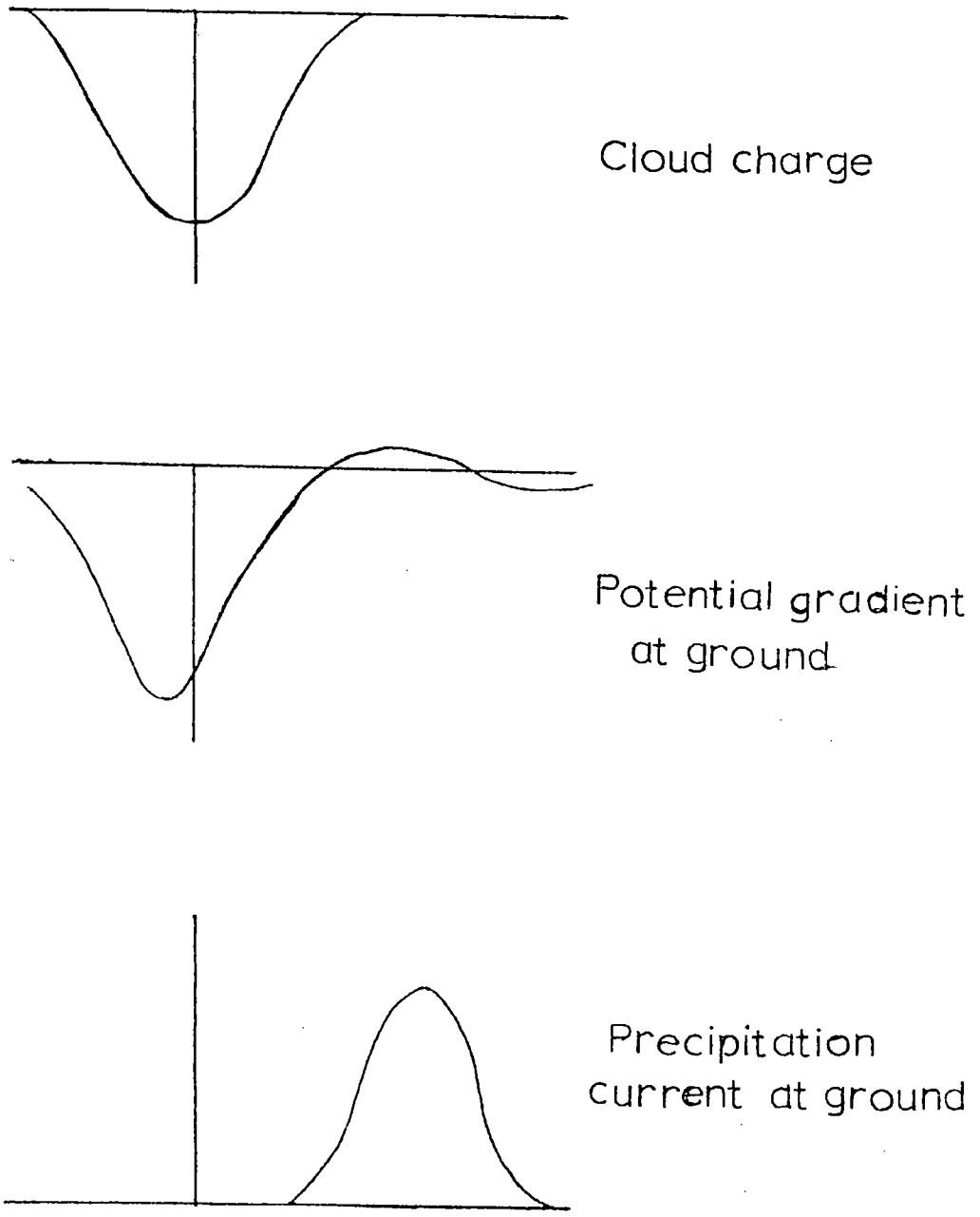

between cloud and ground is nearly always present, and so the potential gradient would be expected to lead the precipitation current; the above argument also leads to the conclusion that if no wind shear is present, then the peaks in potential gradient and precipitation current would be simultaneous.

The second case, that of a stationary developing cloud above the observer, is less simple as steady conditions do not prevail within the cloud. Initially, the potential gradient is affected by the increasing positive space charge of the falling precipitation; when the precipitation starts to reach the ground, the effect of the negative cloud charge will be dominant. Consequently a peak of positive precipitation current leads a peak of negative potential gradient (Fig. 2.10).

As Chalmers points out, the examples taken are very much simplified, with actual conditions most probably being represented by the third case, that of a moving cloud which is also changing. Nevertheless, time lags between potential gradient and precipitation current have been observed with either leading on different occasions (for example RAMSAY and CHALMERS, 1960); there may well be clouds where movement is more important than development, or vice versa.

One prediction of Chalmers is that, due to snow falling more slowly, its space charge will have a greater effect, and so the case of precipitation current leading would be most likely in a developing snow cloud. Observations during quiet snow have certainly shown instances when the precipitation current leads. Another interesting consequence of his ideas is that time lags in the mirror image effect would be due to both the time of fall of the precipitation from the cloud and

FIG. 2.10 Electrical behaviour of a stationary developing cloud (from ~~Reiter~~ Chalmers, 1965)

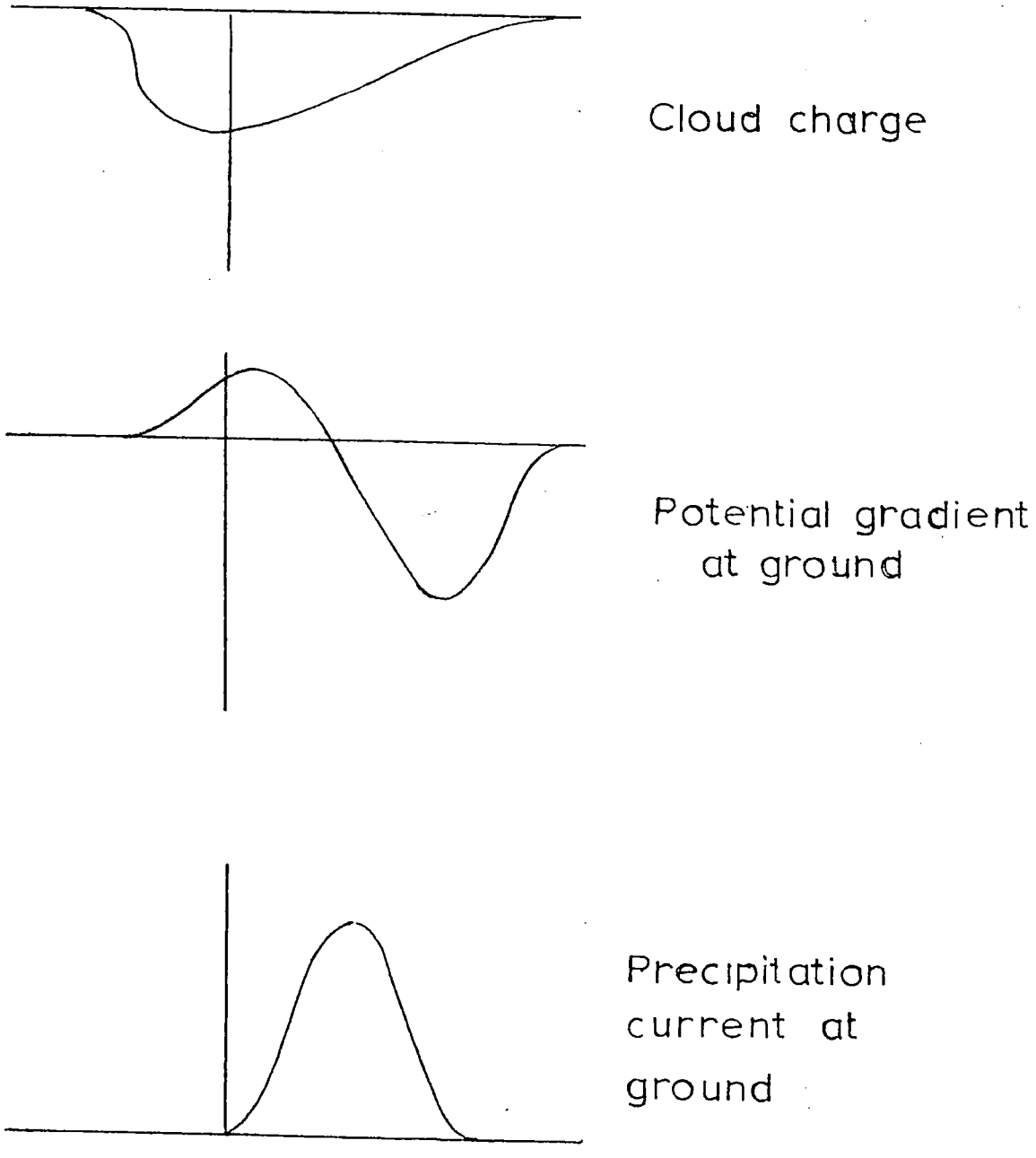

any wind shear between cloud and ground in the case of a stationary developing cloud. In a moving cloud, only the wind shear could produce any time lag. These ideas are developed in a subsequent chapter.

2.4 The relationship between the meteorological and electrical activity in quiet precipitation.

Electrically quiet precipitation falls from extensive layer clouds which produce steady, uniform precipitation, while showers and thunderstorms produce heavier rain and much more violent conditions, both electrically and meteorologically. An interdependence between the degree of meteorological and electrical activity of clouds thus seems possible. The conclusion of REITER (1965, 1968) that the electrical behaviour of steady precipitation is controlled by the degree of stability, and hence turbulence, in the atmosphere supports this idea.

The melting layer appears to be an important feature both electrically and meteorologically. Radar observations normally show a distinct echo from the melting region, and electrical observations have also shown it to be a region of strong electrical activity. Charging has been found in clouds up to about the $-10^{o}C$ level, almost certainly associated with the presence of ice. However, there is also evidence for charging in "warm" clouds, where no ice is present and so different charging processes are at work. The type of charging process, and the degree of electrical activity, may well then be determined by the meteorological conditions, in particular temperature, within the cloud.

As mentioned in the previous section, the time lags observed in the mirror-image effect may be the consequence of the wind profile between the cloud and the ground affecting the falling precipitation. If this is so, the wind profile will have a considerable influence on the electrical features

of quiet precipitation as seen at the ground. GROOM and CHALMERS (1967) have suggested that the apparent absence of the inverse relation in summer observations of RAMSAY and CHALMERS (1960) and themselves could be due to the greater height of the melting level; a longer time of fall of the precipitation could produce a consequently longer time lag in the mirror image effect, disguising any inverse relation.

Recent work by STRINGFELLOW (1969) and ASPINALL (1970) has indicated the existence of "cells" of electrical activity within the cloud, of horizontal dimensions of a few kilometres, and independent of wind speed. Convective cells within meso-scale precipitation areas have already been mentioned (Sec.2.1.3); these also have dimensions of the order of kilometres.

2.5 The proposed investigation.

The purpose of the present work is to investigate the electrical behaviour of quiet precipitation with the aim of explaining the observed effects in terms of possible charging processes in and below the cloud. The influence of the prevailing meteorological conditions will also be considered. It is hoped that a systematic investigation of periods of quiet precipitation over a period of several months will help to clarify the nature and origin of the inverse relation and the mirror-image effect by considering the relevant meteorological conditions on each occasion.

2.5.1 Representation of the inverse relation and the mirror-image effect.

In order to compare different periods of precipitation, some method is needed of representing the degree to which the

inverse relation and the mirror-image effect are present. Previous workers have used various methods, not all strictly comparable, with often only short intervals during a period of steady precipitation being examined. Methods of evaluating any time lags in the mirror-image effect have also differed; sometimes time lags between corresponding maxima or minima have been used, or time differences between the instants when the records changed sign.

More recent work, starting with that of OWOLABI and CHALMERS (1965), has expressed the relation between potential gradient and precipitation current in terms of the correlation between the two records. A period of precipitation exhibiting the inverse relation and mirror-image effect with no additional random effects would show perfect correlation between potential gradient and precipitation current. Any time lag in the mirror-image effect is then shown by maximum correlation occurring for one record shifted with respect to the other by the appropriate time difference.

The correlation between the records can be expressed as a statistical quantity, the correlation coefficient, which describes both entire records. This coefficient has a value of + 1.0 for a direct relationship and - 1.0 for an inverse relationship between the records (Fig. 2.11). As random effects increase, so the correlation coefficient approaches a value of zero when the two records are completely random. The correlation coefficient and its statistical background are described in Chapter 5.

The availability of modern digital computers permits the

FIG. 2 11 Correlation between two records

(a) Direct correlation

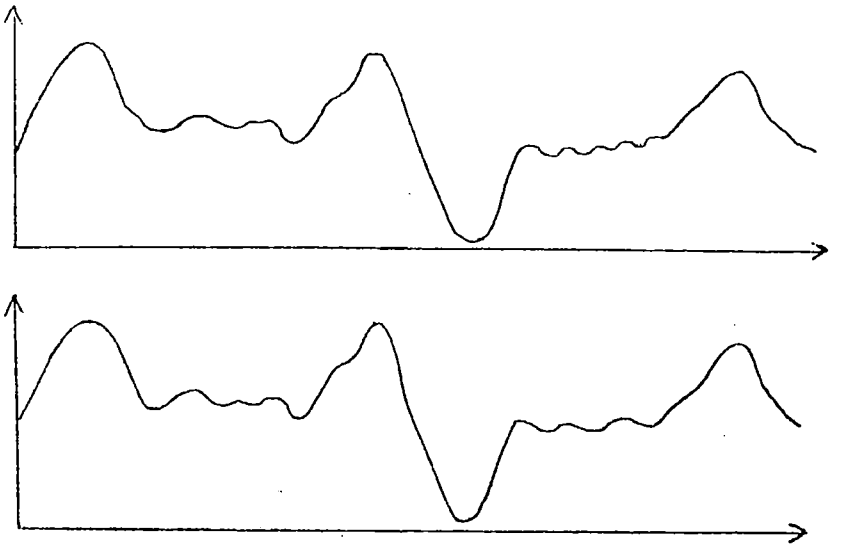

(b) Inverse correlation

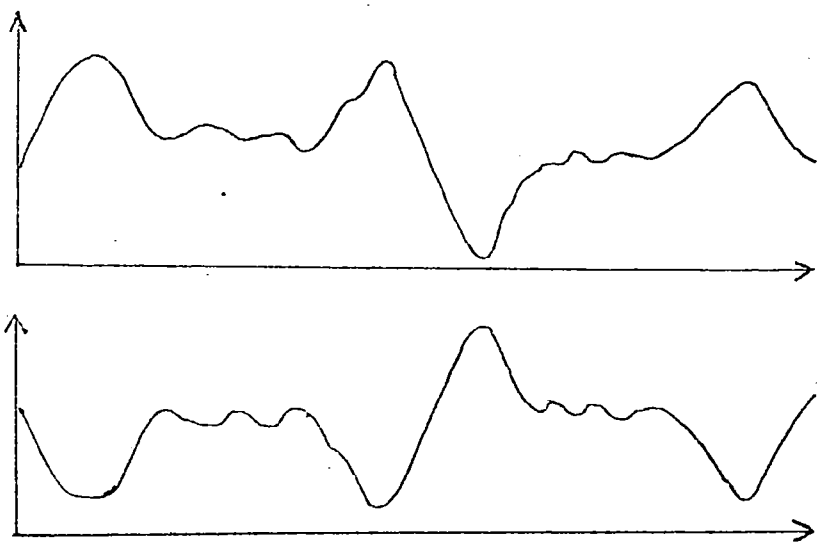

(c) No correlation

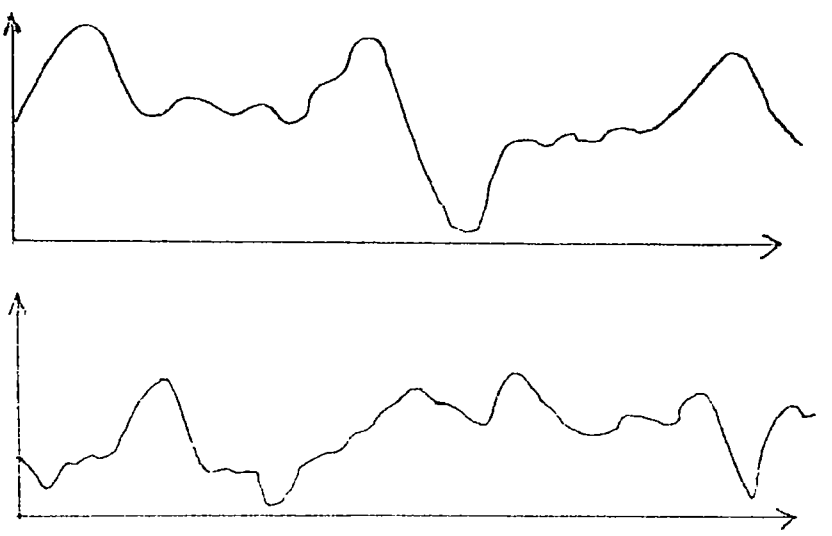

processing of the large quantities of data involved in the calculation of correlation coefficients and other statistical quantities from sets of readings taken at frequent intervals over long periods of time. In the case of the electrical behaviour of precipitation, the effects of the great variability in conditions both within a single set of records and between different occasions can be minimised by adopting a statistical approach. Such an approach is thus now possible by using the digital computer to handle the data and calculate the relevant statistical quantities.

2.5.2 A statistical method of representation

It has already been described how the relationship between potential gradient F and precipitation current I in quiet precipitation can be described by functional relationships of the form:

$$I = - a(F - C) \qquad (2.1)$$

Such an expression indicates the presence of both the inverse relation and the mirror-image effect. The former is present if the constant a is positive, while the latter will be most noticeable if the simultaneous values of I and F fit the expression at all times (ignoring for the moment the effect of any time lag). In actual cases, such an expression as above will fit simultaneous values of I and F to a greater or lesser degree; the extent to which this is true is indicated by the value of the correlation coefficient between the two records. It is thus proposed in the present work to express the mirror-image effect in terms of the correlation coefficient between the two records of potential gradient and precipitation current. This method also has the advantage of indicating any

time lag by the maximum correlation coefficient occurring for one record shifted with respect to the other by this amount. The expression 2.1 will then apply to values of I and F when one record has been shifted by the appropriate time lag.

The inverse relation and mirror-image effects can occur independently of each other if their usual definitions are taken; this is illustrated in Fig. 2.12. In Fig 2.12(a), both effects occur; a perfect mirror-image effect would result in a correlation coefficient of - 1.0, as there is inverse correlation between the records. Fig 2.12(b) shows a case of mirror-image effect with no inverse relation; the correlation coefficient will still be negative. Finally, Fig. 2.12(c) shows the case of neither effect being present, with the correlation coefficient being positive (direct correlation).

It can therefore be said that the inverse relation is present if the mean values of the potential gradient and precipitation current records are of opposite sign (constant a in Eq. 2.1 is positive); and the mirror-image effect can be said to be present if a significant inverse correlation exists between the two records (i.e. a negative correlation coefficient). It is proposed to adopt this convention in the present work, thus treating both effects in statistical terms.

2.5.3 The description of precipitation as "quiet"

So far, while the term "quiet" has been often mentioned, no precise definition has been given. This is partly because

FIG. 2.12 Statistical representation of the inverse relation and mirror-image effect

(a) Both present

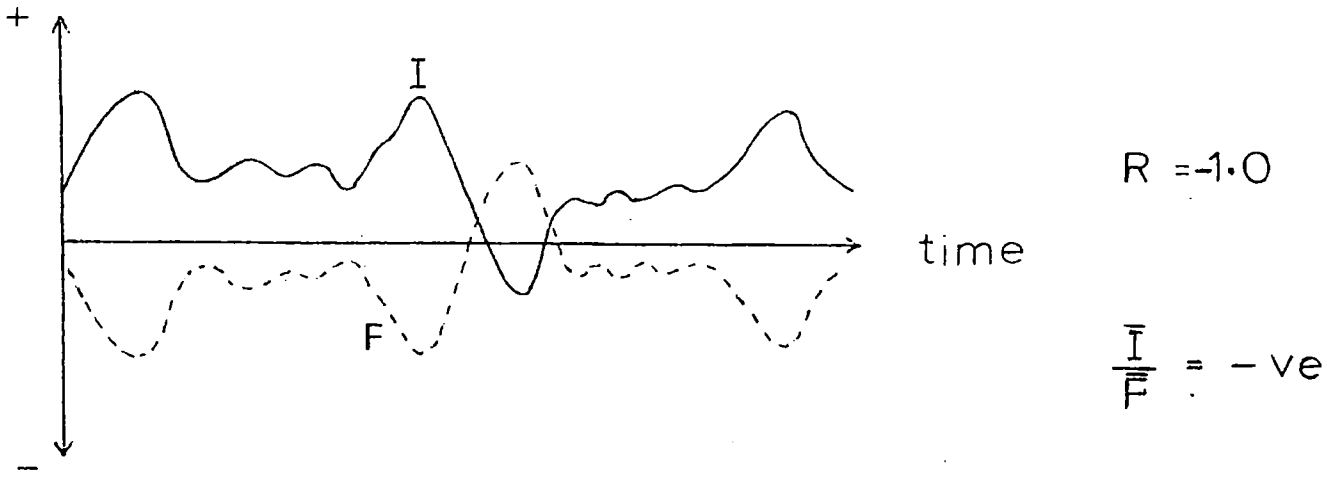

(b) Mirror-image effect only

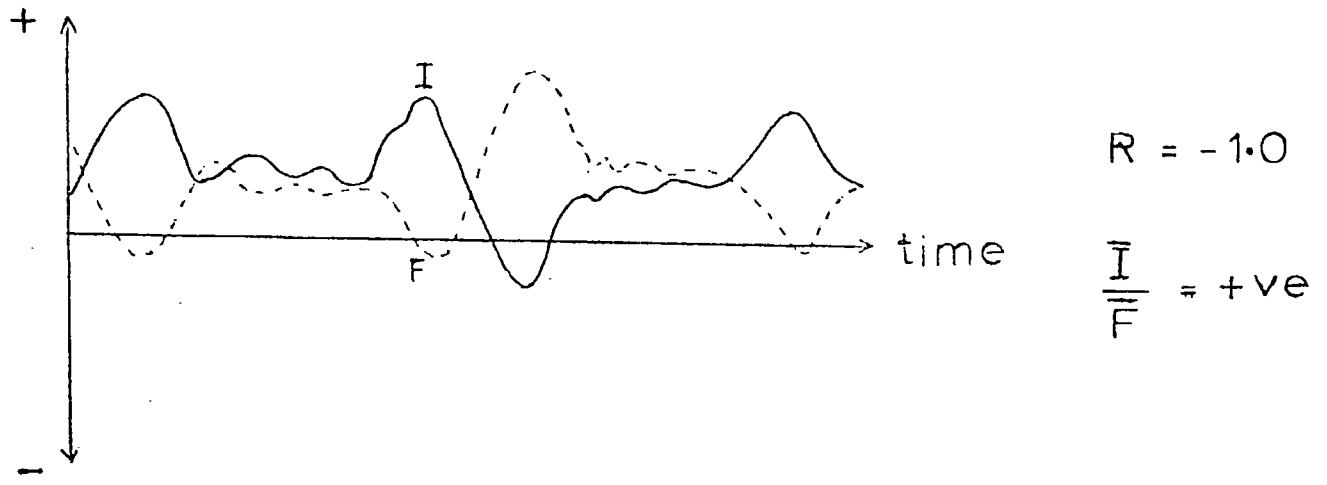

(c) No inverse relation or mirror image effect (but direct correllation)

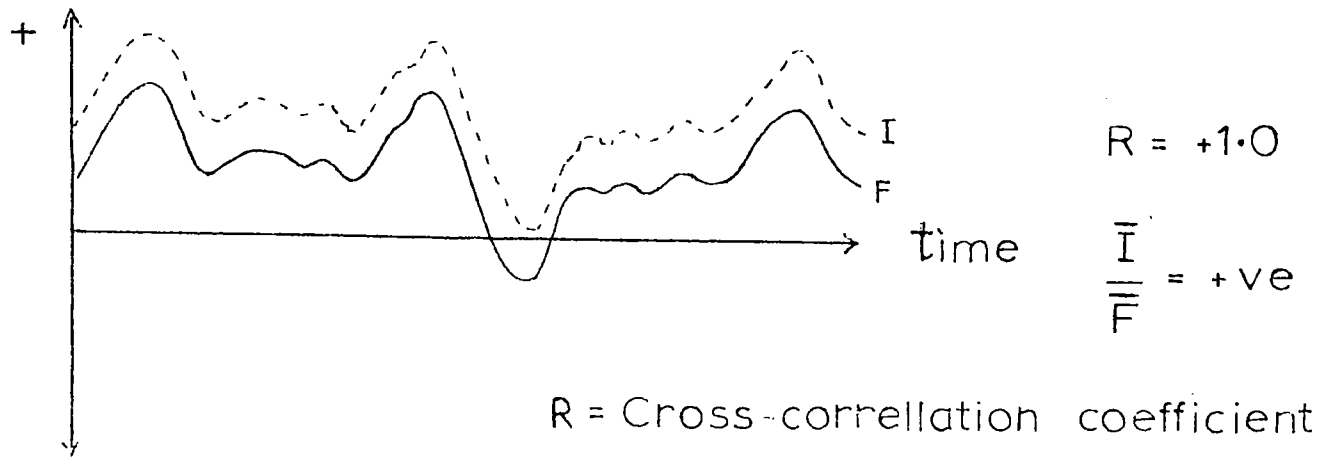

R = Cross-correllation coefficient

Precipitation current I

Potential gradient F

previous workers have not all used exactly equivalent definitions. The purpose in limiting the present investigation to periods of quiet precipitation is to ensure that conditions in and below the cloud are as straightforward as possible, and so, in particular, periods when point discharge currents occur between cloud and ground are excluded.

Such periods are usually evident from the high values of potential gradient and the much more violent behaviour of the record. Thus, for example, ASPINALL (1970) restricted measurements to periods when the potential gradient was less than 1000 Vm^{-1} in magnitude, and only slow changes in potential gradient were occurring. This practice will be followed, except that experience showed that the limitation on potential gradient values could be increased to 1500 Vm^{-1} before there was usually any significant change in the character of the record.

To avoid showers or other short periods of precipitation, records of duration shorter than one hour will not be considered as "quiet"; neither will records exhibiting frequent and large variations and producing sign reversals above a rate of, say, five per hour. It is hoped that the conclusions of the present work will make possible a much more precise definition of quiet precipitation.

CHAPTER 3

The Instrumentation of the Recording Site

3.1 The measurement of precipitation current density

3.1.1 General principles

The precipitation current is one of several atmospheric electric currents present during steady precipitation. In order to measure the precipitation current density (current per unit surface area), the effects of other currents collected by the measuring apparatus must be considered.

The conduction current is the ohmic electric current caused by the movement of atmospheric ions under the influence of the potential gradient, and is present in both fair weather and disturbed conditions. In quiet precipitation, the conduction current density is unlikely to exceed 10 pAm^{-2} in magnitude but can still be comparable with the precipitation current density.

The vertical movement of ionic charges in convective or turbulent motions of the air can produce a "convection current" to any portion of the Earth's surface isolated in order to measure the precipitation current density. For the convection current to be significant, vertical air motions greater than the ionic velocities due to conduction are needed, together with a space charge gradient between adjacent levels. The magnitude of this current is also unlikely to exceed 10 pAm^{-2} in quiet precipitation.

When the potential gradient is sufficiently high, point discharge will produce atmospheric ions of opposite sign to

the potential gradient; this may modify the precipitation current, due to ion capture by the falling precipitation. The value of potential gradient above which point discharge becomes significant is difficult to specify. An isolated metal point will start to discharge at a potential gradient of about 1000 Vm^{-1}, but there is evidence that natural objects such as trees do not discharge until much higher values have been reached. In the present work, periods when point discharge occurs are excluded, such periods usually being evident from the behaviour of the potential gradient and precipitation current records.

If a portion of the Earth's surface is isolated to measure the current flowing to it, a bound charge proportional in magnitude to the atmospheric potential gradient will be produced on it. A change of potential gradient will cause a corresponding change in the bound charge, with consequently a "displacement current" being measured in addition to the other atmospheric currents. The displacement current is proportional to the rate of change of potential gradient and could be a serious source of error; a rate of change of potential gradient of 5 Vm^{-1} s^{-1} will produce a displacement current density of about 50 pAm^{-2}, as large as precipitation current densities often recorded during quiet precipitation. It is essential that any apparatus designed to measure precipitation currents allows for the effects of displacement currents.

3.1.2 The design of apparatus to measure precipitation current density

The obvious method of measuring the precipitation current density is to isolate a portion of the Earth's surface, and

to measure the charge or current transferred to this portion by precipitation, having first eliminated conduction, convection and displacement currents. Precipitation current collectors based on this principle can be classified as "exposed" or "shielded", depending on whether or not the collecting surface is exposed to the atmospheric potential gradient.

3.1.3 The exposed collector

This type of collector normally consists of a circular plate mounted level with, but isolated from, the earth's surface. Conduction, convection and displacement currents will be measured in addition to the precipitation current, and so some method of compensation for these additional currents must be devised.

One method, originally devised by WILSON (1916), uses a second inverted plate to measure the additional currents, but not the precipitation current. The currents measured by the two plates are subtracted to estimate the precipitation current density. A system of instantaneous compensation for conduction and displacement currents was devised by KASEMIR (1955). A current-measuring circuit, effectively having a time constant equal to the relaxation time of the atmosphere, instantaneously subtracts the conduction and displacement currents from the total current to a single isolated plate. This method has the disadvantage, however, of integrating the precipitation current density with the time constant of the measuring circuit.

An alternative approach is to measure the potential gradient and conductivity separately, from which the displacement and conduction currents can be determined for subtraction

from the total collector current. RAMSAY and CHALMERS(1960) used a double electrometer valve in the current-measuring circuit to perform the subtraction at the same time as the current was being measured, while ASPINALL (1970) used a computer to calculate the precipitation current density from recorded potential gradient, conductivity and collector current values.

It is doubtful whether any of these methods effectively compensates for convection currents; furthermore ASPINALL (1972) has found evidence of a "mechanical transfer current" of ions to an exposed receiver, due to small-scale air motions.

3.1.4 The shielded collector

In this type of collector, the collecting surface is shielded from the atmospheric potential gradient, eliminating the conduction and displacement currents. The collecting surface is usually shielded by a raised and earthed metallic cylinder surrounding it, which also largely eliminates the effects of convection currents.

This type of collector has the disadvantage, however, of not collecting all the precipitation, particularly under windy conditions. Selective capture of larger precipitation particles is possible under such conditions, as these are affected less by the wind. If larger particles are charged differently from smaller ones, a distortion as well as reduction of the precipitation current could result.

RAMSAY and CHALMERS (1960), however, operated both exposed and shielded receivers in quiet precipitation, and did not detect any significant differences in the measured

precipitation currents. During similar precipitation, OWOLABI and CHALMERS (1965) found two shielded collectors to give consistent readings when situated up to 1 km apart. Under quiet conditions, it would therefore seem that a shielded receiver can give meaningful readings.

3.1.5 The choice of collector

Since quiet precipitation conditions were to be studied, and the associated meteorological conditions were also expected to be quiet, it was decided to use a shielded collector. As this type of collector is easier to maintain and operate, it should prove more reliable for continuous operation in both rain and snow than an exposed collector.

The design of the collector is shown in Fig. 3.1, and is based on that of SCRASE (1938), but using a larger diameter shield and modern P.T.F.E. insulators. A shielding cylinder of height twice its diameter has been shown by OWOLABI and OLOAFE (1969) to provide the best shielding of the collecting surface, and so a shield of 1 m height and 0.5 m diameter was chosen. The collecting surface is an inverted cone of diameter 30 cm. A shield to prevent drops splashing from the rim of the cylinder into the collecting cone limited the effective diameter of the collecting surface to 25 cm, giving a collecting area of 0.049 m^2. The collecting cone empties through a hole in its base into a brass cup, from which the water runs out through a rubber tube. The collector is constructed from aluminium.

The precipitation current is measured by a Rank Nucleonics d.c. amplifier, housed in the space beneath the collecting cone. The connection from the collecting cone to the amplifier input

FIG. 3.1 The shielded precipitation collector

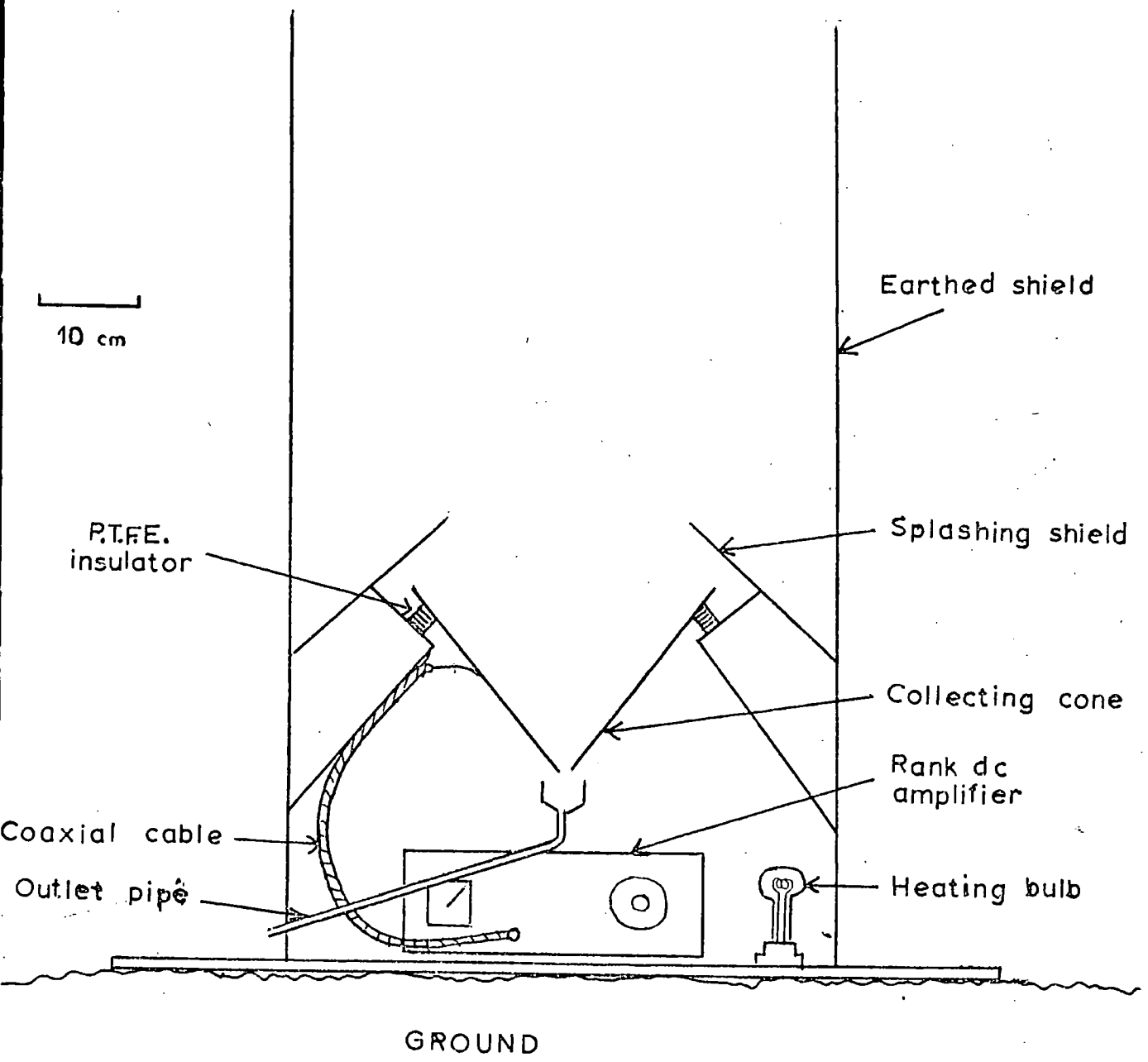

is by coaxial cable, firmly attached to the collector to prevent any spurious signals due to movement of the cable. A 0 to 1 mA recorder output was fed from the amplifier to the Observatory laboratory.

To minimize condensation on the P.T.F.E. insulators and in the amplifier, two 60 W mains bulbs were continually run beneath the cone, connected in series to prolong their life.

The constructed collector is shown in Fig. 3.2.

3.1.6. The operation of the collector

The collector proved as reliable in operation as had been hoped, any failures usually being due to loss of insulation of the collecting cone. To maintain the necessary high resistance of about 10^8 ohm across the P.T.F.E. insulators, they were cleaned about once a fortnight to remove any dirt or grease by wiping with a clean tissue dampened with carbon tetrachloride. Loss of insulation was noticeable by a gradual drift of the Rank output from zero until a constant full-scale deflection resulted.

During the summer, the formation of spiders' webs across the insulators and between the collecting cone and the shielding cylinder sometimes caused loss of insulation, particularly when they became damp. This problem could be minimized by each morning running a screwdriver around the space between the cone and shield to break the webs, but they often re-formed by night.

The collector was run continuously, with the Rank amplifier usually set to give a full scale reading of 1 pA, representing a precipitation current density of about 20 pAm^{-2}. The

FIG. 3.2 The shielded precipitation collector

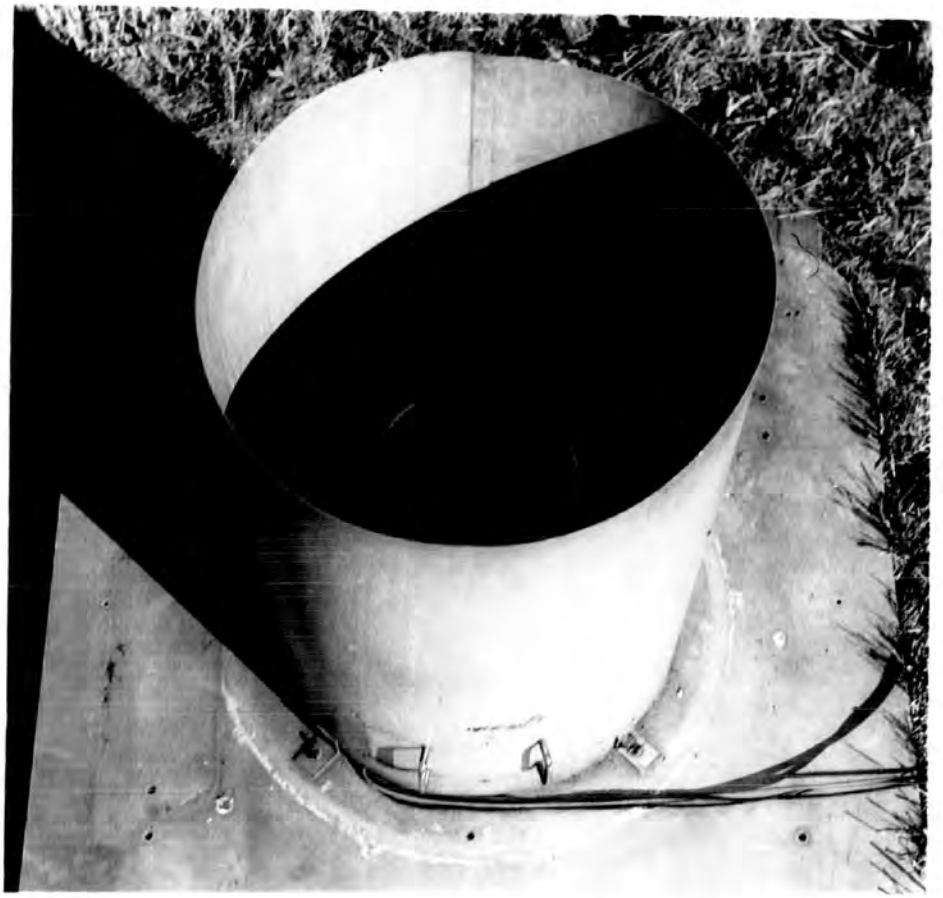

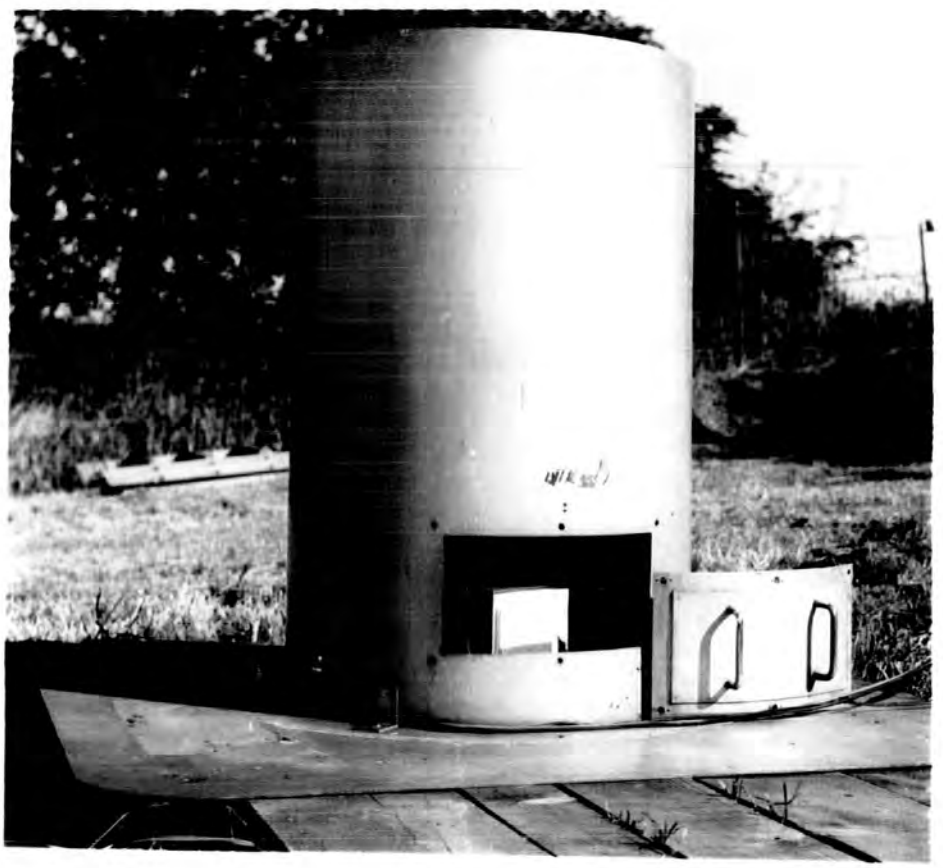

shielding was perfectly adequate, with no deflections attributable to potential gradient changes or conduction currents being observed when precipitation was not falling.

The collector also functioned during snow, but the effects of wind were then far more noticeable, with any wind speed in excess of about 5 ms^{-1} considerably reducing the precipitation current measured. The collector, however, continued to operate when up to 15 cm of snow was lying on the ground, which would almost certainly have prevented an exposed collector from operating. Eventually the shielded collector failed when the outlet pipe froze, causing the brass cup to fill with water, which shorted to the collecting cone whenever a drop fell from it.

3.1.7 Recommendations for future work

For measurement in quiet precipitation, use of the shielded receiver is probably as accurate a method of measurement as use of the exposed receiver. Both types of collector could benefit from the use of integrated circuit F.E.T. amplifiers, a wide range of which are now available. These units may offer a performance equal to that of the conventional Rank d.c. amplifier or Vibrating Reed Electrometer, but occupy far less space, can be made completely weatherproof and avoid the need for an outside a.c. mains supply.

3.2 The measurement of potential gradient

3.2.1 The field mill

Of the various instruments used to measure potential gradient, the field mill was chosen for the present work as

it offers the best combination of sensitivity, response and ease of use. The principle of operation of the field mill has been described elsewhere (for example CHALMERS, 1967), and so only the methods of sign discrimination will be considered here.

As the conventional field mill produces a sinusoidal output voltage signal, it cannot directly distinguish between positive and negative potential gradients, and so some method of sign discrimination is needed.

One method is to offset the zero of the field mill by applying a bias voltage to a second stator mounted above the rotor (see Fig. 3.3), which applies a constant artificial potential gradient to the lower stator. Any external potential gradient is then added to or subtracted from this artificial value. A similar approach is to apply a known voltage at intervals to a normally earthed guard ring surrounding the stator and rotor. The sign of the potential gradient is found by the direction of the deflection produced on the field mill output.

Alternatively, a phase sensitive device can be used, as the phase of the alternating field mill signal will shift by 180° when the sign of the potential gradient changes. By comparing the phase of the field mill signal with that of a reference signal of constant phase, the potential gradient sign can be determined.

In the present work, the field mills were expected to operate continuously under adverse weather conditions, and so a simple design was required. A new design of field mill, that of LANE - SMITH (1967), avoided the need for separate

FIG. 3.3 Basic design of a field mill

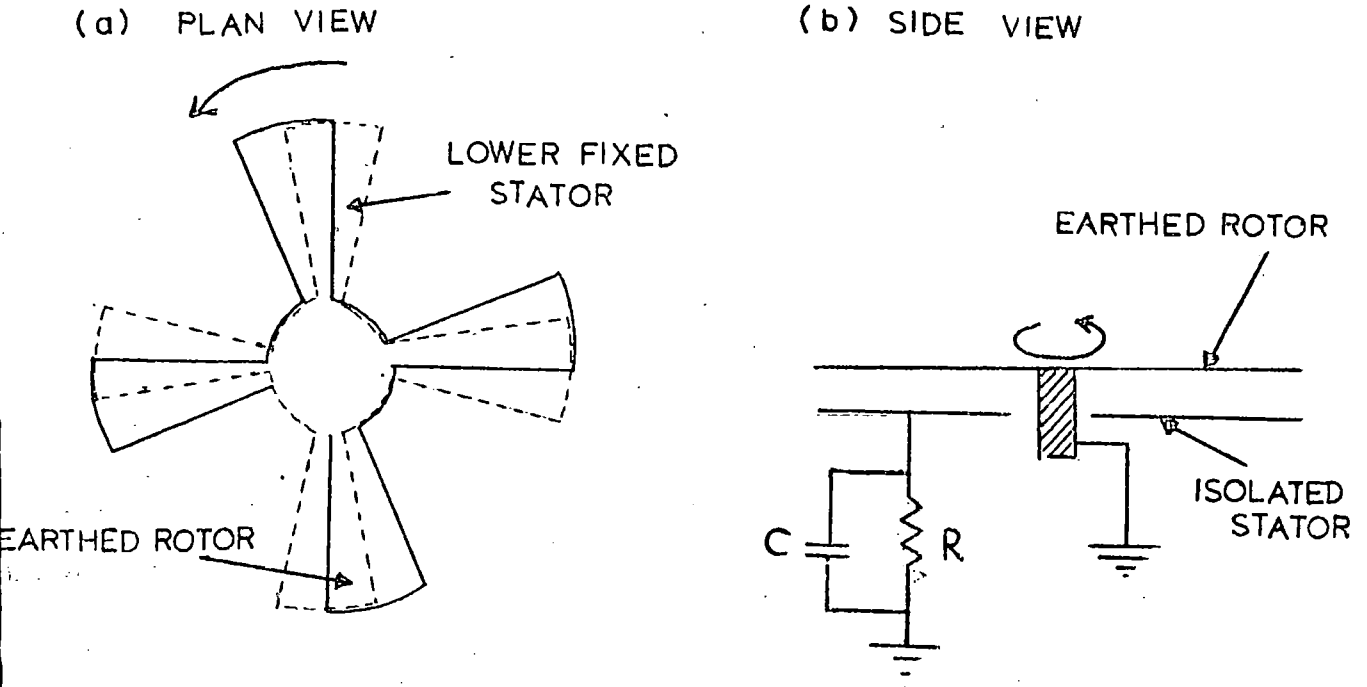

FIG. 3.5 Field mill output voltage (Lane-Smith design)

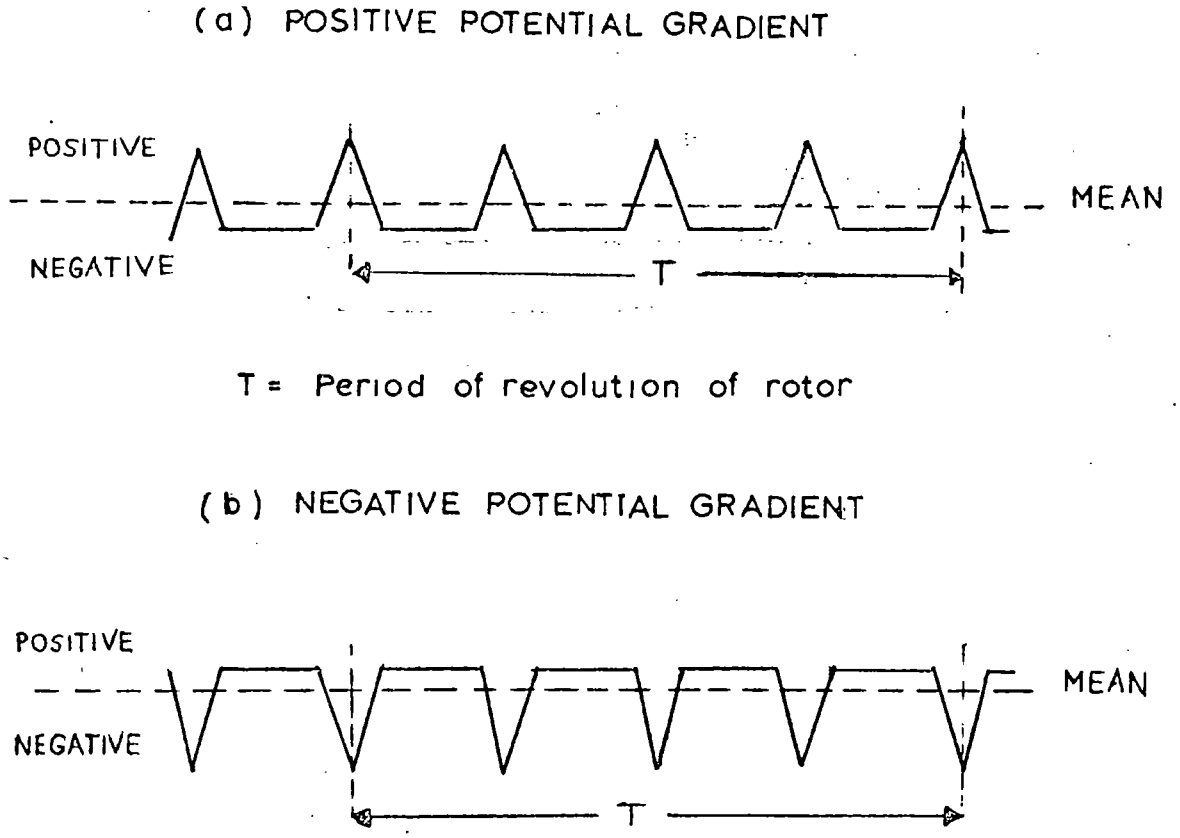

sign discrimination, and so this design was adopted.

3.2.2 The field mill design of Lane - Smith

This design of field mill avoids the need for a separate method of sign discrimination by producing an asymmetric triangular waveform, whereas conventional field mills produce a symmetric sinusoidal waveform. This is achieved by using a stator and rotor with $22\frac{1}{2}^{\circ}$ arms, instead of the usual 45° arms. The waveforms from the stator of both types of mill are shown in Fig. 3.4, after integration by the parallel resistance and capacitance between the stator and earth. The waveforms produced by the Lane - Smith field mill for equal positive and negative potential gradients are shown in Fig. 3.5, where it can be seen that reversal of the potential gradient results in an inverted waveform.

Since the waveform is asymmetrical about the zero voltage level, there is a greater peak voltage in one direction than in the other, depending on the sign of the potential gradient. After amplification, the signal from the field mill is passed into a "detector" circuit, which gives a d.c. output proportional to the difference between the peak voltages reached by the signal. The sign of this output will be the same as that of the potential gradient. High frequency spurious noise or low frequency sinusoidal pick-up do not usually affect the detector output, as these produce equal positive and negative voltage deflections.

3.2.3 The constructed field mills

Three identical field mills were constructed, two for use at the Observatory and one for calibration purposes

FIG. 3.4 Principle of operation of the Lane-Smith field mill

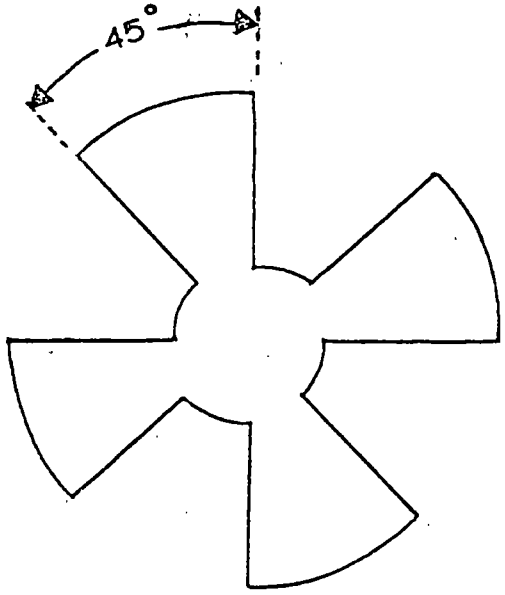

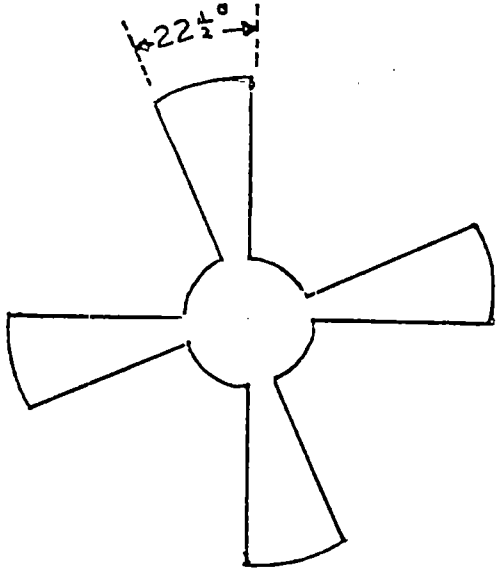

VOLTAGE OUTPUT FROM FIELD MILL

CONVENTIONAL FIELD MILL

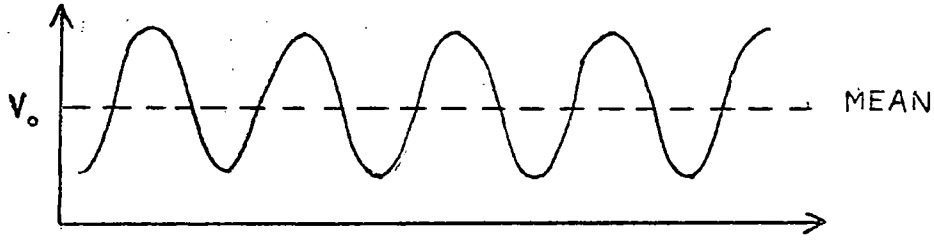

LANE-SMITH FIELD MILL

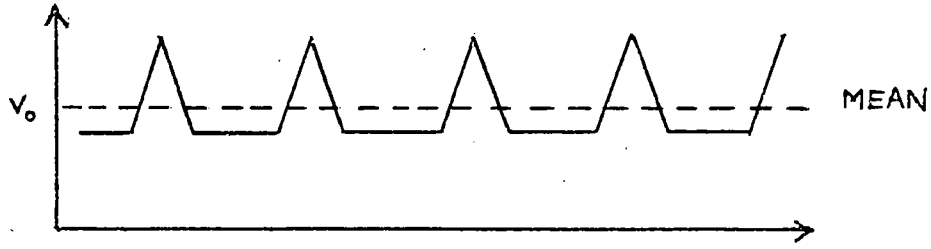

(see Sec. 3.2.5) and to act as a spare. The design and dimensions are shown in Fig. 3.6.

The field mills were constructed from aluminium, with the stator insulated from the base plate by nylon bolts. Originally gramophone-type a.c. synchronous motors were used, but these proved liable to overheating, and in one case burnt out. Capacitor start a.c. motors were substituted, and these proved completely reliable.

The motor and electronic amplifier, which was constructed on Veroboard, were housed in a weatherproof aluminium box, and separated by an earthed screen to prevent hum pick-up by the amplifier (Fig. 3.7). The d.c. supply for the amplifier was provided externally through coaxial cable, and the output to the Observatory laboratory was also by coaxial cable. The input to the amplifier from the stator was by means of screened microphone cable. The mills were mounted inverted to protect them from the rain (Fig. 3.8).

3.2.4 The electronics

The frequency of the input signal from the stator was about 200 Hz, and so an audio amplifier was used to amplify the input signal, typically of a few millivolts amplitude. The circuit, based on the design of STRINGFELLOW (1969), is shown in Fig. 3.9. The first two stages form a "bootstrapped" current amplifier, providing the necessary high input impedance of the circuit. The third stage is a voltage amplifier of gain about 100, being set by the potentiometer R_V. The final stage is an emitter follower, acting as a buffer between the amplifier and detector circuits.

FIG. 3.6 Construction of the field mill

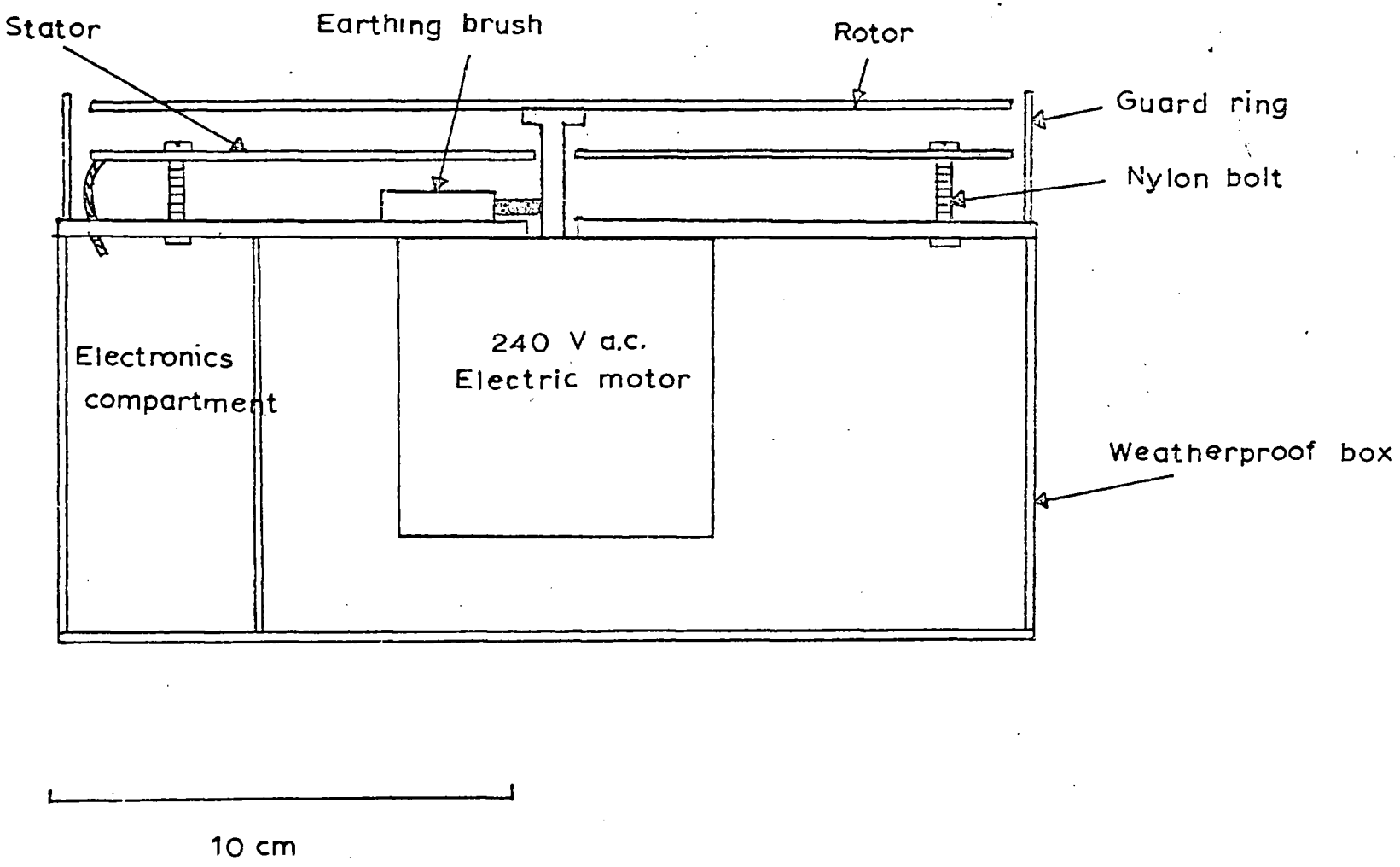

FIG. 3.7 The field mill

FIG. 3.8 The inverted field mill

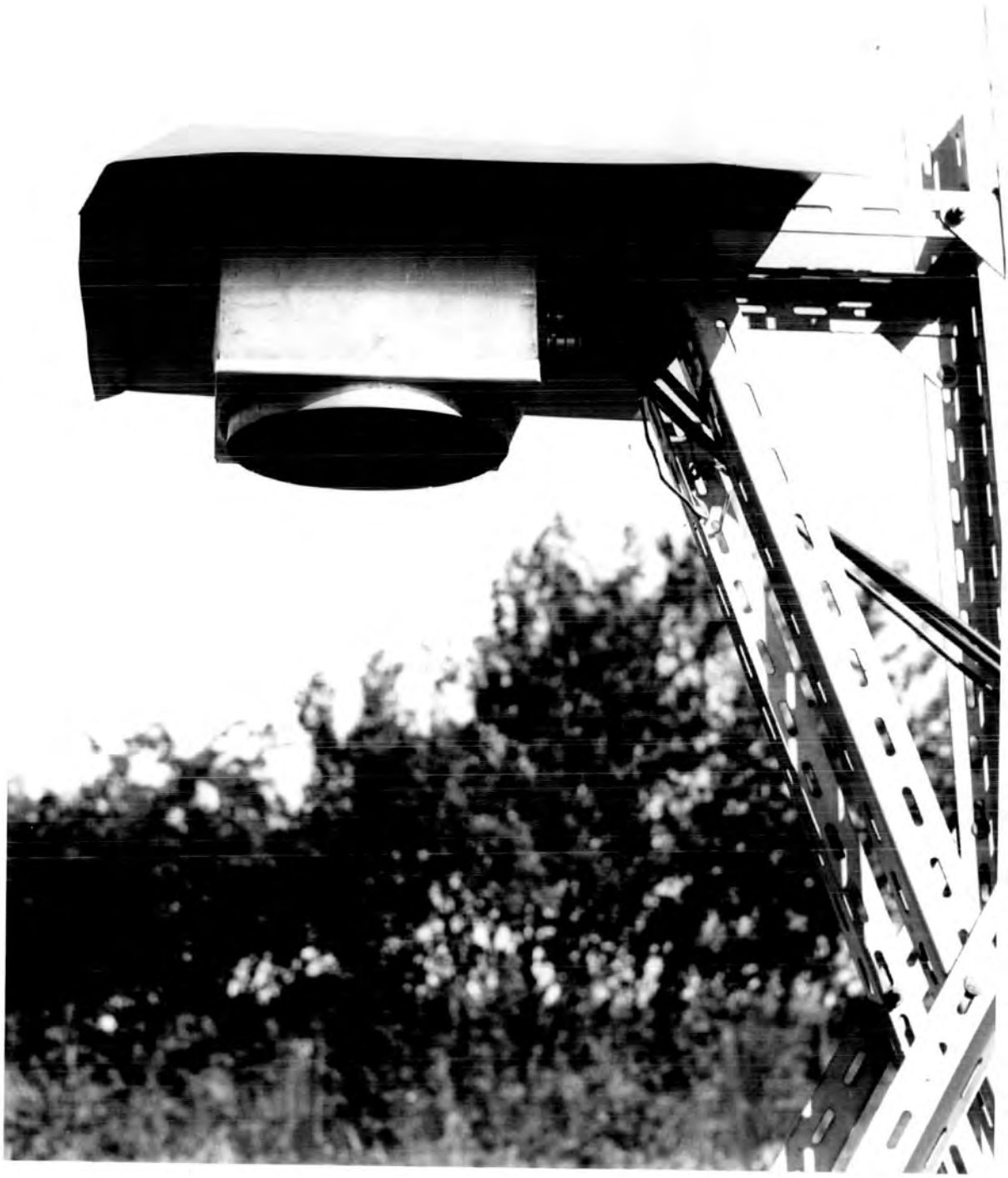

FIG. 3.9 The field mill amplifier

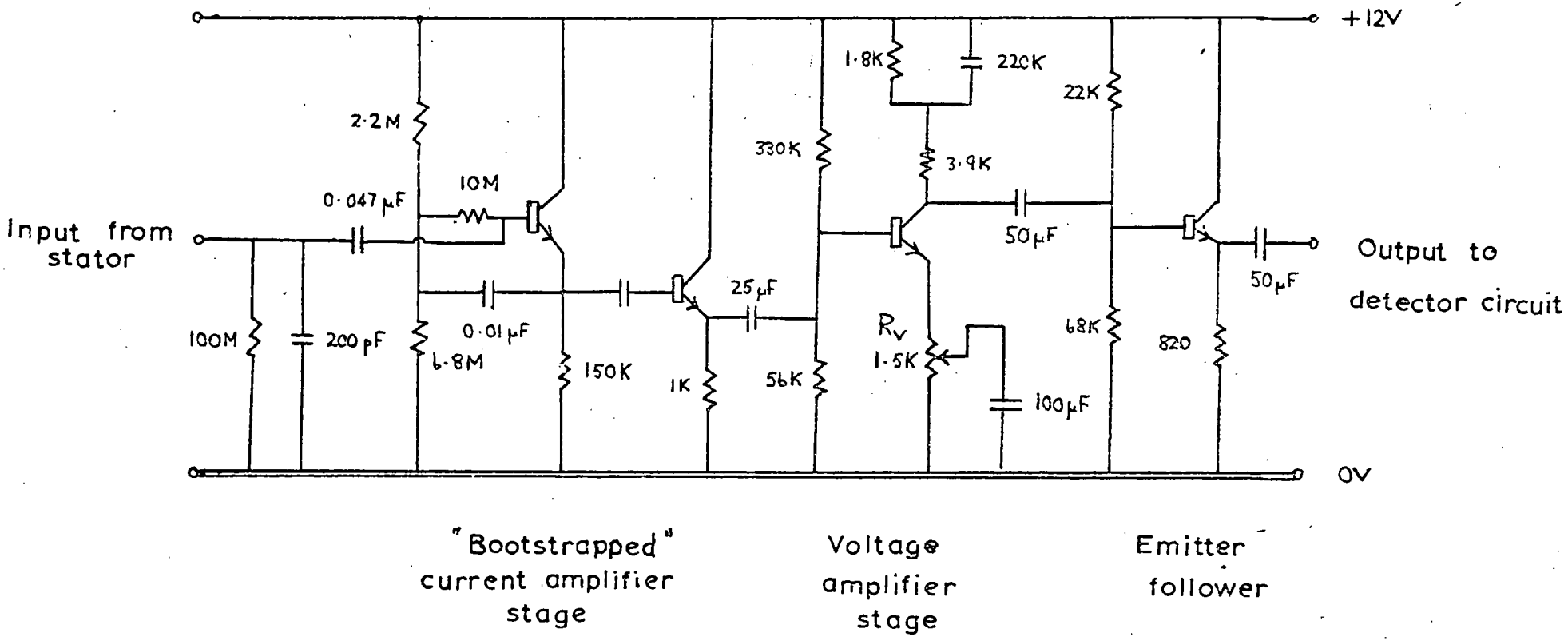

All transistors BC109

The detector circuit is shown in Fig. 3.10, and is a 4 - diode network, giving a d.c. output proportional to the difference between the peak voltages attained by the a.c. signal from the amplifier. The detector circuit output is set to zero by adjustment of resistor R.

The detector circuits for the outside field mills were housed in the Observatory laboratory, connected to the amplifiers in the field mills through coaxial cable.

3.2.5 Calibration of the field mills

The field mills were calibrated by applying known potential gradients, and measuring the corresponding detector circuit outputs. A 1 m diameter circular metal plate was mounted around the stator, the centre of the plate having been suitably cut out, and another 1 m diameter plate mounted 5 cm above. Known voltage differences were applied across the plates; for example a difference of 20 V produced a potential gradient of 1000 Vm^{-1} at the stator.

A typical calibration is shown in Fig. 3.11. The slight difference in slopes for positive and negative potential gradients is probably due to small differences in the characteristics of the diodes in the detector circuit. A more serious feature is the reduced response at low potential gradients, due to the presence of noise and other spurious signals of amplitude comparable to the detector output. These effects were allowed for during the calculation of the potential gradient values from the detector output values on the computer, by using suitable calibration equations for each part of the calibration curve.

FIG. 3.10 The detector circuit

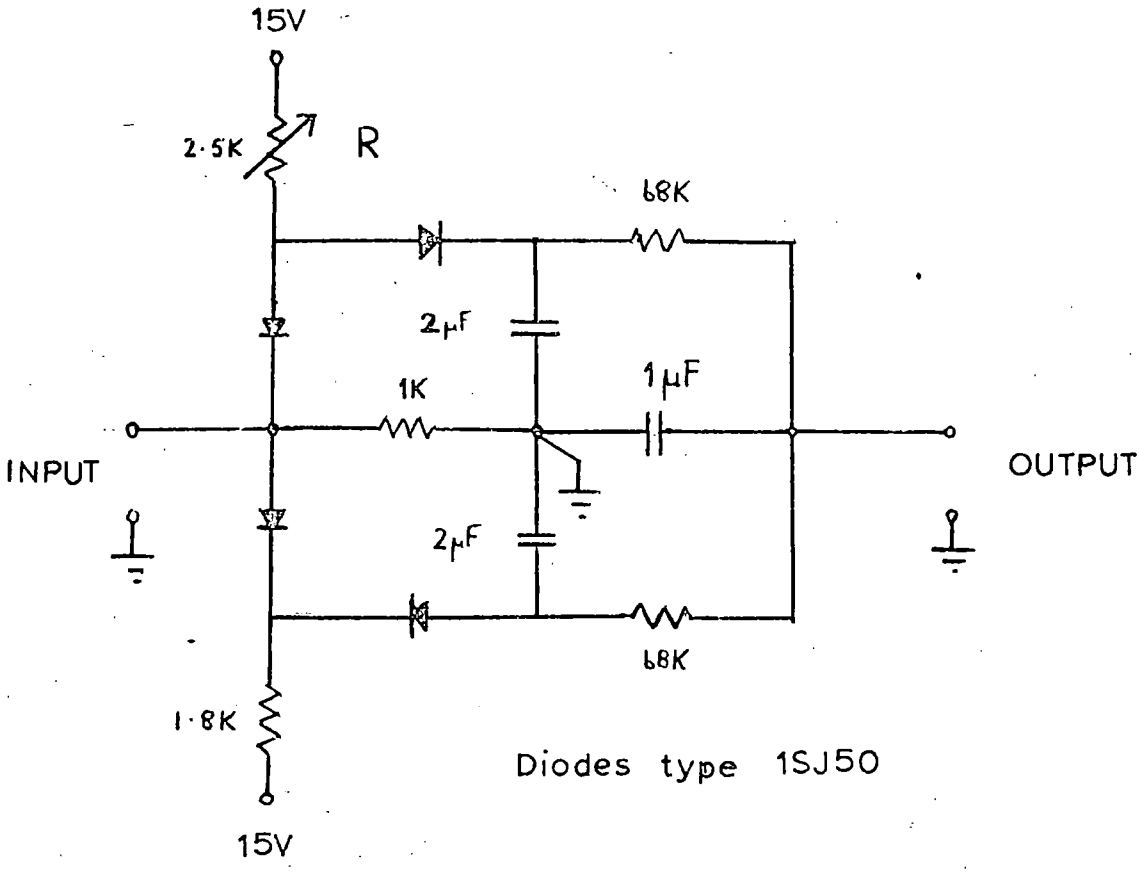

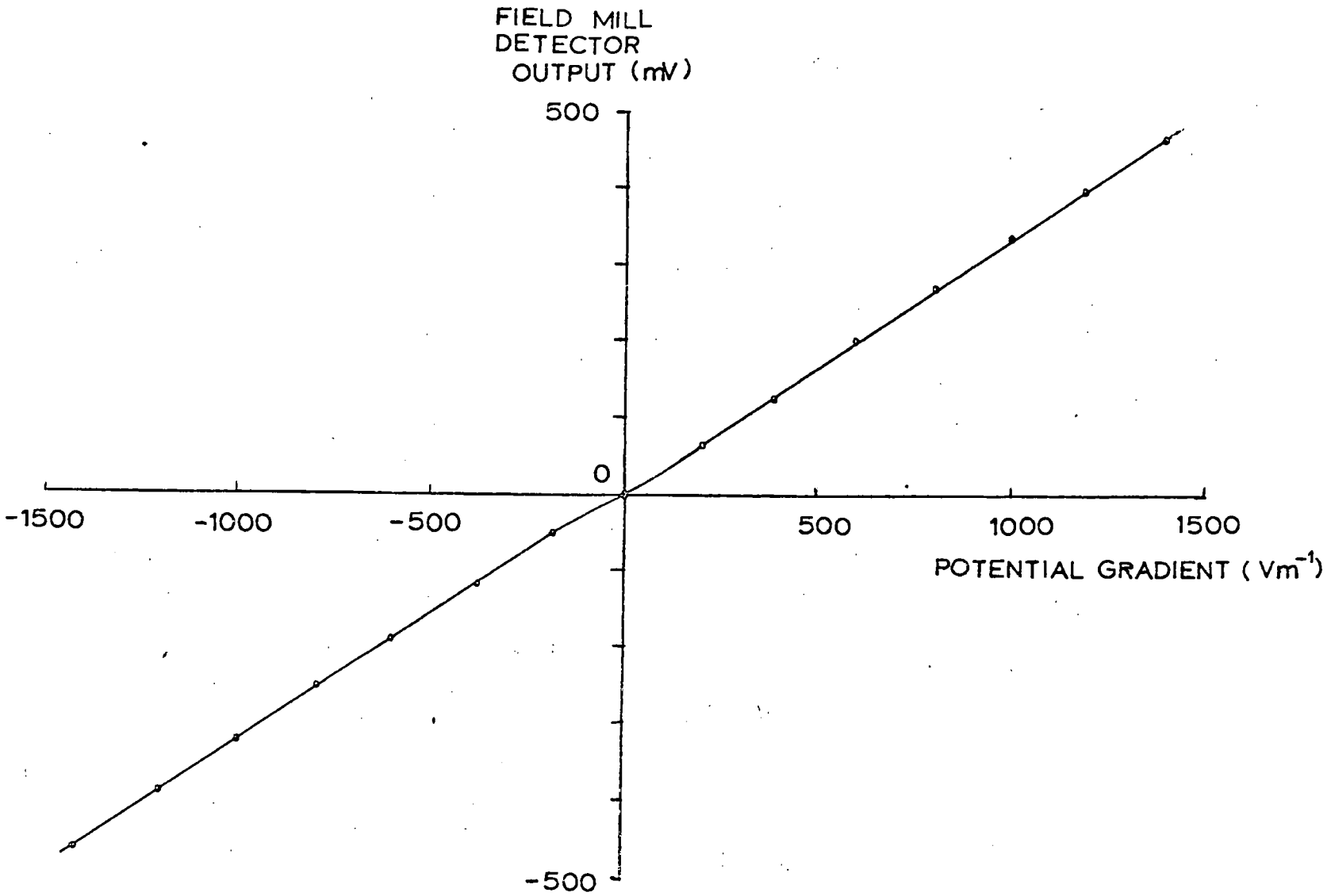
FIELD MILL
DETECTOR
OUTPUT (mV)
500
0
-500
-1500
-1000
-500
500
1000
1500
POTENTIAL GRADIENT (Vm^{-1})

Serious errors could arise at high values of potential gradient, when the input signal from the stator may be so great that the amplifier "clips" the waveform, as illustrated in Fig. 3.12. Any circuit, such as the detector circuit, measuring the amplitude of the signal will give a spuriously low output in such an instance, and in extreme cases the output may even decrease with increasing potential gradient.

To avoid this happening, the amplifier gain was set so that clipping was certain not to occur, not only within the calibrated range, but for potential gradients about 20% in excess of the calibrated range. Thus, for the calibrated range of 0 to $\pm$ 1500 Vm^{-1}, reduction in the detector output did not occur until the potential gradient was in excess of 2000 Vm^{-1}. The few occasions when spuriously low values of potential gradient still resulted could usually be recognised from the behaviour of the chart records.

Unless a field mill is run level with the Earth's surface, the atmospheric potential gradient will be distorted by whatever structure the mill is mounted upon. The field mill mounted inverted on a stand at 1 m height and the mill on the mast at 10 m will both distort the potential gradient they are measuring. To allow for this, an "exposure factor" is determined for each mill by comparing its output with that of a mill running upright with its stator at ground level, well away from the stand or mast. The ratio between the potential gradient measured by the upright and inverted mills is the "exposure factor" of the inverted mill. To minimize the effects of any localised space charges on either of the mills,

the exposure factor is evaluated for several hours of readings, taken in calm, fair-weather conditions.

The exposure factor for the ground inverted mill was found to be 1.2, while that for the 10 m mast mill was 1.4. To find the true potential gradient values, the inverted field mill readings must be multiplied by this factor.

3.2.6 Operation of the field mills

The ground inverted mill has operated continuously since August 1971, with only occasional interruptions for cleaning and re-calibration. The mast field mill has proved less reliable, being more exposed to the weather and less accessible in the event of failure, but nevertheless has been available for most recording periods. The calibrations of both mills have been checked monthly, and no significant variations were noticed apart from slight drifting of the zero readings, due to backlash in the preset resistors used in the detector circuit.

3.3 The rain switch

3.3.1 Introduction

The precipitation current collector and the field mill outputs were initially recorded on a Honeywell Brown potentiometric chart recorder, later to be replaced by the data handling system described in Chapter 4. It was obviously wasteful to record the instrument outputs continuously, and so a method of automatic switching of the recording system was needed. This would switch on the recording system at the start of precipitation, and if possible switch it off when precipitation ceased.

FIG. 3.12 Clipping of field mill signal

(a) Unaffected signal : peak voltage V_o

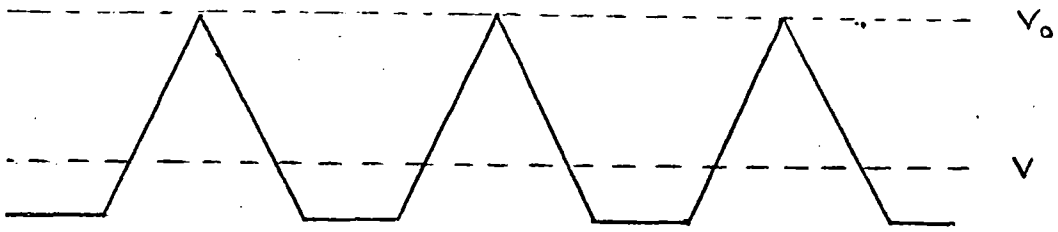

(b) Clipped signal : peak voltage V_c instead of true value V_o

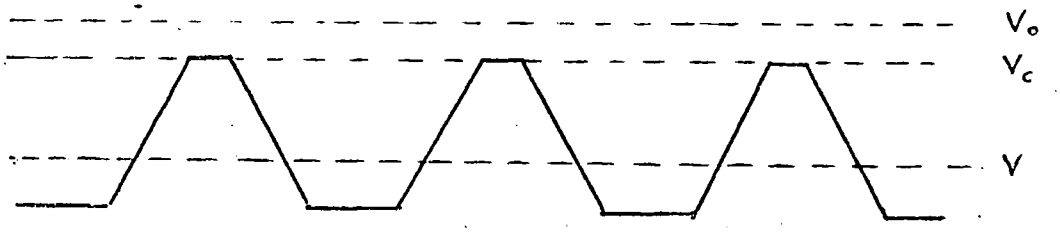

FIG 3.13 The rain switch circuit

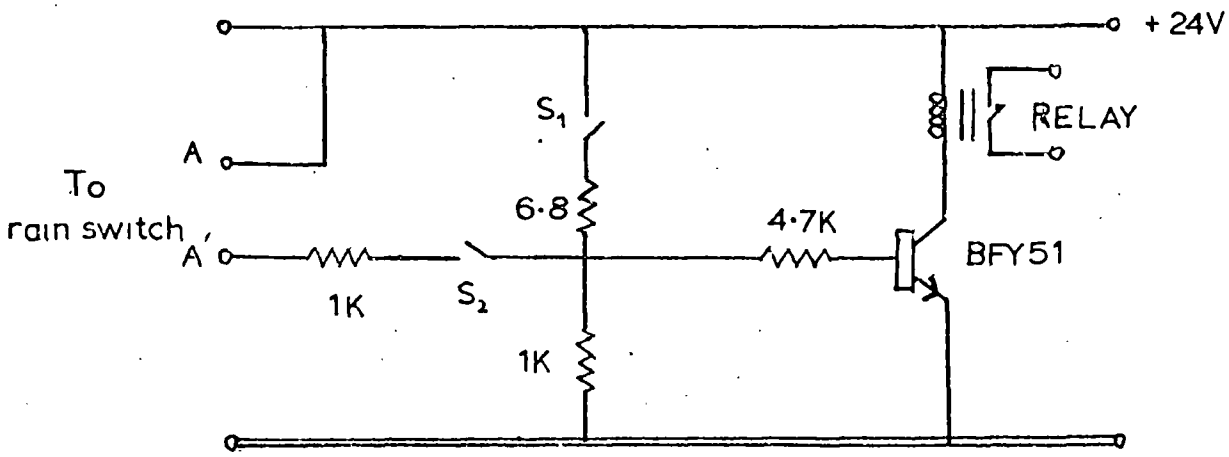

1. When S_1 closed , relay closed
2. S_2 closed, S_1 open : relay closed by rain switch shorting across A A'
3. S_1 S_2 open : relay open

It is possible to use the precipitation current collector for this purpose, as it gives an output only during periods of rain or snow. However any drift due to loss of insulation or shorting of the insulators would have also initiated recording, and there may have been uncertainty at low values of precipitation current. It was thus decided to use a separate device which did not rely on the collector output.

3.3.2 The rain switch design

Previous designs of rain switch or detector, such as that of COLLIN (1967), have used two exposed contacts separated by blotting paper, or similar material, which loses its insulation when damp. A current can then flow, triggering a relay or other device.

A switch was thus built, consisting of a lower metal plate, separated from an upper wire grid by a sheet of blotting paper. Connections were made to the plate and the wire grid, which passed sufficient current when the paper was dampened by rain to close a transistor-driven relay (Fig. 3.13). An improvement was soon made by replacing the wire grid and plate arrangement by a single sheet of "Veroboard", which consists of narrow copper strips fixed to an insulating backing sheet. The connections were made to two strips, separated by another two strips, which short when dampened by rain or snow. Placing a sheet of blotting paper over the strips prevented the rain switch drying during short breaks in precipitation. The constructed rain switch is shown in Fig. 3.14.

FIG. 3.14 The rain switch

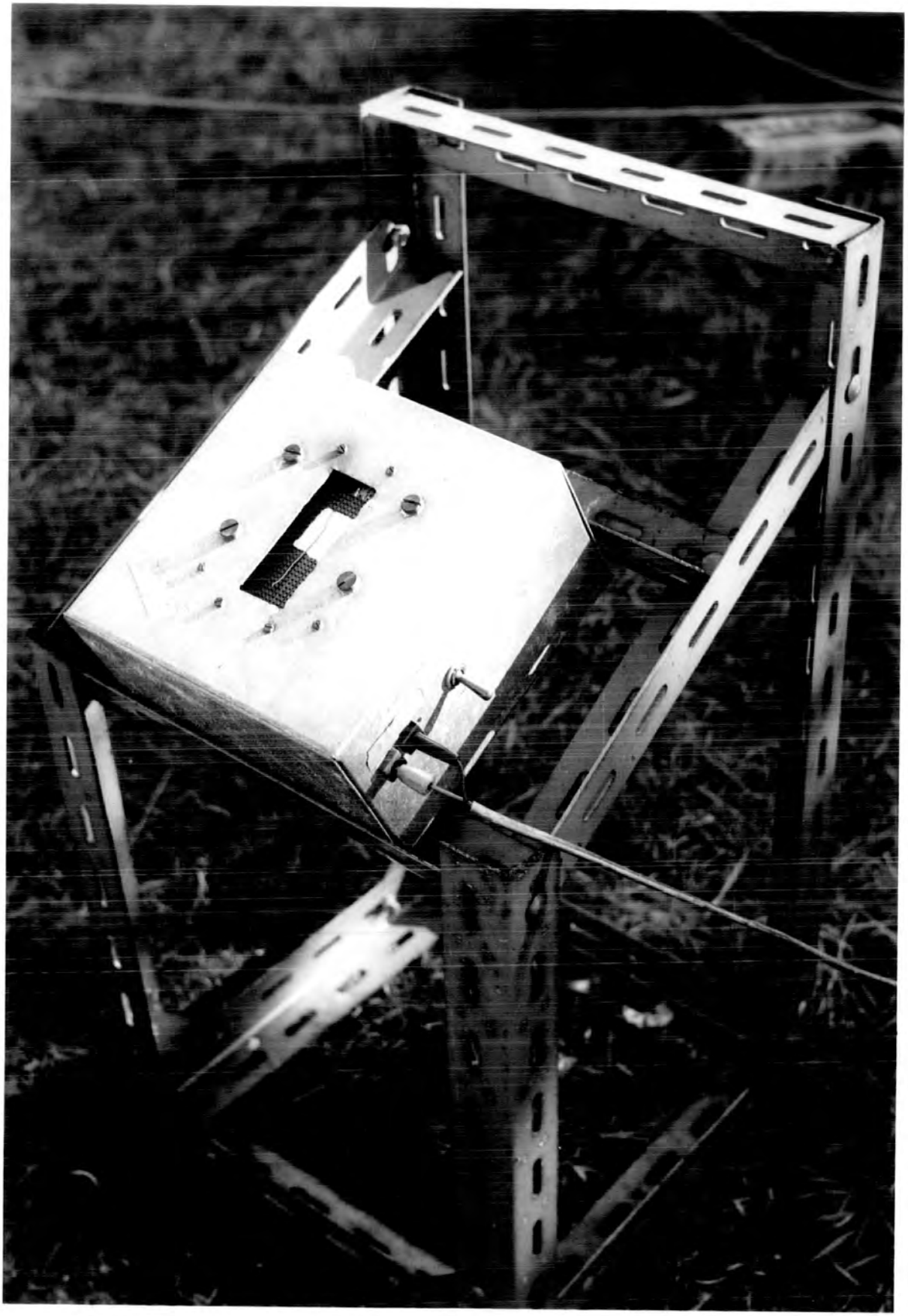

The relay was connected to the on-off switch of the chart recorder, switching it on when the relay closed, and switching it off again when the rain switch dried after the end of precipitation. When the chart recorder was replaced by the data handling system, the relay was used to start the channel selector and tape recorder (see Chapter 4).

3.3.3 Operation of the rain switch

The rain switch proved very useful, particularly when precipitation started or finished overnight. The relay would close a few minutes after the start of precipitation, and open again about an hour after the end of precipitation. Heating of the rain switch might have made it dry out faster, but it was felt that this could cause uncertainty in switching during light precipitation.

The switch also functioned during snow, but tended to freeze, causing the relay to remain closed. Heating may well have been useful in these conditions, and it is recommended that it is adopted in any future design of rain switch, especially for use in snow.

3.4 The recording site

3.4.1 The Observatory

Durham Observatory is located about 1 km S.W. of Durham (Ordnance Survey grid reference NZ 267424) on a slight hill, at a height of 120 m above sea level (Fig. 3.15). The precipitation current collector, field mills and rain switch were set up in a field adjoining the Observatory, shown in Figs. 3.16 and 3.17. The field slopes gently downwards away

FIG. 3.15 The recording site at Durham Observatory

FIG. 3.16 The instrumentation at Durham Observatory

FIG. 3.17 View from the top of the Observatory field

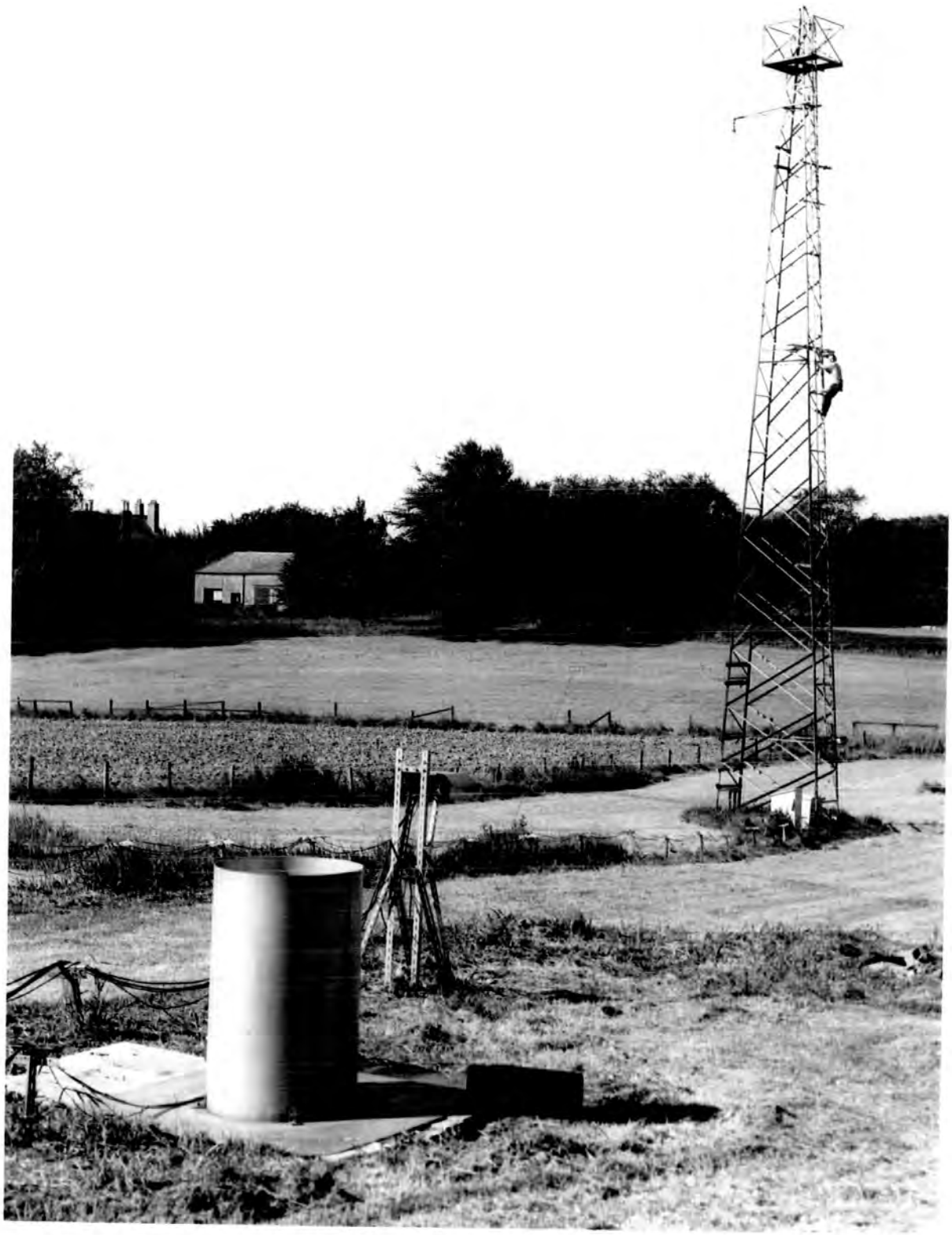

from the Observatory.

To avoid any distortion of the potential gradient at the ground by the 21 m mast, the ground field mill and precipitation current collector were located away from the mast, at a distance nearly equal to its height. They were also located away from the top of the field, where a hedge and some bushes could have caused shielding effects. The mast field mill was located at 10 m height, as the distortion of the potential gradient is considerably larger at higher points on the mast.

Meteorological readings are continually made at the Observatory, and these records were used to obtain the meteorological conditions during each recorded period of precipitation.

3.4.2 Power supplies at the recording site

The field mills and precipitation current collector required a.c. mains supplies, and in addition the field mills used a + 12V d.c. supply for the amplifiers. A power distribution board, housed in a weatherproof cabinet, was set up in the Observatory field, fed from the Observatory laboratory through an isolation transformer. A d.c. power supply, providing the + 12 V supply, was also run from the board to minimize any voltage drop along the connecting cables running to the field mills.

All connecting cables were carried about 1 ft. above the ground, to protect them against snow and dampness. An outside earth was provided by a copper earthing strip running from an earthing plate buried beneath the mast to the Observatory laboratory. All outside equipment and d.c. supplies

inside the laboratory were earthed to this strip to avoid earth loops.

3.5 The recording of the data

3.5.1 The chart recorder

Initially, a Honeywell-Brown multi-point potentiometric chart recorder was used to record the instrument outputs. This recorder has 16 channels, printed sequentially, each with its number for identification. Each instrument output, after reduction to the 0 to $\pm$ 2.5 mV recorder range, was connected to two channels. Thus the ground field mill was connected to channels 1 and 9, the mast field mill to channels 3 and 11, and the precipitation current collector to channels 5 and 13, the remaining channels being shorted to give a zero reading. Each instrument reading was printed every 15 s.

The on-off recorder switch was connected through the rain switch (Sec. 3.3), so that the recorder operated automatically during periods of precipitation.

3.5.2 The data handling system

To facilitate computer analysis of the recorded data, the chart recorder was subsequently replaced by the data handing system, fully described in the next chapter. The data was then recorded on magnetic tape for subsequent playback into a "Data Capture Unit", a device which prints the recorded data values on a paper roll. The values on the paper roll are then punched on to computer cards.

The system has an input range of -1 V to - 11 V, and so three d.c. amplifiers were constructed to amplify the field

mill detector and precipitation current outputs to this range.

3.5.3 The d.c. amplifiers

Two designs of d.c. amplifier were required, one to convert the 0 to ± 500 mV detector circuit output to the - 1 V to - 11 V range of the data handling system, and the other to similarly convert the 0 to ± 1 mA output from the Rank amplifier in the precipitation current collector.

The circuits, using Radiospares 709 integrated circuit operational amplifiers, are shown in Fig. 3.18. Two operational amplifiers are used in the second circuit, one to produce most of the voltage gain, and the second to bias the output to a negative polarity. The characteristics of the constructed circuits are shown in Fig. 3.19.

3.5.4 The final system

The instrumentation in its final form is shown in Fig. 4.13 . The right-hand instrument rack contains the field mill detector circuits and d.c. amplifiers, with the ± 15 V power supply beneath. The left-hand rack contains the rain switch relay circuit, the recording system of the data handling system and at the top the Farnell L30T power supply. The inputs to the recording system were monitored on a 4 channel 0 to 1 mA pen recorder, which was allowed to record continuously. This system was used for the entire series of recordings from January to June, 1972.

FIG. 3.18 D.C. Amplifier circuits

(a) Field mill detector d.c. amplifier

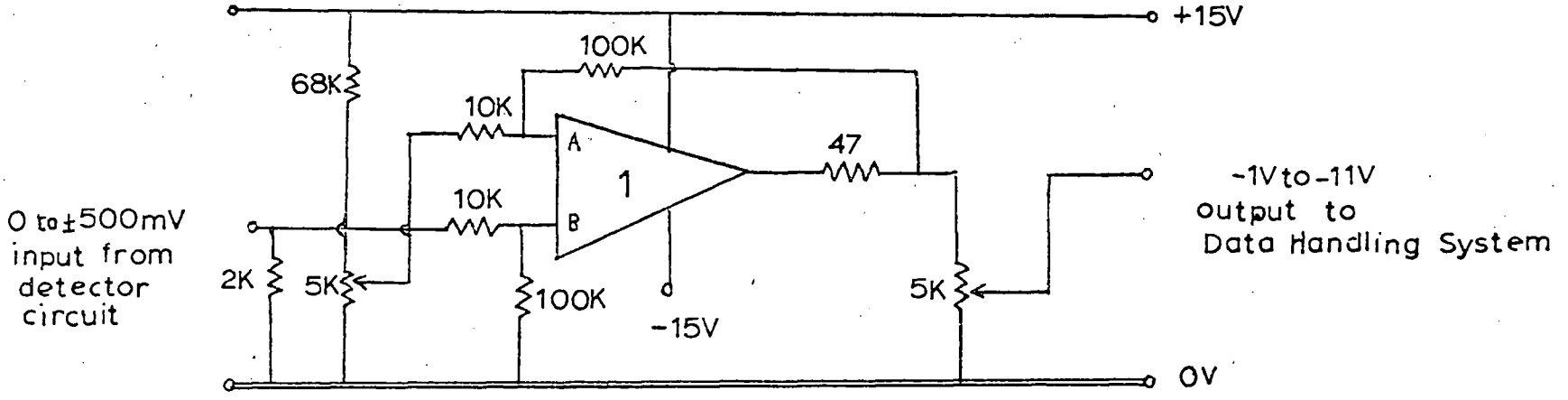

(b) Precipitation current collector d.c. amplifier

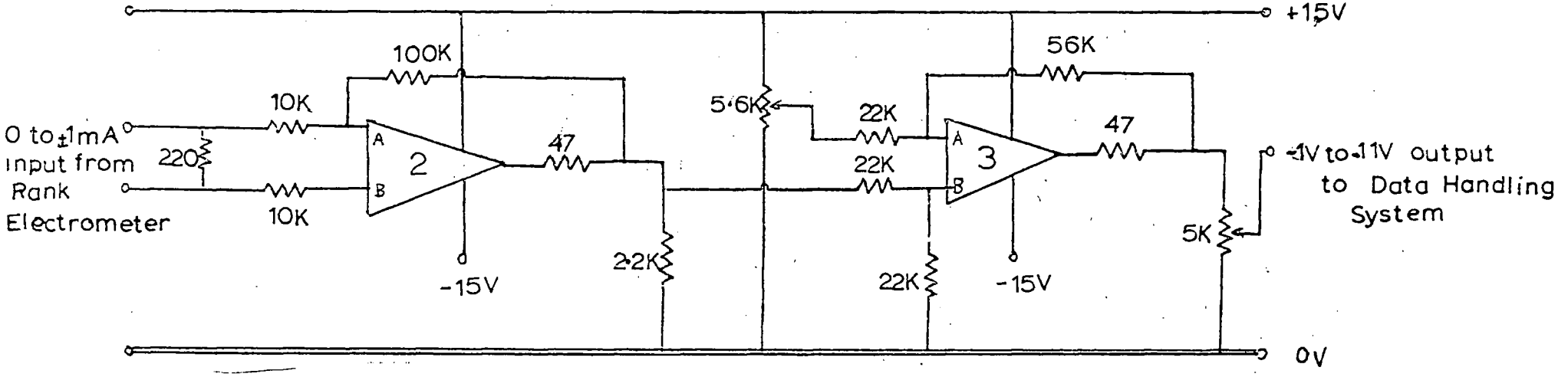

All i.c. amplifiers μA709 : gains of 10, 10 and 2·5 for respectively 1, 2, and 3.

FIG. 3.19 The d.c. amplifier characteristics

(a) Field mill detector amplifier

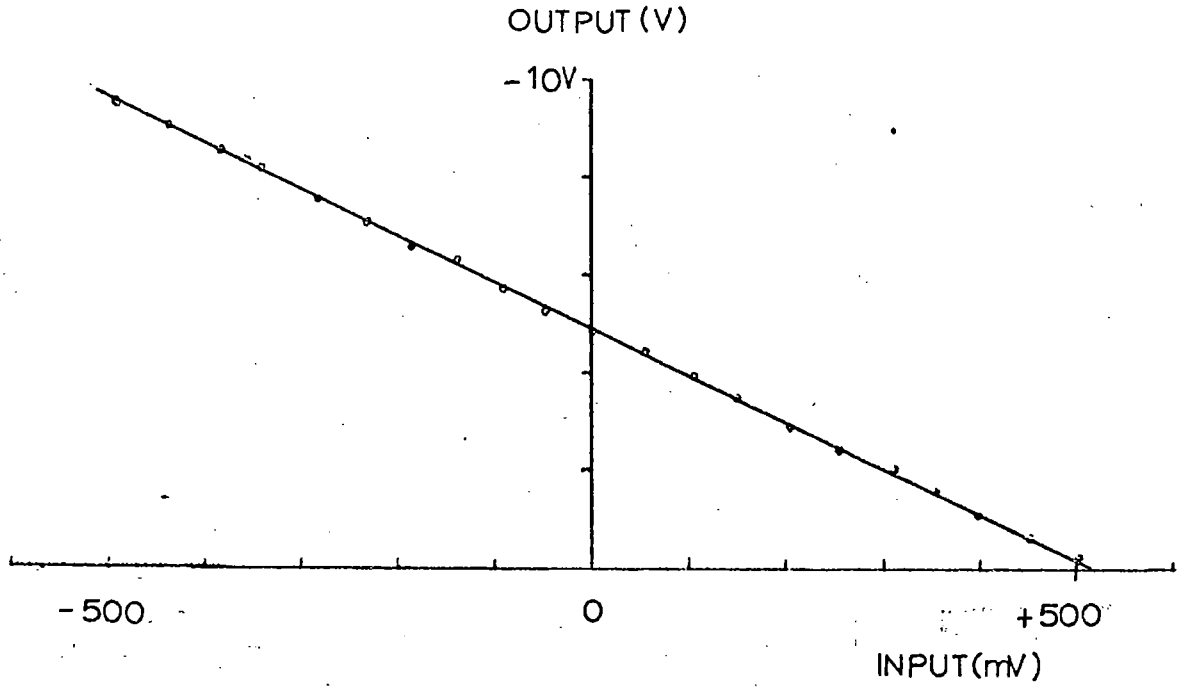

(b) Precipitation current collector amplifier

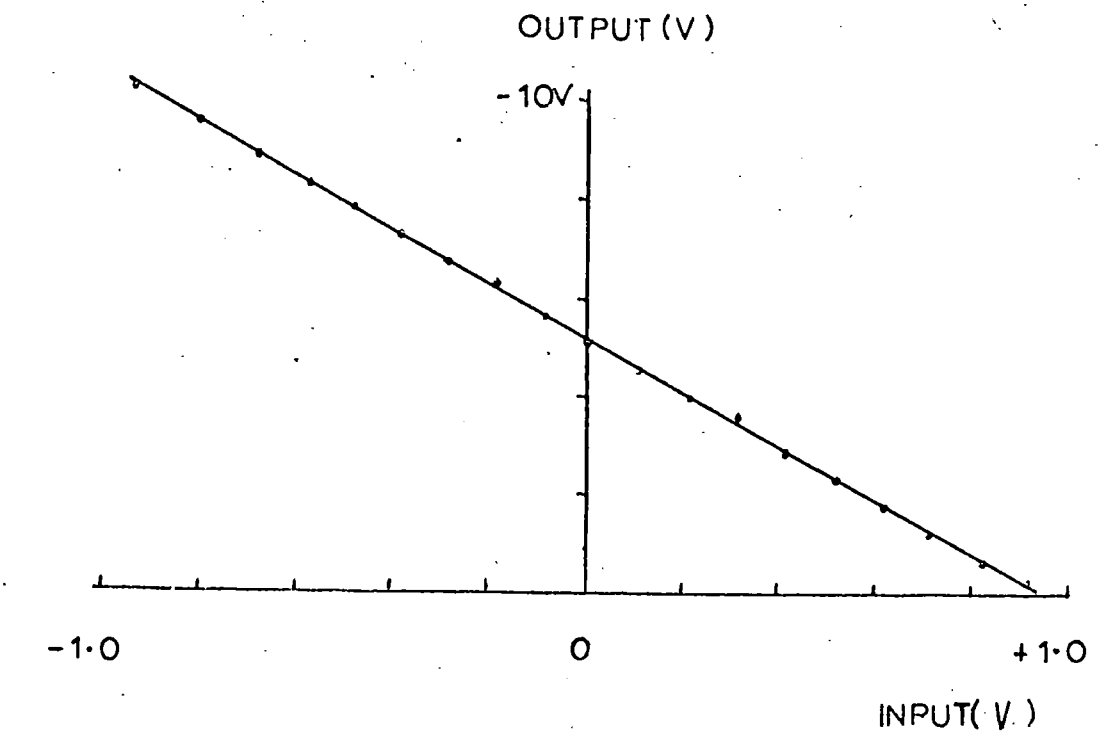

CHAPTER 4

The Data Handling System

4.1 The need for a data handling system

To perform the statistical analysis of the data recorded during periods of precipitation, it is essential to use a digital computer for the large amount of calculation involved. To do this, the recorded data must be presented in a form suitable for input to the computer. At Durham University, the computer(an IBM 360/67) uses punched cards as the usual form of input, and less commonly punched paper tape. A system was thus required to present the field mill and precipitation current collector outputs either as values punched on cards or paper tape, or in a form readily convertible to such.

These requirements would have been met by a data logging system, many types of which are available commercially. A data-logging system converts a number of analogue inputs from measuring instruments into an output of punched cards, punched paper tape or magnetic tape suitable for direct input to a computer, and can also give a printed record of the data values. Inquiries showed that such a system, even on the comparatively small scale needed for the author's requirements, was beyond the resources of the research group, and so alternative methods had to be considered.

4.2 The "D - Mac" chart reader

Initially, a chart recorder was used to record the field mill and precipitation current collector outputs. It soon became evident that reading the chart values by eye for subsequent punching on to cards would be tedious and time consuming, and so some form of chart reading device was necessary.

The Computer Unit at Durham possessed a "D - Mac" chart reader, a device which enables chart records, maps and diagrams to be produced as a series of values punched on paper tape. By tracing the chart record with a pen connected to the reader, the x and y co-ordinates of any pen position can be punched on the paper tape by pressing a trigger button. Thus by following the potential gradient and precipitation current records with the pen, their values in terms of the pen co-ordinates could be obtained on a punched paper tape.

This method still proved somewhat tedious, however, particularly with long records. Moreover, the "D - Mac" had been designed to interface with the previous computer at Durham, an Elliott 803, and so a considerable proportion of the overall computing time would have been needed to convert the paper tape data to a format suitable for the present computer. Also, the Computer Unit could not give an assurance that the "D - Mac" could be repaired if a serious fault occurred, and so this method of handling the data was not adopted.

4.3 The chosen system

At the same time as the author was considering various methods of data handling, a colleague, Mr. C.D. Jones, had a similar requirement for processing data from mobile equipment being used for outdoor turbulence measurements. His intention was to record the data on a portable magnetic tape recorder for playback at the laboratory in Durham and subsequent conversion to computer input. By recording the author's data also on magnetic tape, it seemed possible to use a common system of data recording and playback.

A Weyfringe "Data Capture Unit" was thus obtained for use in both playback systems. This device consists of a digital voltmeter with a printer, enabling the voltmeter readings to be automatically printed as a series of values on a paper roll. By using a suitable playback system to enable the magnetic tape to be replayed on to the Data Capture Unit, a printed record of the data values can be obtained. The data values on the paper roll can then be punched on to computer cards by the Punching Staff of the Computer Unit.

This system proved capable of producing the data as computer input with a minimum of intervention by the observer, as both recording and playback could be performed automatically once started. A chart recorder was, however, retained to provide an immediate visual record during recording, which enabled any faults or errors to be recognised before playback, together with any sections of tape containing data unsuitable for playback.

4.4 The recording system

4.4.1 Introduction

This system was adapted from that designed by Mr. C.D. Jones for his portable equipment, differing mainly in the detail design of circuits and the use of a single polarity power supply. The author is indebted to Mr. C.D. Jones for the use of his original design.

A schematic outline of the recording system is given in Fig. 4.1. The inputs from the measuring instruments are switched successively by the channel selector to the voltage-to-frequency converter. This conversion is necessary as the tape recorder can record only a.c. signals, and so the d.c. signals from the measuring instruments must be converted to enable them to be recorded.

A "blanking pulse" is necessary to separate the signals from adjacent channels; it provides a triggering pulse for the printer when the tape is replayed into the Data Capture Unit. The input to the tape recorder is thus shorted for 0.5 s by the blanking unit during the switch from one channel to the next. To ensure that the blanking pulse remains synchronised with the channel switching, the blanking unit is driven by the channel selector drive.

FIG. 4.1 The recording system

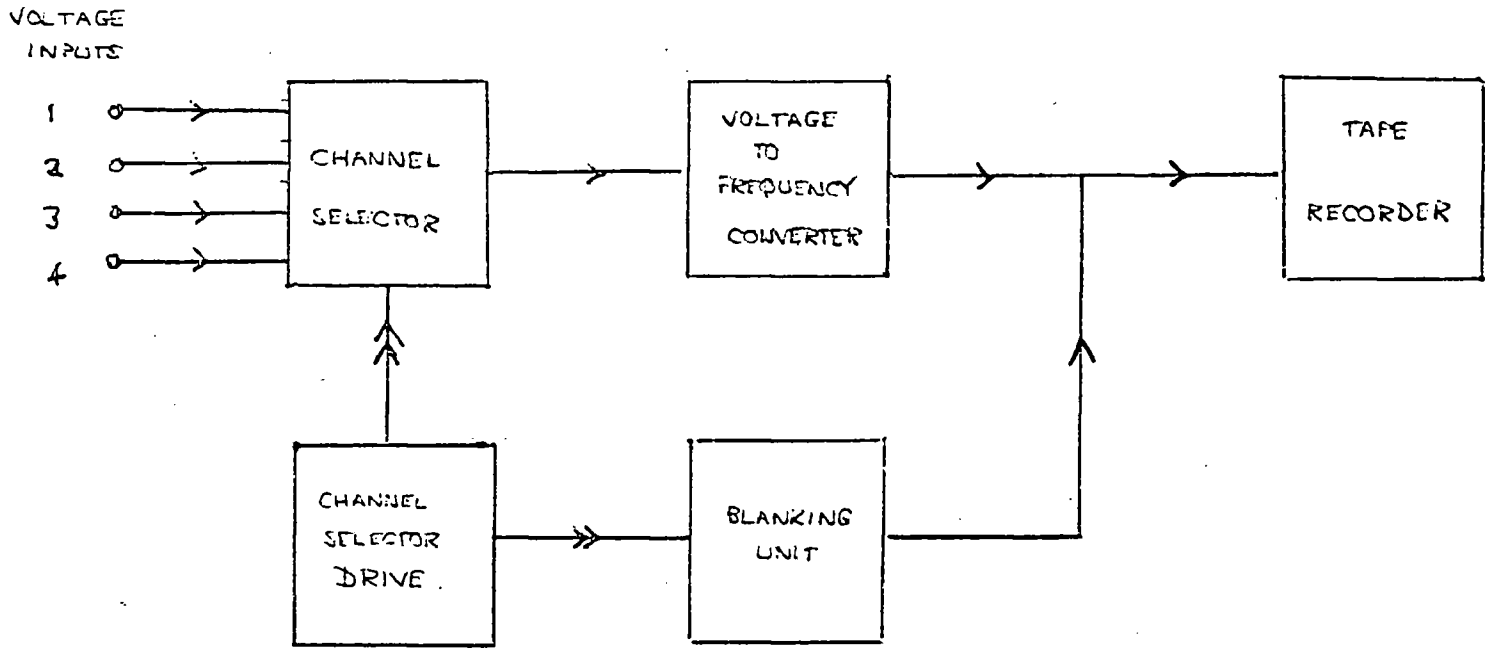

	INPUTS	VOLTAGE RANGE	FREQUENCY RANGE
1	GROUND POTENTIAL GRADIENT	-1V to -11V	100 to 1900 Hz
2	MAST POTENTIAL GRADIENT		
3	PRECIPITATION CURRENT		
4	REFERENCE VOLTAGE	-6V	1000 Hz

4.4.2 The channel selection

The channel selection is performed by a 12-way uniselector, triggered every 7.5 s by the channel selector drive. Each input channel is connected to 3 inputs of the uniselector, making it in effect a 4-way selector. The channel selector drive circuit, shown in Fig. 4.2, consists of an astable multivibrator of period 7.5 s, and a monostable multivibrator of period 50 ms. The output of the astable circuit is differentiated to provide a trigger pulse for the monostable circuit every 7.5 s; this causes the reed switch S_1 to close for 50 ms which in turn triggers the uniselector to advance to the next channel. Each input channel is thus sampled for 7.5 s every 30 s, during which it is connected through the voltage-to-frequency converter to the tape recorder.

The astable multivibrator is also used to provide a trigger pulse for the blanking unit, described in Sec.4.4.4.

4.4.3 The voltage-to-frequency converter

The circuit design of MOLYNEUX and DE'SA (1963) was adopted for this purpose, as it gives a good linear relationship between input voltage and output frequency over a wide voltage range. The circuit is shown in Fig. 4.3, and the characteristic of the constructed circuit in Fig. 4.4.

As can be seen from the characteristic a minimum input of about - 0.5 V is necessary for the circuit to fire, and so an input range of - 1.0 V to - 11.0 V was chosen, giving

FIG. 4.2 The channel selector drive

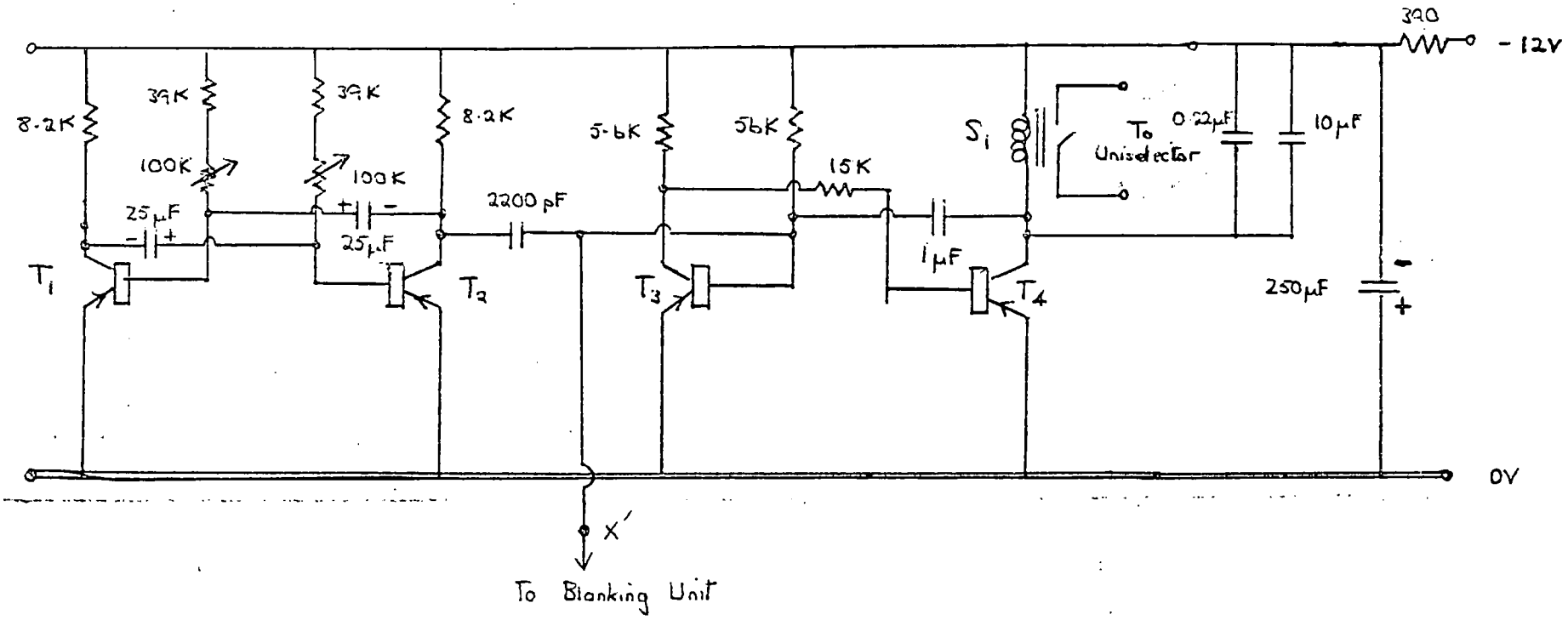

ASTABLE MULTIVIBRATOR

Time constant = 7·5s

MONOSTABLE MULTIVIBRATOR 1

Time constant = 50 ms

Transistors T_1, T_2 type ZTX501

T_3, T_4 type ACY40

FIG. 4.3 The voltage-to-frequency converter

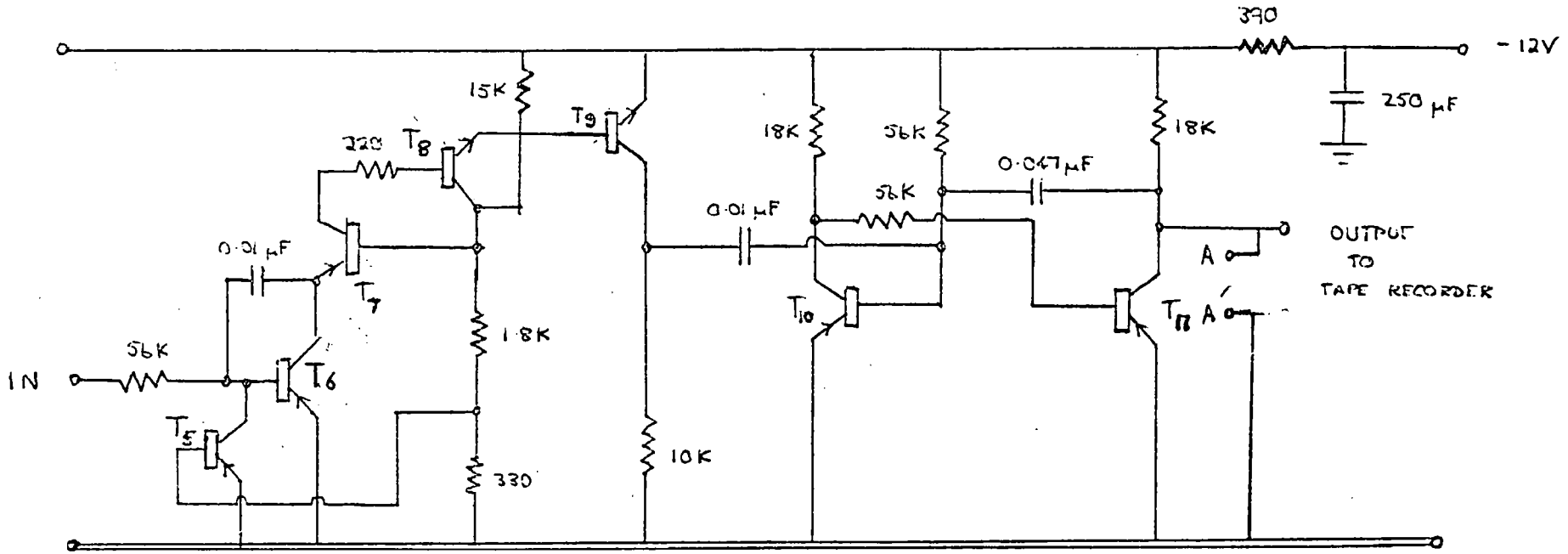

VOLTAGE TO FREQUENCY CONVERTER

MONOSTABLE MULTIVIBRATOR 2

Time constant = 0·4ms

Transistors	T_5, T_7	type	OC200
	T_6	type	2S303
	T_8, T_9	type	2S701
	T_{10}, T_{11}	type	ZTX501

FIG. 4.4 Characteristic of the voltage-to-frequency circuit

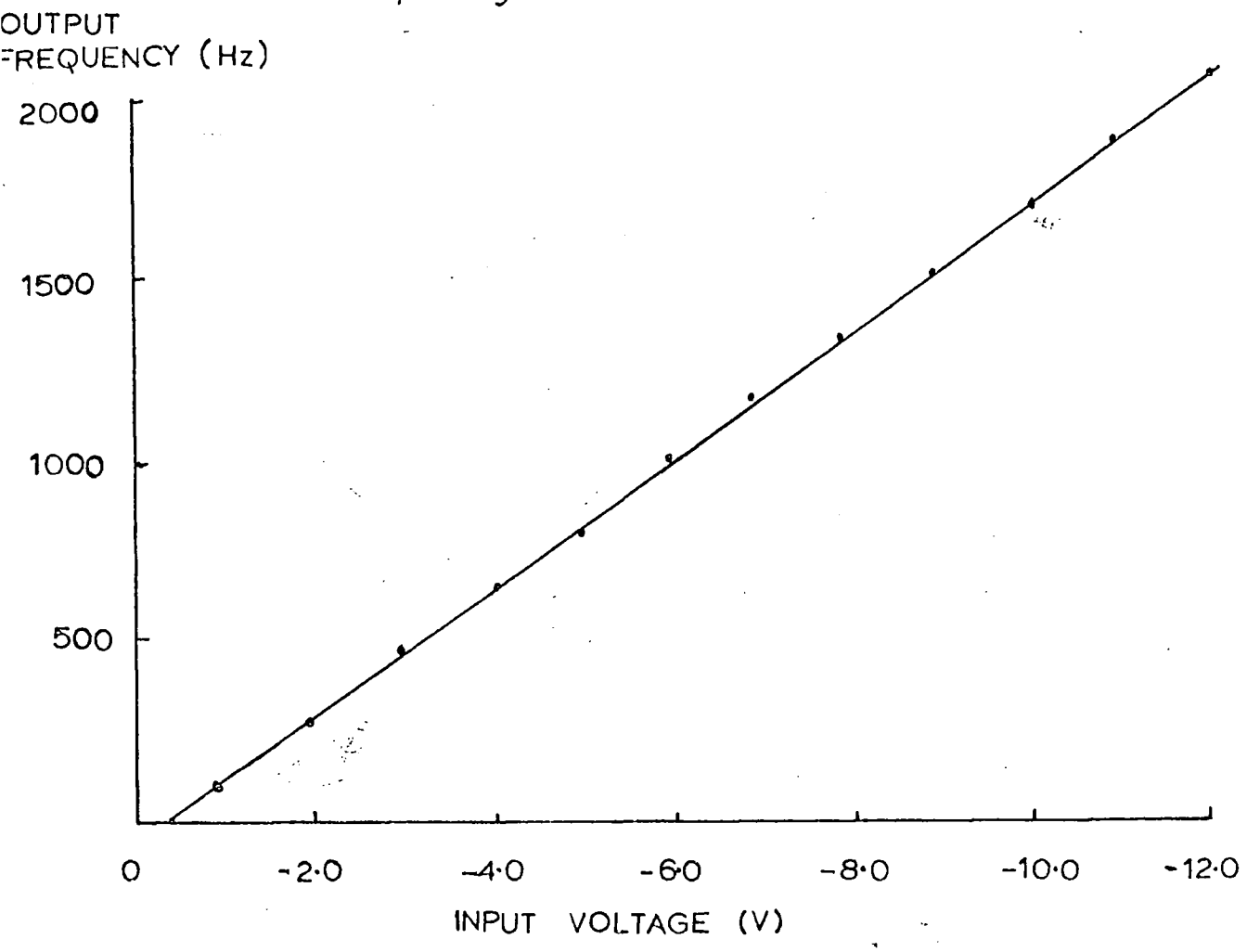

FIG. 4.5 (a) The voltage-to-frequency circuit output

(b) The monostable circuit output

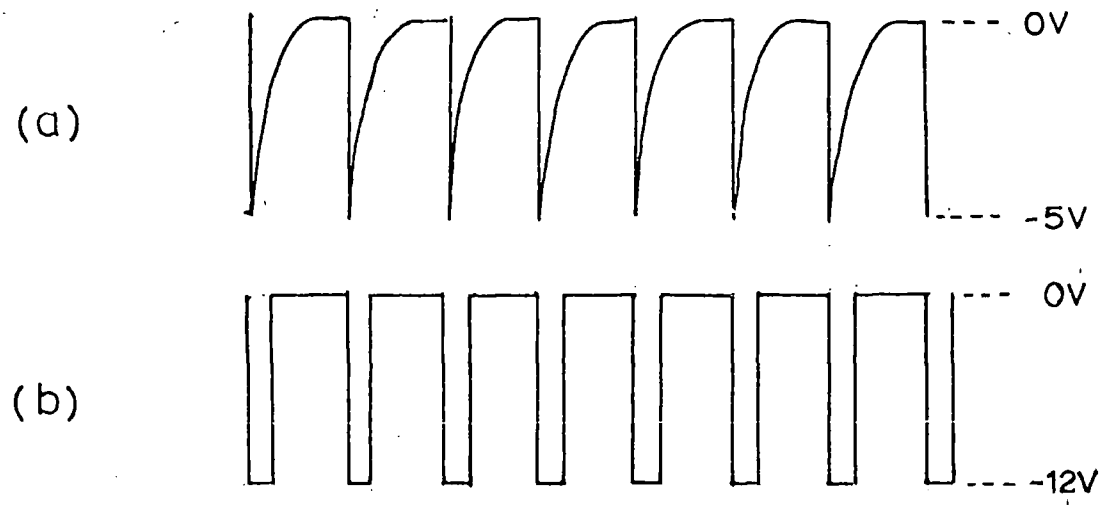

an output frequency range of 100 Hz to 1900 Hz. The d.c. amplifiers used to amplify the field mill and precipitation current collector outputs (Sec. 3.5.3) were consequently biased to give - 6.0 V output for a zero input signal, and so producing a 1 kHz signal for recording. A negative potential gradient, for instance, increases the d.c. amplifier output from - 6.0 V, while a positive potential gradient decreases the output to below - 6.0 V. Hence the higher frequency signals on the tape recorder correspond to negative potential gradients or precipitation currents, and the lower frequencies to positive inputs.

The voltage-to-frequency converter output consists of a series of "spikes", shown in Fig. 4.5. This form of output proved unsuitable for recording due to the frequency response of the tape recorder at the low running speeds used, which caused considerable attenuation of the higher frequency signals. The converter output is thus passed through a monostable circuit to convert the spikes to square pulses, which proved far more suitable for recording. This improvement in the frequency response of the recorder can be seen from Fig. 4.6.

4.4.4 The blanking unit

The blanking pulse, described in Sec. 4.4.1, is produced by a monostable circuit, triggered by the astable circuit of the channel selector drive. The monostable circuit, shown in Fig. 4.7, has a period of 0.5 s, during

FIG. 4.6 The playback signal

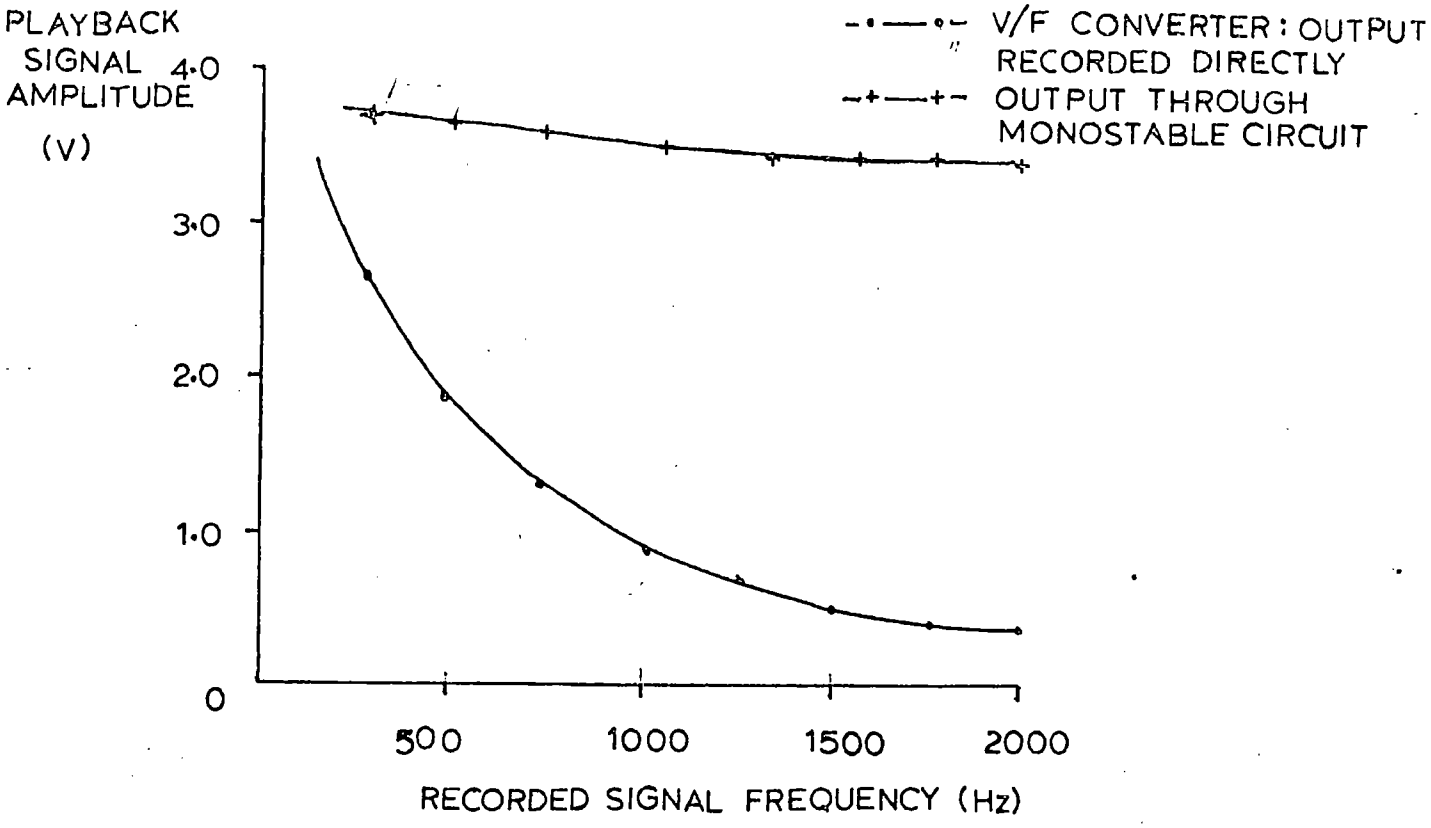

FIG. 4.7 The Blanking unit

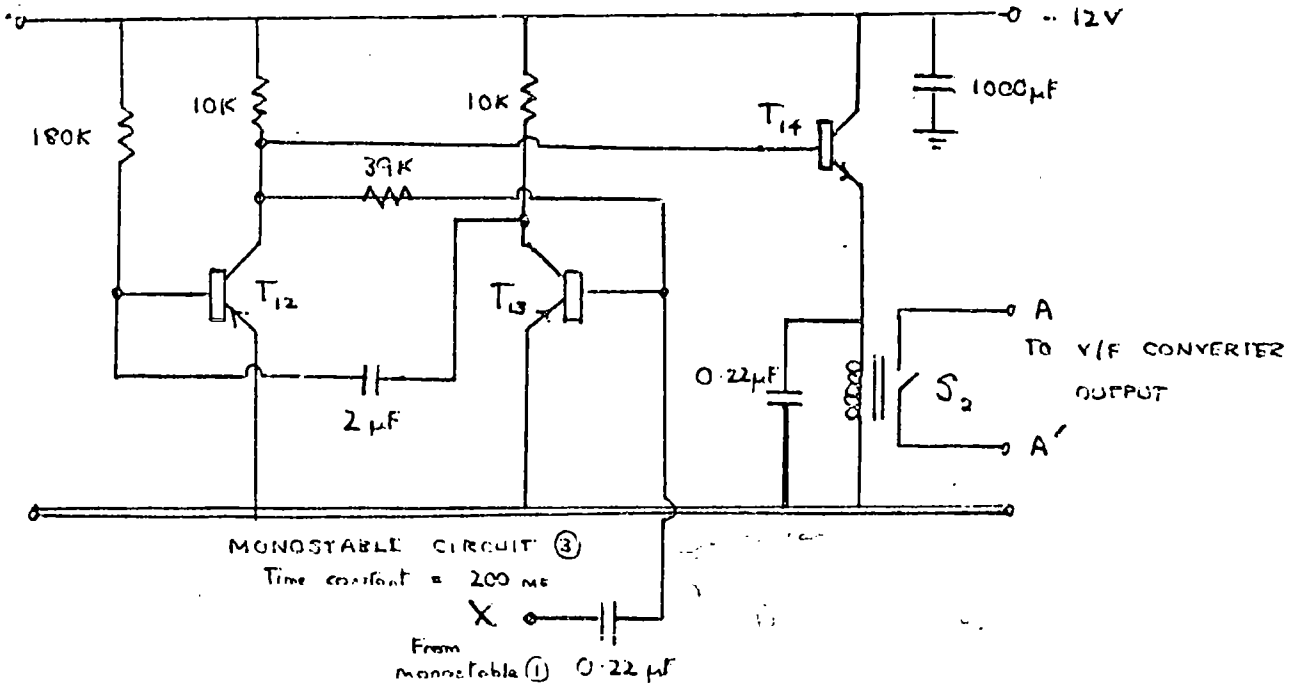

Transistors T_{12}, T_{13} type ZTX501

T_{14} type AC128

which the reed switch S_2 closes, shorting out the input to the tape recorder. A blank pulse of 0.5 s duration is thus produced on the tape each time the input channel switches.

4.5 The tape recorder

A Philips model 4308 tape recorder was used for recording the data. As it was expected that recording would sometimes be necessary overnight, a recording time of about 12 hours per tape was thought necessary. The lowest running speed of the tape recorder, $1\,^7/_8$ i.p.s. (4.75 cms^{-1}) gave $4\,^1/_4$ hours running time with a 7 inch spool of double-play tape, so the recorder was altered to run at just less than $^{15}/_{16}$ i.p.s. (2 cms^{-1}) by adjusting its pulley drive system. This gave a running time of 9 hours for double play tape; subsequently some triple-play tape was obtained, which gave the required running time of 12 hours.

As mentioned in Sec. 4.4.3, reducing the running speed caused attenuation of the higher frequency signals if the voltage-to-frequency converter output was recorded directly. For example, a 100 Hz signal had an amplitude of 3.5 V when played back, while a 1.8 kHz signal had an amplitude of only 0.5 V, which prevented correct operation of the playback system. Changing the output of the converter to square pulses successfully overcame this problem.

The microphone input to the tape recorder was used to record spoken comments at the start or end of the tape, and for identification of the tape. The recording and

playback could be monitored through the tape recorder loudspeaker if required.

4.6 The playback system

4.6.1 Introduction

This system, outlined in Fig. 4.8, enables the recorded tape to be replayed into the Data Capture Unit, which prints the recorded data values on a paper roll. The recorded series of frequency modulated signals from successive input channels is reconverted to a series of analogue voltage signals by the frequency-to-voltage converter, having first passed the signal through the pulse shaper to ensure that all the frequency pulses are identical square pulses. The converter provides two outputs, a 0 to 200 mV output to the digital voltmeter of the Data Capture Unit, and a 0 to 5 V output to the print trigger unit.

4.6.2 The pulse shaper

While the difficulty of the poor frequency response of the tape recorder had been largely overcome, the output frequency pulses still tended to be rounded and slightly attentuated at the higher frequencies. To restore the square shape of the pulses a Schmitt trigger circuit was used, producing 4 V amplitude square pulses throughout the frequency range of recording. The circuit is shown in figure 4.9.

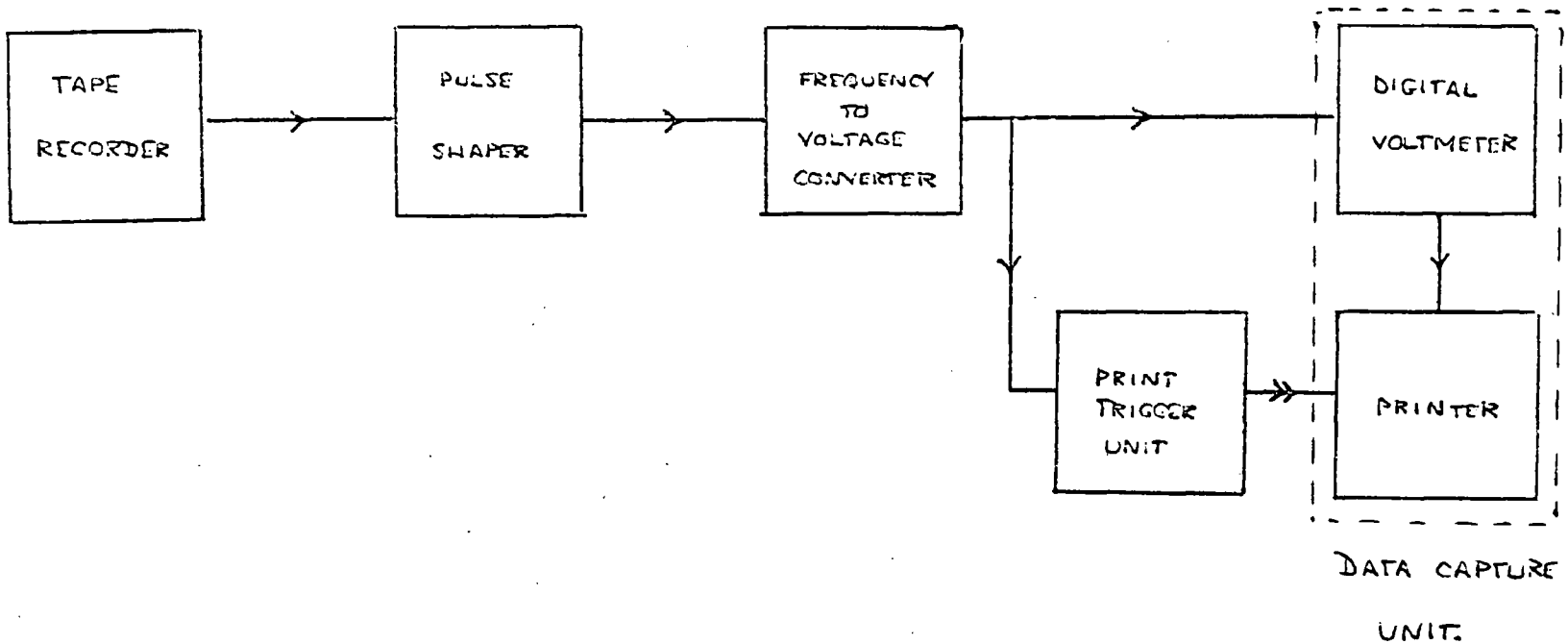
TAPE RECORDER
PULSE SHAPER
FREQUENCY TO VOLTAGE CONVERTER
DIGITAL VOLTMETER
PRINT TRIGGER UNIT
PRINTER
DATA CAPTURE UNIT.
PATH OF PLAYBACK SIGNAL
PATH OF CONTROL PULSE

FIG. 4.9 The pulse shaper

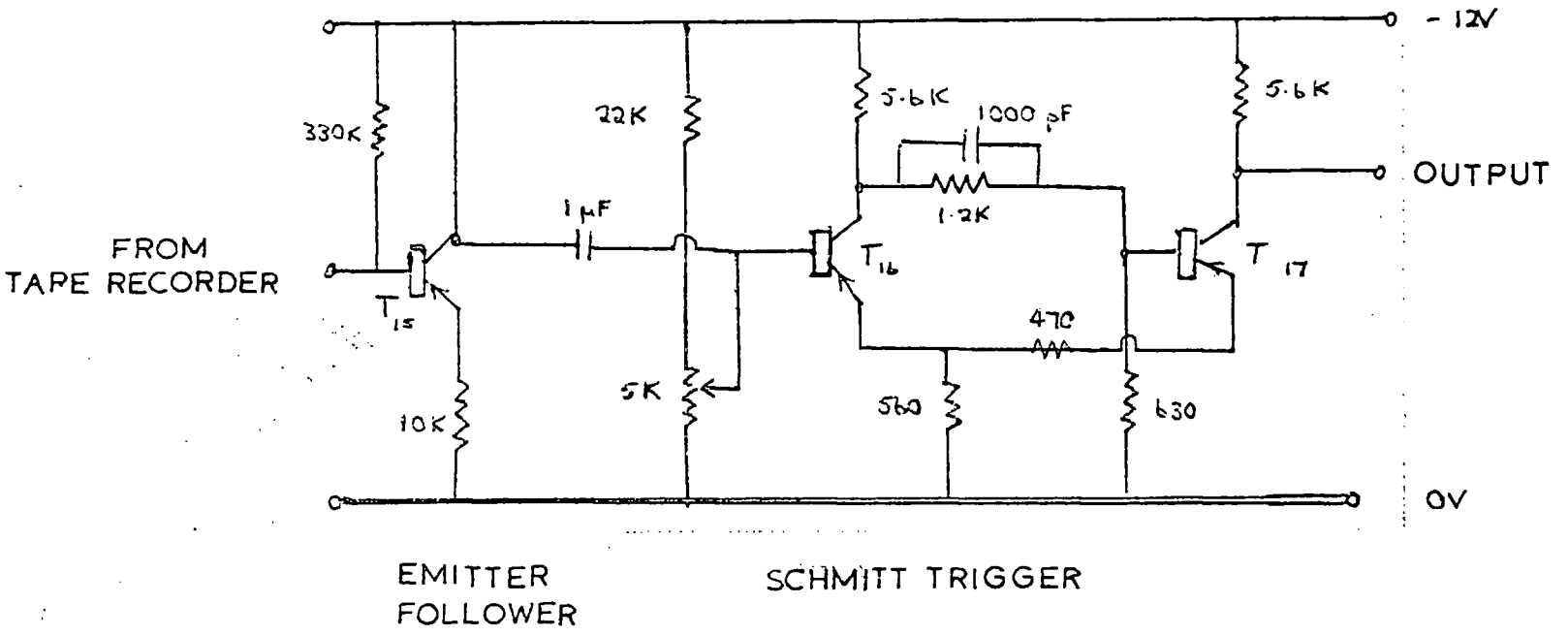

Transistors type ZTX501

4.6.3 The frequency-to-voltage converter

This circuit (Fig.4.10) consists of a monostable multivibrator and an integrating circuit, buffered by an emitter follower. As the pulse length of the Schmitt trigger output could vary slightly at differing frequencies, the monostable circuit ensures that all the pulses have a length of 0.5 ms. These pulses, when passed into the integrating network R_I, C_I, will then produce a voltage output dependent solely on the pulse repetition frequency.

The output from the converter is thus a series of d.c. voltages proportional to the original recorded signals from the input channels, separated by 0.5 s blanking pulses. The full output is used as input to the print trigger unit (Sec. 4.6.4), while a 0 to 200 mV output is taken for display on the digital voltmeter of the Data Capture Unit; the value of this voltage is printed out.

4.6.4 The print trigger unit

The print trigger unit (Fig. 4.11) produces the trigger pulse needed for automatic printing of the digital voltmeter reading. The voltage output from the frequency-to-voltage converter is first differentiated by the network R_D, C_D. The next stage is a reverse-biassed emitter follower circuit, which only passes the required trigger pulse, eliminating any spurious pulses or noise of lesser amplitude.

The trigger pulse is then amplified to provide an input suitable for the first monostable circuit. This

FIG. 4.10 The frequency-to-voltage converter

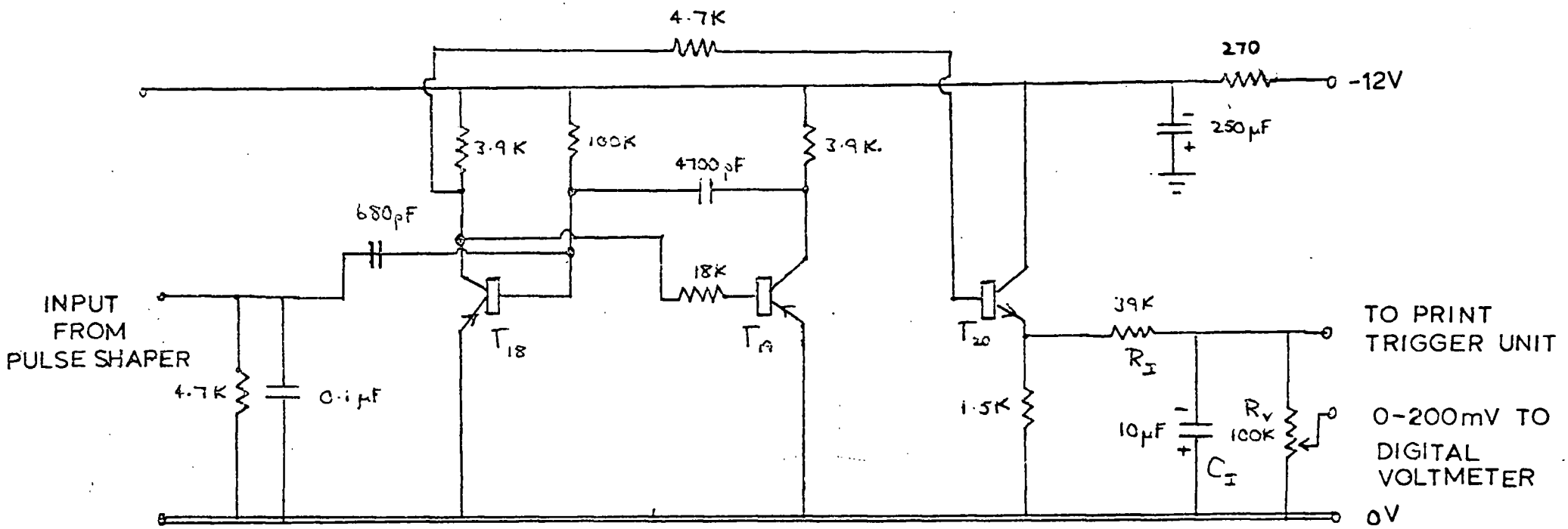

MONOSTABLE CIRCUIT 4
Time constant = 0·5ms

EMITTER FOLLOWER

INTEGRATING CIRCUIT

Transistors type ZTX501

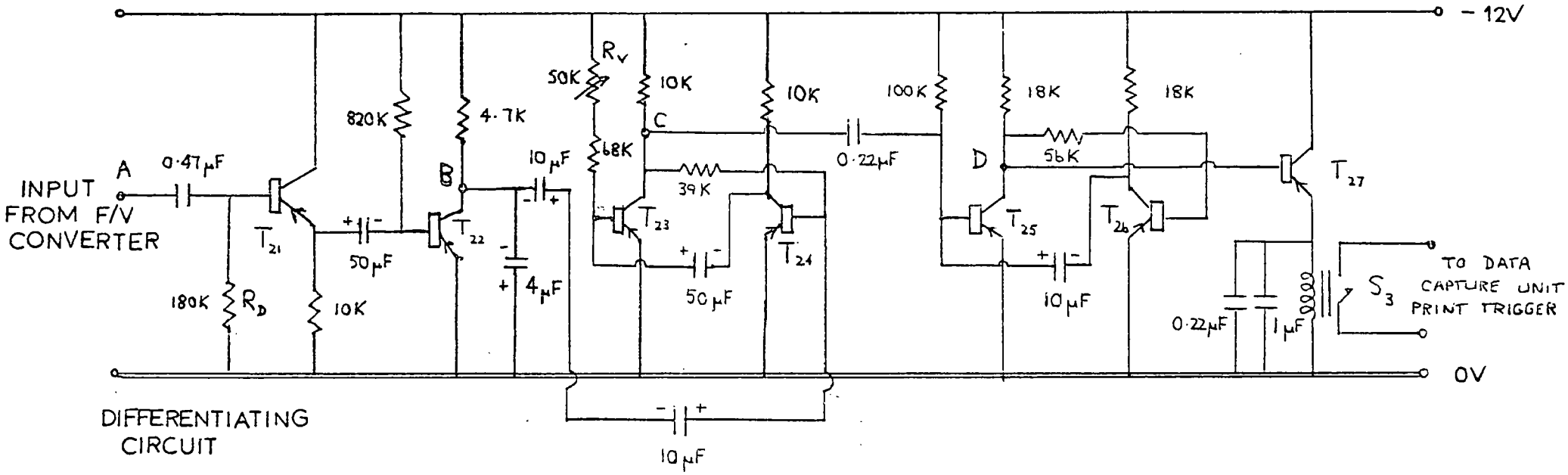

Transistors T_{21} , T_{27} ACY40
T_{22} to T_{26} ZTX501

Waveforms at points A, B, C, D shown in Fig. 4 12

circuit acts as a 5 s time delay, so that the printer is triggered only when the voltage on the digital voltmeter has reached a steady value between blanking pulses. This is achieved by taking the output from the collector of transistor T_{23}, where the output appears only after the time constant of the circuit has elapsed. The second monostable circuit, of period 1 s, is then triggered, closing reed switch S_3 for this time interval, which causes the current digital voltmeter reading to be printed by the Data Capture Unit.

The triggering process is illustrated in Fig. 4.12, where waveforms at various points in the circuit are shown. The method adopted has the advantage that the printing can be triggered from the same track on the tape on which the data values are recorded.

4.7 Construction of the data handling system

The electronic circuitry of the recording and playback units was constructed on "Veroboard", a circuit board consisting of copper strips fixed to an insulating backing board. The circuit boards were constructed as plug-in boards mounted on 19-inch aluminium panels suitable for standard instrument racks. Any alteration or replacement of components was then easily performed by removing the appropriate board. Power supplies for the system were provided by a Farnell L30T twin power unit for the recording system, which was located at the Observatory, and a single L30 power unit for the playback system, located at the Atmospheric Physics laboratory at Durham.

FIG. 4.12 Print trigger unit waveforms

(time intervals not to scale)

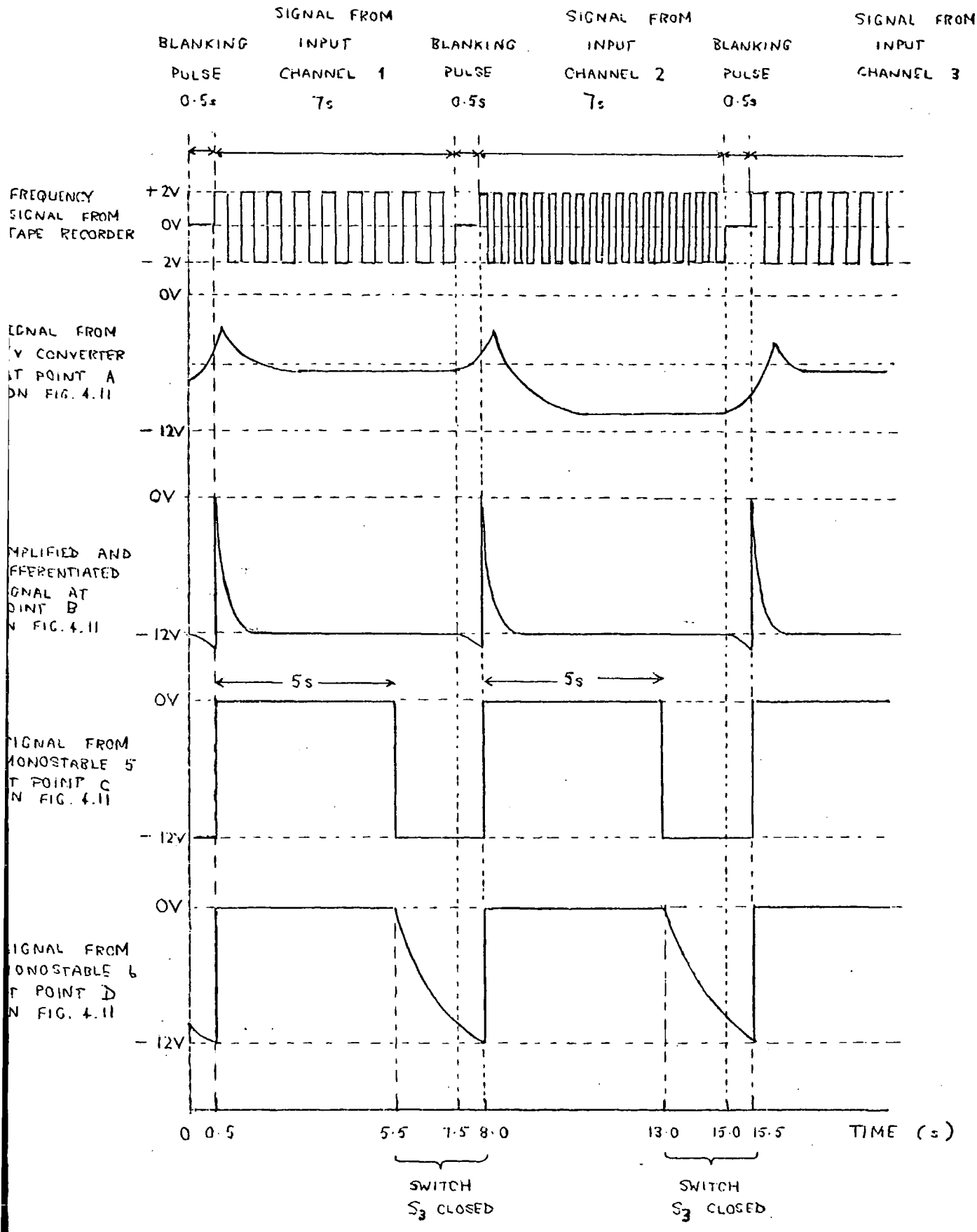

The constructed recording system is shown in Fig. 4.13, and the playback system in Fig. 4.14.

4.8 Operation of the system

The recording unit at the Observatory was arranged to switch on automatically when precipitation started by having the uniselector power supply and the tape recorder mains supply connected through a relay operated by the rain switch (described in Chapter 3). When a period of precipitation was expected, the tape recorder would be set, the recording unit switched on and tested, and the Uniselector power supply and tape recorder mains supply then connected through the rain switch relay. When precipitation started, the relay would close, starting the uniselector and tape recorder. When the precipitation had stopped, and the rain switch dried, then the relay would open, and the recording stop. The system could also be switched on or off manually if required.

To replay a tape recording, the relevant tape was taken with the tape recorder to the laboratory in Durham for replay into the Data Capture Unit. The paper roll containing the printed data values, after checking for any printing errors or missing values, was then taken to the Computer Unit for punching on to cards.

The overall performance of the system proved quite adequate, as can be seen from the linear relationship between the input voltage and the digital voltmeter reading shown in Fig. 4.15. The main problem to arise was an uncertainty in the printer triggering during replay

FIG. 4.13 The recording equipment

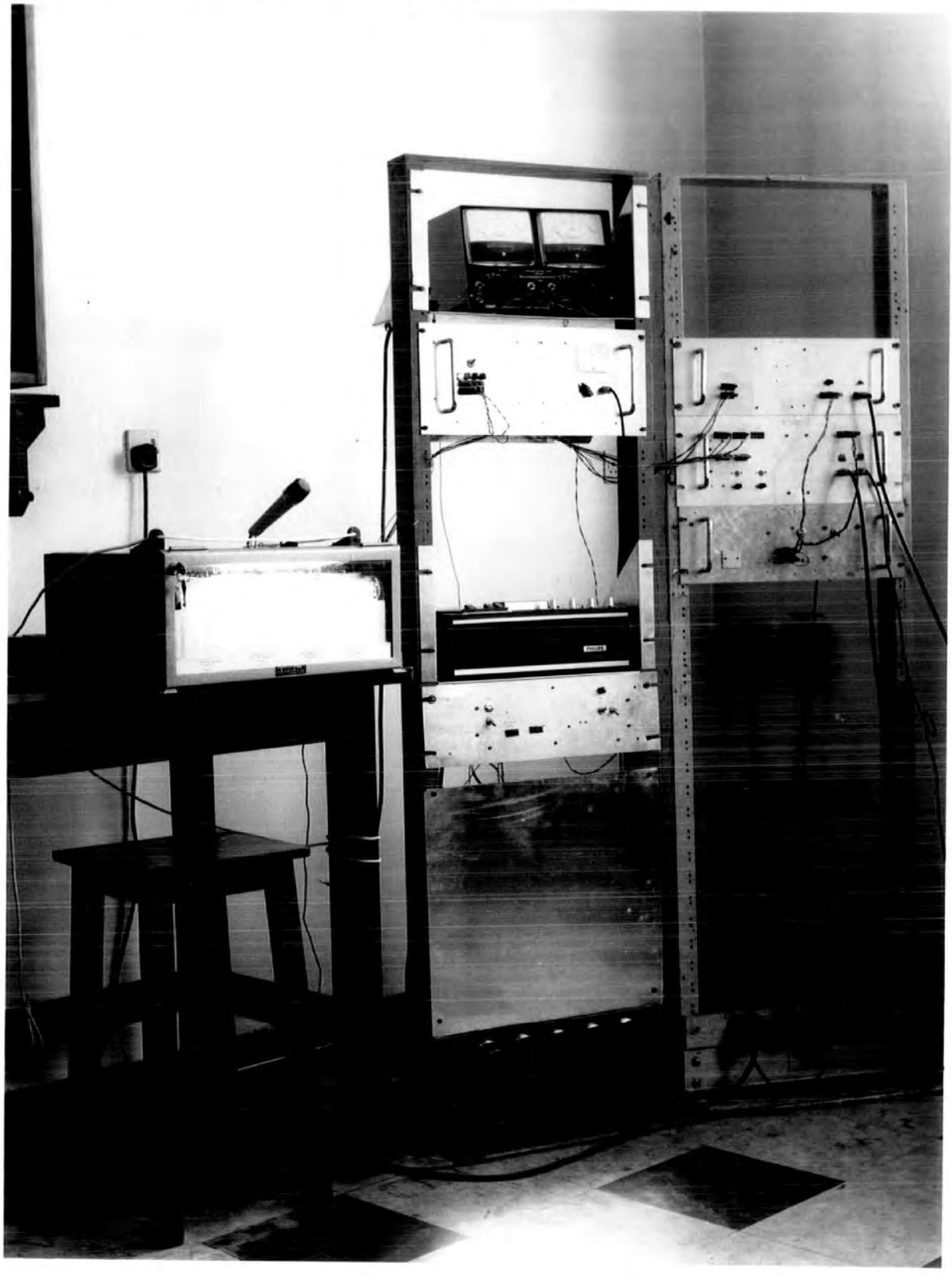

FIG. 4.14 The playback system

FIG. 4.15 The recording system transfer characteristics

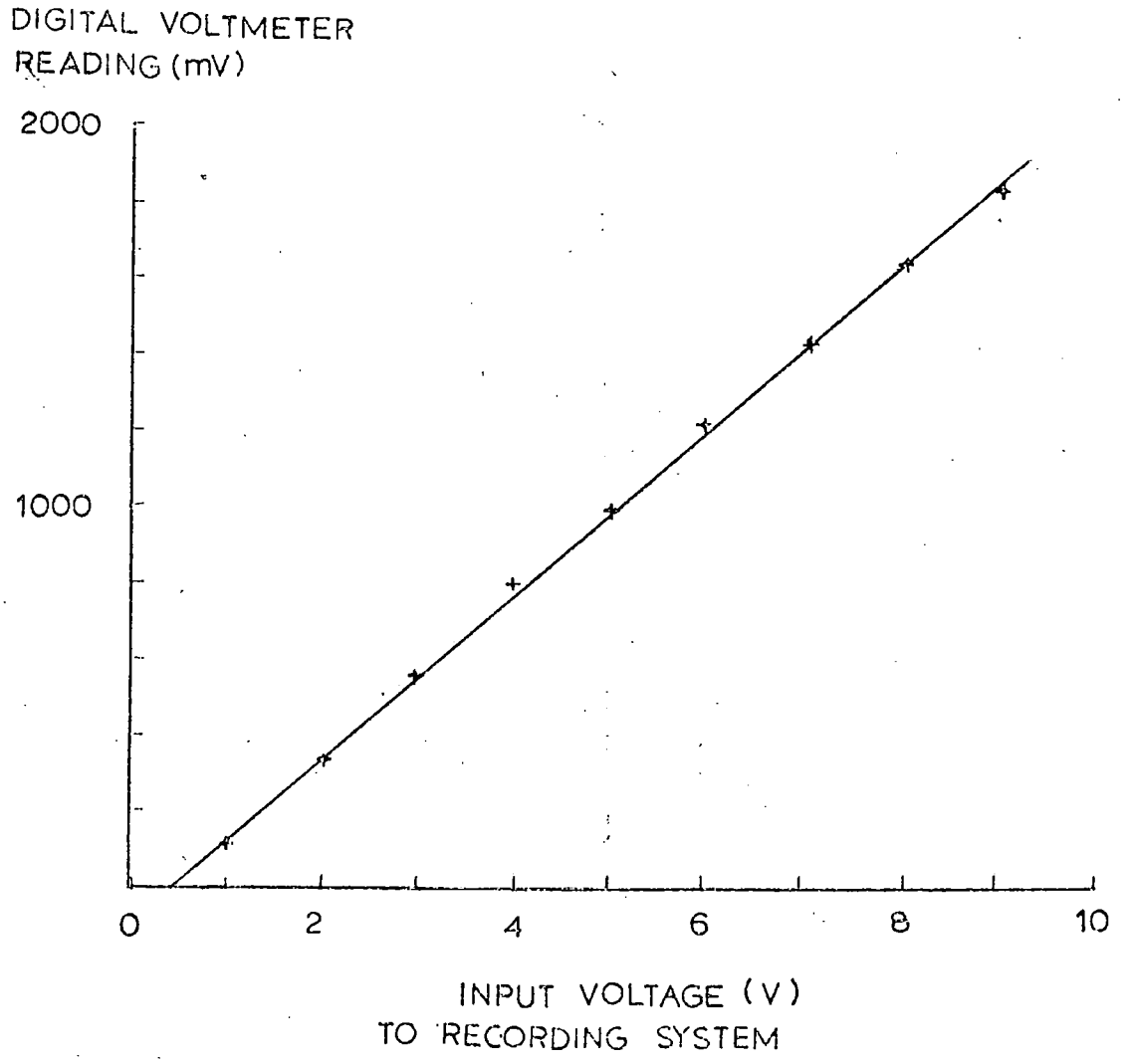

of very high or very low voltage values. High values, producing digital voltmeter readings close or equal to the 2.000 mV full scale reading, sometimes resulted in premature triggering of the printer, with a false low value being printed. Very low voltage values failed to fire the voltage-to-frequency converter, resulting in a blank signal for that channel, and also occasionally produced uncertainties in triggering. Such points could be noticed on the printout, and any missing or incorrect values corrected before the printed roll was taken for punching on to cards.

A reference voltage was recorded on one channel to detect any fluctuation in the tape speed, during either recording or playback, which would affect the frequency signal replayed from the tape recorder, and consequently the calibration of the system. If a noticeable fluctuation had occurred (the greatest observed was 5%), the printed voltage values were suitably corrected by the computer during the analysis of the data.

It was found convenient to open-circuit one channel of the uniselector, causing every twelfth channel recorded on the tape to be blank. This enabled any point on the tape to be located easily, say, for correction of the printout, by noting the location of the preceding blank channel on the indicator on the tape recorder which metered the running of the tape. The "blanked" channel was chosen as one of the reference voltage channels, so that no precipitation current or potential gradient values were lost.

The calibration of the system was checked at intervals by recording and replaying a series of input voltages covering the - 1 V to - 11 V range. No noticeable drift was detected during the 9 months the system was in use.

4.9 Suggestions for future use

The Data Handling System proved as versatile as had been hoped, fulfilling the requirements of both the author and his colleague, Mr. C.D. Jones. Its main application in the future will most likely be for outdoor recording, and so the use of integrated circuits would be advantageous for reducing the physical size and the power requirements. Several designs of integrated circuit which have recently become available can perform both the d.c. amplication of the measuring instrument outputs and the channel selector function, which would enable the uniselector to be eliminated.

CHAPTER 5

Statistical Analysis of the Data

5.1 Statistical theory

In this chapter, the statistical methodsused in the analysis of the precipitation data will be described, and an outline given of the series of computer programs written to perform this task. Detailed explanations or proofs of the statistical principles involved will not be given, as they are readily available in standard text books such as BENDAT and PIERSOL (1966).

It has already been explained in Chapter 2 how the relationship between potential gradient and precipitation current during quiet precipitation can be expressed in terms of the correlation between the two records. The properties of correlation functions and some of their uses, as relevant to the present work, will now be described.

5.1.1 The correlation function

Correlation functions can be used to discover whether a functional relationship exists between two variables x and y, such that $y = f(x)$. In the present application in atmospheric electricity, the possibility of a linear relationship between potential gradient and precipitation current is being investigated. The linear correlation between the two variables x and y can be expressed in terms of the correlation

coefficient r, given by

$$r = \frac{1}{N\sigma_x\sigma_y} \sum_{i=1}^{N} (x_i - \bar{x})(y_i - \bar{y}) \qquad (5.1)$$

where the variables x and y are expressed as a series of N observations (x_1, y_1), (x_2, y_2).....(x_N, y_N), with mean values $\bar{x}$, $\bar{y}$, and standard deviations σ_x, σ_y.

The value of r varies between + 1.0 for an absolute direct relationship between the two variables, and - 1.0 for an absolute inverse relationship. A coefficient $r = 0$ implies no relationship. In practice, errors in the values of x_i and y_i due to measurement or random effects will cause a deviation from any linear relationship, and so coefficients of magnitude 1.0 will never be attained. Similarly, two series (x_i, y_i) which are not related may still give a non-zero correlation coefficient, due to random variations in their measured values.

5.1.2 Cross-correlation with time lags

Maximum correlation between two time series may not necessarily occur for simultaneous values, as was assumed above; from the expected behaviour of the potential gradient and precipitation current during quiet precipitation, maximum correlation may occur for one or other record leading. The correlation coefficient can also be expressed as a function of a time lag τ between the series:

$$r(\tau) = \frac{1}{N\sigma_x\sigma_y} \sum_{i=1}^{\tau} (x_i - \bar{x})(y_{i+\tau} - \bar{y}) \qquad (5.2)$$

where $\tau = 0, \pm 1, \pm 2, \ldots\ldots \pm L$. The maximum lag number

L is of necessity less than N, the number of observations of x and y.

The expression 5.2 will be used to calculate the correlation coefficient $r(\tau)$ for each set of potential gradient and precipitation current values. A plot of $r(\tau)$ against the time lag τ for either record lagging will enable the time lag for maximum correlation to be determined. Such a plot is termed a "cross-correlogram"; a typical example is shown in Fig. 5.1.

5.1.3 Autocorrelation

Just as two time series can be cross-correlated, a single time series can be correlated with itself to determine the correlation of given values x_i with previous ones $x_{i-\tau}$. This is known as "autocorrelation", with an autocorrelation coefficient $a(\tau)$ given by

$$a(\tau) = \frac{1}{N\sigma_x^2} \sum_{i=1}^{N-\tau} (x_i - \bar{x})(x_{i+\tau} - \bar{x}) \qquad (5.3)$$

where again $\tau = 0, \pm 1, \pm 2, \ldots \pm L \quad (L < N)$

A plot of $a(\tau)$ against time lag τ is termed an "autocorrelogram". Its main use is in determining the degree of "persistence" in the series, and in detecting any periodic variations. Thus, if a series x_i exhibits a high degree of persistence, the value of $a(\tau)$ will be larger for a particular value of τ than for a series with a small degree of persistence (Fig. 5.2) This may mean that subsequent values of x_i are not completely independent of their predecessors, as is required for many statistical results to be valid. The problem of deciding if the values x_i are independent is discussed later (Sect. 5.1.6).

FIG 5.1 A typical cross-correlogram

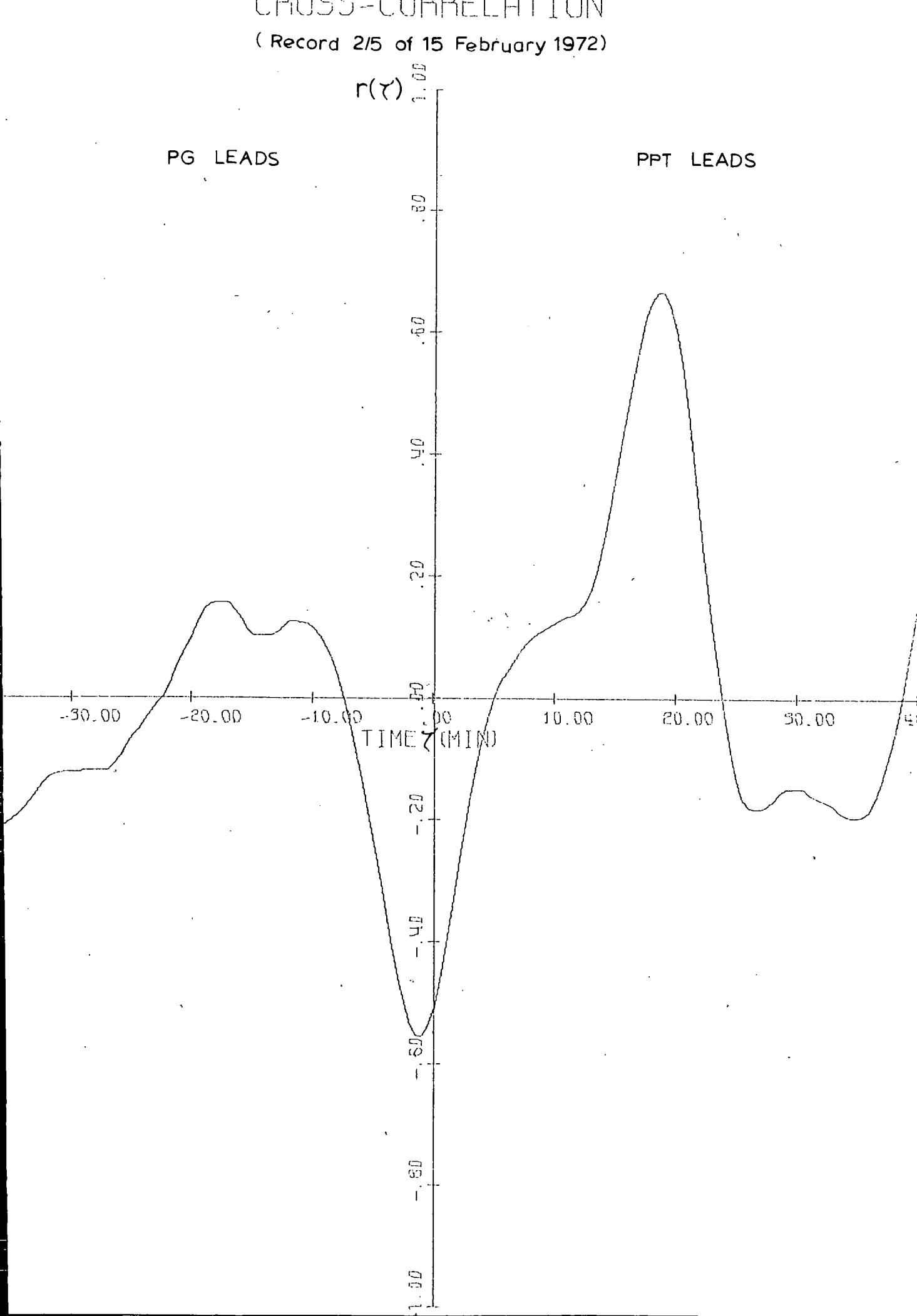

Fig. 5.2 The autocorrelogram

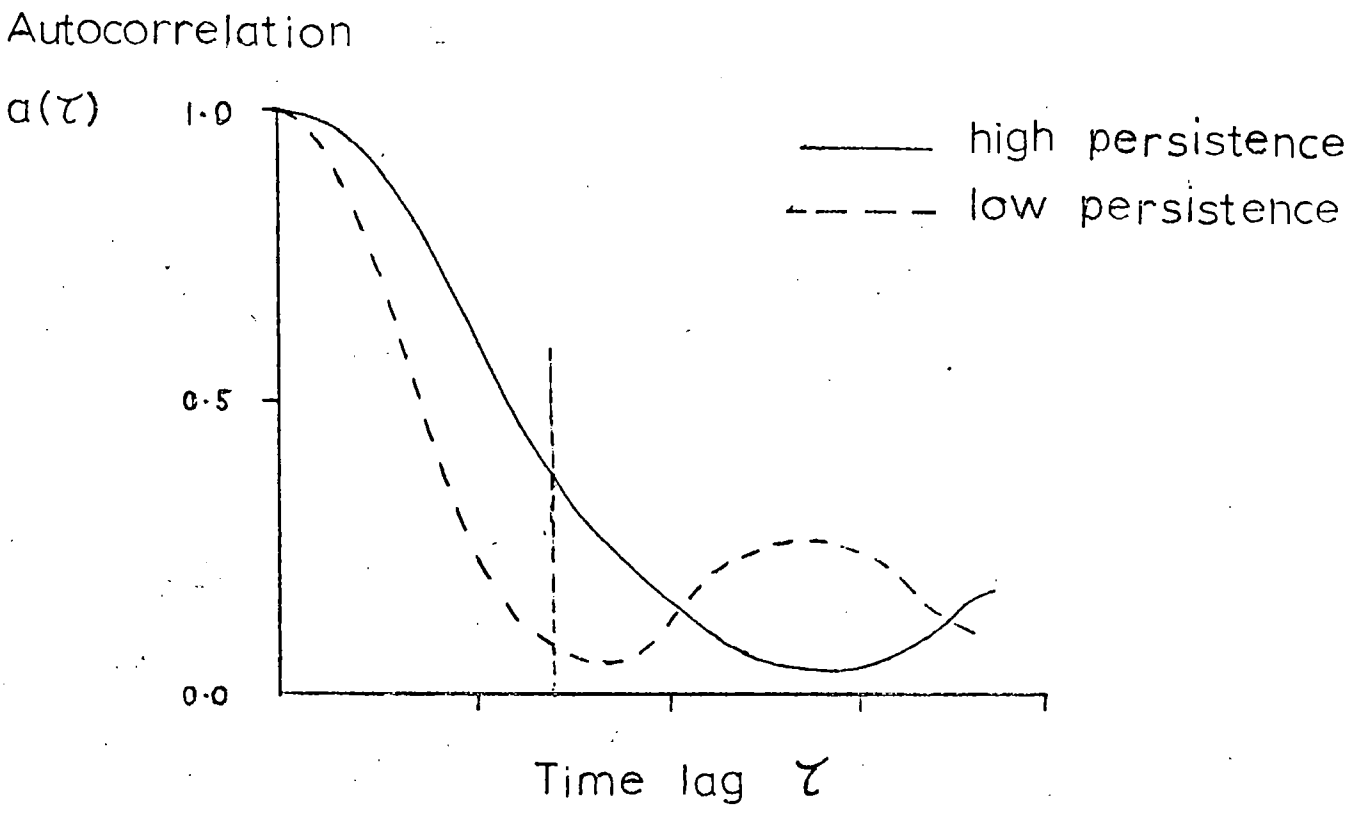

Fig. 5.3 Autocorrelation of a sinusoidal series

(a) series $x(t) = X \sin \frac{2\pi t}{T}$

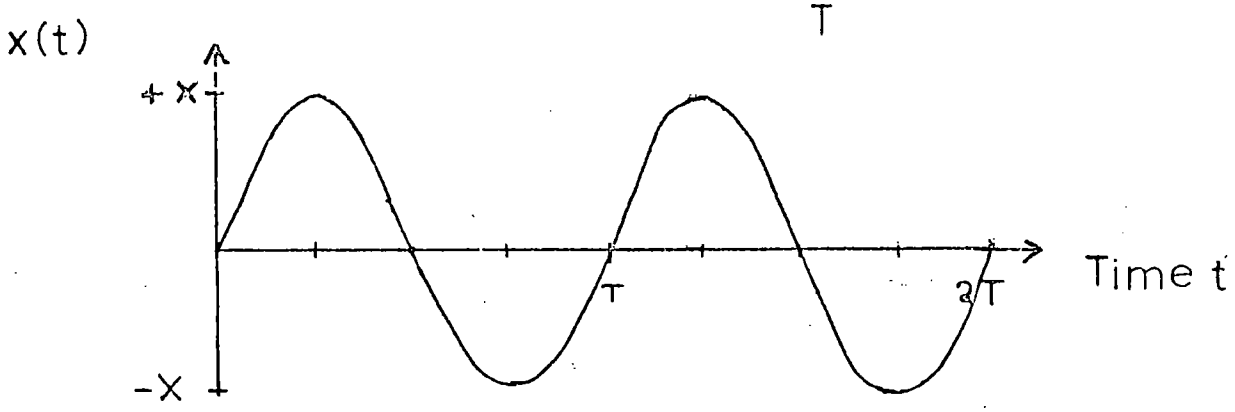

(b) autocorrelogram $a(\tau) = \cos \frac{2\pi t}{T}$

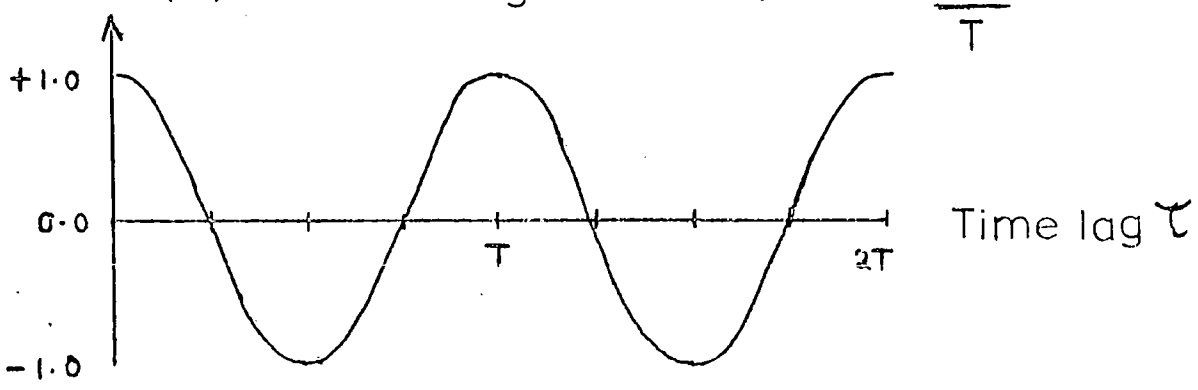

5.1.4 Correlation of periodic series

The autocorrelogram is useful in detecting any periodic behaviour of the series x_i. In the case of a purely sinusoidal variation

$$x(t) = X \sin \frac{2\pi t}{T}$$

where T is the period and X the amplitude, the autocorrelogram will have the form

$$a(\tau) = \cos \frac{2\pi\tau}{T} \qquad (5.4)$$

This is a cosine function with a period equal to that of the series x(t); positive correlation maxima will occur at τ = 0, T, 2T..... and negative maxima at $\tau = \frac{T}{2}, \frac{3T}{2}, \frac{5T}{2}$... (Fig.5.3).

Random noise in the observations x_i of a periodic series will reduce the amplitude of the periodicity of $a(\tau)$, but it will often still be evident.

The cross-correlogram of two sinusoidal series will also be a cosine function, again with maxima recurring with the time period of the series. In the present work, the correlation of two series separated by a time interval t′ is more relevant. The cross-correlogram between the series

$$x(t) = X \sin \frac{2\pi t}{T}$$

and

$$y(t) = Y \sin \frac{2\pi(t + t')}{T}$$

will have the form

$$r(\tau) = \cos \frac{2\pi(\tau + t')}{T} \qquad (5.5)$$

which has maximum positive values at t′, T + t′, 2T + t′ .... and maximum negative values at $\frac{T}{2} + t'$, $\frac{3T}{2} + t'$, $\frac{5T}{2} + t'$..... (Fig.5.4). The maxima are again occurring at intervals of T,

Fig. 5.4 Cross-correlation of two sinusoidal time series separated by a time lag t'

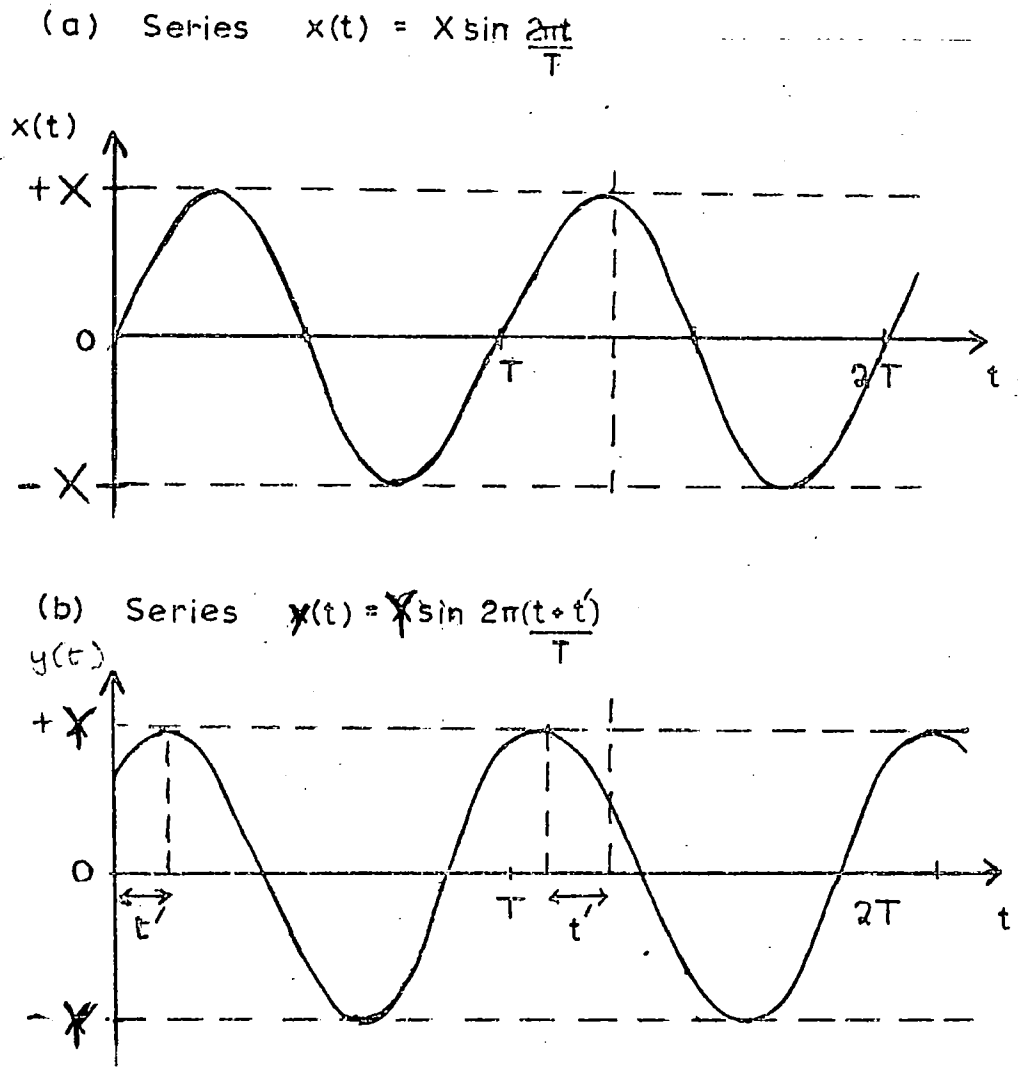

but are now shifted by the time lag t' of $x(t)$ behind $y(t)$.

5.1.5 The statistical significance of correlation maxima

It can be shown that two time series which are not infinite in length can produce spurious values of correlation coefficient, even if they are completely unrelated. Random unrelated series, for instance, seldom give a zero cross-correlation coefficient. A given correlation coefficient value must therefore be tested for significance, as it may have arisen purely by chance.

The usual tests of significance estimate the probability of the calculated correlation coefficient arising by chance out of random data. If this probability is less than 0.05, i.e. less than 5 times in 100 estimates, the coefficient is usually considered to be significant, the "significance level" being in this case 95%. Values which would arise less than once in 100 estimates are considered to be highly significant, the significance level then being 99%.

If the random data of the time series are distributed normally, the correlation coefficient values calculated from a number of samples of the given series will be similarly distributed about the true value. The probability of a certain value of correlation coefficient arising by chance can then be estimated by a standard statistical procedure known as the "Student t-test". A value of the coefficient t can be calculated from the correlation coefficient r by the relationship:

$$t = \frac{r\sqrt{N_r - 2}}{1 - r^2}$$

where N_I is the number of independent observations of the series. The quantity $N_I - 2$ is often termed the "number of degrees of freedom."

Statistical tables are available which give values of t corresponding to values of r which could arise from uncorrelated data; these values are given at various levels of significance.

The number of independent observations, N_I, depends on the persistence of the individual series, and is not necessarily the same as the number of observations N. The method of estimating N_I is outlined in the following section.

5.1.6 The autocorrelation interval

The autocorrelation function described in Section 5.1.3 can be used to estimate an "autocorrelation interval" for a time series; observations of this time series made at a time separation less than this interval are not independent. AWE (1964) has shown analytically that the autocorrelation interval L_o is given by

$$L_o = \int_{-\infty}^{\infty} a^2(\tau)\, d\tau \qquad (5.7)$$

He also showed that a good estimate can be obtained by evaluating $a^2(\tau)$ over only the central maximum of the autocorrelogram. As an autocorrelogram is symmetrical about the $\tau = 0$ axis, the autocorrelation interval can be evaluated for a time series by:

$$L_o = 2\sum_{L=1}^{M} a^2(\tau)\,\Delta t \qquad (5.8)$$

where the first minumum of the autocorrelogram occurs at the Mth time lag, and Δt is the sampling interval between successive values of the time series.

The total number of observations of the time series, N is then divided by L_o to determine the effective number of independent observations N_I, i.e.

$$N_I = \frac{N}{L_o} \Delta t \qquad (5.9)$$

Usually N_I will be less than N, and is therefore used as the number of observations for tests of significance.

5.1.7 The nature of physical data

Data representing physical phenomena can be generally classified as being either deterministic or random. Deterministic data can be described by an explicit mathematical expression, and so an accurate prediction of future behaviour can be made. For random data no such explicit expression can be deduced, and so probability functions and statistical quantities have to be used to describe their behaviour. Atmospheric electrical processes will generally produce largely random data, and so statistical methods of analysis are required.

Random data can in turn be divided into two categories; stationary and non-stationary. The statistical properties of non-stationary data, such as the mean or the variance, continually vary with time, so that different samples of the data would give different statistical values. Stationary data show no such variation. Fig 5.5 illustrates the differences between the two types of data.

FIG. 5.5 Stationary and non-stationary processes

(a) stationary

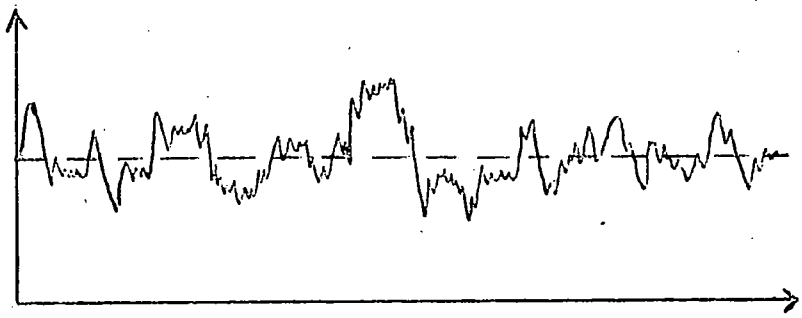

(b) non-stationary — mean not constant

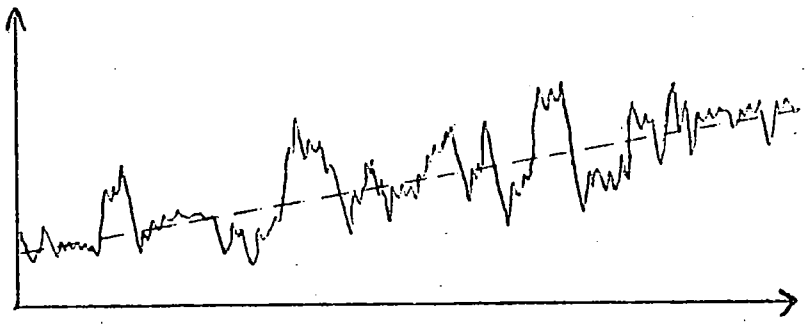

(c) non stationary — variance not constant

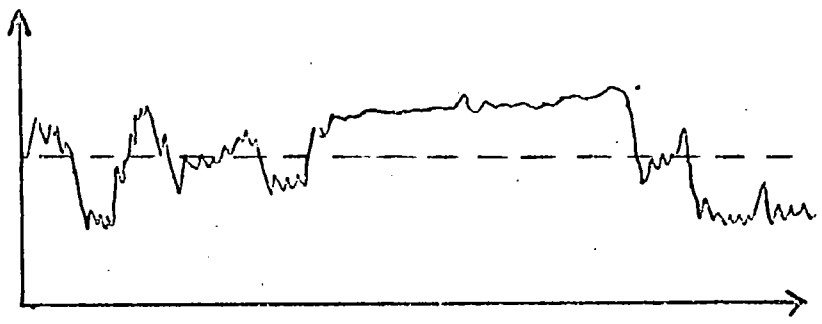

(d) non stationary variance and mean not constant

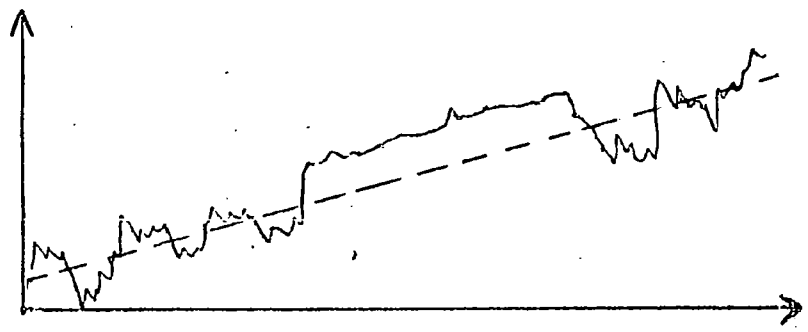

The statistical theory and results of the preceeding sections assume that the data are stationary. No theory has yet been developed for non-stationary data, and so all the data in the present investigation have to be treated as stationary. It will be evident, however, from the precipitation records shown in subsequent Chapters that this is not strictly true in these cases, particularly if only short records are being analysed. However, when the means and standard deviations of a parameter do not vary significantly between statistical samples, it is said to be "weakly stationary", and the above statistical theory can be considered to be applicable.

Many of the records of potential gradient and precipitation in the present work appear to be weakly stationary, particularly if lasting many hours. The main effect on the correlograms if a record is in fact non-stationary will be to increase the values of correlation coefficient, rather than alter the general form of the correlogram.

For stationary or weakly-stationary data, a useful feature of the cross-correlation coefficient r is that it indicates how much of the variability of one parameter is due to the variability of the other. This proportion is given by r^2, so that a maximum cross-correlation coefficient of, for example, 0.80, implies that 0.64 of the variability of the one parameter is due to the other.

5.2 The computer programs

Calculation of the various statistical quantities for each set of precipitation data was carried out on the I.B.M.

360/67 computer at Durham University. A series of programs was written which first converted the "raw" data values (i.e. digital voltmeter readings) to potential gradient and precipitation current density values, then calculated the auto and cross-correlations and other statistical quantities, and finally presented the results in printed and graphical form.

The programs were written in the computer language Fortran IV, and so, because of the specialised nature of this language, will not be presented in detail. By using the system of computer operation known as the "Michigan Terminal System", or M.T.S., each program could be stored in the computer in a unit of storage space known as a "file". Each file has an identifying name which enables the program (or data) stored in it to be called (or accessed) as required. The program to calculate the auto and cross correlations, for instance, was stored in the file CORPROG; on each computer run, this file would be accessed and the program executed, using the current set of data to calculate the correlations.

5.2.1 A typical computer run

Figure 5.6 shows schematically the various stages of a typical computer run. The raw data, consisting of the digital voltmeter values produced by the data handling system, are converted to potential gradient and precipitation current density values by the program CALPROG; these values are then stored in the file RAINDATA. The opportunity to

FIG. 5.6 The computing procedure

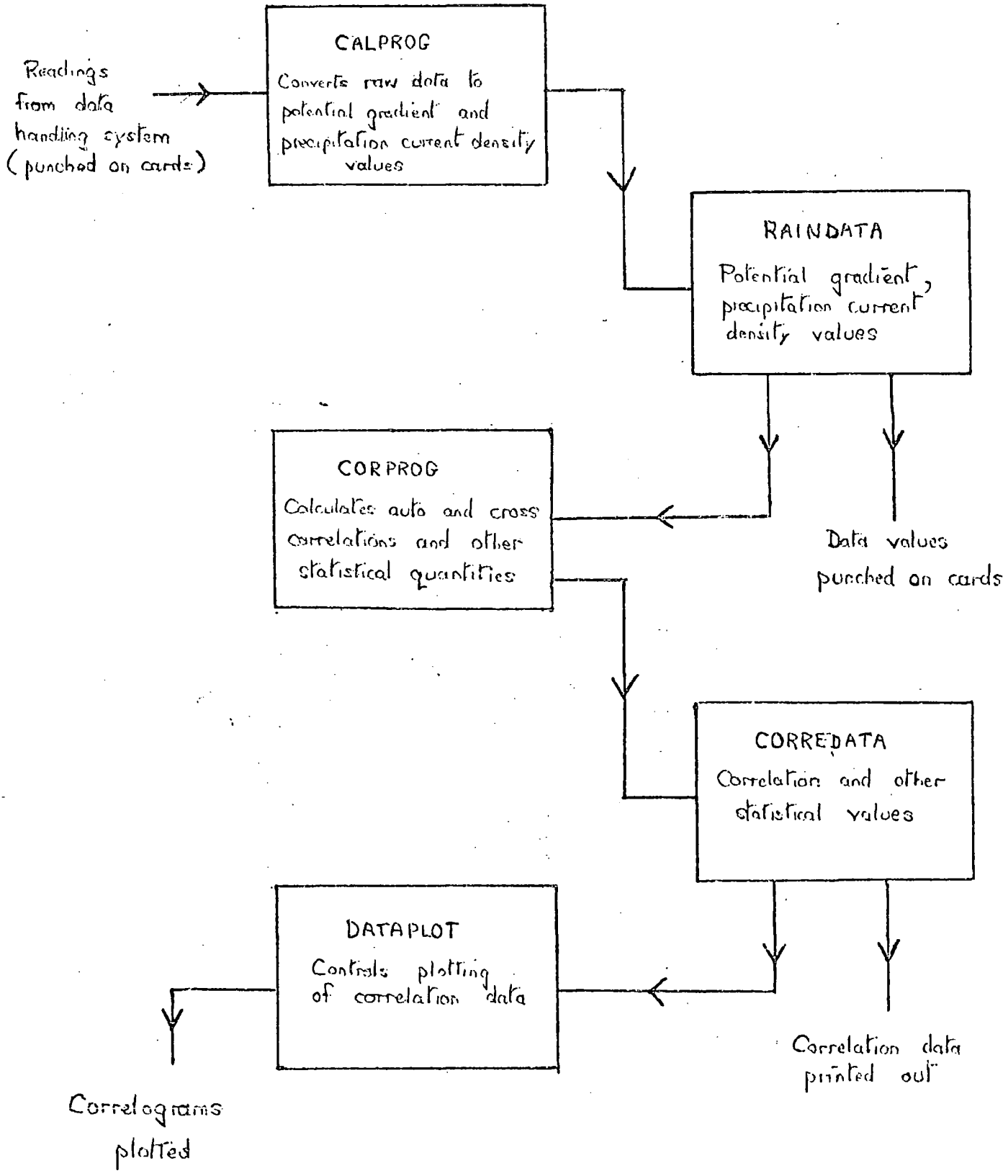

correct for any non-uniformity in the field mill calibrations (see Sect. 3.2.5) was taken at this stage.

The auto and cross correlations are then calculated by the program CORPROG, using the data stored in RAINDATA as input, and placing the calculated correlation values in CORREDATA. The correlation values are also printed out as required.

A useful feature of the Durham computer facilities is the availability of a series of standard programs, or "subroutines", which can be adapted to the requirements of an individual user. The "Scientific Subroutines Package" (or S.S.P.) includes programs for calculating auto and cross correlations and many other statistical quantities, and was thus extensively used.

The third stage of the computer run is the plotting of the correlograms by the computer graph plotter. This device enables any set (or sets) of data to be automatically plotted; its use in the present work is described below.

5.2.2 The presentation of the computer output

Altogether, three types of computer output proved useful: the standard print-out, plotted output, and punched output. The standard form of print-out monitors the progress of a particular computer run, or "job", and the results of the various calculations can also be listed.

The plotting facility was extensively used, with two main applications. The first was plotting the correlograms for each set of data, using the calculated values of correlation coefficient stored in the CORREDATA file (Fig.5.6). The other

application was in presenting wind and temperature profiles for periods of precipitation, using data from the Daily Aerological Record published by the Meteorological Office. A program was written to calculate wind speed, direction and temperature values from the coded data presented in the Aerological Record, and plot these against height. Examples of these plots and their applications are given in subsequent Chapters.

The contents of the RAINDATA file were punched on to cards on each occasion; if needed, this enabled the data to be run at a later date more readily, as conversion to true values of potential gradient and precipitation current density is not then required.

CHAPTER 6

Examples of Precipitation Records

6.1 Introduction

Three periods of quiet precipitation recorded during the present work will now be presented in detail to illustrate the electrical and meteorological behaviour typical of such precipitation. A period of disturbed precipitation will also be examined briefly, by way of comparison.

Except for the disturbed precipitation, when no statistical calculations could be made as the recorded instrument values were often off-scale or changing rapidly, the electrical and meteorological behaviour will be presented in the following order:

(a) The synoptic meteorological situation, using information from the Daily Weather Report of the Meteorological Office.

(b) The electrical records of potential gradient and precipitation current density, as obtained at Durham Observatory.

(c) The correlograms and other statistical quantities, calculated from the electrical recordings.

(d) The meteorological conditions at Durham during the precipitation, obtained from the Observatory records.

(e) Appropriate Aerological profiles, i.e. temperature - height and wind - height, at either Shanwell, Hemsby or Aughton, the nearest meteorological stations taking upper - air measurements. These were calculated and

plotted by computer from data in the Daily Aerological Record of the Meteorological Office.

Information on all the periods of quiet precipitation during which records were obtained is presented in Chapter 7.

6.2 The records of the 17 and 18 January, 1972

An occluded front running from the west of Scotland through to south - west England produced periods of rain, sleet and snow from 08 20 on the 17th to 07 00 on the 18th. The front remained virtually stationary throughout this period, and so provided a good example of the different characteristics of rain and snow in otherwise similar conditions, as both originated from the same frontal system.

6.2.1 The period of rain

Rain started at Durham at 08 20 and continued throughout the morning until about 14 00, when sleet began to fall. The synoptic situation at 12 00 is shown in Fig. 6.1, together with the approximate extent of the area of precipitation.

The chart record of potential gradient and precipitation current density from 10 00 to 15 30 is reproduced in Fig. 6.2. The record during steady rain shows the inverse relation and, to a lesser extent, the mirror image effect, with the potential gradient apparently leading. After 14 00, sleet was falling and the electrical record becomes much more disturbed, sometimes going off - scale and showing larger and more rapid variations. Only the portion of record up to 14 00 is thus considered to be quiet.

FIG. 6.1 Synoptic situation at 12Z on 17 January 1972

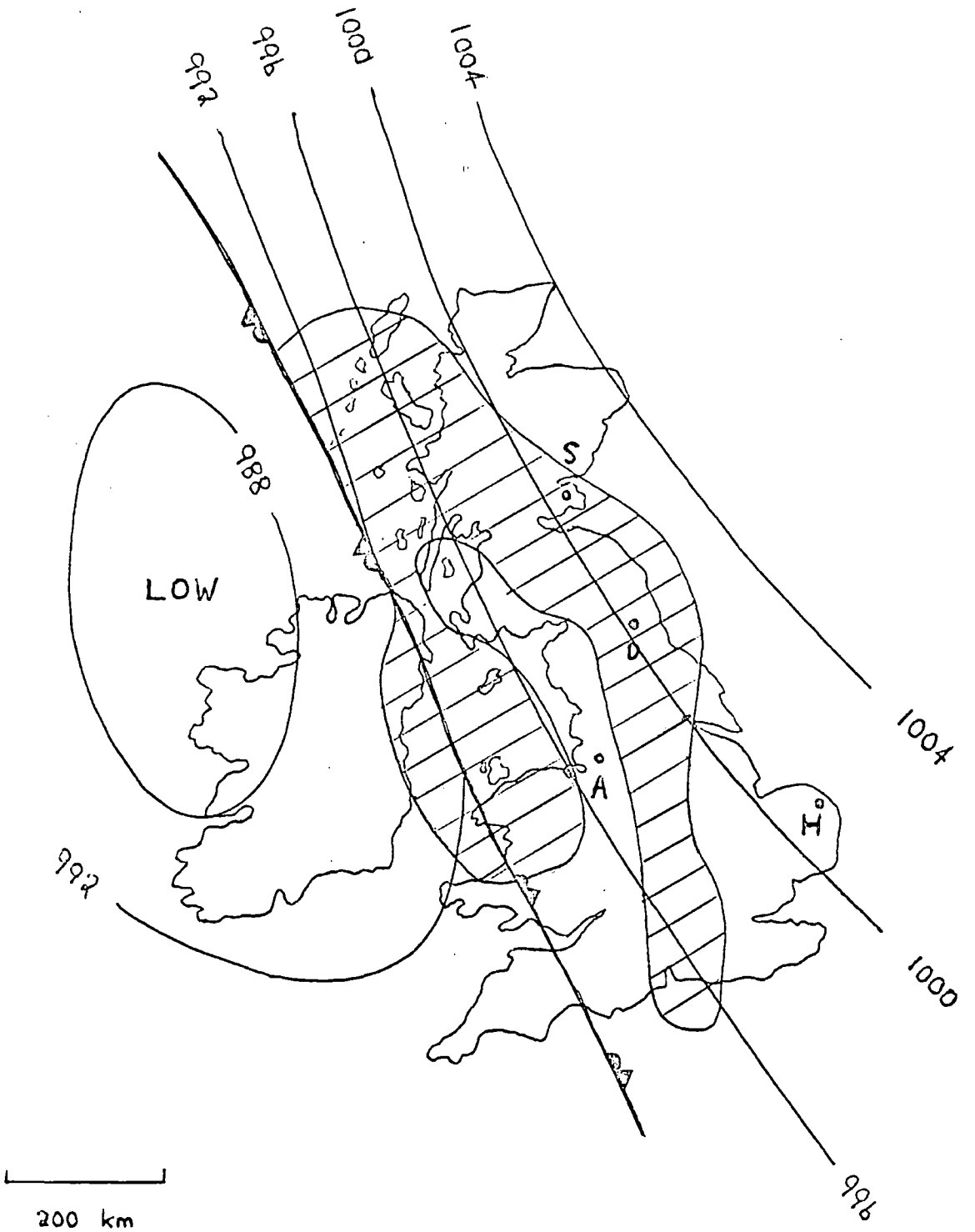

FIG. 6.2 Precipitation record of 17 January 1972

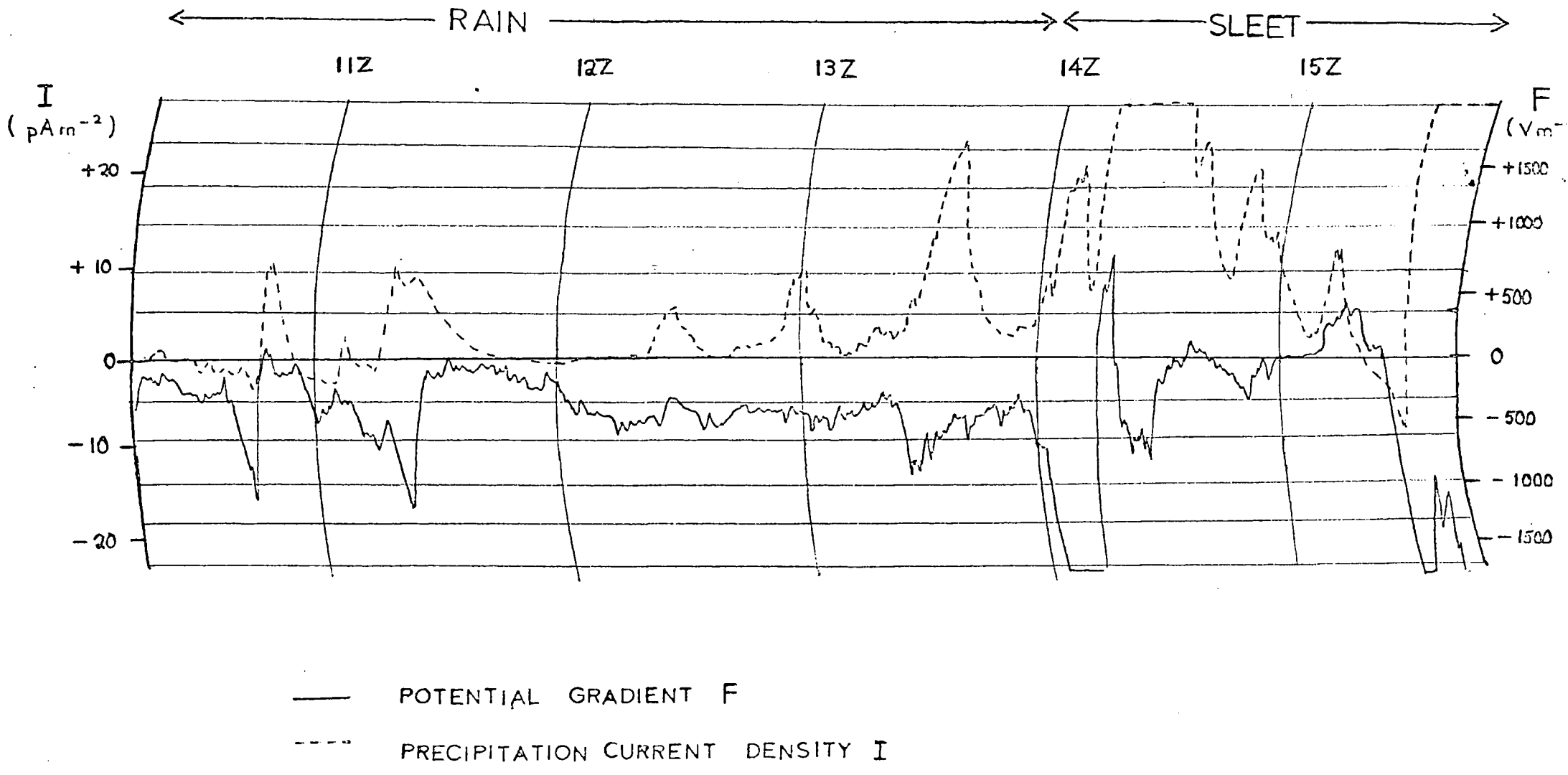

6.2.2 The statistical properties of the record

The auto and cross-correlograms were calculated for the portion of record between 08 20 and 14 00. Fig. 6.3 shows the cross-correlogram between potential gradient and precipitation current; maximum, negative, correlation occurs for potential gradient leading by 6 minutes, the value of correlation coefficient, - 0.67, being very nearly significant at the 99% level. It should be noted that the cross-correlation at zero lag is very small, and so if only simultaneous values of potential gradient and precipitation current had been considered, no significant correlation would have been found.

The negative cross-correlation maximum, with the potential gradient leading, agrees with the situation suggested by the chart record, of a mirror - image effect with potential gradient leading.

The autocorrelograms (Fig. 6.4) indicate that the precipitation current has more persistence than the potential gradient, as at a given time lag, the precipitation current generally has a larger value of autocorrelation coefficient than the potential gradient.

Table 6.1 gives some other statistical quantities calculated for this record. The inverse relation is evident, the mean potential gradient being negative, and the mean precipitation current positive.

6.2.3 The meteorological properties

Table 6.1 also summarises the meteorological situation at Durham during the period of rain. The mean rate of rainfall

FIG. 6.3. CROSS-CORRELATION

17 January 1972

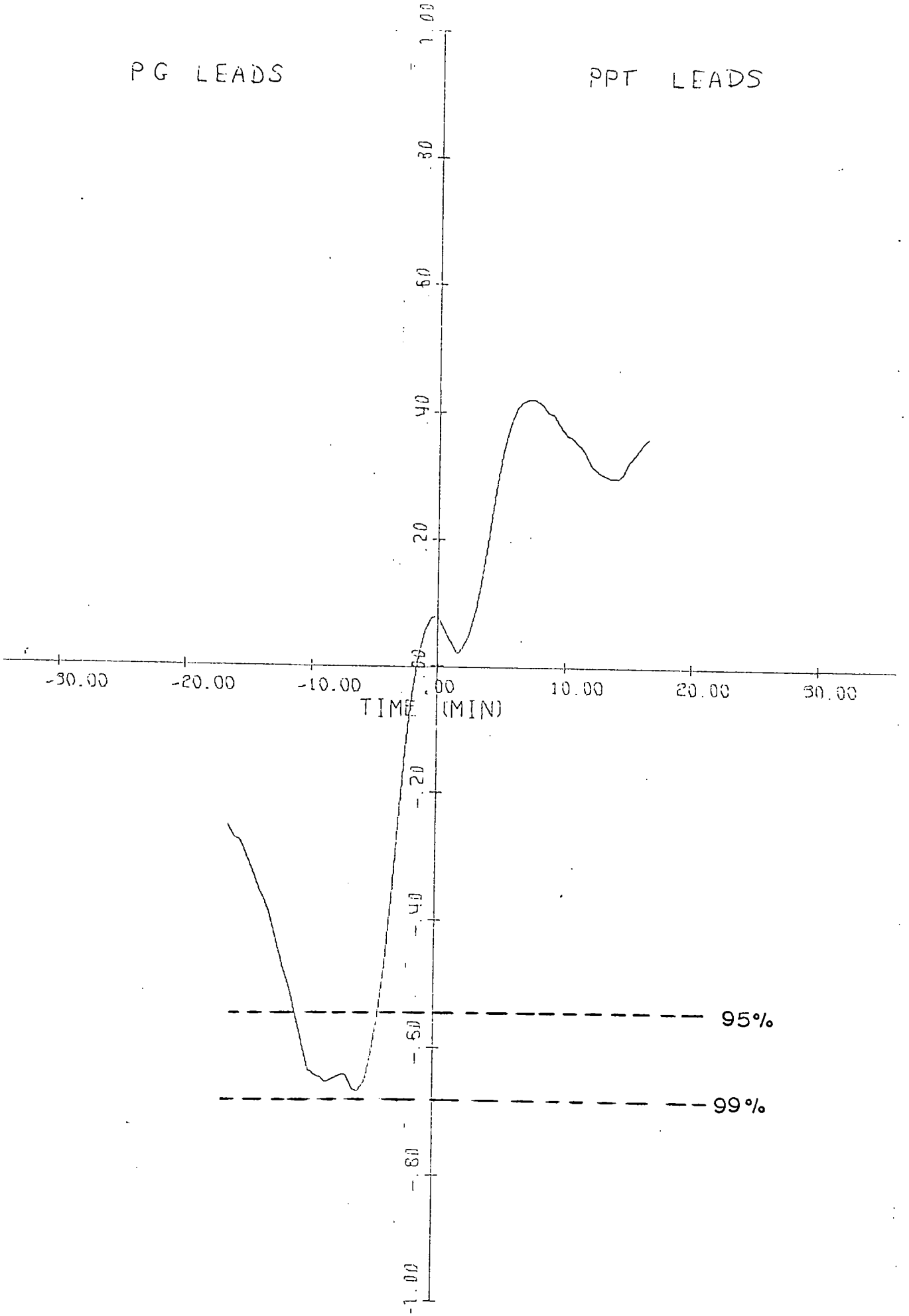

FIG. 6.4 17 January 1972

Durham

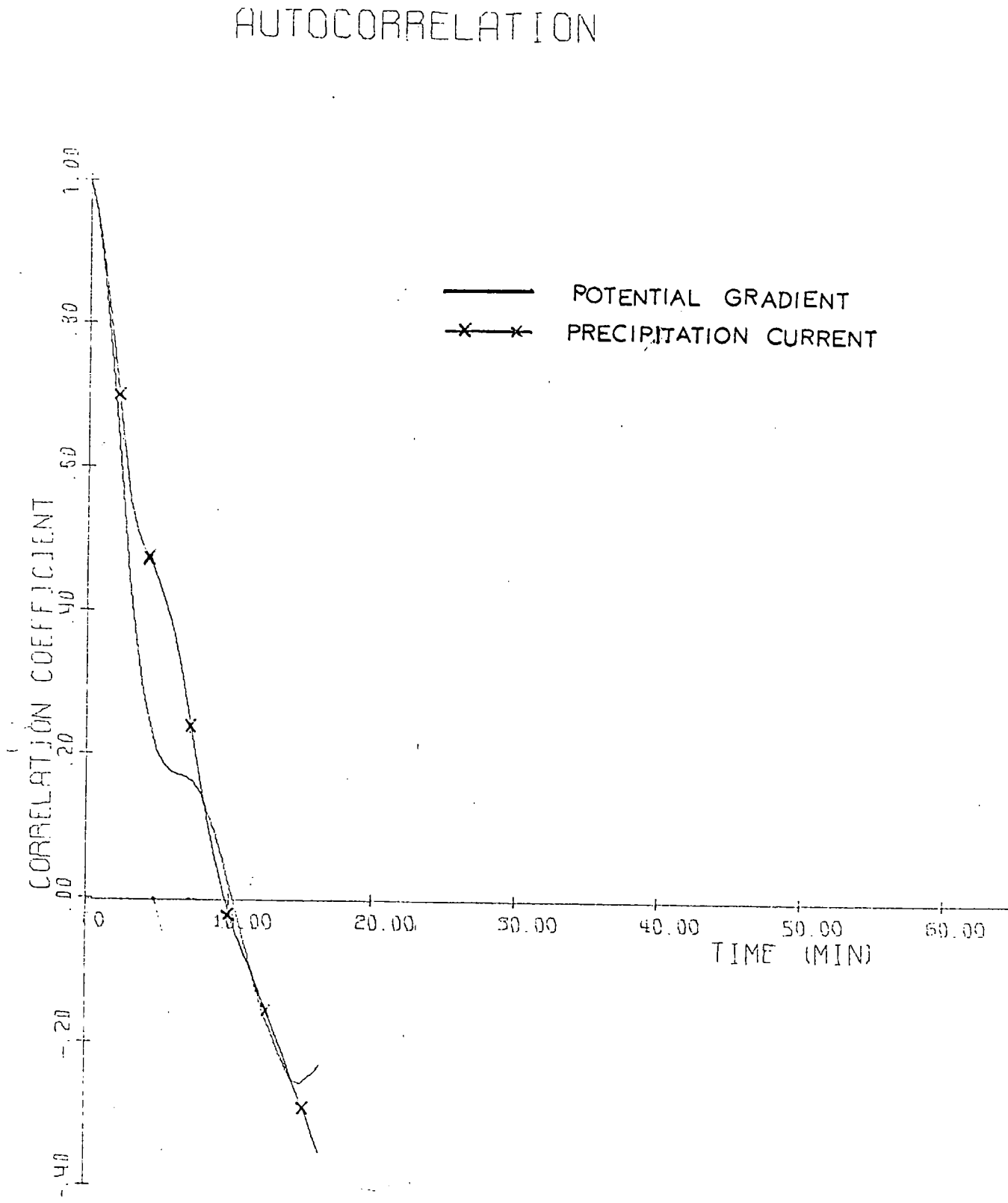

TABLE 6.1 CHARACTERISTICS OF SEVERAL PERIODS OF PRECIPITATION

			17 JAN Quiet rain	17/18 JAN Quiet snow	2/3 MAY Quiet rain		26 JAN Disturbed rain
Potential Gradient	Mean	Vm^{-1}	-420	+175	-280		-
	Standard deviation	Vm^{-1}	450	465	510		-
	% positive values		11	82	23		-
Precipitation current density	Mean	pAm^{-2}	+2.5	-3.5	-4.0		-
	Standard deviation	pAm^{-2}	10.1	7.6	9.0		-
	% positive values		73	14	11		-
Cross correlation coefficient	Maximum value		-0.67**	-0.77***	-0.34*	+0.26	-
	Time lag	min	-6	+1	+22	-24	
Meteorological conditions at Durham	Mean rate of rainfall	$mm\ hr^{-1}$	0.7	0.7	0.7		2.3
	Surface wind speed	ms^{-1}	6.0	5.0	2.0		10

Cross-correlation coefficient significance level: * 95% ** 99% *** 99.9%

Time lag is positive for precipitation current leading, negative for potential gradient leading.

and surface wind speed were somewhat above the usual values found during quiet precipitation.

Figs. 6.5 to 6.8 are aerological profiles at 12Z (12 00 G.M.T) at Shanwell and at 11Z at Hemsby. The location of these stations, together with a third, Aughton, is shown in Fig. 6.1. Unfortunately Durham is a considerable distance from any of these stations, at respectively 200, 300 and 175 km, and so local conditions at Durham may vary considerably from those at any of the stations. However, by choosing the station at which the meteorological situation is closest to that at Durham a good indication of the local aerological situation should be available, particularly in the extensive cloud systems producing quiet precipitation.

The temperature profile at Shanwell clearly shows the frontal surface, between 1.0 and 1.2 km. altitude. The melting level is at 0.5 km. No wind data from Shanwell was available and so the profiles at Hemsby are also shown, although this was outside the area of precipitation. The frontal surface is again evident in the temperature profile, while the wind speed profile shows a region of negative shear (speed decreasing with height), between 0.9 and 1.2 km altitude. Such a region proved to be a characteristic feature of most profiles during quiet precipitation, whether or not a frontal surface was present. The wind direction veers slightly up to 1.9 km, but otherwise hardly varies.

6.2.4 The period of snow

The sleet which had started at 14 00 gradually turned to snow, and a period of quiet snow followed from 20 30 on the 17th

FIG. 6,5 Shanwell 12Z 17 January 1972

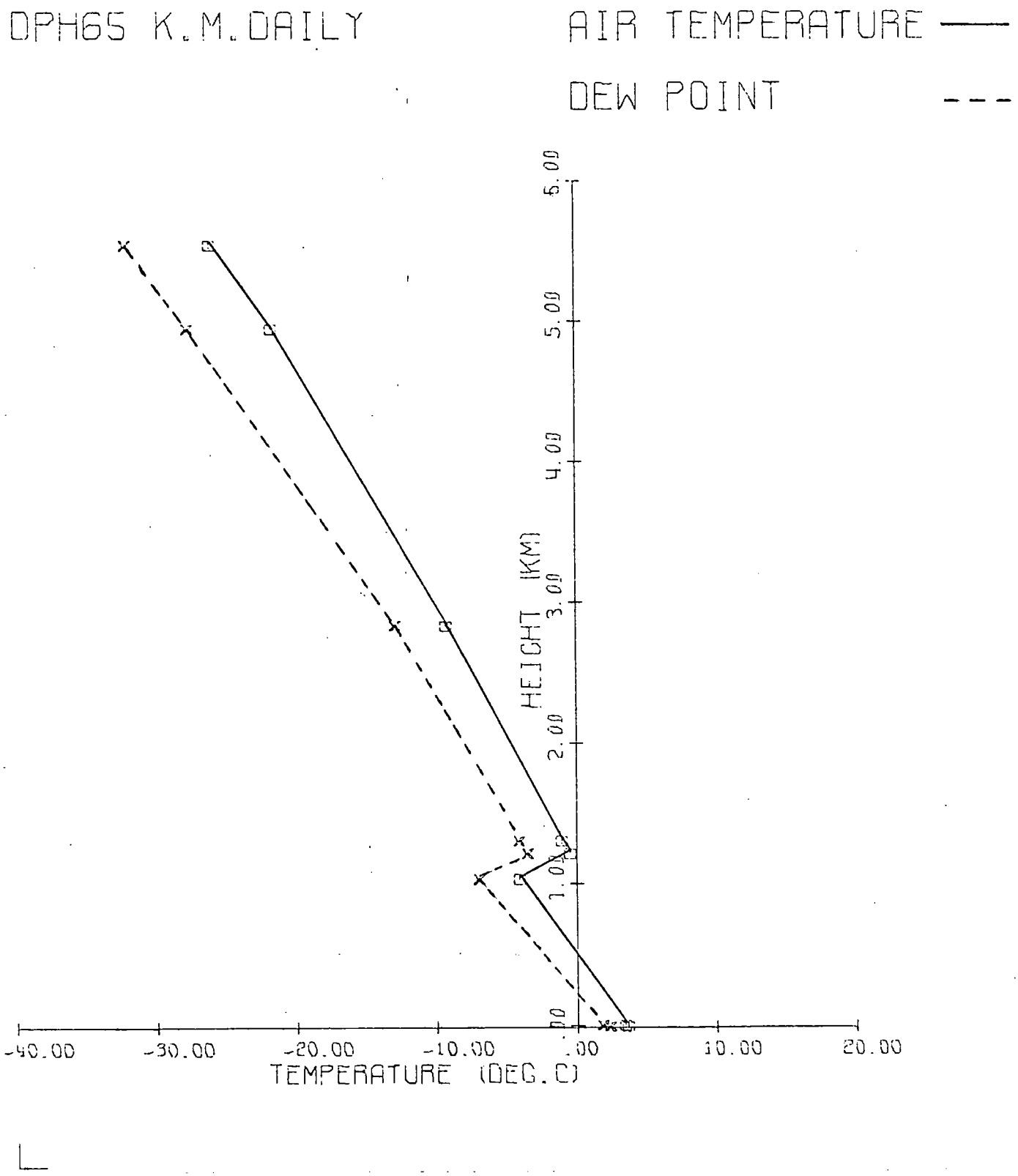

FIG. 6.6 Hemsby 11Z 17 January 1972

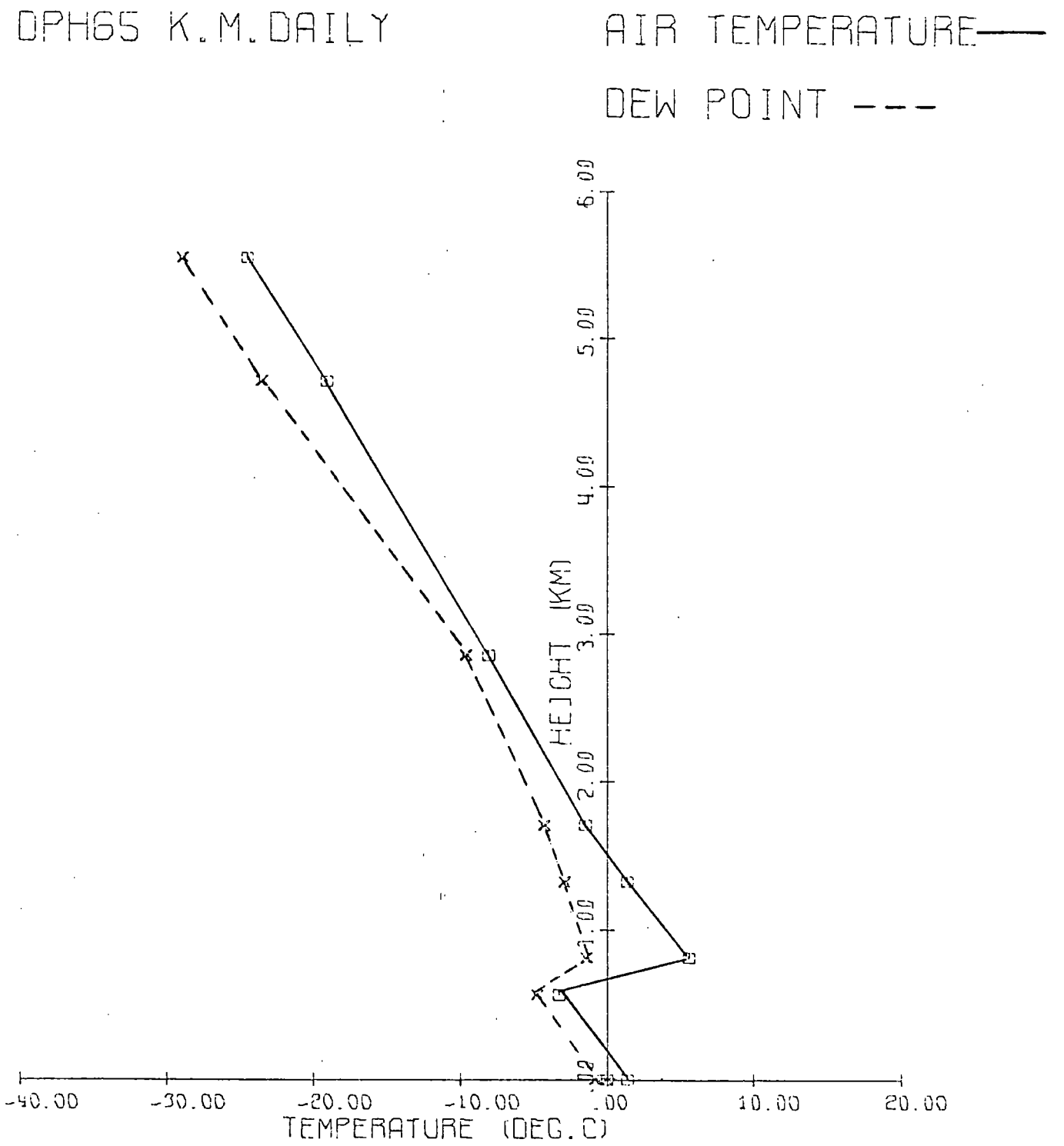

FIG.6.7 Hemsby 11Z 17 January 1972

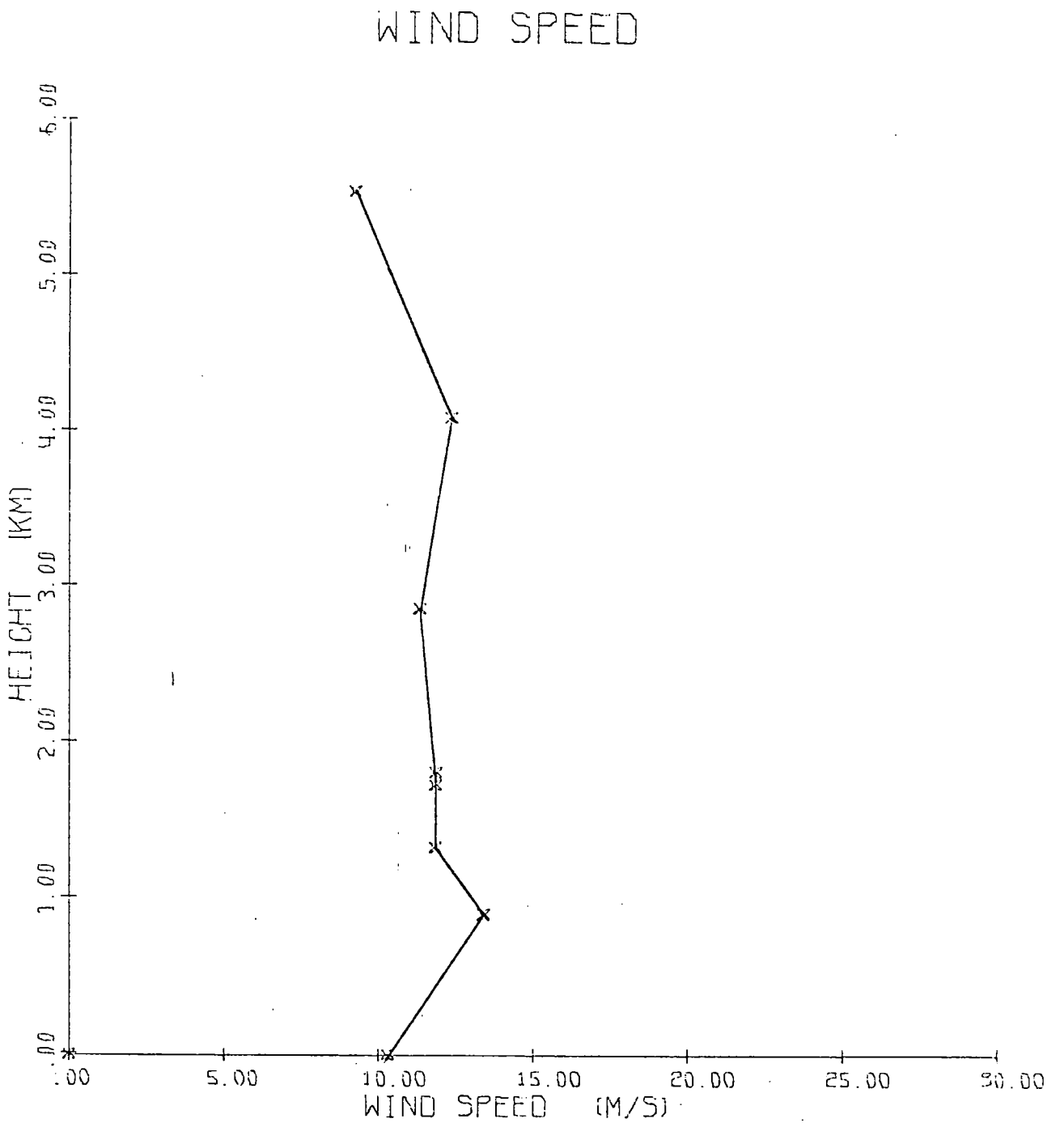

FIG. 6.8 Hemsby 11Z 17 January 1972

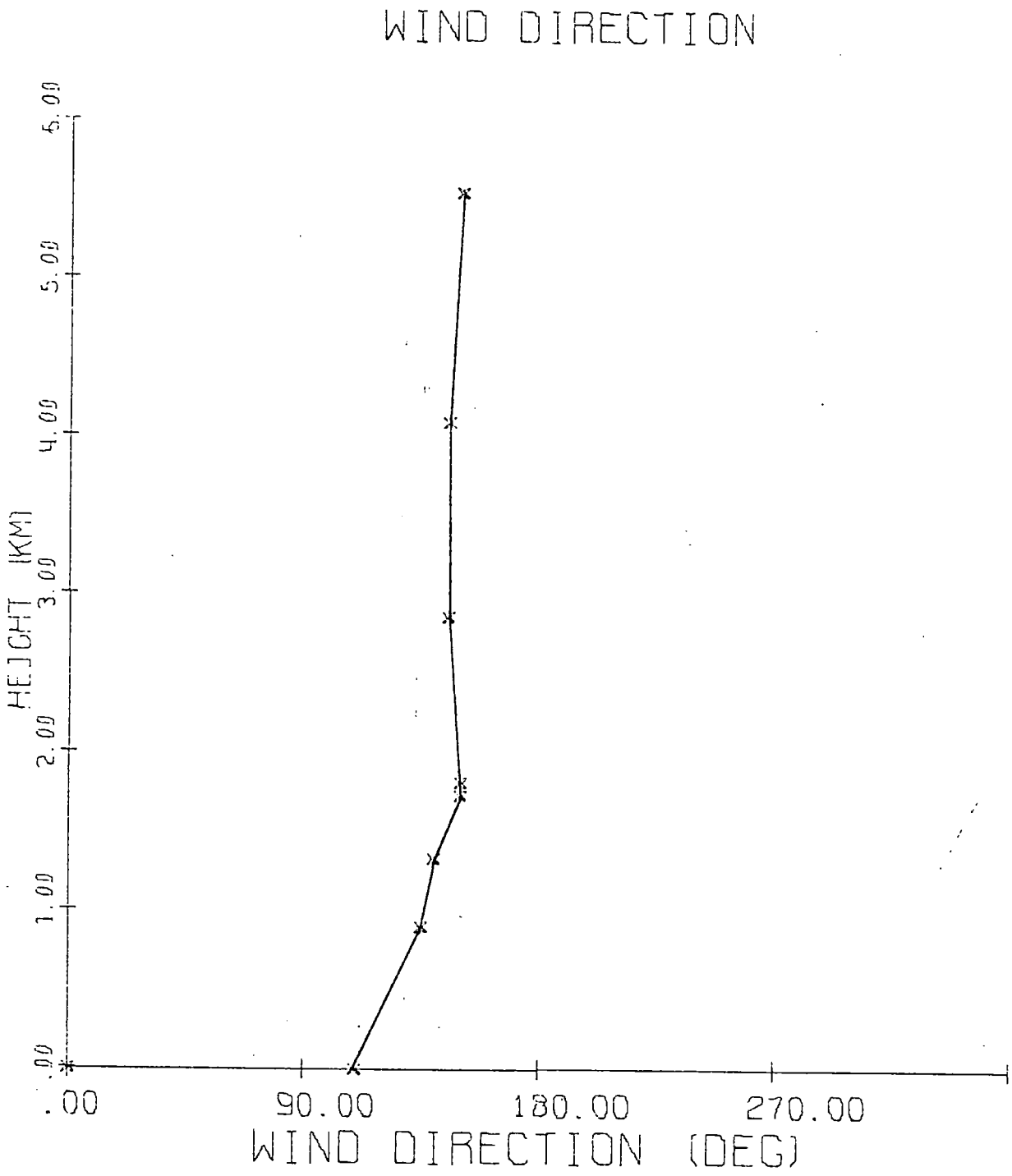

until 07 00 the next morning, apart from a short period from 23 15 to 23 50 when conditions were disturbed. The synoptic situation at 00 Z on the 18th (Fig. 6.9) showed little change, with the occluded front hardly moving.

The electrical record from 23 40 to 04 30 is shown in Fig. 6.10. Initially conditions are disturbed, but after 23 50 quiet snow is falling, with both the inverse relation and mirror-image effect being prominent. The signs of the potential gradient and precipitation current are largely opposite to those during quiet rain, the former being positive and the latter negative.

The prominence of the mirror-image effect is confirmed by the cross-correlogram of Fig. 6.11, with a maximum correlation coefficient of -0.77, highly significant at the 99.9% level, between potential gradient and precipitation current. In this case, however, precipitation current leads by about 1 min. The autocorrelograms (Fig. 6.12) again show the precipitation current to have more persistence.

The meteorological conditions at Durham (Table 6.1) show little change from those during the rain earlier, the mean rate of rainfall being the same and the wind speed slightly less. The aerological profiles at Shanwell are also similar to those earlier, with a prominent frontal zone in the temperature profile (Fig. 6.13), and a region of negative wind shear from 0.3 to 1.8 km (Fig. 6.14). It should be noted, however, that the surface wind speed at Shanwell (15.5 ms^{-1}) is considerably greater than that at Durham (5 ms^{-1}).

6.3 The record of the 2nd and 3rd May, 1972

While the records of the 17 and 18 January were in many

FIG. 6.9 Synoptic situation at 00Z on 18 January 1972

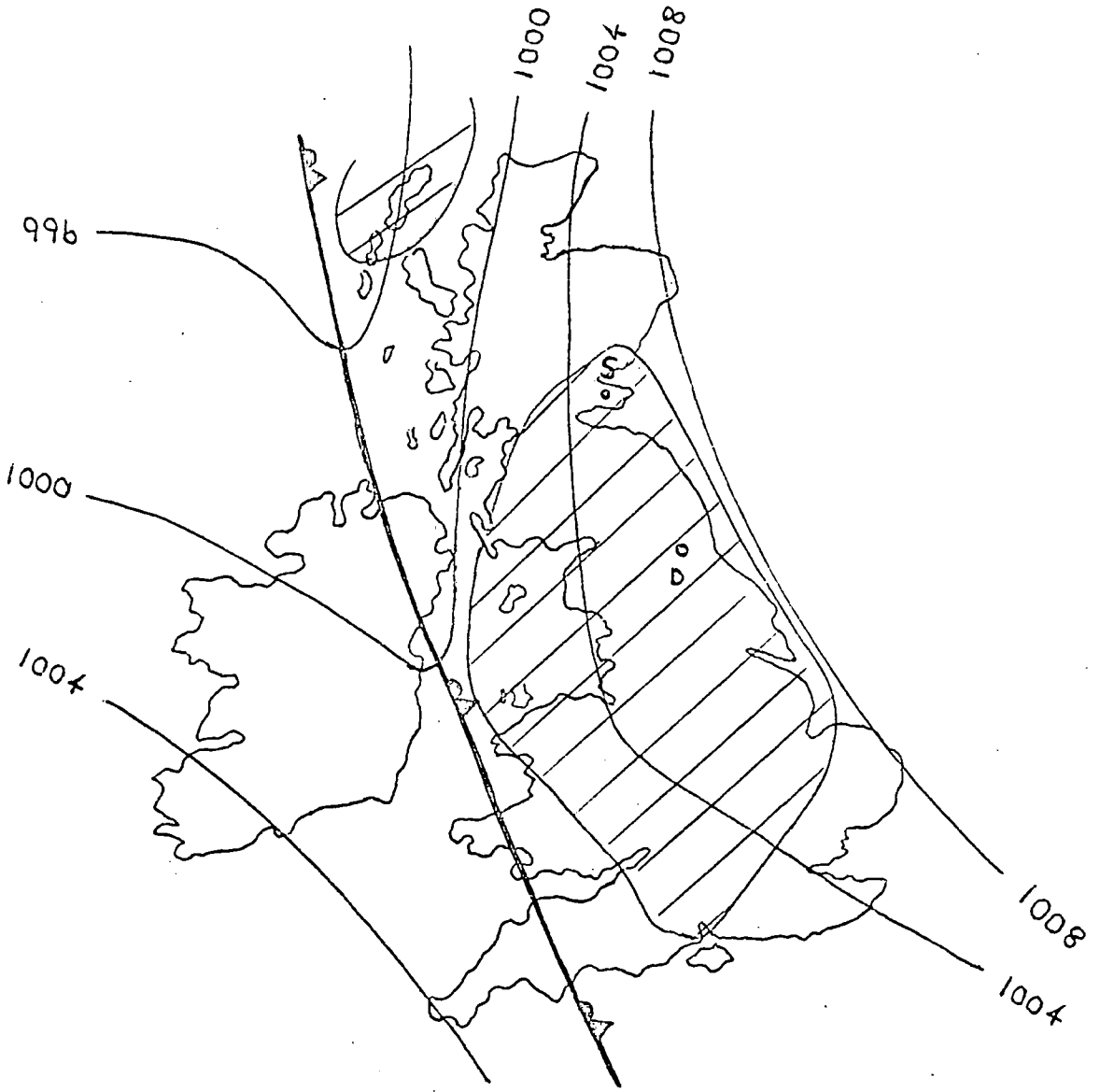

1004 Isobars

Approximate area of precipitation

D DURHAM

S SHANWELL

FIG. 6.10 Precipitation record of 17/18 January 1972

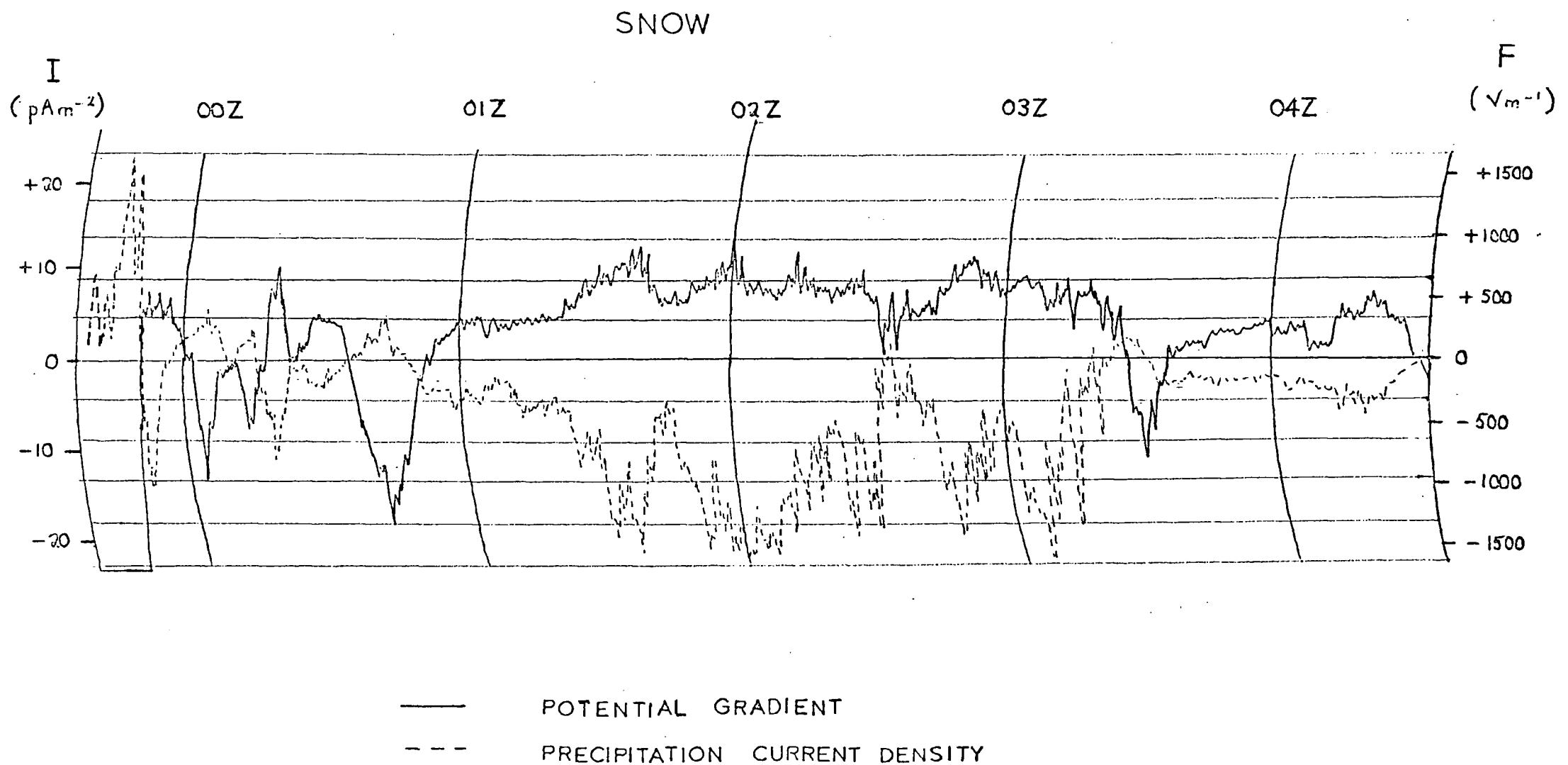

FIG. 6.11

17/18 January 1972 (Snow)

Cross correlogram

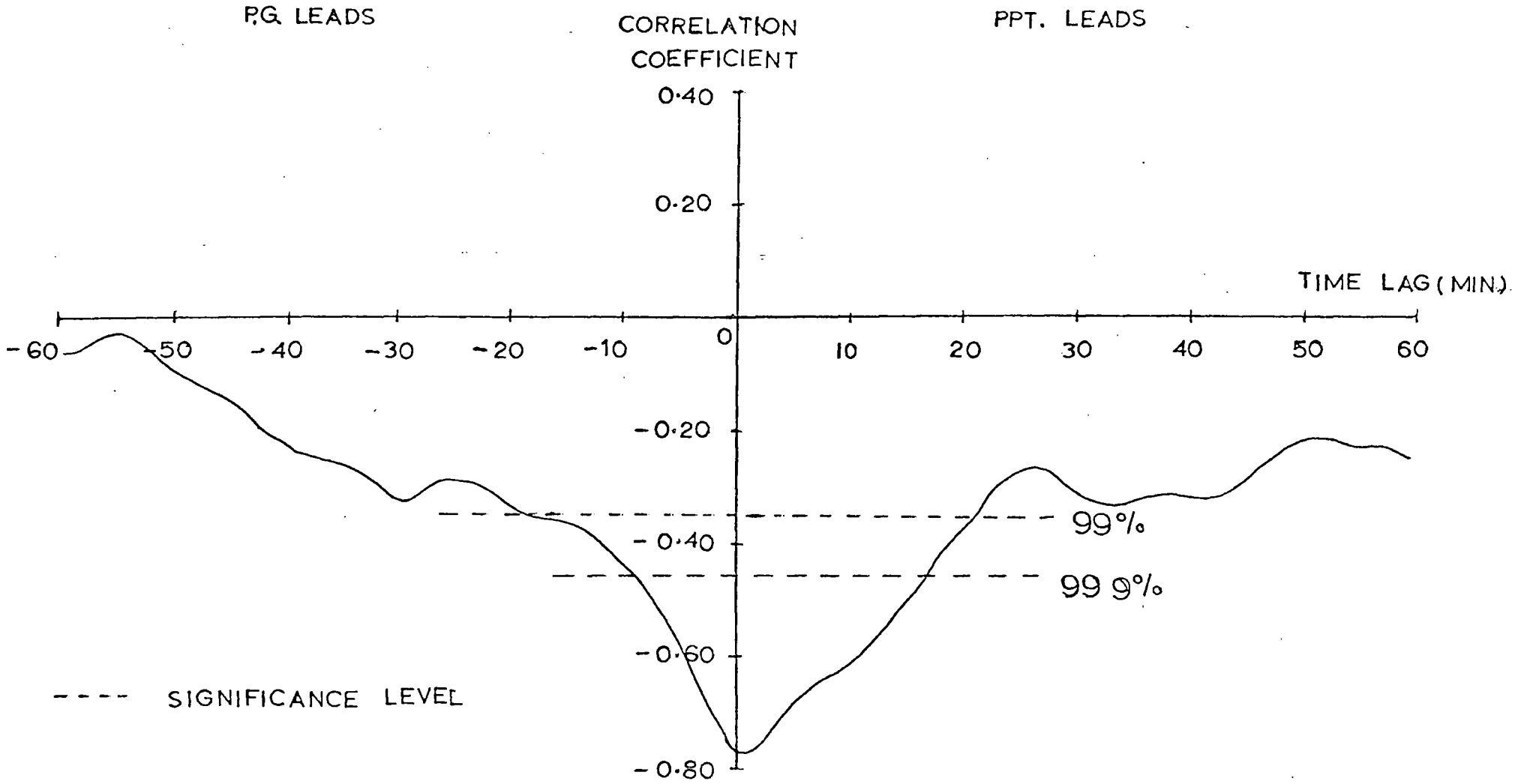

FIG 6.12

17/18 January 1972
SNOW

Autocorrelogram

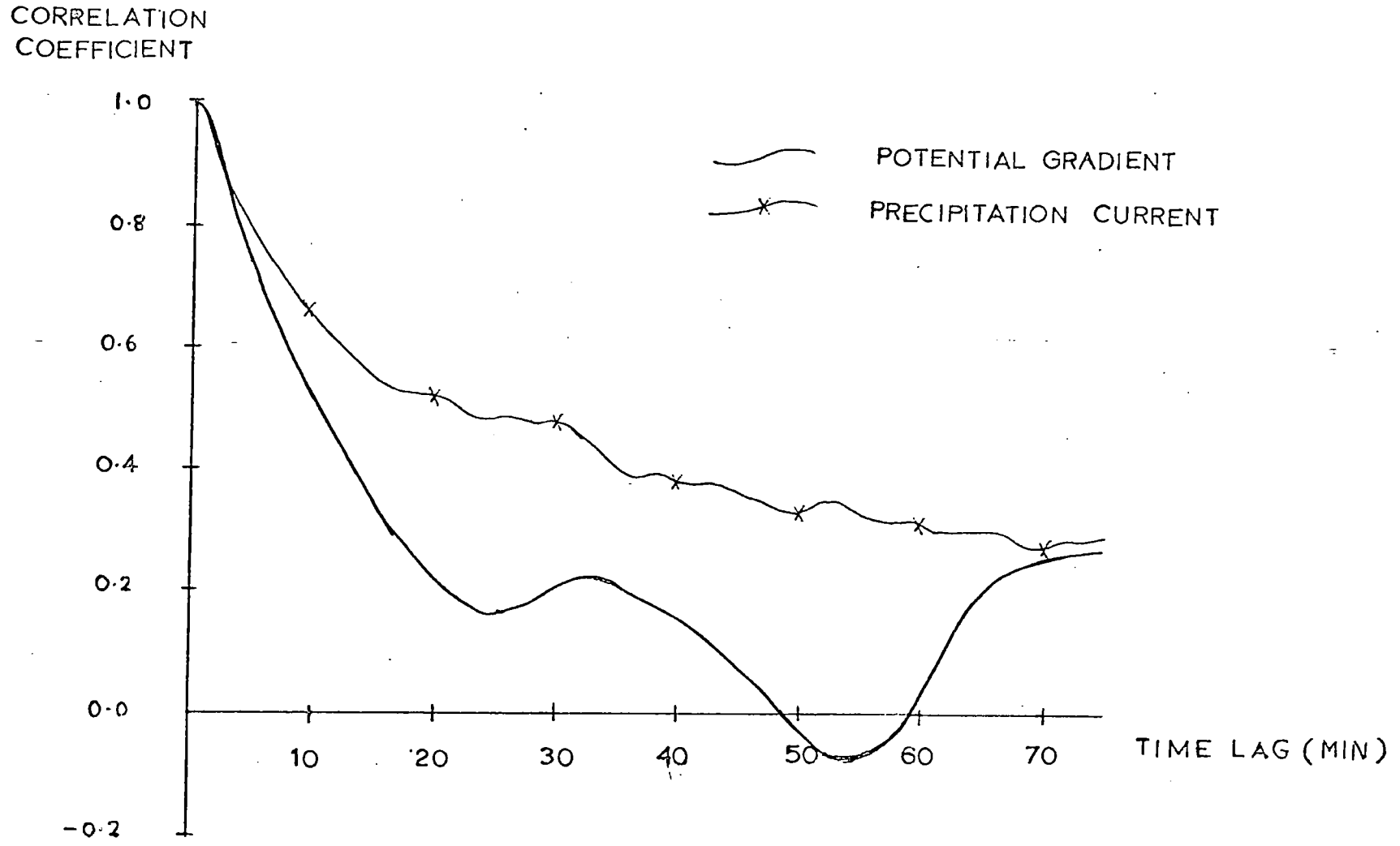

FIG. 6.13 Shanwell 23Z 17 January 1972

DPH65 K.M.DAILY

AIR TEMPERATURE ——

DEW POINT - - -

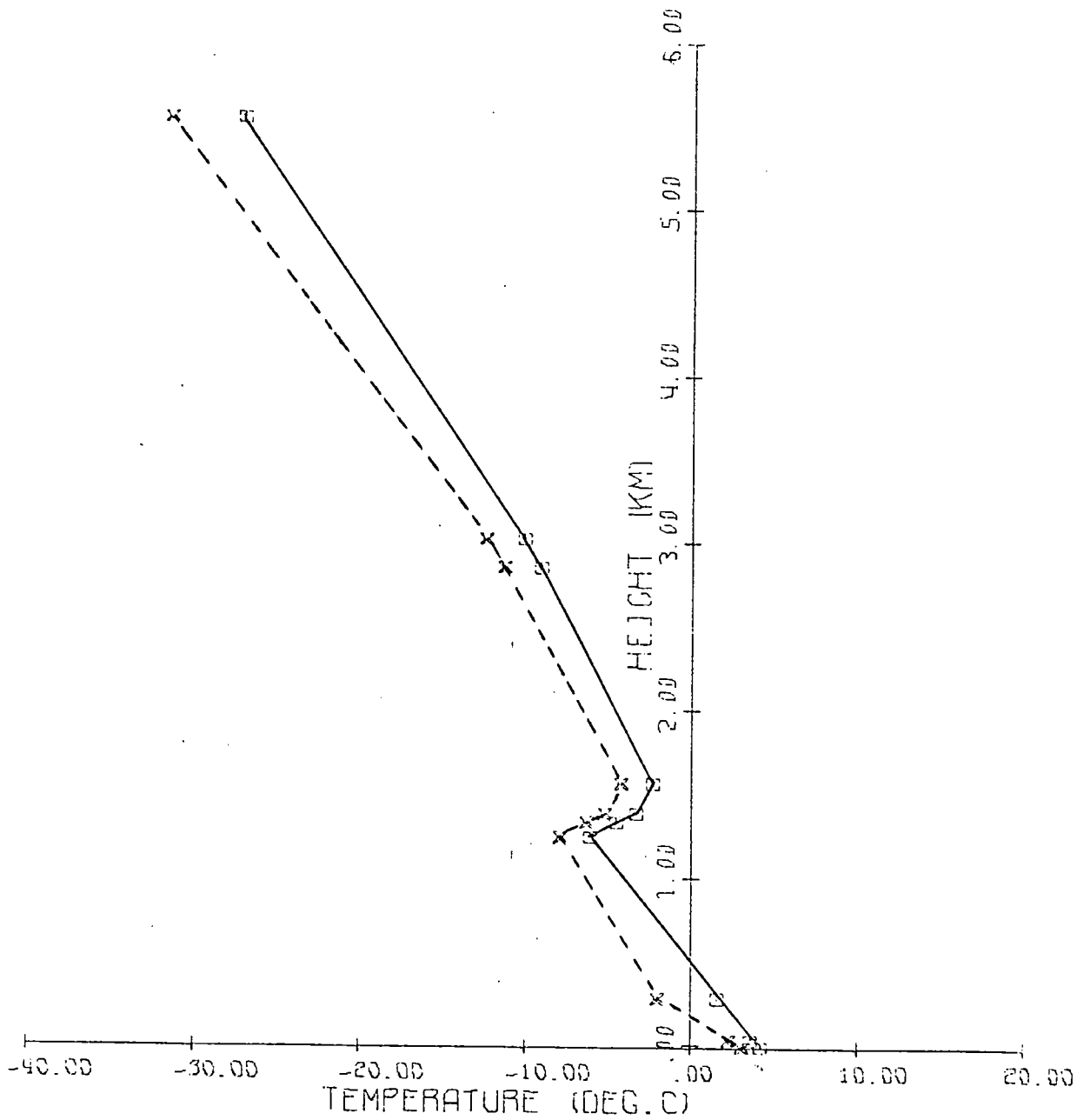

FIG.6.14 Shanwell 23Z 17 January 1972

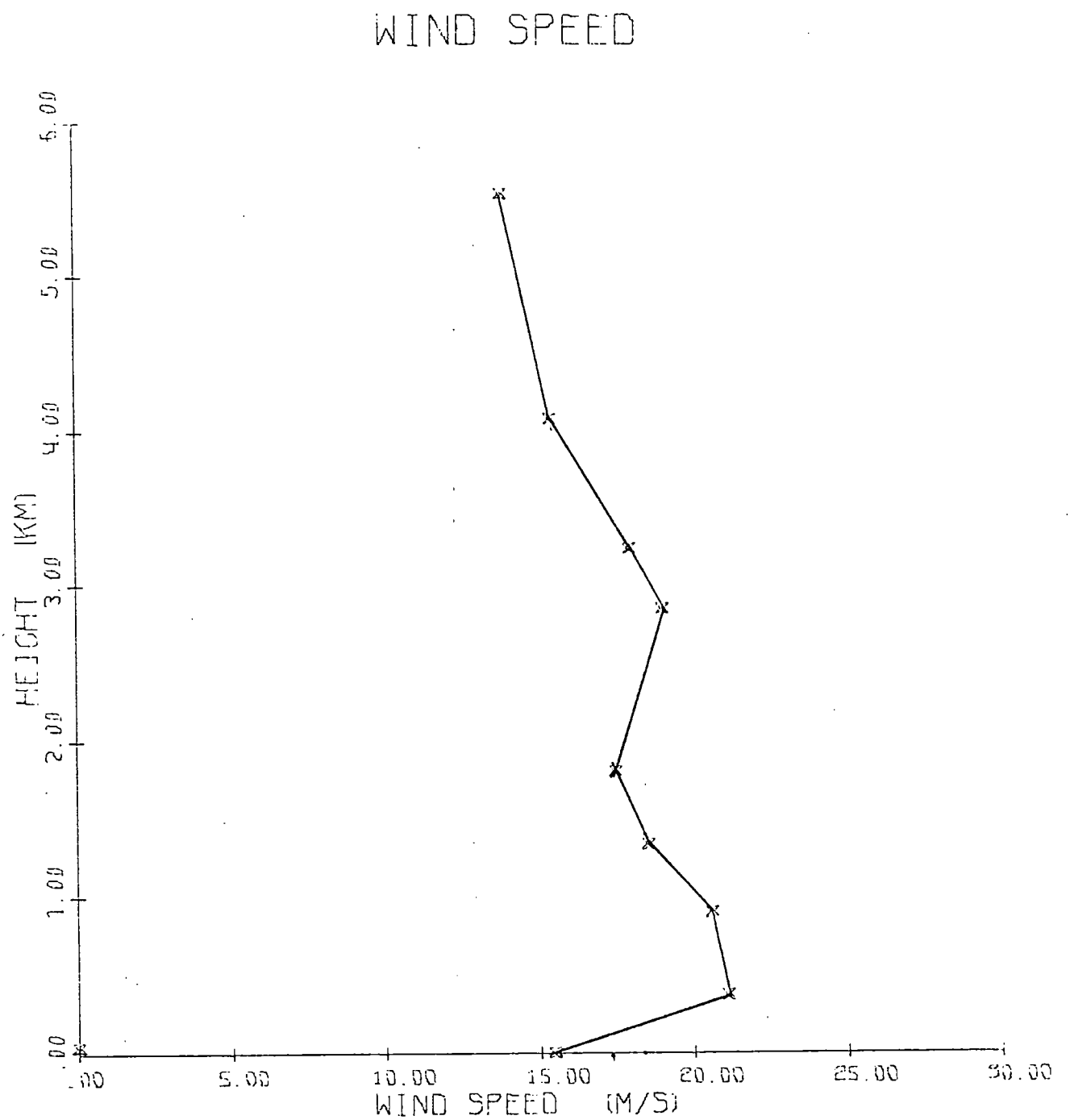

Shanwell

FIG. 6.15 23Z 17 January 1972

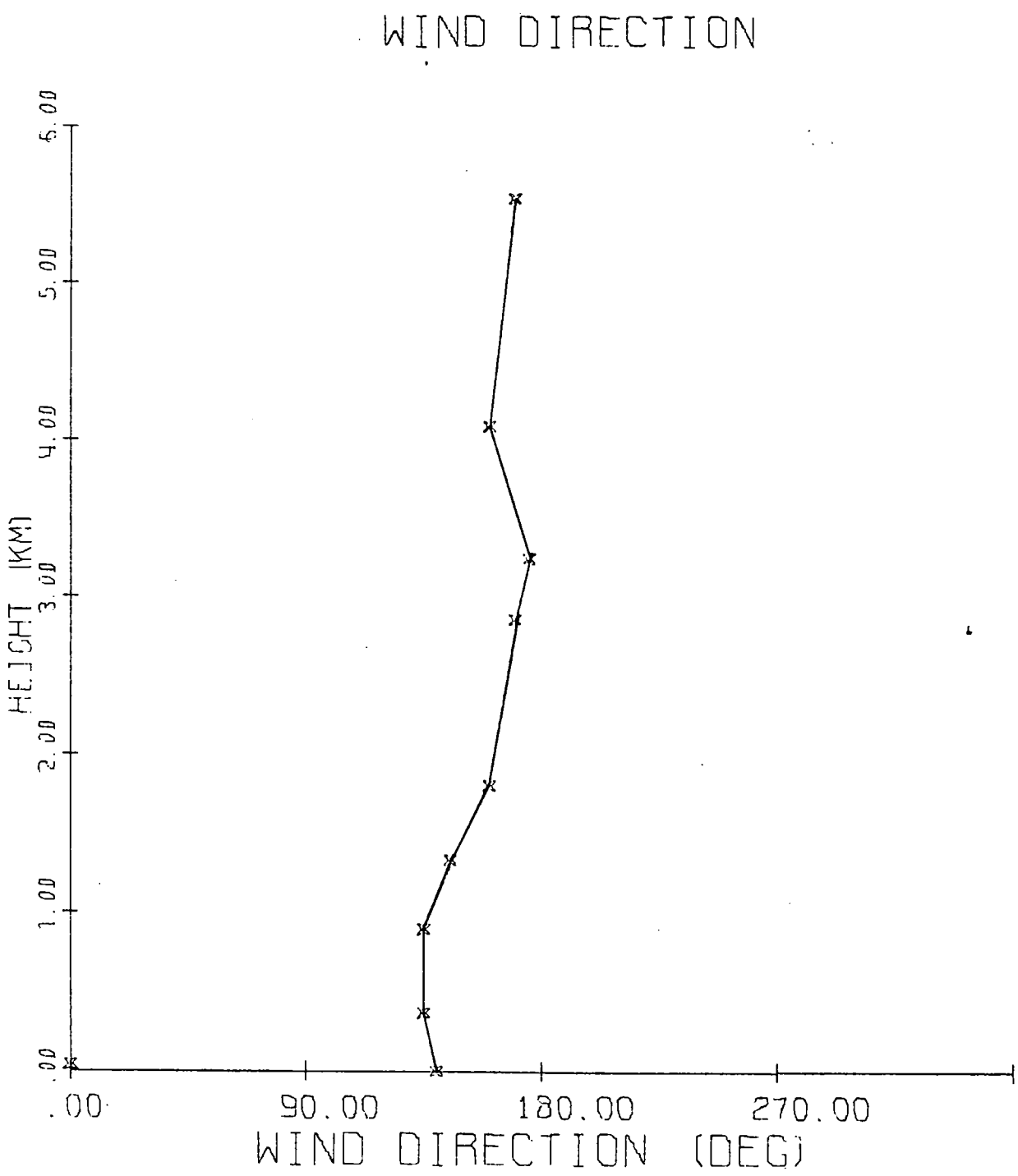

ways typical of the majority of periods of quiet precipitation, a few instances showed different behaviour. Several periods of quiet rain were characterised by the very quiet conditions and the long duration of the rain, as well as by the electrical behaviour: one of these periods is now presented.

6.3.1 The period of rain

Quiet rain fell at Durham for no less than 20 hours, from 18 00 on the 2nd May to about 14 00 the following day. The synoptic situations at 00Z and 12Z of 3rd May are shown in Fig. 6.16; a very slow moving region of precipitation persisted over northern England, probably associated with the weak occluded front which appears on the synoptic situation at 12Z. Conditions were very quiet, with winds being light and variable.

The electrical record is reproduced in Fig. 6.17 for the entire period of precipitation. An interesting feature is the different behaviour of the potential gradient and precipitation current in the earlier and later parts of the record. Initially, until about 03 30, the two records appear to follow each other closely, with the potential gradient leading by about 15 minutes. There is neither an inverse relation nor mirror-image effect evident. Subsequently, the character of the record changes, with both effects being evident at times, and with the precipitation current now appearing to lead.

6.3.2 Statistical results

The electrical behaviour apparent from the chart record is confirmed by the cross-correlogram of Fig. 6.18. Two maxima are evident; one, significant at the 95% level, for precipitation current leading by 22 minutes, with a second broad maximum for

FIG. 6.16 Synoptic situation of 2/3 May 1972

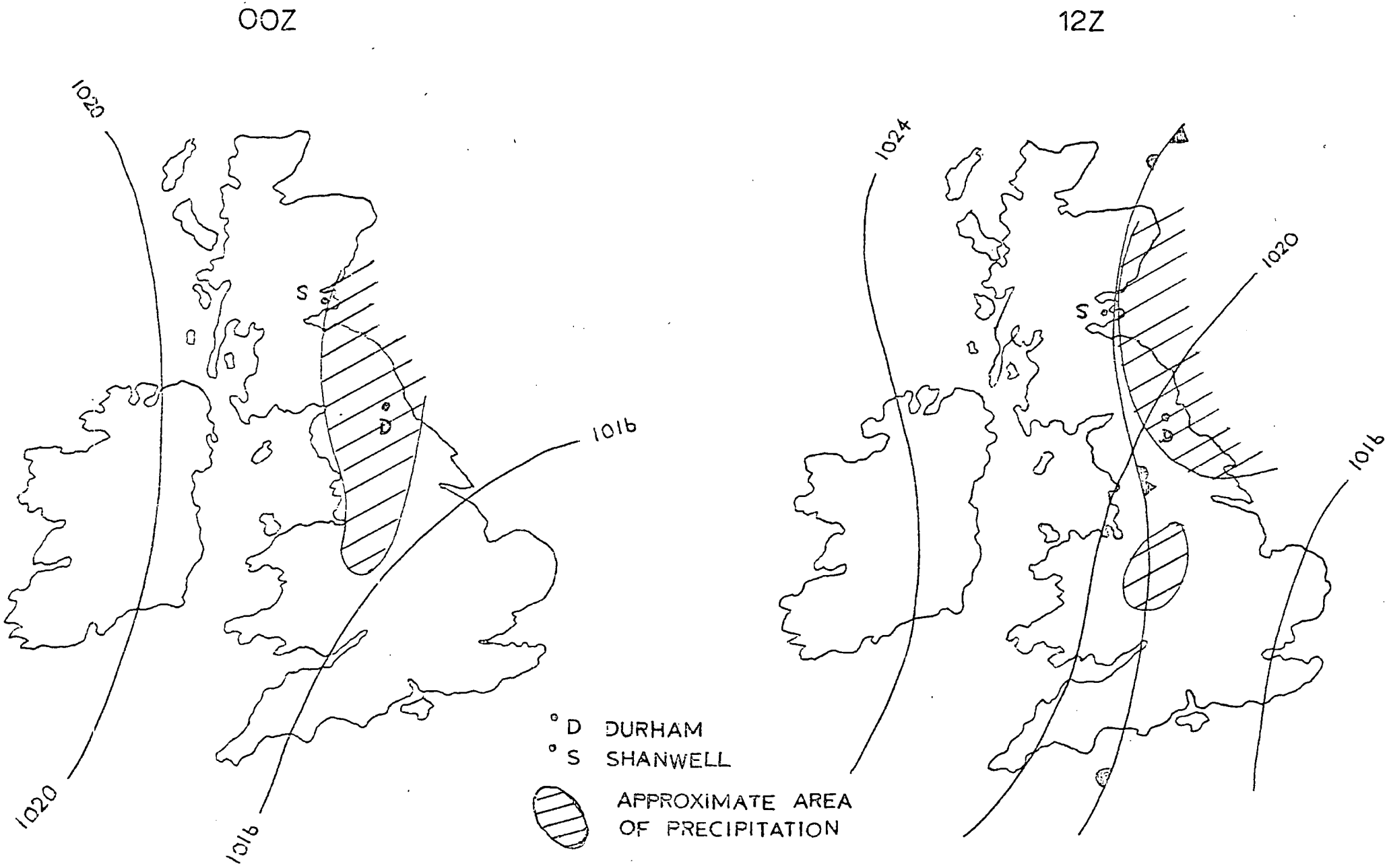

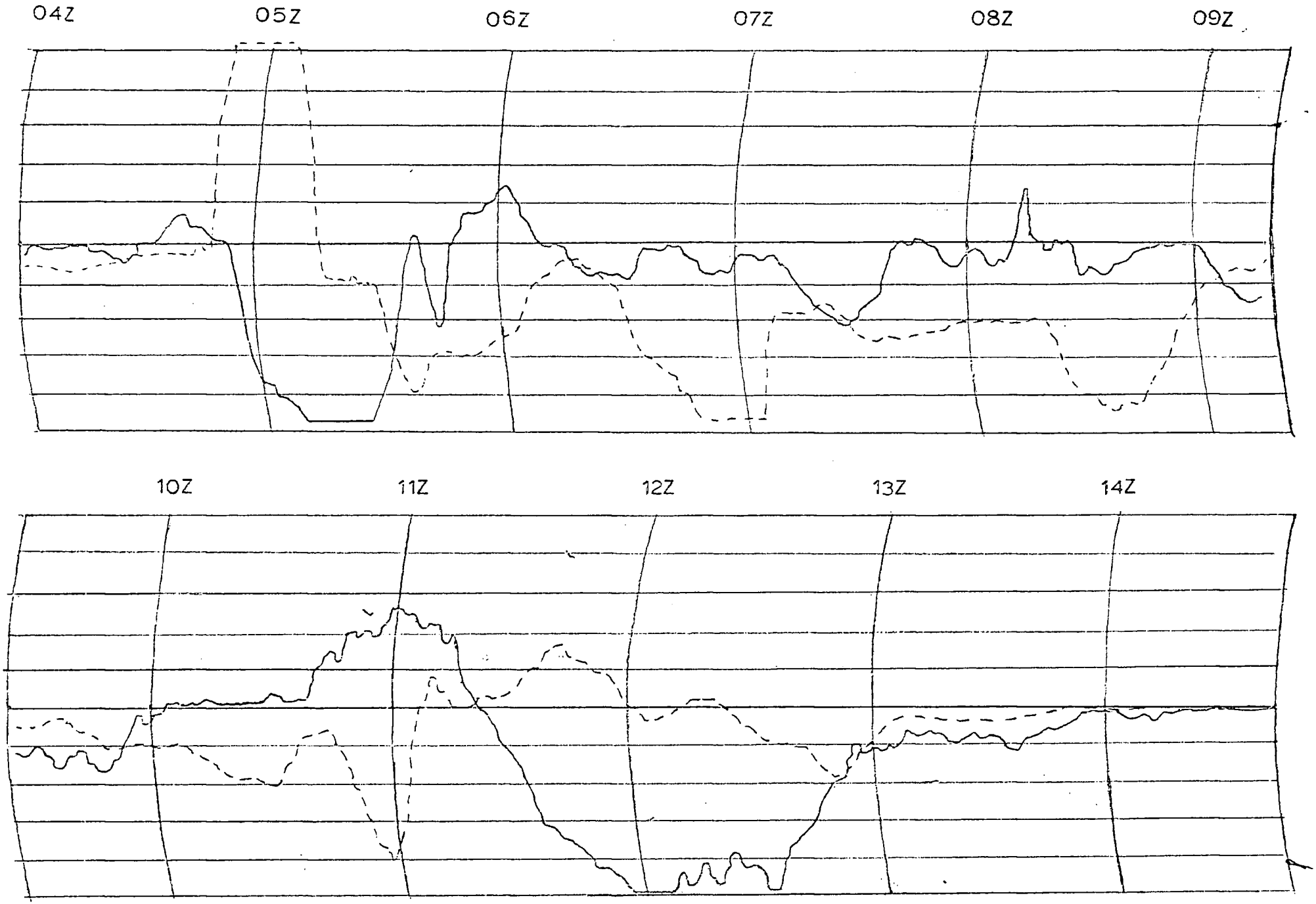
04Z
05Z
06Z
07Z
08Z
09Z
10Z
11Z
12Z
13Z
14Z

FIG. 6.18

2/3 May 1972

Cross-correlogram

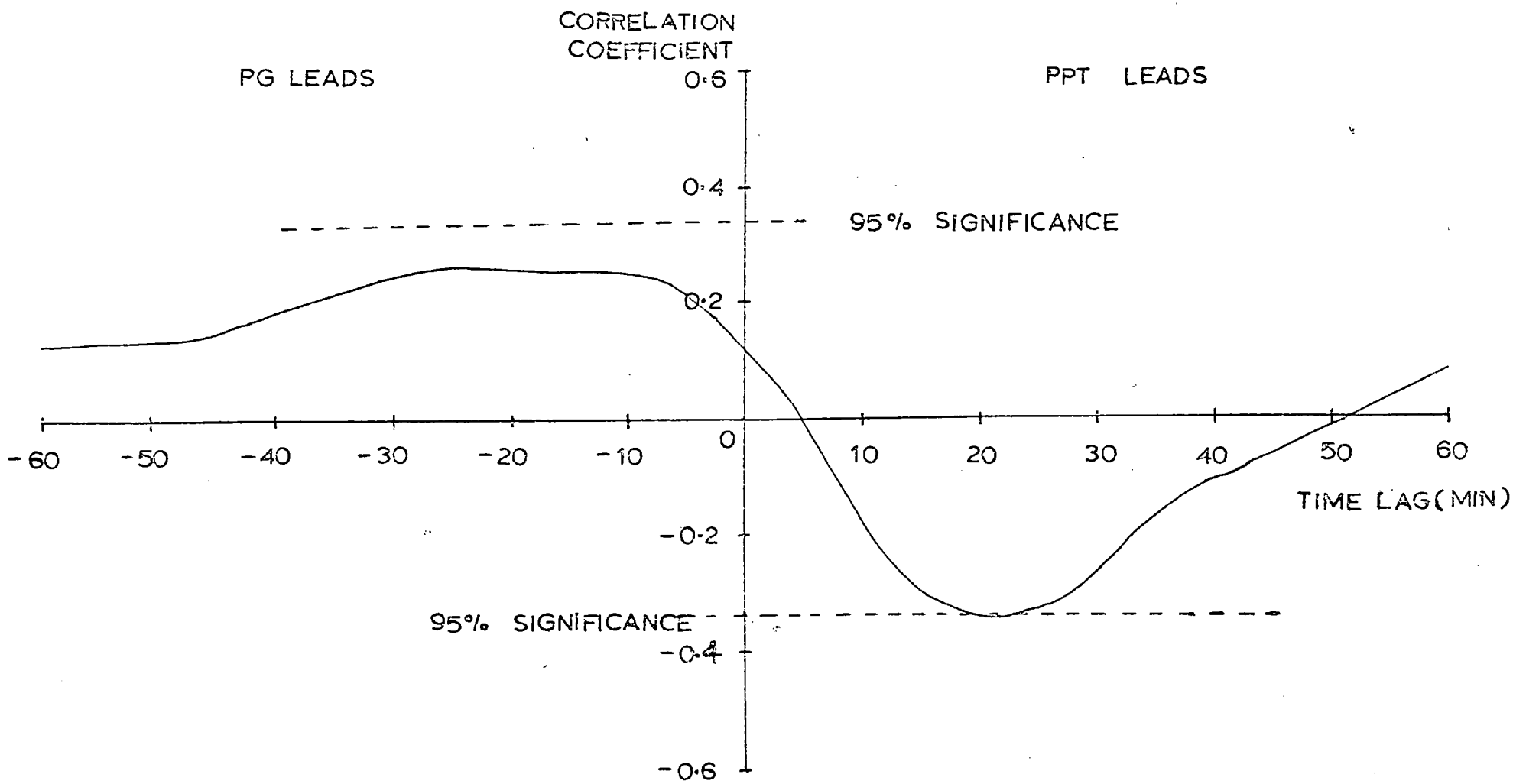

potential gradient leading by about 20 minutes. The first maximum is negative, indicating a mirror-image effect with the precipitation current leading by 22 minutes. The second is positive, corresponding to the earlier part of the record, where the potential gradient and precipitation current follow each other closely.

The autocorrelograms (Fig. 6.19) indicate considerable persistence in both the potential gradient and precipitation current, due to their show variation; maxima on the chart record recur at intervals of about 90 minutes. There is also a suggestion of a secondary, faster, periodicity of about 35 minutes in the precipitation current.

6.3.3 Meteorological situation

The quietness of the electrical behaviour is reflected in the meteorological conditions. The mean wind speed at Durham (Table 6.1) is particularly low. The aerological profiles at Shanwell, at 23Z on the 2nd May also show particularly low wind speeds (Fig. 6.21) of less than 5 ms^{-1} at as high as 3 km altitude. Also noticeable is the absence of any region of negative wind shear. The wind direction profile of Fig. 6.22 does however show a considerable change in wind direction between 1 and 2 km; this may well be erroneous, as no similar shift occurs in the profile at 11Z on 3rd May, when conditions otherwise are very similar.

6.4 A period of disturbed precipitation: 26 January, 1972.

By way of comparison, a period of disturbed precipitation will now be briefly examined. One such period occurred during

Autocorrelogram

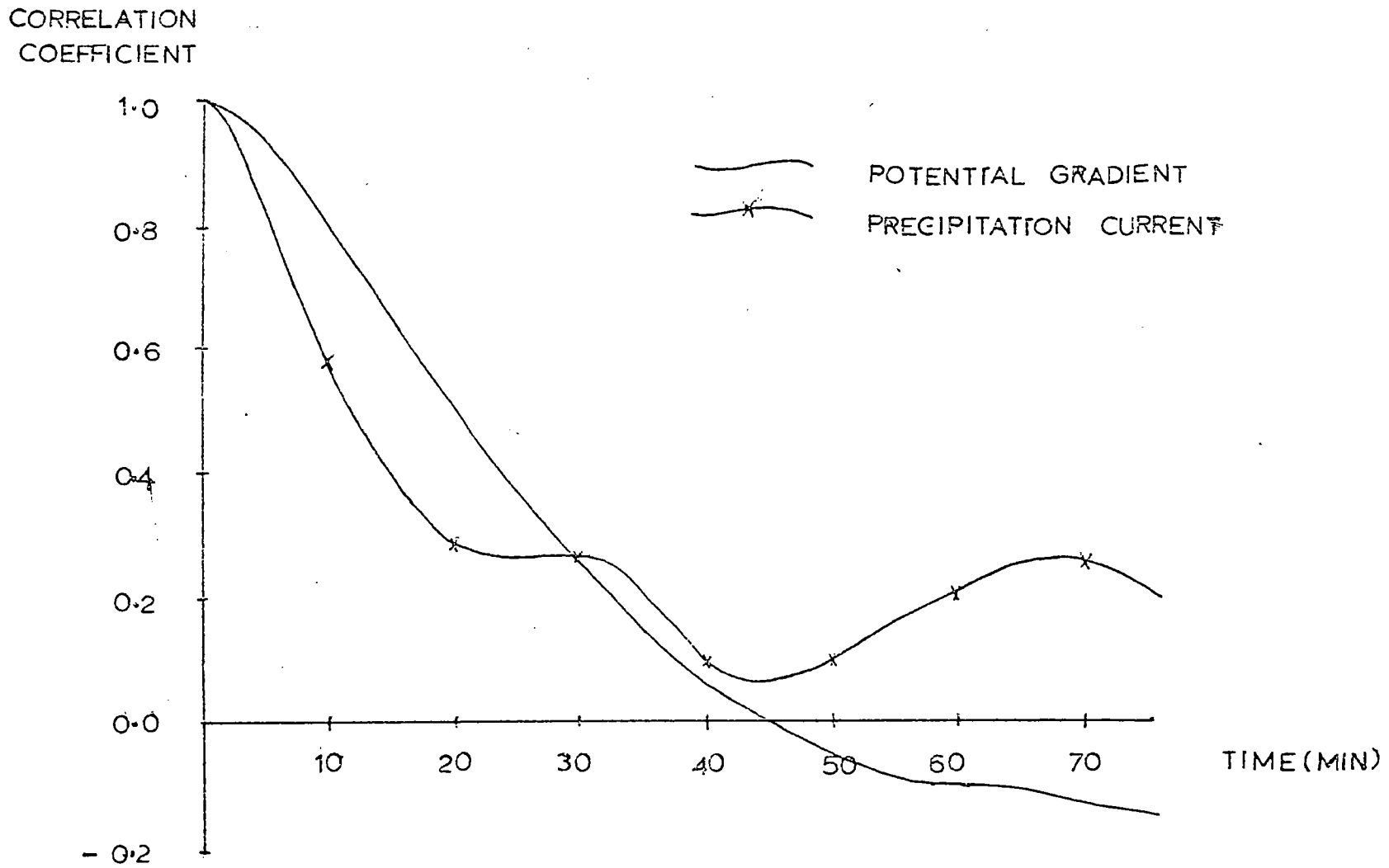

FIG. 6.20 Shanwell 23Z 2 May 1972

DPH65 K.M.DAILY

AIR TEMPERATURE —

DEW POINT – – –

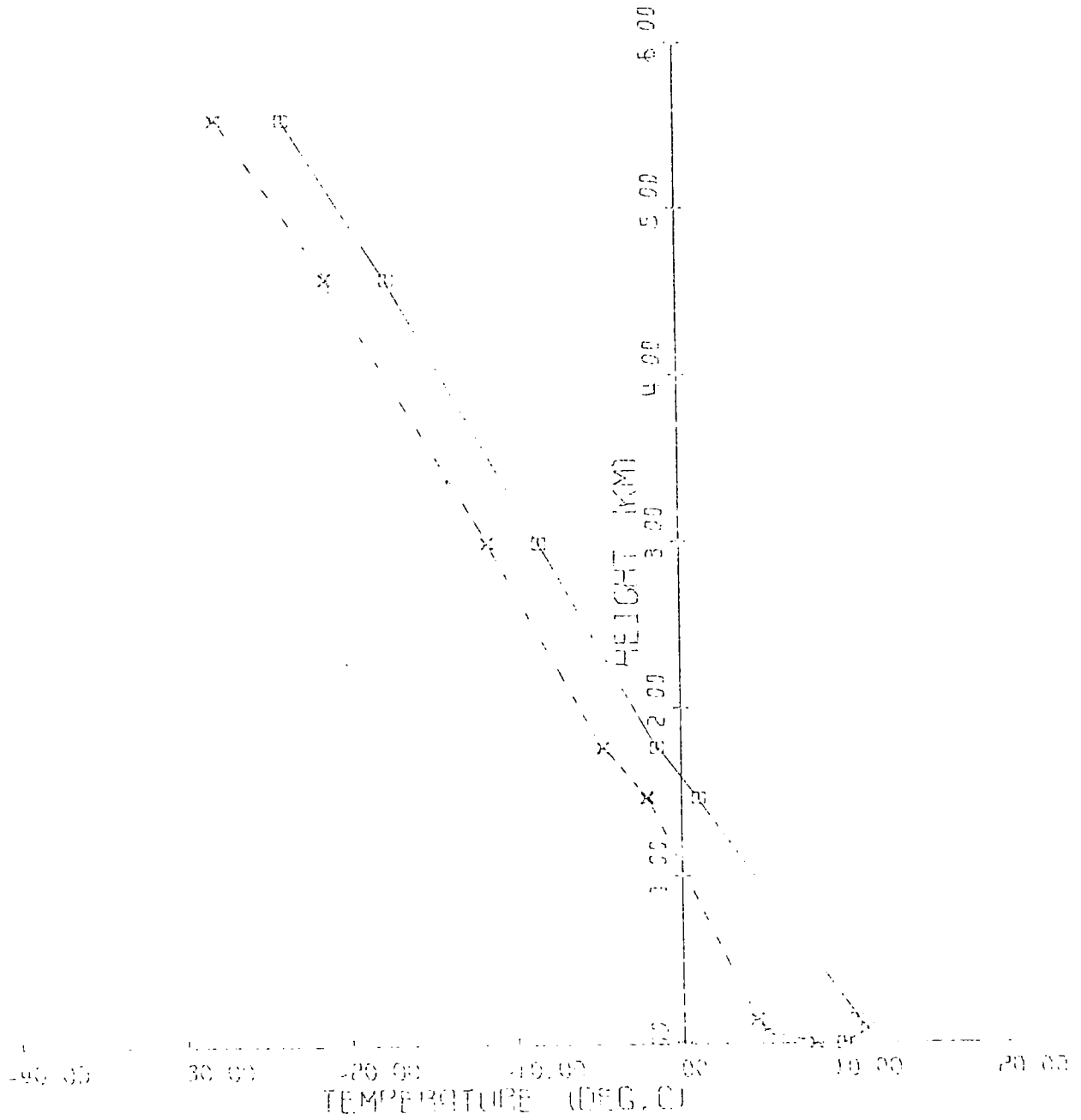

FIG. 6.21 Shanwell 23Z 2 May 1972

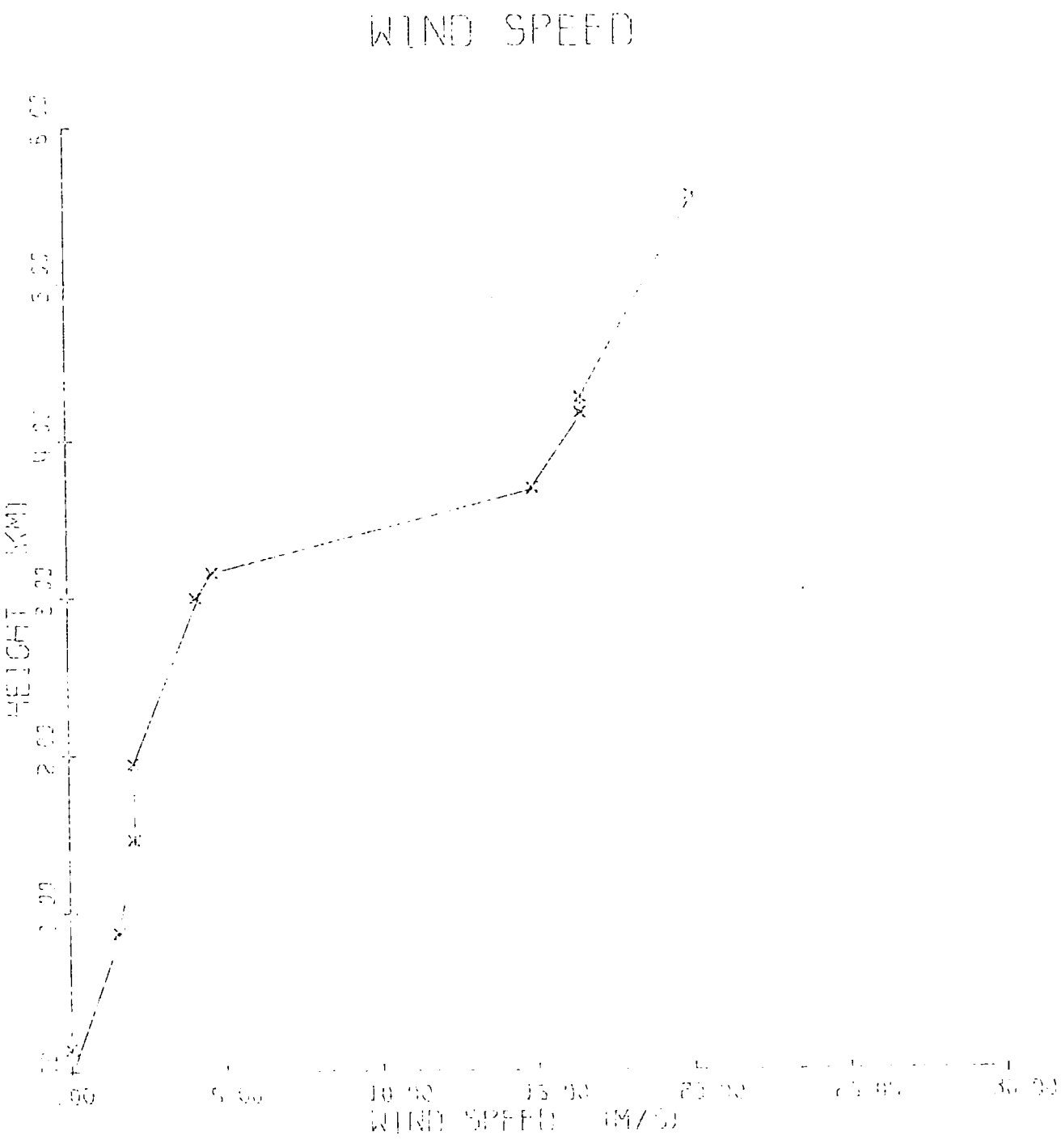

FIG. 6.22 Shanwell 23Z 2 May 1972

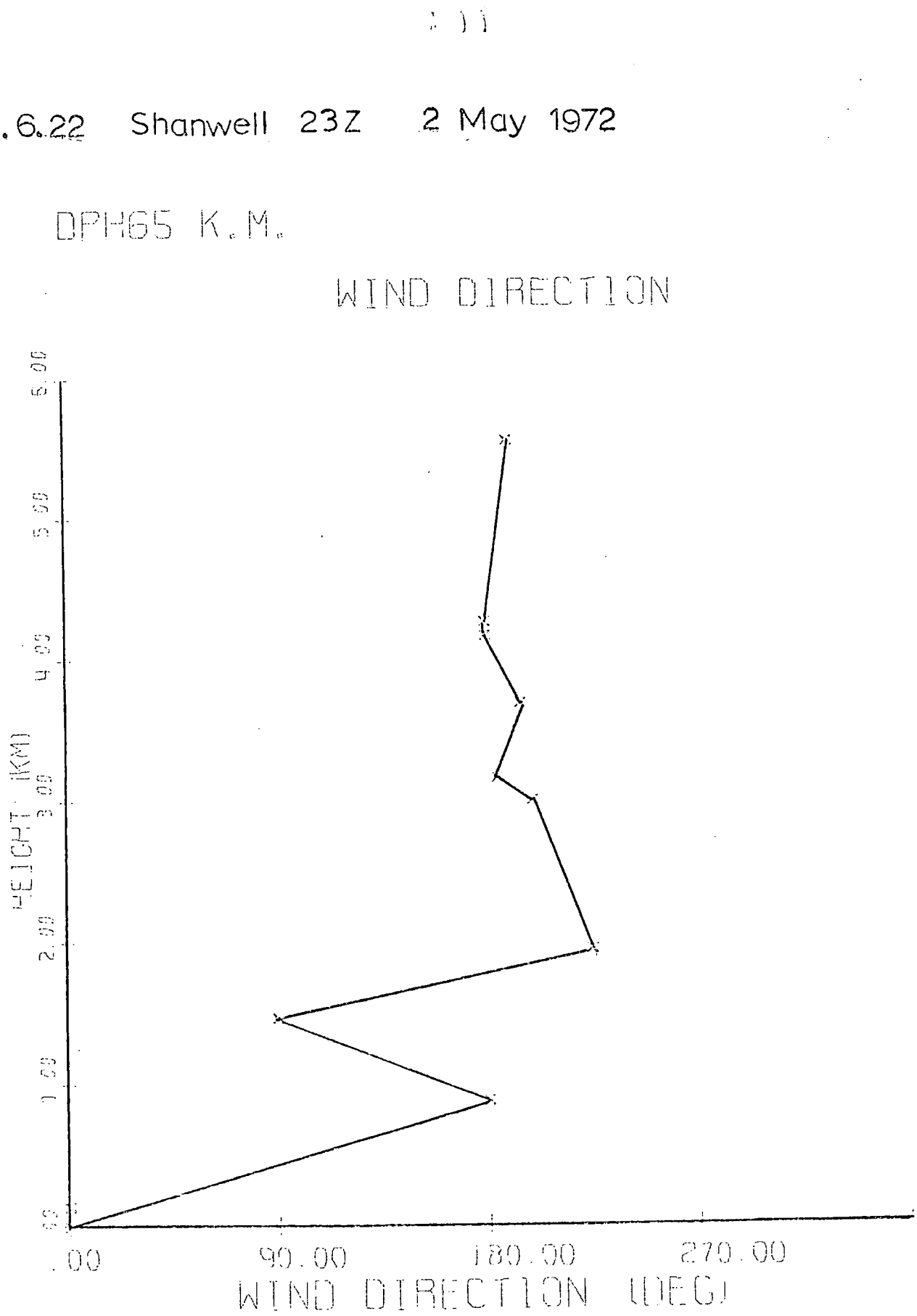

the late afternoon and evening of the 26 January 1972, producing heavy continuous rain at Durham from about 13 30 to 22 10, except for the period from 17 45 to 19 15, when the rain was somewhat lighter. The synoptic situation is shown in Fig. 6.23; a fast-moving frontal system associated with a depression moving eastwards across northern England.

6.4.1 The electrical behaviour

A portion of the precipitation current record is shown in Fig. 6.24. The record shows much more rapid and frequent changes in precipitation current than during quiet precipitation; note that the precipitation current density values are also much greater. No reliable potential gradient record is available on this occasion, as for much of the time the record was off-scale, or changing too quickly to be distinguished. An idea of the behaviour during disturbed precipitation can be obtained from Fig. 6.25, where the electrical record during a less violent period of disturbed precipitation on 3 Februrary 1972 is reproduced. On this occasion a mirror-image effect is also noticeable, indicating that it is not limited to conditions of quiet precipitation.

6.4.2 The meteorological situation

The meteorological conditions at Durham are shown in Table 6.1; the rate of rainfall was much higher, at 2.3 mm hr^{-1} than usual in quiet precipitation, as was the mean surface wind speed, at 10 ms^{-1}. Aerological profiles at Shanwell at 11Z (Figs. 6.26 to 6.28) show a similar situation, with considerable wind shear near the ground, and wind speeds of up to 15 ms^{-1}, at 3 km. altitude.

FIG. 6.23 Synoptic situation of 26 January 1972

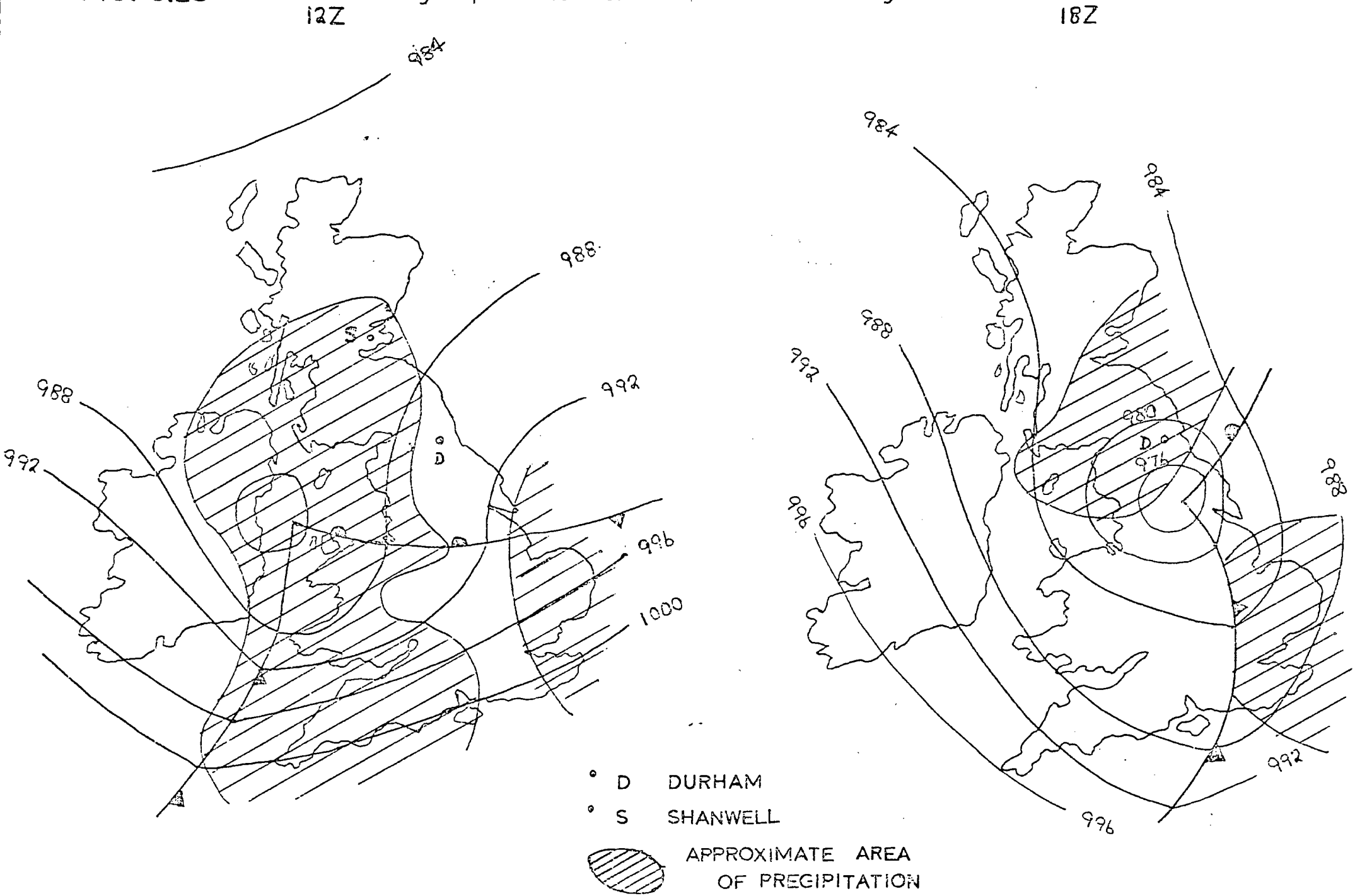

FIG. 6.24 Precipitation current record of 26 January 1972

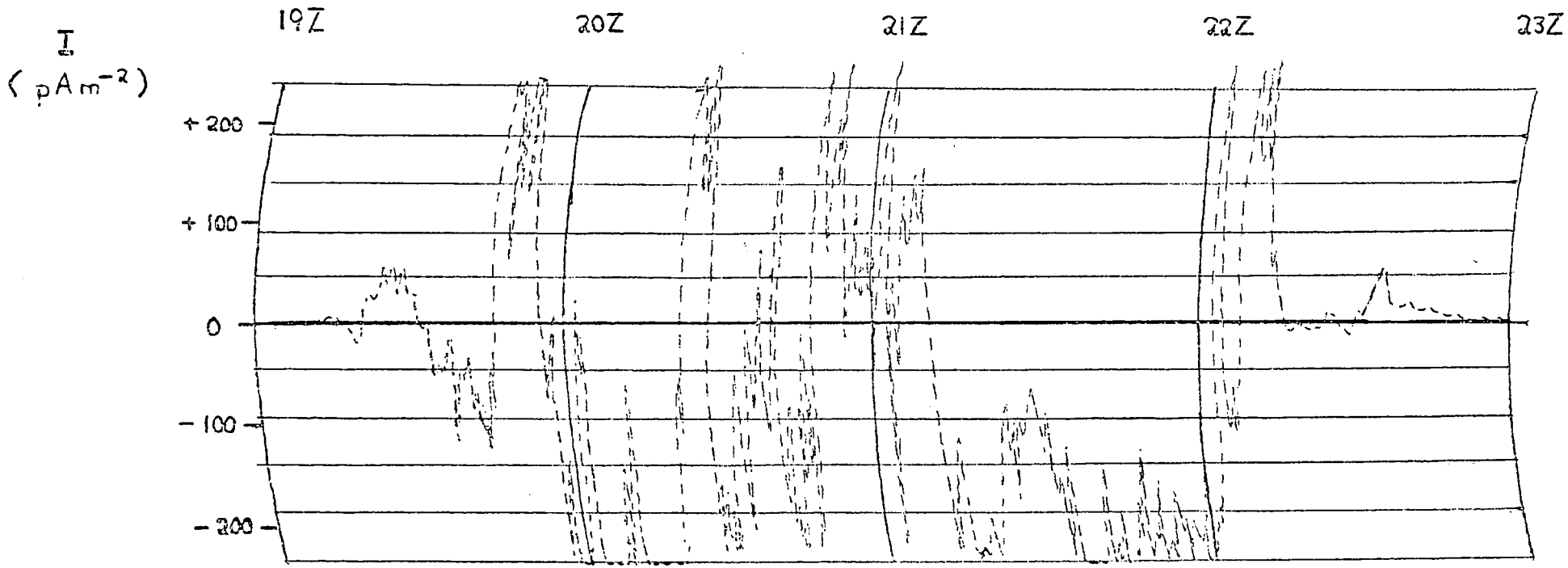

FIG. 6.25 Precipitation record of 3 February 1972

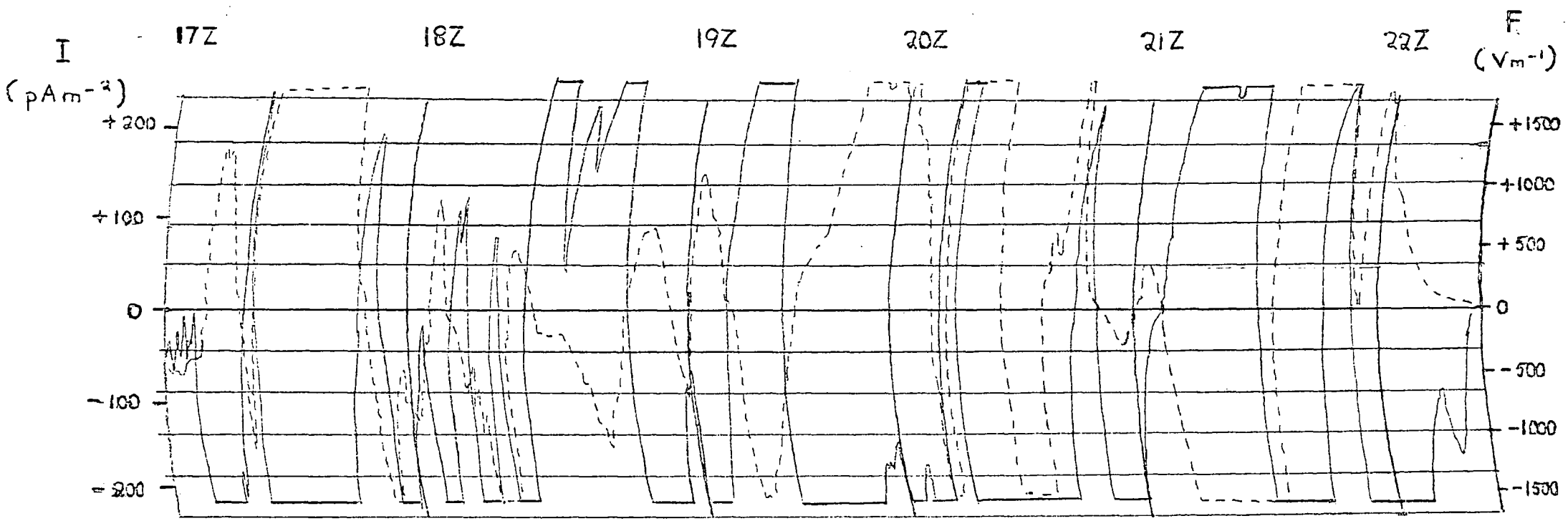

——— POTENTIAL GRADIENT

– – – – – PRECIPITATION CURRENT DENSITY

FIG. 6.26 Shanwell 11Z 26 January 1972

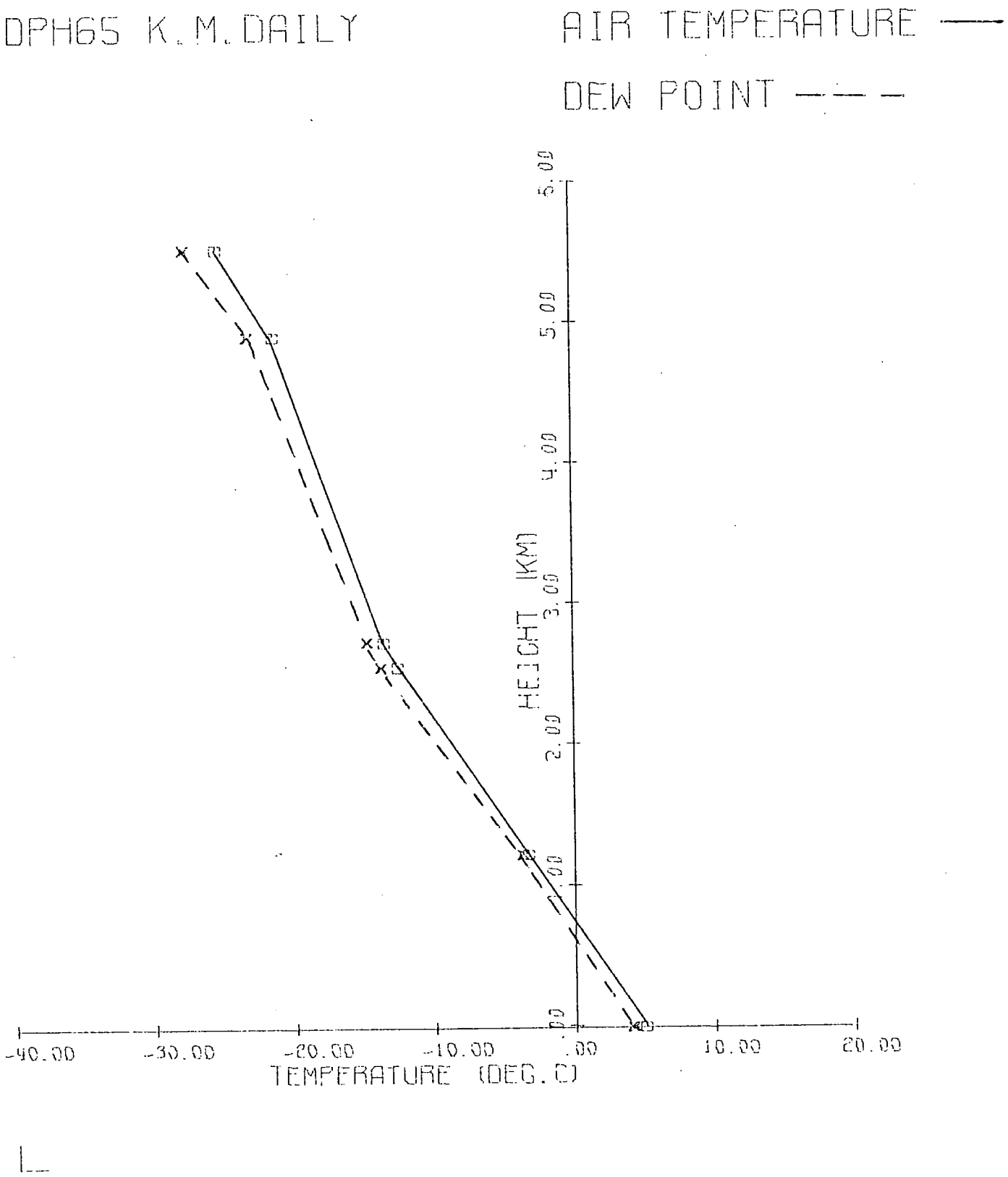

FIG. 6.27 Shanwell 11Z 26 January 1972

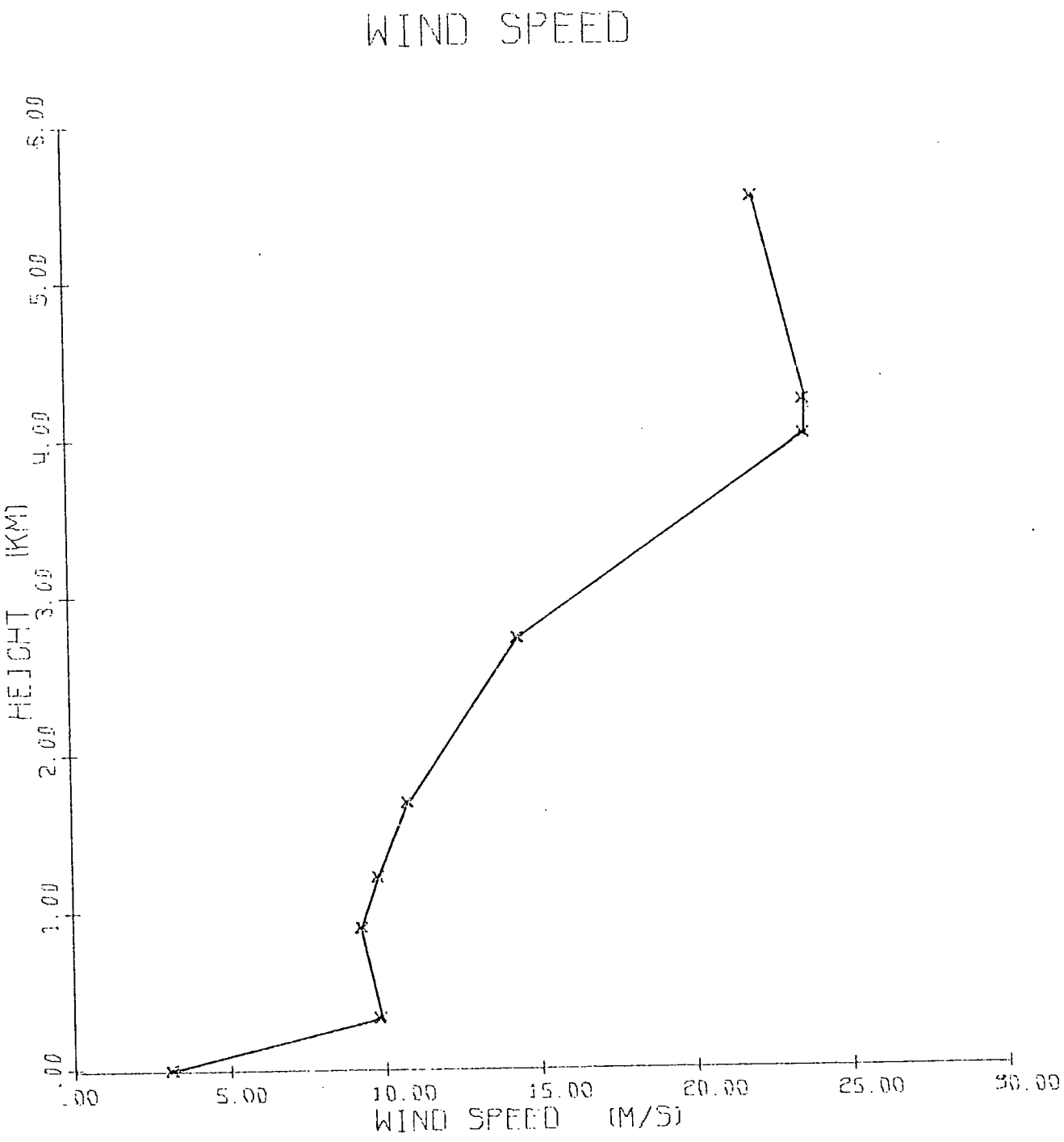

FIG. 6.28 Shanwell 11Z 26 January 1972

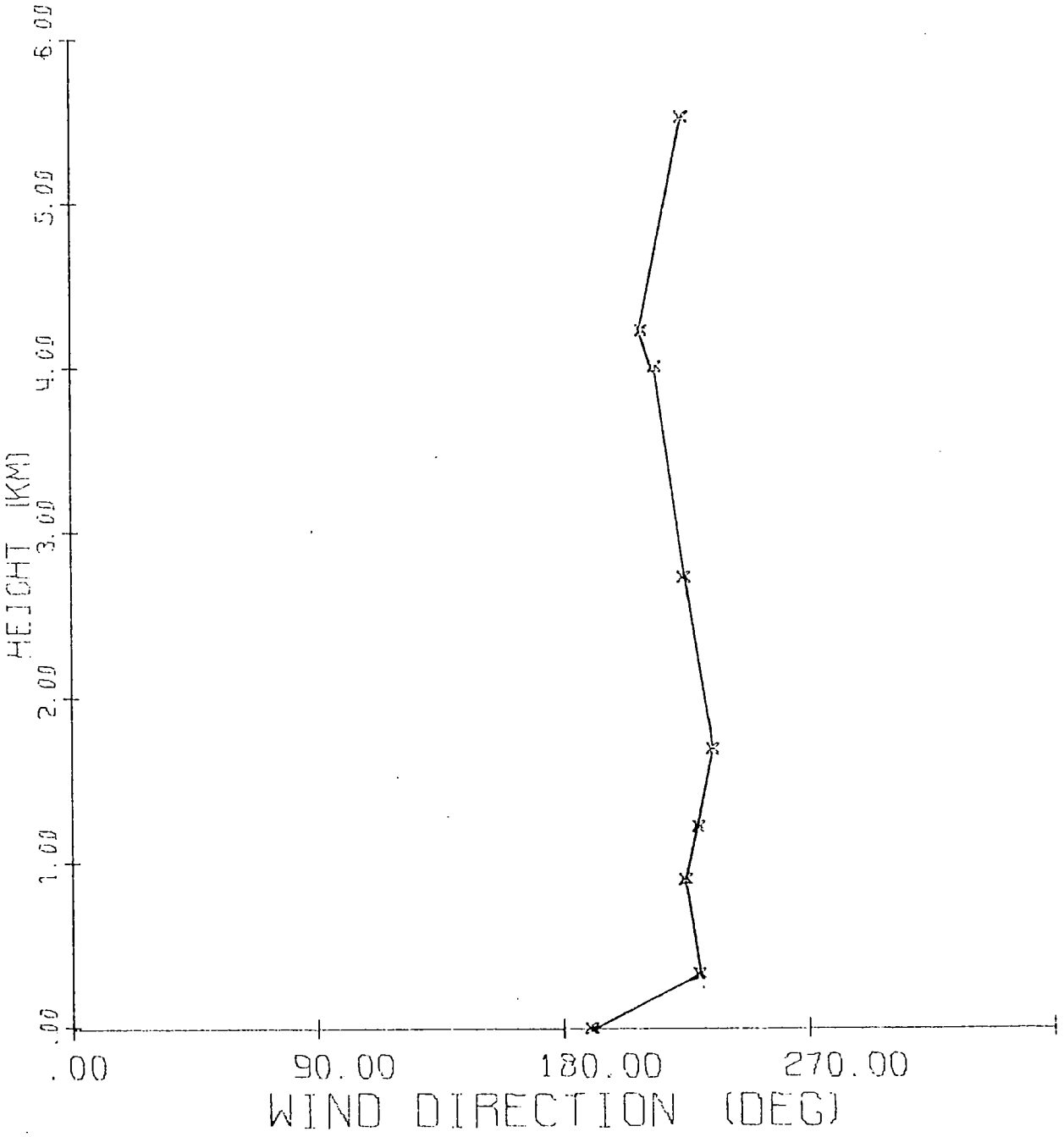

CHAPTER 7

Results of the Quiet Precipitation Measurements

7.1 Introduction

The results of the quiet precipitation measurements at Durham during the period January to June 1972 are now presented, together with the associated meteorological conditions for each occasion. The data handling system recorded nearly all instances of quiet precipitation during this period, and so the results can be taken as characteristic of quiet precipitation in general during these six months. A few chart records of quiet precipitation had been obtained during the previous spring and summer, but with one or two exceptions were not suitable for analysis. The results of the precipitation measurements will consequently be confined in this Chapter to the periods recorded during 1972, although some earlier records will be considered later.

7.2 The electrical properties of the quiet precipitation records.

Table 7.1 lists the electrical characteristics of all the periods of quiet precipitation recorded between January and June, 1972. The mean values and standard deviations of the potential gradient and precipitation current density are given, together with the percentage of positive values of these parameters during the record. The values are those recorded every 30 seconds by the data handling system. Altogether 35 periods of quiet precipitation, amounting to 195 hours, were recorded; this represented about 90% of all quiet precipitation during the six months,

TABLE 7.1 ELECTRICAL PROPERTIES OF PERIODS OF QUIET PRECIPITATION AT DURHAM

RECORD NO.	DATE (1972)		RECORD START	RECORD FINISH	MEAN VALUES		STANDARD DEV.		% POSITIVE VALUES	
			G.M.T.	G.M.T.	POTENTIAL GRADIENT	PPT. CURR. DENSITY	POTENTIAL GRADIENT	PPT. CURR. DENSITY	POTENTIAL GRADIENT	PPT. CURR. DENSITY
					$V m^{-1}$	$pA m^{-2}$	$V m^{-1}$	$pA m^{-2}$		
1/1 +	7/8		21 20	04 00	-670	-	660	-	15	45
1/2	8/9		19 00	03 45	-	-	-	-	7	78
1/3	11		10 30	14 30	-755	-	500	-	2	100
1/5	16.	JAN	19 50	23 50	-240	+0.5	505	7.0	30	47
1/6	17		08 20	14 00	-420	+2.5	450	10.1	11	73
1/7 ++	17/18		20 30	07 00	+175	-3.5	465	7.6	82	14
2/1 ++	1/2		18 15	01 30	+95	-0.8	190	24.4	82	16
2/3	6/7		19 20	02 30	-235	-8.0	250	4.3	10	0
2/4	8	FEB	17 50	22 30	-310	-	375	-	5	90
2/5 +	15		12 20	13 50	-670	+3.4	600	23.0	18	75

\+ Sleet
++ Snow

Other periods are rain

(cont.)

TABLE 7.1 (Continued)

RECORD NO.	DATE (1972)		RECORD START	RECORD FINISH	MEAN VALUES		STANDARD DEVIATIONS		% POSITIVE VALUES	
			G.M.T.	G.M.T.	POTENTIAL GRADIENT	PPT. CURR. DENSITY	POTENTIAL GRADIENT	PPT. CURR. DENSITY	POTENTIAL GRADIENT	PPT. CURR. DENSITY
					Vm^{-1}	pAm^{-2}	Vm^{-1}	pAm^{-2}		
3/1	1		02 00	09 50	-630	+1.7	500	1.7	11	95
3/5	6		17 00	23 15	-520	+2.1	340	2.5	5	79
3/6	7	MAR	16 45	21 00	-40	+0.5	420	6.3	23	57
3/7	8		01 30	13 30	-520	+5.0	515	4.2	13	98
3/10	30		06 00	10 00	-960	-	420	-	0	7
3/11	31		15 00	18 15	-	-	-	-	1	100
4/2	6/7		23 45	03 15	-490	+1.1	560	2.3	21	51
4/4	8		02 45	04 10	-405	+2.9	420	2.4	11	90
4/5	8/9		16 25	03 15	-500	+7.5	475	4.8	1	100
4/6	10	APR	03 00	08 45	-520	+5.8	480	2.5	10	99
4/7	26/27		22 00	00 30	-550	+2.7	540	6.6	10	61
4/8	29		09 25	11 55	-145	+2.2	-	-	43	94

(cont.)

TABLE 7.1 (Continued)

RECORD NO.	DATE (1972)		RECORD START	RECORD FINISH	MEAN VALUES		STANDARD DEVIATIONS		% POSITIVE VALUES	
			G.M.T.	G.M.T.	POTENTIAL GRADIENT	PPT. CURR. DENSITY	POTENTIAL GRADIENT	PPT. CURR. DENSITY	POTENTIAL GRADIENT	PPT CURR DENSITY
					Vm^{-1}	pAm^{-2}	Vm^{-1}	pAm^{-2}		
5/1	2/3	MAY	18 00	13 00	-280	-4.0	510	9.0	23	11
5/2	5/6		16 10	06 45	-675	+1.7	335	1.2	7	97
6/5	4/5		22 00	04 00	-775	+6.8	630	11.5	13	67
6/6	7		06 30	11 00	-350	+10.5	820	8.8	42	100
6/7	9		07 10	09 45	-480	+2.0	440	6.8	10	37
6/8	10		05 10	08 15	-510	+2.7	320	6.0	11	72
6/9	10/11		22 15	08 00	-330	+9.1	430	5.6	1	100
6/11	12	JUN	10 10	12 45	-	-	-	-	56	32
6/13	18		01 15	05 30	-	-	-	-	4	26
6/14	19		10 00	13 45	-280	+6.0	795	8.8	38	82
6/16	26		06 45	11 30	+150	-2.3	470	11.9	73	48

POTENTIAL GRADIENT VALUES IN Vm^{-1} (GIVEN TO NEAREST 5 Vm^{-1})

PRECIPITATION CURRENT DENSITY VALUES IN pAm^{-2}

records being unavailable on the other occasions due to instrumental failure, or faulty recording.

It should be noted that periods of light or intermittent drizzle and very light rain were excluded due to the very small precipitation currents and consequently the uncertain behaviour of the collector in such conditions.

7.2.1 Quiet rain

Apart from two instances of snow and two of sleet, all the recordings were made during rain. The mean potential gradient on most occasions of rain was negative, and the mean precipitation current was positive. The "inverse relation" thus applied overall in these cases. The same conclusions can be made if the percentage of positive values of these two parameters is examined; 22 of the 29 periods of rain had mostly negative values of potential gradient and at the same time mostly positive precipitation current.

Taking the records when this situation applied, the overall mean potential gradient was -490 Vm^{-1}, and the overall mean precipitation current density + 4.6 pAm^{-2}.

There were, however, a number of instances when overall the inverse relation did not apply, or the usual signs of the electrical quantities were not found. Record 6/16 of the 26 June, for instance, shows the inverse relation, but with a mean positive potential gradient and mean negative precipitation current. The long record 5/1 of the 2 and 3 May, already referred to in Chapter 6, has mean potential gradient and mean precipitation current both negative; a similar instance is record 2/3 of the 6 and 7 February. There was, incidentally, no instance of the

mean potential gradient and precipitation current both being positive.

7.2.2 Quiet snow and sleet

The two periods of quiet snow (records 1/7 and 2/1) both showed an inverse relation, but with a negative precipitation current and a positive potential gradient. Their magnitudes were similar to those during rain, although it should be remembered that the collector is likely to be less efficient at collecting snow than rain, particularly at wind speeds in excess of a few metres per second.

The two periods of sleet, records 1/1 and 2/5, differed in behaviour, with negative potential gradient in both cases but an overall inverse relation only in the latter case. All other periods of sleet between January and April produced disturbed precipitation.

7.3 The potential gradient and precipitation current correlograms

Auto and cross-correlograms were calculated for 21 of the periods of quiet precipitation, the data on other occasions being unsuitable or unavailable. All the cross-correlograms between potential gradient and precipitation current showed a maximum, with one or other record leading. Cross-correlograms between the ground and mast potential gradient records were also calculated on a number of occasions, and showed a very high correlation for simultaneous readings, hence indicating that there was no significant difference between the two records. Consequently only the ground potential gradient will be considered when analys-

ing the precipitation records.

Table 7.2 lists the important features of the quiet precipitation correlograms. The autocorrelation intervals, as well as indicating the degree of persistence in a record, were used in evaluating the significance of the cross-correlation maxima, as was explained in Chapter 5.

7.3.1 Quiet rain cross-correlograms

Nearly all records showed a maximum of negative cross-correlation, usually with the potential gradient leading the precipitation current. The "mirror-image" effect was thus present in nearly all records. Most of the cross-correlation maxima are statistically significant, some at the 99.9% level, indicating a high degree of significance. The time lags are mostly of a few minutes, ranging from 0.5 to 7.5 minutes for the potential gradient leading. One exception is record 6/5, where there is a much longer time lag of 61 minutes. The correlation is not significant in this case, however, and so the maximum may well have no physical significance; moreover point discharge may have occurred during part of the record.

A number of records, however, show different behaviour. Three (4/5, 5/1 and 6/16) still have a maximum of negative correlation, and hence show the mirror-image effect, but with the precipitation current leading, by as much as 22 minutes. The first two cases show significant cross-correlation, and it is likely that the third case is also physically meaningful, as it is significant at the 90% level.

Two records, 4/2 and 5/2, have a maximum of positive correlation, with the precipitation current leading by 11 and 29 minutes

TABLE 7.2 CORRELATION OF POTENTIAL GRADIENT AND PRECIPITATION CURRENT DURING QUIET PRECIPITATION

RECORD NO.	DATE (1972)		RECORD START	RECORD FINISH	COMMENTS	AUTOCORRELATION INTERVAL (MINUTES)		CROSS CORRELATION MAXIMUM	
	DAY	MONTH	G.M.T.	G.M.T.		POT.GRAD.	PPT.CURR. DENSITY	COEFFICIENT	TIME LAG (MINUTES)
1/1	7/8	JAN	21 20	04 00	Sleet	19	32	-0.47	+5.5
1/2	8/9		19 00	03 45		10	16	-0.58***	-0.5
1/3	11		10 30	14 30		14	14	-0.67**	-7.5
1/6	17		08 20	14 00		N/A	7	-0.67**	-6.0
1/7	17/18		20 30	07 00	Snow	15	N/A	-0.77***	+1.0
2/1	1/2	FEB	18 15	01 30	Snow A	20	20	-0.93**	+1.0
2/5	15		12 20	13 50	Sleet	4	8	-0.56* +0.67**	-1.0 +19.0
3/1	1	MAR	02 00	09 50		11	14	-0.27	-2.5
3/5	6		17 00	23 15		10	21	-0.80***	-3.5
3/7	8		07 30	13 30		14	23	-0.63*	-2.0

(cont.)

Notes at end of table

TABLE 7.2 (Continued)

RECORD NO.	DATE (1972)		RECORD START	RECORD FINISH	COMMENTS	AUTOCORRELATION INTERVAL (MINUTES)		CROSS CORRELATION MAXIMUM	
	DAY	MONTH	G.M.T.	G.M.T.		POT.GRAD.	PPT.CURR. DENSITY	COEFFICIENT	TIME LAG (MINUTES).
4/2	6/7	APR	23 45	03 15		11	11	$+0.61^{**}$	+11.0
4/4	8		02 45	04 10		13	14	-0.85^{***}	-4.0
4/5	8/9		16 25	03 15		25	31	-0.48^{*}	+1.5
4/7	26/27		22 00	00 30		14	11	-0.45	-4.0
5/1	2/3	MAY	18 00	13 00		34	37	-0.34^{*}	+22.0
5/2	5/6		16 10	06 45		13	20	-0.12 $+0.32^{*}$	-1.5 +29.0
6/5	4/5	JUN	22 00	04 00	B	N/A	N/A	-0.38	-61.0
6/6	7		06 30	11 00		20	65	-0.70^{*}	-2.0
6/9	10/11		22 15	08 00		45	37	-0.32	-3.0
6/14	19		10 00	13 45		9	8	-0.62^{**}	-4.0
6/16	26		06 45	11 30		15	26	-0.54	+20.0

Time lag positive for precipitation current leading: negative for potential gradient leading.

A Correlations obtained from part of record only

B Possibility of point discharge during part of record.

Correlation coefficients significant at * 95% level
** 99% level
*** 99.9% level

respectively. The latter record also has a secondary maximum of negative correlation for potential gradient leading by 1.5 minutes, but although this is not statistically significant, the chart record (see Chapter 6) does suggest that this may be a real feature for part of this period of rain.

It is interesting to note that two of the periods of rain, 5/1 and 6/16, which did not show the most common correlation behaviour, also did not have the usual electrical properties; in the former case there was no overall inverse relation, and in the latter case the signs of the potential gradient and precipitation current were opposite to those usually found during rain. Also, the three cases of a maximum of positive correlation all occured for the precipitation current leading.

7.3.2 Quiet snow and sleet cross-correlations

The two periods of snow, 1/7 and 2/1, both show a strong negative cross-correlation, the precipitation current leading by 1.0 minutes in both cases. This implies a strong mirror-image effect, and this indeed was seen in the chart record 1/7 reproduced in Chapter 6. The direction of the time lag is, of course, opposite to that usually found during quiet rain, when the potential gradient usually leads. It should be noted that the correlation for record 2/1 was calculated for only part of the period of snow, when the data were almost certainly non-stationary, and so the cross-correlation coefficient is probably enhanced in value.

The behaviour of the periods of sleet, 1/1 and 2/5, again differed. The former record behaved similarly to snow, with the precipitation current leading by 5.5 minutes; there was no overall inverse relation in this case. The second period, when

there was an inverse relation, behaved similarly to rain, with a maximum of negative correlation for potential gradient leading. There was, however, a second,more significant,maximum of positive correlation for precipitation current leading by 19 minutes.

7.3.3 The autocorrelograms

The autocorrelograms show both the potential gradient and precipitation current to have considerable persistence, with autocorrelation invervals ranging from 4 to as much as 65 minutes. Particularly noticeable is the similarity between the values for the two electrical quantities,although occasionally, as for records 3/5 and 6/16, the persistence of the precipitation current appears to be approximately double that of the potential gradient. Generally, the precipitation current shows slightly greater persistence than the potential gradient during a given record.

7.4 The meteorological conditions during quiet precipitation

Table 7.3 summarises the meteorological conditions at Durham during each period of quiet precipitation, and also gives the general synoptic situation at the time. The meteorological readings were those from Durham Observatory, adjoining the site where the electrical measurements were made.

The mean rates of rainfall rarely exceeded 1.0 mm hr^{-1}, with 1.2 mm hr^{-1} being the greatest rate. By comparison, periods of disturbed precipitation rarely produced rates of rainfall less than 1.0 mm hr^{-1}, and often 2.0 mm hr^{-1} or higher. A heavy shower can produce rain at a rate of 5 mm hr^{-1} or more. Some of the values of rainfall rate given for quiet precipitation may be somewhat high, as on occasion heavier rain preceding or follow-

TABLE 7.3 METEOROLOGICAL CONDITIONS AT DURHAM DURING PERIODS OF QUIET PRECIPITATION

RECORD	DATE (1972)		DURATION	MEAN RATE OF RAINFALL	MEAN WIND SPEED	COMMENTS	SYNOPTIC SITUATION
	DAY	MONTH	hr	mm hr^{-1}	ms^{-1}		
1/1	7/8	JAN	6.7	0.8	4.5	Sleet	Occluded front approaching from SW
1/2	8/9		8.8	0.8	5.0		do.
1/3	11		4.0	1.0	7.0		Warm front passing from S
1/5	16		4.0	0.4	5.0		Cold front approaching from E
1/6	17		5.7	0.7	6.0		Stationary occluded front to W
1/7	17/18		10.5	0.7	5.0	Snow	
2/1	1/2	FEB	7.3	0.9	5.0	Snow	Occluded front passing from SW
2/3	6/7		7.2	0.2	3.0		Wave depression across S of Britain
2/4	8		4.4	0.2	5.0		Occluded front passing from SW
2/5	15		1.5+	1.2	9.5	Sleet	Occluded front passing from W

Notes at end of table

(cont.)

TABLE 7.3 (Continued)

RECORD	DATE (1972)		DURATION	MEAN RATE OF RAINFALL	MEAN WIND SPEED	COMMENTS	SYNOPTIC SITUATION
	DAY	MONTH	hr	mm hr^{-1}	ms^{-1}		
3/1	1		7.8	0.4	3.5		Near-stationary occluded front to N
3/5	6		6.3	0.5	7.5		Occluded front passing from SW
3/6	7		4.3	0.1	3.5		Occluded front over central Scotland
3/7	8	MAR	6.0	0.3	1.5		No feature other than depression over N France
3/10	30		4.0	1.2	4.0		No feature
3/11	31		3.3	0.6	2.0		Near-stationary warm front to SW
4/2	6/7		3.5	0.6	3.0		Occluding frontal system passing from SW
4/4	8		1.4	0.4	3.0		Stationary declining occluded front across N Scotland
4/5	8/9	APR	10.8	0.2	2.5		Same system as above.
4/6	10		5.8	0.4	7.0		Occluded front passing from NW
4/7	26/27		2.5	0.6	2.5		Cold front passing from N
4/8	29		2.5	-	5.5		Occluded front passing from W

(cont.)

TABLE 7.3 (Continued)

RECORD	DATE (1972)		DURATION	MEAN RATE OF RAINFALL	MEAN WIND SPEED	COMMENTS	SYNOPTIC SITUATION
	DAY	MONTH	hr	mm hr^{-1}	ms^{-1}		
5/1	2/3	MAY	19.0	0.7	1.5		Weak depression to N of Scotland
5/2	5/6		14.6	0.3	2.0		Depression over SW England
6/5	4/5		6.0	1.1	3.5		Frontal system passing from SE
6/6	7		4.5	0.5*	2.5		Cold front passing from SW
6/7	9		2.6	0.3	0.5		Depression over Irish Sea, trough passing to S.
6/8	10	JUN	3.1	0.6	4.5		Depression to SE, trough passing
6/9	10/11		9.8	0.7	4.5		Depression moving N over North Sea
6/11	12		3.6	0.4	1.0		No feature
6/13	18		4.2	0.3	7.0		Weak occluding frontal system
6/14	19		3.8	0.5	3.0		Troughs passing from W
6/16	26		5.8	0.9	1.0		Cold front passing from W

Rate of rainfall to nearest 0.1 mm hr^{-1}
Mean wind speed to nearest 0.5 ms^{-1}

* Estimated rate of rainfall

\+ Not entire period of precipitation

Total duration of periods of quiet precipitation : 195.3 hr

ing a period of quiet precipitation could not be easily distinguished on the rainfall record: the minimum rainfall detectable was 0.04 in. (very nearly 1 mm.).

Mean wind speeds were quite low, usually in the range 3 to 5 ms^{-1}, the highest being 9.5 ms^{-1} during the period of sleet on 15 February. The mean wind speed during the 9 June record was as low as 0.5 ms^{-1}.

The periods of quiet precipitation mostly originated in frontal systems, typically from an occluded front crossing the British Isles from a westerly direction. The classic frontal system as presented in Chapter 2, with separate warm and cold fronts, was not common during the six-month period; when it did occur, the precipitation was nearly always disturbed. On a few occasions no large scale synoptic feature such as a front was evident, and so precipitation was probably due to weak troughs of low pressure, or to convergence causing the large-scale ascent of moist air needed to produce the precipitation.

7.5 The charge on quiet precipitation

For a period of precipitation producing a total rainfall (depth) H, and a mean precipitation current density I, the mean charge per unit volume Q is IT/H, where T is the duration of the precipitation period. Expressing I in pAm^{-2}, H in mm and T in hr, and taking the density of rainwater as 1 gm cm^{-3}, Q is then given by

$$Q = 3.6 \frac{IT}{H} \qquad (7.1)$$

and represents either the charge per unit volume (pC cm^{-3}) or the charge per unit mass (pC gm^{-1}). An alternative form is:

$$Q = 3.6 \frac{I}{R}$$

where R is the mean rate of rainfall (mm hr^{-1}).

Table 7.4 presents the values of Q for most of the recorded periods of precipitation, and also the total charge per unit area brought down by the precipitation on each occasion. The periods of rain with the usual positive precipitation current and negative potential gradient produced an overall mean charge per unit mass of 32 pC gm^{-1}.

TABLE 7.4 MEAN PRECIPITATION CHARGE DURING QUIET PRECIPITATION PERIODS AT DURHAM

RECORD NO	DATE (1972)		DURATION	MEAN VALUES			TOTAL PPT. CHARGE
				RATE OF RAINFALL	PPT.CURR. DENSITY	PPT. CHARGE/ UNIT MASS	
	Day	Month	hr	mm hr^{-1}	pAm^{-2}	$pC\ gm^{-1}$	C x 10 $^{-9}$
1/5	16	JAN	4.0	0.4	+0.5	+5	+8
1/6	17		5.7	0.7	+2.5	+14	+5[illegible]
1/7	17/18		10.5	0.7	-3.5	-17	-125
2/1	1/2		7.3	0.9	-0.8	-31	-204
2/3	6/7	FEB	7.2	0.2	-8.0	-17	-24
2/5	15		1.5 *	1.2	+3.4	+10	+17 *
3/1	1		7.8	0.4	+1.7	+14	+98
3/5	6	MAR	6.3	0.5	+2.1	+14	+43
3/6	7		4.3	0.1	+0.5	+18	+7
3/7	8		6.0	0.3	+5.0	+68	+109

* Not entire period of precipitation

(cont.)

TABLE 7.4 (Continued)

RECORD NO	DATE (1972)		DURATION	MEAN VALUES			TOTAL PPT. CHARGE
				RATE OF RAINFALL	PPT.CURR. DENSITY	PPT. CHARGE/ UNIT MASS	
	Day	Month	hr	mm hr^{-1}	pAm^{-2}	$pC\ gm^{-1}$	C x 10 $^{-9}$
4/?	6/7	APR	3.5	0.6	+1.1	+7	+14
4/4	8		1.4	0.4	+2.9	+29	+15
4/5	8/9		10.8	0.2	+7.5	+16	+34
4/6	10		5.8	0.4	+5.8	+52	+104
4/7	26/27		2.5	0.6	+2.7	+14	+21
5/1	2/3	MAY	19.0	0.7	-4.0	-16	-212
5/?	5/6		14.6	0.3	+5.0	+56	+246

(cont.)

TABLE 7.4 (Continued)

RECORD NO	DATE (1972)		DURATION	MEAN VALUES			TOTAL PPT CHARGE
				RATE OF RAINFALL	PPT. CURR. DENSITY	PPT. CHARGE/ UNIT MASS	
	Day	Month	hr	mm hr $^{-1}$	pAm^{-2}	pC gm^{-1}	C x 10^{-9}
6/5	4/5		6.0	1.1	+6.8	+13	+86
6/6	7		4.5	0.5**	+10.5	+76	+171
6/7	9		2.6	0.3	+2.0	+24	+22
6/8	10	JUN	3.1	0.6	+2.7	+16	+29
6/9	10/11		9.8	0.7	+9.1	+80	+568
6/14	19		3.8	0.5	+6.0	+43	+82
6/16	26		5.8	0.9	-2.3	-9	-45

** Mean rate of rainfall for 1 hour portion of record.

CHAPTER 8

Analysis of the Quiet Precipitation Results

8.1 The relationship between potential gradient and precipitation current

The quiet precipitation measurements between January and June 1972 showed that the inverse relation and mirror-image effect were usually present. These findings will now be compared with those of previous investigations, and the possible origins of the two effects discussed.

8.1.1 Previous work : the inverse relation

The behaviour of quiet rain and snow found in the present work largely agrees with that found by previous workers. CHALMERS (1956) concluded from measurements during 38 periods of quiet rain that the precipitation current was most often positive, with an average density of + 3.8 pAm^{-2}, and the potential gradient negative, with an average of - 176 Vm^{-1}. In the present work, those periods of rain when the usual inverse relation applied had overall averages for the two electrical quantities of respectively + 4.6 pAm^{-2} and - 490 Vm^{-1}.

RAMSAY and CHALMERS (1960) quote mean values from 31 periods of rain, but classified by precipitation rate. Their values are from one - minute averages however, whereas

those quoted above from Chalmers are for $4\frac{1}{2}$ minute averages. Table 8.1 lists Ramsay and Chalmers mean values for rates of rainfall up to 1.80 mm hr^{-1}; their overall mean values are + 3.27 pAm^{-2} for precipitation current density and - 93 Vm^{-1} for potential gradient.

The mean potential gradient found in the present work is thus greater than both the values quoted above. This may well be due to the slightly different definition of quiet precipitation, with a limit of $\pm$ 1500 Vm^{-1} taken for the potential gradient, whereas Chalmers, for instance, limits his measurements to the $\pm$ 800 Vm^{-1} range. Also the electrical quantities were usually averaged over the entire period of precipitation.

Although only two periods of snow were recorded during the period January to June 1972, both showed the same electrical features of a strong inverse relation, with negative snow falling in a positive potential gradient. CHALMERS (1956), using the same method as for rain, concluded that during quiet snow, the precipitation current was usually negative, with a mean density of - 3.5 pAm^{-2} for 25 separate periods of snow. This value compares with mean values of - 3.5 and - 0.8 pAm^{-2} for the two periods in the present work. Chalmers, however, found the mean potential gradient to be also negative, with a value of - 57 Vm^{-1}. Other workers such as REITER (1965), however, have more often found the potential gradient to be positive. MAGONO and ORIKASA (1966) found the charge of individual snowflakes

TABLE 8.1. The quiet precipitation measurements of Ramsay and Chalmers (1960)

(Readings during Winter 1957/8)

RAINFALL RATE ($mm\ hr^{-1}$)	NO. 1-MINUTE AVERAGES	MEAN POTENTIAL GRADIENT (Vm^{-1})	MEAN PRECIPITATION CURRENT DENSITY (pAm^{-2})
< 0·18	962	− 89	+ 0·34
0·18–0·60	219	− 83	+ 5·33
0·60–1·20	267	−116	+ 8·48
1·20–1·80	147	− 95	+ 9·88

TABLE 8.2. Distribution of the mirror-image effect (from Ramsay and Chalmers, 1960)

No. of quiet precipitation periods showing stated time lag:

	RAIN	SNOW	SLEET	"WET SNOW"	TOTAL
No time delay	6	1	1	1	9
Ppt. current leads	3	3	1	0	7
Pot. gradient leads	5	0	0	0	5
Total	14	4	2	1	21

in light, quiet snow to be usually negative with the potential gradient positive, as had been concluded earlier by MAGONO and KIKUCHI (1963). It would appear then that the two periods of snow in the present work are typical of quiet snow.

8.1.2 Previous work : the mirror-image effect

RAMSAY and CHALMERS (1960) were probably the first to make any systematic investigation of the mirror-image effect and the time delays between corresponding features of the potential gradient and precipitation current variations. One of the problems in dealing with this effect is the different conditions under which records have been taken, and the different methods of determining whether the effect is present. SIMPSON (1949), who first drew attention to the effect, mainly considered electrical records where the potential gradient was high enough to produce point discharge, and so the precipitation was not quiet. As can be seen from a record of "disturbed" precipitation reproduced in Chapter 6, a mirror-image effect can indeed be present in such conditions.

RAMSAY and CHALMERS (1960) investigated 21 occasions when the mirror-image effect was detected in quiet precipitation. They considered the effect to be present if the precipitation current and potential gradient had maxima in opposite directions at or close to the same time, and determined any time lags by plotting the precipitation current values against the simultaneous values of potential gradient. A time lag results in successive points follow-

ing roughly an ellipse, the direction of rotation indicating which electrical quantity is leading.

Their distribution of time lags is given in Table 8.2, where it appears that the potential gradient most commonly leads during rain, and the precipitation current during snow, although other situations did occur. This largely agrees with the observations of the present work, except that no case of zero time lag was found. This may well be due to Ramsay and Chalmers' method being unable to distinguish time lags which were small, or possibly varying during the period of precipitation.

The use of the cross-correlation coefficient to detect the mirror-image effect and associated time lags was first suggested by OWOLABI and CHALMERS (1965), who found maximum correlation during a shower of sleet and snow for the potential gradient leading by 40 seconds. They used a graphical method, however, to determine this lag. The correlation approach has been used extensively in more recent studies by ASPINALL (1970) and STRINGFELLOW (1969), who used a computer to calculate the correlation coefficients directly from the potential gradient and precipitation current values. Their results also suggest that the potential gradient generally leads during rain and the precipitation current during snow.

Later in this chapter, the possible origins of the inverse relation and mirror-image effect will be considered. Those occasions when different electrical behaviour of quiet precipitation has been observed will be discussed in

Chapter 9. Before this, however, some relationships found between the electrical and meteorological conditions must be mentioned.

8.2 The variation of electrical and meteorological activity

8.2.1 Rate of rainfall

A connection between the potential gradient F, precipitation current density I and rate of rainfall R was first suggested by SIMPSON (1949), who found that the relationship between these quantities could be expressed as

$$I = -0.0133\ R(F - 400)$$

where I is in pAm^{-2}, R in mm hr^{-1} and F in Vm^{-1}.
The results of Ramsay and Chalmers have already been quoted; they suggested that the average values of precipitation current increased with the rate of rainfall at the time, although the potential gradient showed no such relationship. STRINGFELLOW (1969) has found a significant correlation on certain occasions between the precipitation current and the rate of rainfall.

Fig. 8.1 shows the values of mean potential gradient $\bar{F}$ and mean precipitation current density $\bar{I}$ plotted against the mean rate of rainfall $\bar{R}$ for many of the periods of quiet rain at Durham. In this instance there appears to be a relationship between the potential gradient and rate of rainfall, rather than for the precipitation current.

The closest connection in fact is apparent if the

FIG.8.1 Mean values of potential gradient and precipitation current density against mean rate of rainfall

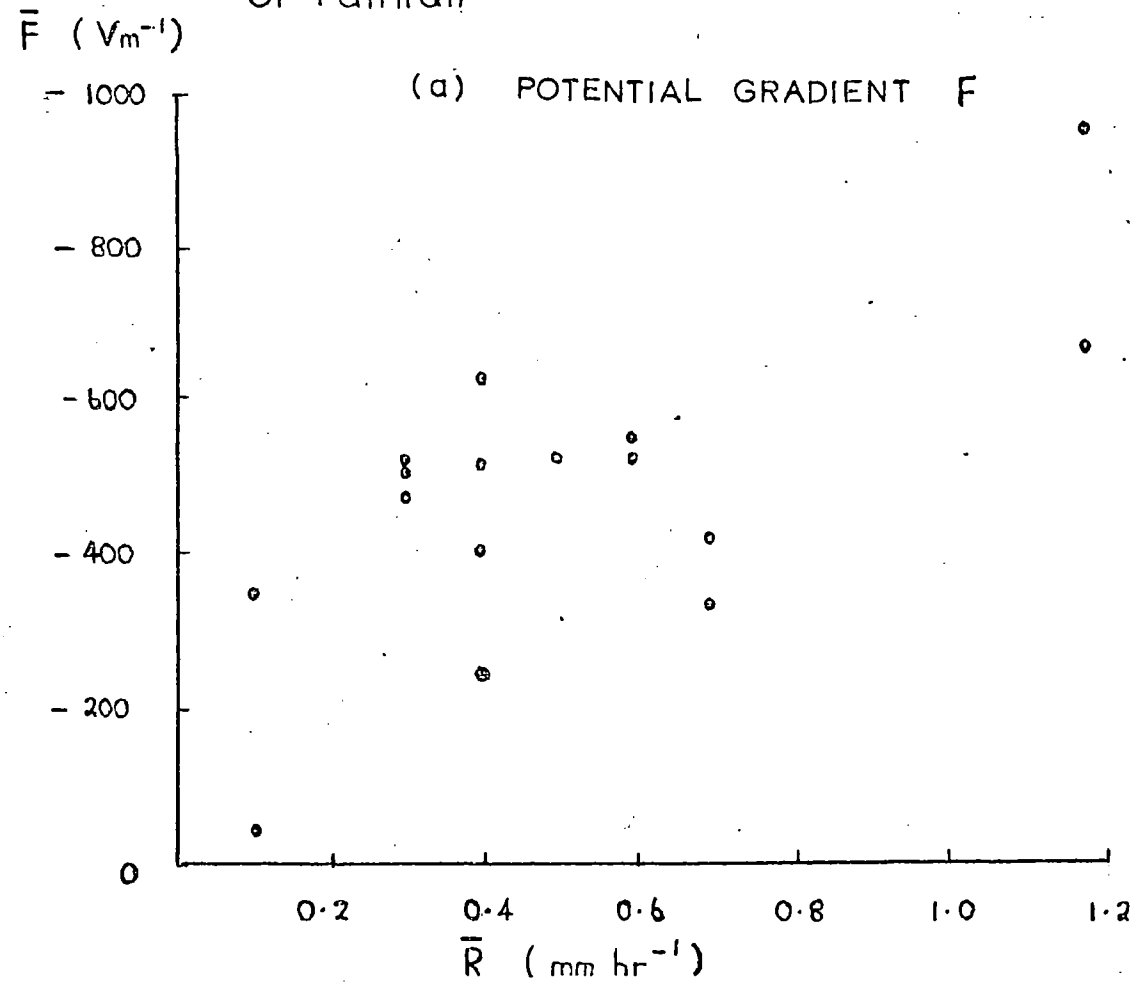

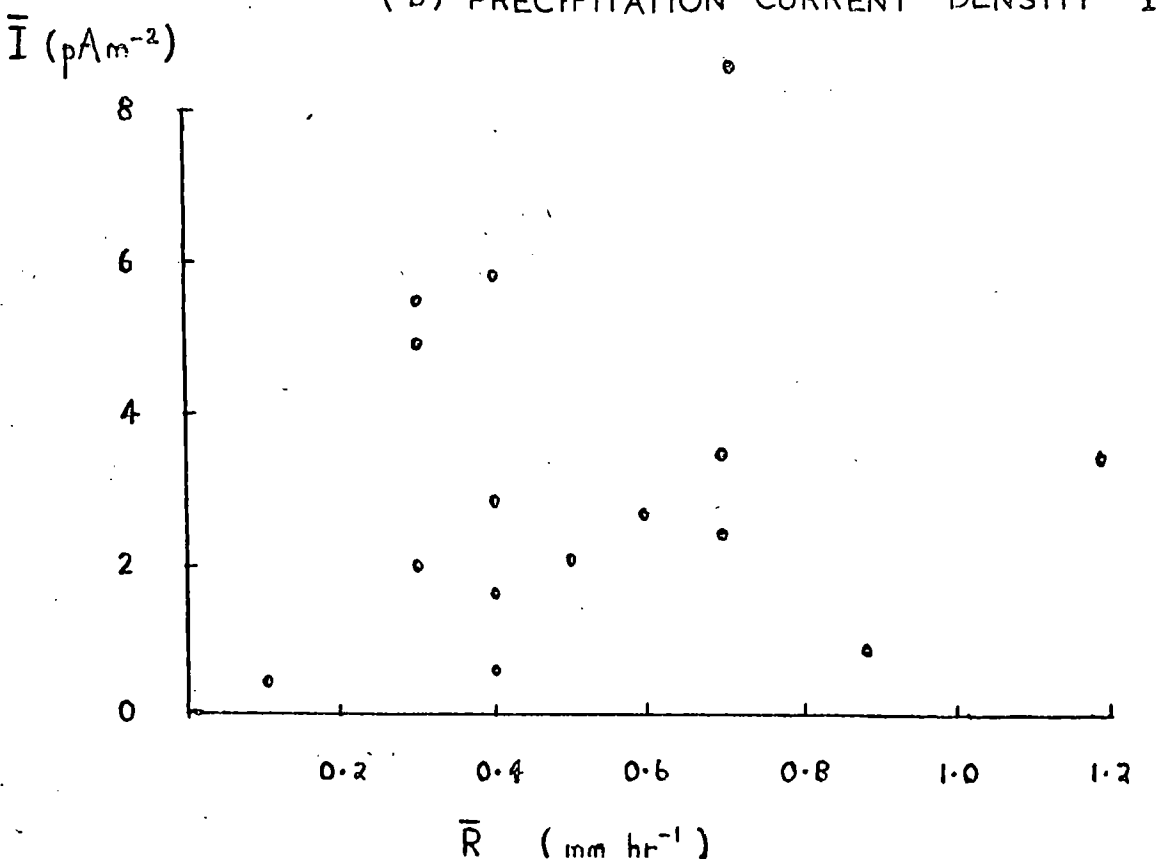

standard deviations of $\bar{F}$ and $\bar{I}$ are plotted against $\bar{R}$. This is done for the same precipitation periods in Fig. 8.2, where a clear relationship is seen for both $\bar{F}$ and $\bar{I}$. The standard deviation of the precipitation current, σ_I, tends to zero for no rainfall, as might be expected. These relationships can also be expressed in terms of the variances S_I and S_F of respectively $\bar{I}$ and $\bar{F}$, as they are just the square of the standard deviations. The relationships suggested by Fig. 8.2 are thus:

$$\sigma_F, \sigma_I \propto \bar{R}$$

$$S_F, S_I \propto \bar{R}^2$$

The connection between the meteorological and electrical activity is thus seen more in the variability of the electrical quantities, rather than in their mean values.

8.2.2 The frequency of sign reversals

The work of REITER (1965, 1968) was mentioned in Chapter 2, and in particular his conclusions on the relationship between the degree of stability in the lower atmosphere and the degree of electrical activity shown by quiet precipitation. He represented the latter quantity by the frequency of sign reversals of the potential gradient, which is easily obtained from a chart record. This may not always be an accurate measure of the variability of the potential gradient, however, particularly during very quiet precipitation when few, if any, sign changes will occur. Nevertheless, if it can be taken as an approximate indication, the conclusions

FIG. 8.2 Standard deviations of potential gradient (σ_F) and precipitation current density (σ_I) against mean rate of rainfall $\bar{R}$ for quiet rain

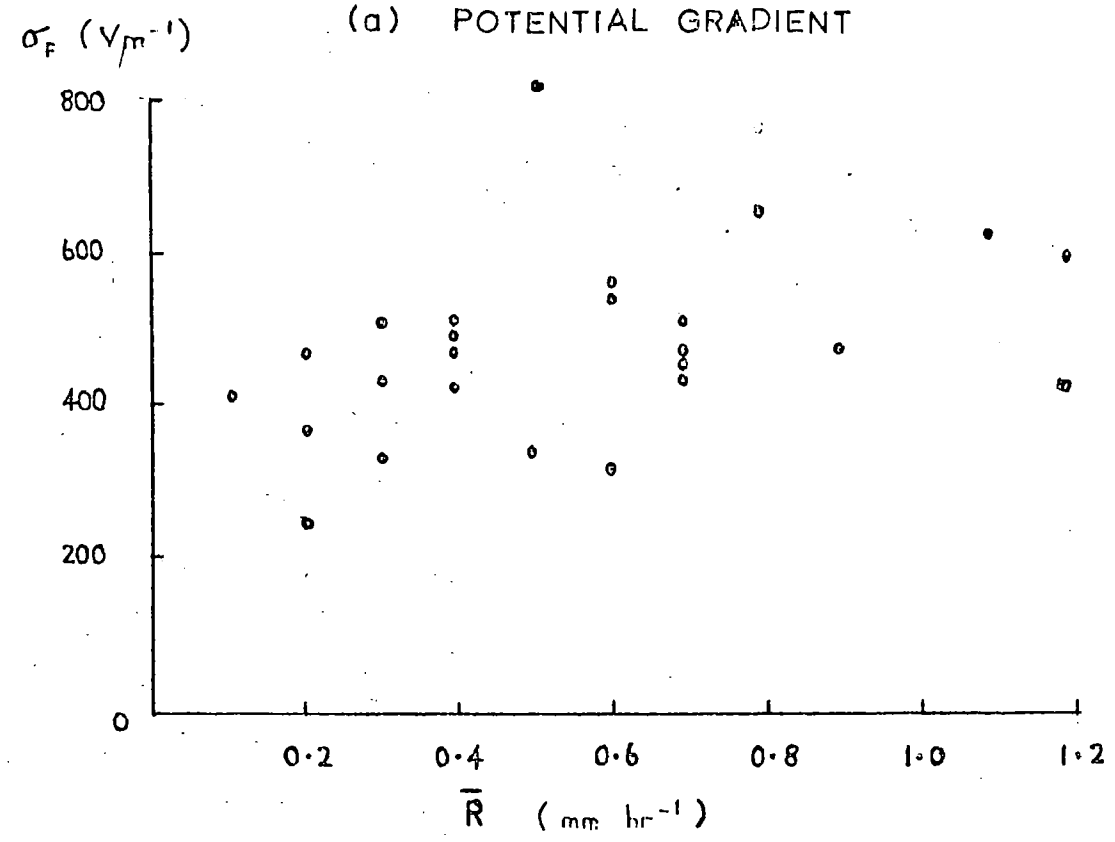

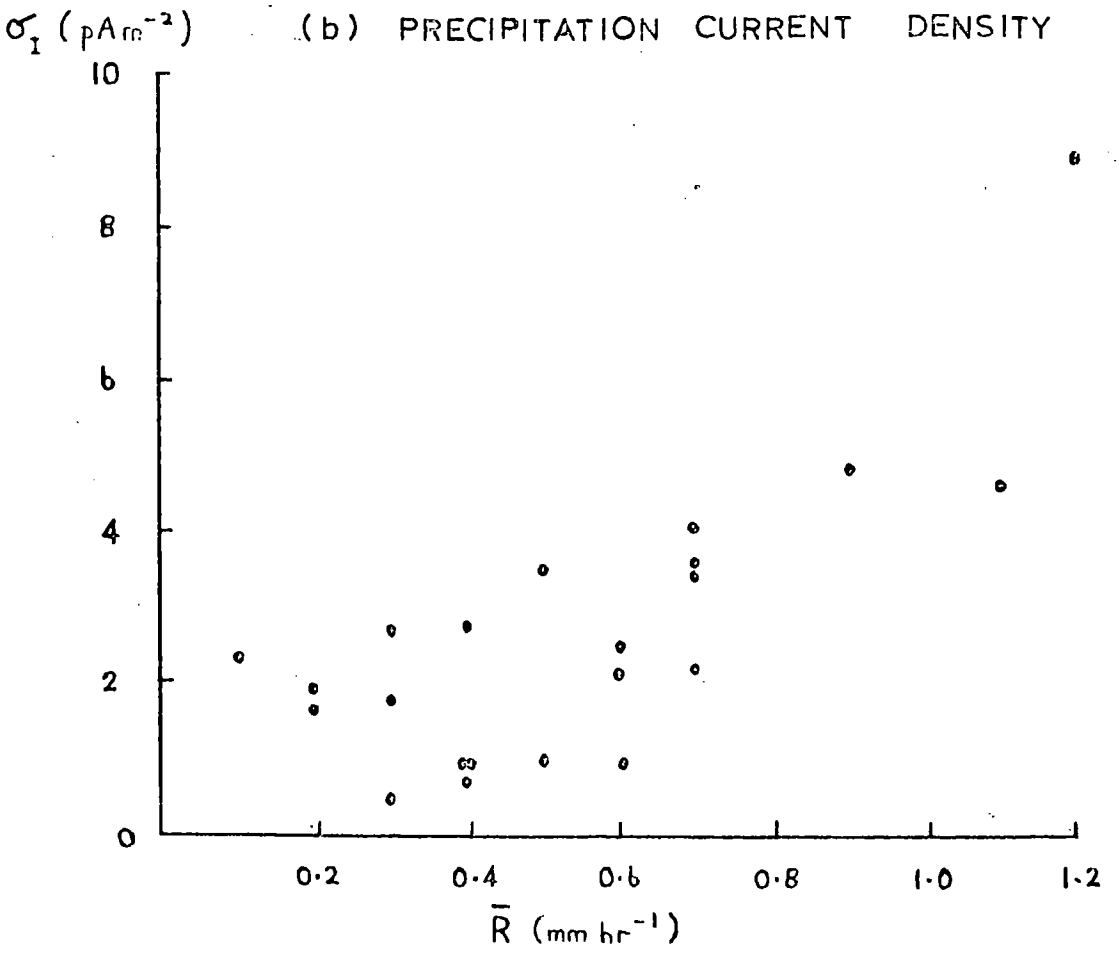

of the previous section suggest that this frequency should also depend on the mean rate of rainfall during a record.

The number of sign reversals per hour of both the potential gradient and precipitation current is plotted against the mean rate of rainfall in Fig. 8.3, for most of the periods of rain, sleet and snow observed at Durham. An increase in the frequency of sign reversals with rate of rainfall is seen for both electrical quantities.

Reiter related the frequency of sign reversals to the degree of stability in the 500 - 700mb layer of the atmosphere (approximately between 2.0 and 5.5 km in altitude), and deduced that the transition from stability to instability occurred when the frequency exceeded 1.5 reversals per hour. This will be considered in Chapter 9, where it is shown that a similar value of frequency can be used to distinguish between quiet and disturbed precipitation.

8.3 The origin of the electrical behaviour

The origins of the usual behaviour of quiet precipitation will now be discussed, the main features for explanation being:

(i) The inverse relation, whereby during rain the mean precipitation current is positive and the mean potential gradient negative, and during snow these signs are reversed.

(ii) The mirror-image effect, whereby there is a significant negative cross-correlation between potential gradient and precipitation current, with the former usually leading during rain and the

FIG. 8.3 Rate of sign reversals (S) against mean rate of rainfall (R) during quiet precipitation

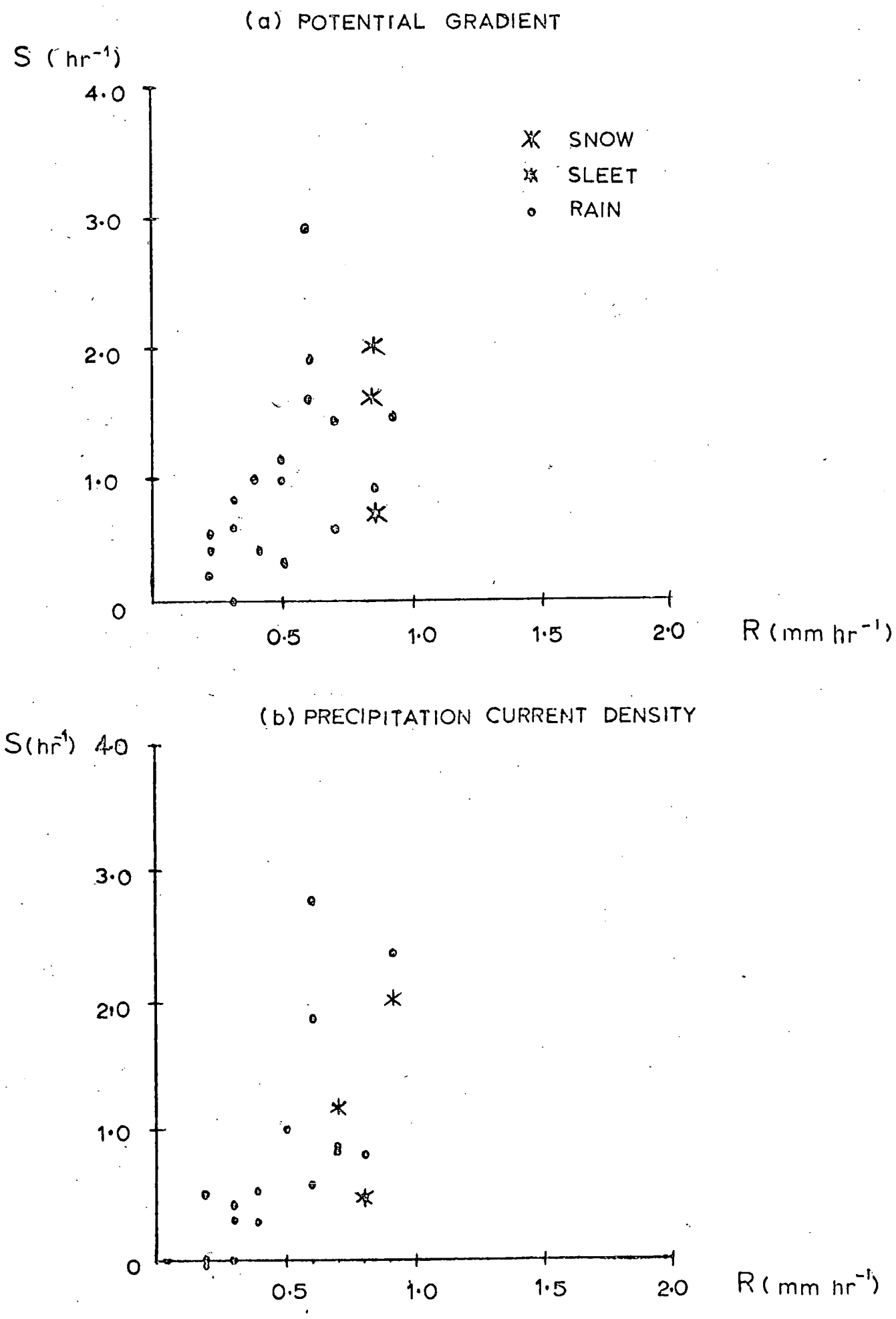

latter during snow.

(iii) The connection between the degrees of electrical and meteorological activity. This is evident in the increase of mean potential gradient with rate of rainfall, and more particularly for the standard deviation (and hence variance) of both potential gradient and precipitation current density. This connection is also evident in the increase in the frequency of electrical sign reversals with precipitation rate.

8.3.1 The inverse relation

It has already been explained in Chapter 2 how Chalmers showed that the inverse relation could be explained by two precipitation charging processes. One process would be situated within the cloud and above the 0°C level, giving negative charge to solid precipitation and leaving behind positive charge within the charging region. The second process would operate at or below the 0°C level, reversing the sign of the precipitation charge and leaving behind a negative charge within the charging region. For snow only the first process will operate, producing the positive potential gradient at the ground, while for rain both processes will operate, resulting in a negative potential gradient at the ground.

It is worthwhile examining the meteorological conditions at Durham during the periods of quiet precipitation to see

if Chalmers' theory is consistent with the conditions at the time: if, for instance, the clouds are found to be mostly at temperatures above $0^{o}C$, or only thin layers of low cloud are present, then his explanation in terms of the two charging processes is unlikely.

8.3.2 The meteorological conditions during the quiet precipitation periods

From the data in the Daily Weather Report and the Daily Aerological Record of the Meteorological Office, it is possible to gain some idea of the structure of the cloud systems producing quiet precipitation, and of the conditions within them. The relevant data were obtained as far as possible for the precipitation periods recorded at Durham, some of the aerological profiles having been presented in Chapter 6. Of particular interest is the cloud structure, but unfortunately this information was not always available, for instance if low cloud at a particular meteorological station obscured higher layers. It has thus only been possible to draw general conclusions as to the altitudes of the cloud layers and the temperatures within them.

The cloud observations published in the Daily Weather Report suggest that three main layers of cloud are usually present during periods of quiet precipitation. An upper layer of cirrus has a base at about 6 km altitude, with a medium layer of alto stratus down to about 3 km and a lower layer of stratocumulus or nimbostratus with a base around 0.5 to 1.5 km. Still lower layers of stratus and

stratus fractus are sometimes present. This cloud structure agrees well with that of precipitating cloud in a frontal system as outlined in Sect. 2.1.4. The layer of nimbostratus is sometimes absent however, particularly at the leading edge of the cloud system; such instances were occasionally observed at Durham, usually when light rain was falling at the start of a period of rain.

An idea of the temperatures within these cloud layers can be obtained by comparing the cloud base values with an appropriate temperature profile. This is done, for the particular case of 12Z of17 January 1972 at Shanwell, in Fig. 8.4, where the cloud base heights at nearby Leuchars are superimposed on the temperature profile. The altrostratus layer, with a base at 3 km and a temperature of -10°C, will extend upwards through the -15°C level. The nimbostratus layer will extend upwards from 1 km through the -5°C level. Taking the melting region as that between 0°C and 2°C, it is 200 m in thickness, and lies below the nimbostratus layer between 500 m and 300 m altitude. On other occasions the melting region was often within the nimbrostratus layer, but was never above for any of the periods of rain recorded between January and June 1972.

A clearer idea of the possible locations of the two charging processes proposed by Chalmers can thus be obtained. The upper process, if associated with solid precipitation, can be in either the nimbostratus or altostratus layers. If the melting level is high, it would be restricted in the nimbrostratus layer to the upper portions, at altitudes above

FIG.8.4 Temperature profile and cloud levels at Shanwell, 12Z 17 January 1972

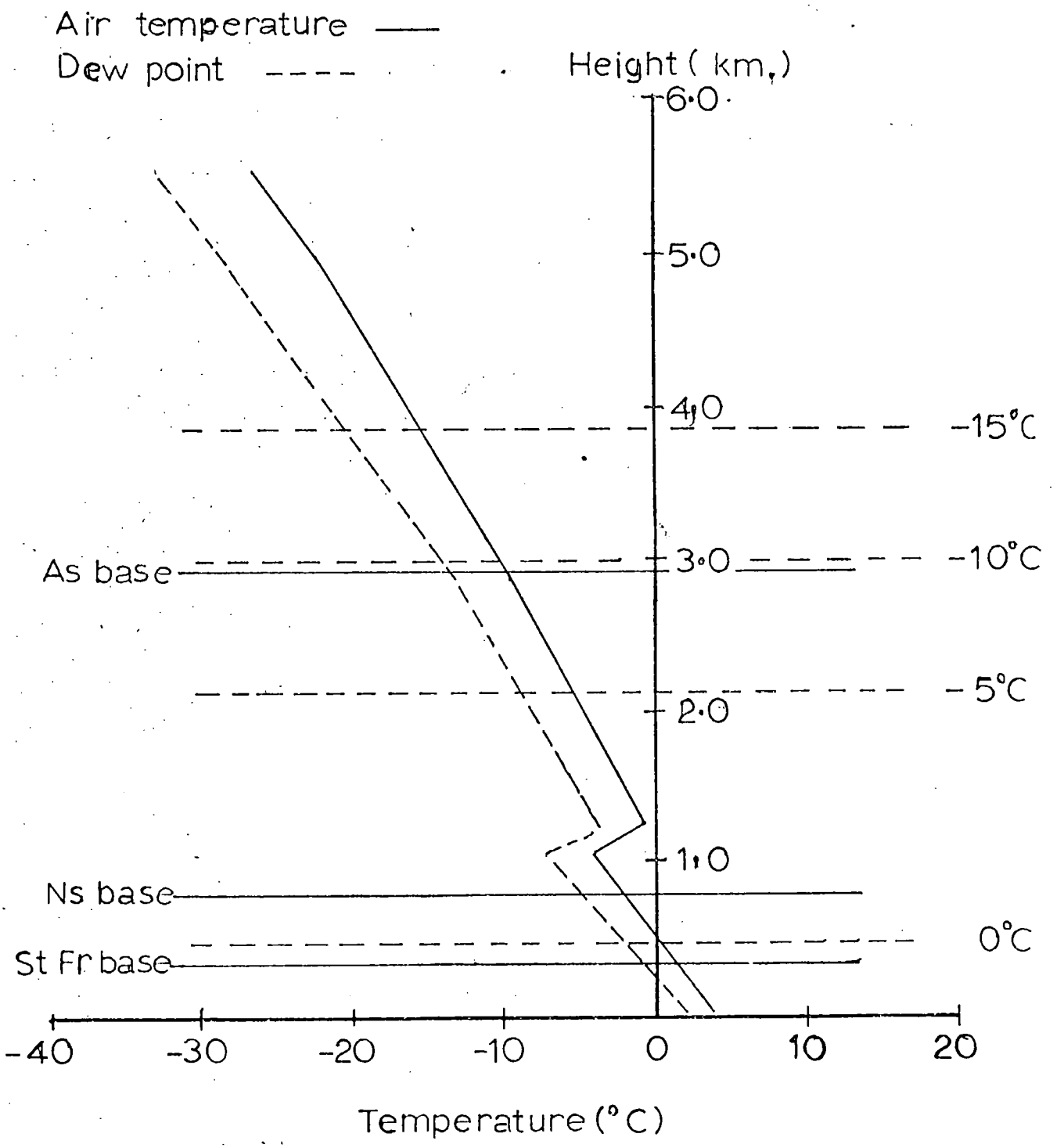

about 1.5 km. The lower process, if associated with melting, could be within or beneath the nimbostratus layer, and so must operate whether or not the melting layer is within the cloud.

8.4 A quiet precipitation cloud model

By making a number of assumptions concerning the charge separation processes within the cloud and the dimensions of the cloud system, approximate mathematical expressions can be deduced for the relationship between the ground potential gradient and the precipitation current density during quiet precipitation. The theory below is based on that of STRINGFELLOW (1969) and MAGONO and ORIKASA (1961), and its predictions will be compared with the results of the quiet precipitation measurements. The charging processes proposed by Chalmers will be assumed to apply.

8.4.1 The snow cloud

The simplest case to consider is the snow cloud, as only one charge separation process is concerned. The potential gradient at the ground, F, is considered to be due to the charge within a cylindrical cloud zone directly above, and to the space charge on the falling precipitation between the cloud and the ground (Fig. 8.5).

A number of assumptions concerning the electrical behaviour of a quiet precipitation cloud are made:

(i) The cloud charges are independent of outside electrical effects.

(ii) Any ionic or space charges in the cloud dissipate only by ionic conduction.

(iii) The rate of charge dissipation depends only on the charge magnitude and the conductivity of the immediate area of the cloud.

(iv) Any charge separation process gives rise to an ionic or cloud charge, and a precipitation charge of opposite sign.

(v) The precipitation current at the ground represents the total current flowing downwards from the charging region.

In the case of the snow cloud, the potential gradient at the ground, F, will be the resultant of that due to the cloud ionic charge (F_ρ) and that due to the space charge of the falling precipitation (F_s).

$$\text{i.e.} \quad F = F_\rho + F_s \qquad (8.1)$$

By integrating over the cloud volume of Fig. 8.5, the potential gradient at any point due to the cloud charges can be found. MAGONO and ORIKASA (1961) showed that, at the ground under the centre of the cylinder, this is

$$F_\rho = \frac{\rho}{\epsilon_o} \left\{ H - \sqrt{(H + h)^2 + R^2} + \sqrt{h^2 + R^2} \right\} \qquad (8.2)$$

where ρ is the cloud space charge density, ϵ_o is the permittivity of free space, h the cloud base height, H the thickness of charging region and R its radius.

FIG. 8.5 Charging Regions in a Snow Cloud

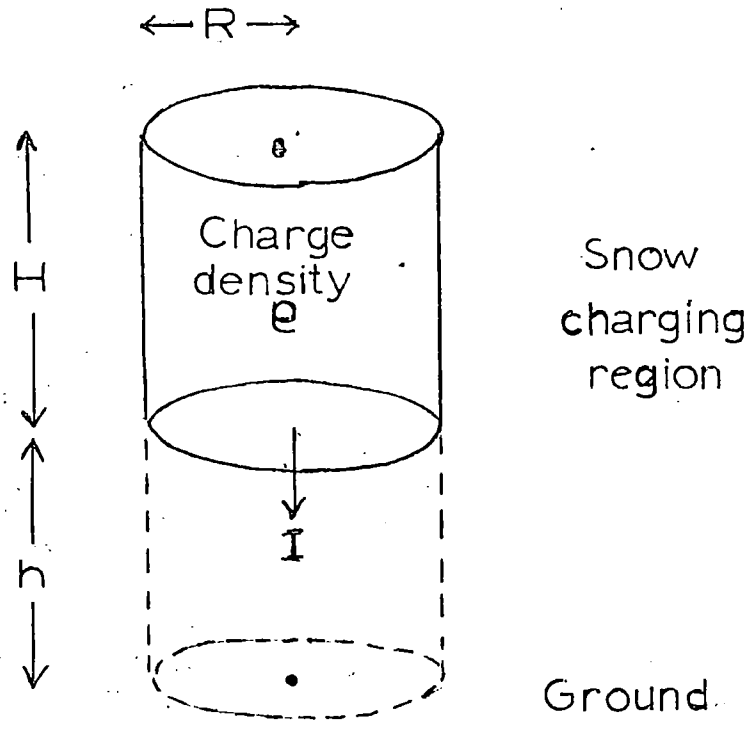

FIG. 8.6 Charging Regions in a Rain Cloud

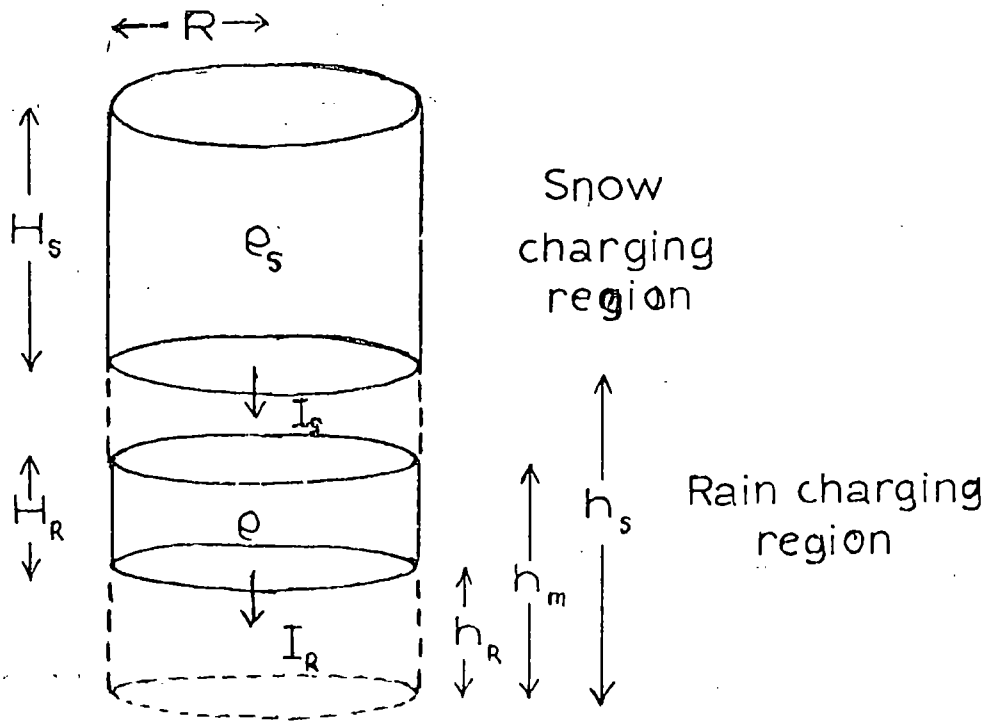

Hence, if the horizontal dimensions of the cloud are large, i.e. $R \gg H, h$ Eq. 8.2 becomes

$$F_\rho \approx \frac{\rho H}{\epsilon_0} \qquad (8.3)$$

It is simplest to consider charging of the precipitation to occur uniformly throughout the cloud charging region: then the cloud charge density ρ will be constant throughout the region and the precipitation current density I will increase linearly with decreasing altitude until the base of the charging region is reached (Fig. 8.5). Assuming that the precipitation current is constant between the cloud and the ground, and again taking $R \gg H, h$, the potential gradient at the ground due to the precipitation space charge, F_s, will be

$$F_s \approx \frac{I}{2\epsilon_0 v} (H + 2h) \qquad (8.4)$$

where v is the fall speed of the precipitation. Hence, the ground potential gradient will be given from Eq. 8.1 by

$$F \approx \frac{\rho H}{\epsilon_0} + \frac{I}{2\epsilon_0 v} . (H + 2h) \qquad (8.5)$$

The only quantity which is not known in this expression is the cloud space charge density ρ. This can be evaluated by the following method.

Consider the cylindrical cloud zone of radius R and height H of Fig. 8.5. Let a precipitation current of

density I leave the base (at height h). The total precipitation current leaving the cloud is then

$$I_{PPT} = \pi R^2 I \tag{8.6}$$

and the total conduction current leaving the cloud will be

$$I_{COND} = \pi R^2 H\rho \cdot \frac{\lambda}{\epsilon_o} \tag{8.7}$$

(since $\pi R^2 H\rho$ is the total cloud charge). λ is the conductivity of the region outside the cloud.
Now, the total current leaving the cloud equals the rate of decrease of the cloud charge, and so

$$\pi R^2 I + \pi R^2 H\rho \frac{\lambda}{\epsilon_o} = -\frac{d}{dt}(\pi R^2 H\rho) \tag{8.8}$$

and so the cloud charge density ρ is given by the differential equation

$$H \frac{d\rho}{dt} = -I - \frac{H\rho}{\tau} \tag{8.9}$$

where $\tau = \epsilon_o/\lambda$ is the relaxation time of the region outside the cloud. Integrating Eq. 8.9 gives

$$\rho = \frac{\tau I}{H}(e^{-t/\tau} - 1) \tag{8.10}$$

assuming $\rho = 0$ when $t = 0$. If it is assumed that the cloud is in quasi-static equilibrium, so that the charge densities are constant, then after about $t > 5\tau$

$$\rho = -\frac{\tau I}{H} \tag{8.11}$$

which is the required expression for ρ. Substituting this in Eq. 8.5 gives

$$F = \frac{I}{\epsilon_0} \left(\frac{2h + H}{2v} - \tau \right) \qquad (8.12)$$

This expression implies that, for the inverse relation to hold during quiet snow, the quantity in brackets in Eq. 8.12 must be negative, so that;

$$\frac{h}{v} + \frac{H}{2v} < \tau \qquad (8.13)$$

In the present work, the inverse relation was seen to hold for two long periods of quiet snow. If the above analysis is reasonably correct, the inequality of expression 8.13 should hold in these cases. Unfortunately, accurate values of τ during snow are not available, but it has been estimated by MAGONO and ORIKASA (1961) to be in the range 10 to 20 minutes.

If the snow charging process is indeed situated within one of the main cloud layers, it should be possible to estimate likely values of h and H and substitute them in expression 8.13. This is done in Table 8.3, with values of h corresponding to the lower nimbostratus and higher altostratus cloud bases. While the values representing charging within the lower layer just satisfy the conditions for the inverse relation, the same does not apply for the higher cloud layer. Even if the fall speed of snow was twice that estimated, this would still be true. In fact it appears that, the lower the height of the charging region, the more likely is the inverse relation.

TABLE 8.3 THE SNOW CLOUD MODEL

Values of $T = h/v_s + H/2v_s$ for various snow charging region dimensions:

height h	thickness H	T
m	m	min
500	500	13
500	1000	17
500	1500	21
1000	500	21
1000	1000	25
1000	1500	29
3000	500	54
3000	1000	58
3000	1500	63

Fall speed of snow, v_s, taken as 1 ms^{-1}

8.4.2 The rain cloud

The theory for the snow cloud can be extended to the case of the rain cloud by considering an extra charging region between the snow charging region and the ground. The most likely location of this second charging region is the melting region, where charging is associated with the transition from snow to rain. The situation for the rain cloud will then be as shown in Fig. 8.6; the potential gradient at the ground will then be the resultant of the cloud space charge in the snow and rain charging regions and the precipitation space charge.

The potential gradient at the ground due to the space charge of the snow charging region, from Eqs. 8.3 and 8.11, will be

$$F_1 = \frac{\rho_s H_s}{\epsilon_o} = - \frac{\tau_s I_s}{\epsilon_o} \qquad (8.14)$$

(where the suffix s refers to the snow regions and R to the rain regions).

Similarly the potential gradient due to the rain charging region will be

$$F_2 = \frac{\rho_R H_R}{\epsilon_o} = - \frac{\tau_R (I_R - I_s)}{\epsilon_o} \qquad (8.15)$$

The potential gradient due to the space charge of the falling snow will be, from Eq. 8.4

$$F_3 = \frac{I_s}{2\epsilon_o v_s} \left\{ H_s + H_R + 2(h_s - h_m) \right\} \qquad (8.16)$$

and, similarly for the falling rain

$$F_4 = \frac{I_R}{2\epsilon_o v_R} (H_R + 2h_R) \qquad (8.17)$$

It is assumed that the fall speed of the precipitation changes from v_s to v_R on melting. Taking $v_R = 5\ ms^{-1}$ and $v_s = 1\ ms^{-1}$, we can write

$$v = v_R = 5v_s$$

If the effect of the melting region is just to reverse the sign of the precipitation current, then

$$I = I_R \approx -I_s$$

and taking $\gamma_R \approx \gamma_s = \gamma$, the ground potential gradient F is

$$F = F_1 + F_2 + F_3 + F_4 \qquad (8.18)$$

$$= \frac{I}{\epsilon_o} \left\{ -\frac{5}{2v}(H_s + H_R + 2h_s - 2h_m) + \frac{1}{2v}(H_R + 2h_R) - \gamma \right\}$$

$$= \frac{I}{\epsilon_o} \left\{ \frac{1}{2v}(-5H_s - 6H_R - 10h_s + 12h_m) - \gamma \right\} \qquad (8.19)$$

Hence, for an inverse relation to apply, the expression in square brackets in Eq. 8.19 is negative and so

$$\frac{1}{2v}(-5H_s - 6H_R - 10h_s + 12h_m) < \gamma \qquad (8.20)$$

Some typical values of H_s, H_R, h_s and h_m are used in

Table 8.4 to test the relationship 8.20 above. τ is again taken to be in the range 10 to 20 minutes. The snow charging region is assumed to lie within either the nimbostratus cloud (with a base at about 1 km) or the altostratus layer at about 3 km. The inverse relation results even when the melting level h_m is high and close to the altostratus layer (e.g. when the value of h_m is 2.5 km and h_s is 3.0 km).

While this theory is very approximate, its general conclusions do agree with the most typically observed behaviour of quiet rain. In the present work the melting level h_m was usually in the range 0.5 to 1.5 km, when the theory predicts an inverse relation, particularly if the snow was charged at higher levels. A few occasions when rain was observed to fall from altostratus cloud alone also showed an inverse relation, which the theory predicts; this is particularly true if the melting level was low, as would actually have been the case.

The main factors which, according to the theory, determine the presence of the inverse relation are the heights h_m and h_s of the two charging regions. The inverse relation would be most probable for a low h_m and a high h_s, when the space charge of the falling snow would have the most effect on the ground potential gradient.

8.4.3 Summary

A simple mathematical model of the electrical structure and behaviour of a cloud system producing quiet precipitation has been seen to account for the observed inverse relation

TABLE 8.4 THE RAIN CLOUD MODEL

Values of $T = (- 5H_s - 6H_R - 10h_s + 12h_m)/2v$

for various charging region dimensions:

Height h_m	height h_s	thickness H_s	T
m	m	m	min
200	1000	500	- 19
500	1000	500	- 13
800	1000	500	- 7
200	500	500	- 11
500	750	500	- 9
200	500	1000	- 15
500	750	1000	- 13
500	3000	500	- 46
1000	3000	500	- 36
2000	3000	500	- 16
2500	3000	500	+ 6
1000	3000	1000	- 40
2500	3000	1000	- 10

Fall speed of rain, v , taken as 5 ms^{-1}

Thickness of rain charging layer, h_R, taken as 200 m

at the ground. In the case of snow, it is most probable for charging occurring in the nimbostratus cloud layer, which will typically have a base at about 1 km and be centred around the -5°C temperature level.

For quiet rain, a second charge separation process in the melting region, acting in the opposite direction to the snow charging process, can account for the inverse relation. The snow charging process can in this case be located at altitudes as high as 3 km, even though the melting level can be also high. The negative potential gradient at the ground could be due to the negative space charge of the falling snow as well as to the negative ionic charge left within the melting region.

It is interesting to compare these conclusions with the observations of precipitating layer clouds mentioned in Sect. 2.1.5, assuming that precipitation charging is indeed associated with its generation. Snowfall was seen to be unlikely from clouds with a base above 1 km, in which case snowfall from altostratus cloud alone is unlikely. The theory of the previous section would not predict an inverse relation in such a case anyway, which suggests that charging was taking place within the nimbostratus layer during the periods of snow observed at Durham.

The origin of the inverse relation in the case of rain is less certain, with charging at the altostratus or nimbostratus layers being possible; there could well be some charging at both levels. The possibility of lower cloud levels being "seeded" by ice crystals falling from upper levels was also mentioned in Sect. 2.1.5. Some

charging at both levels would be consistent with the few cases observed at Durham of rain from altostratus cloud alone, when the inverse relation was still present.

8.5 The origin of the mirror-image effect

It has been seen how the inverse relation during quiet precipitation can be explained in terms of charging processes operating at different heights in the cloud system. Since the mirror-image effect is usually also present, any explanation of its origin will have to be based on an electrical structure in and below the cloud consistent with the presence of the inverse relation.

The mirror-image effect can be considered in the case of quiet precipitation as being a consequence of small variations in electrical activity superimposed on the overall inverse relation. These variations are seen at the ground as fluctuations in the potential gradient and precipitation current. Thus CHALMERS (1967) considered that the same factors which produce the inverse relation also operate in the case of the mirror-image effect, that is the leaving behind in the cloud of a charge opposite to that on the precipitation. The mirror-image effect involves changing conditions, however, and not necessarily the "quasi-static" state assumed for discussion of the inverse relation.

Chalmers' theories as to the possible origins of the mirror-image effect were discussed in Sect. 2.3.2; these will now be examined in terms of the observations of the present work.

8.5.1 Moving and stationary clouds

Chalmers argued that if the mirror-image effect was a consequence of the variation of electrical activity in the cloud, it could be due to either a moving cloud with regions of greater and lesser activity passing the observer, or to a stationary, developing cloud. In an actual period of precipitation, of course, both situations may be present to some extent, but it seems reasonable to expect that in at least some cases one or other situation will predominate.

To decide which situation applies in a particular case, an estimate of the likely period of variation of electrical activity within the cloud is needed. Some indication can be gained from the electrical relaxation time of the atmosphere, which as mentioned earlier is generally taken to be of the order of 10 to 20 min. for quiet precipitation. A cloud moving at 10 ms^{-1} will travel 12 km in a time of 20 min., so that any development in activity with this time period seems unlikely to be detected by a stationary observer, unless the development is particularly widespread over a large area of cloud. At low wind speeds, say 2 to 3 ms^{-1}, the cloud would only travel a kilometre or so in an hour, in which case the effects of electrical development could well be predominant as seen at a fixed location on the ground.

For most of the Durham records, the ground wind speeds were in the range 3 to 6 ms^{-1} (or above), so that the moving cloud situation might be expected. According to Chalmers, this results in a mirror-image effect at the ground with the potential gradient leading, which was indeed usually

found (Table 7.2).

Chalmers attributed the time difference between the two electrical records to the time of fall of the precipitation from the charging region being longer than the time taken by the portion of cloud from which it originated to travel across to be vertically above the observer. One possible reason for this difference could be wind shear between the cloud and the ground, resulting in the horizontal velocity of the precipitation decreasing as it nears the ground and so falling behind the portion of cloud in which it originated.

8.5.2 Theory of the time lags

A method will now be derived for estimating time lags (and their direction) for the mirror-image effect during quiet rain, assuming that they are due solely to wind shear between the charging region and the ground. This involves a number of assumptions concerning the physical behaviour of the precipitation as it falls from the cloud. These are:

(i) The precipitation particles travel horizontally at the speed of the wind, and vertically at their terminal fall speed: this is taken as 5 ms^{-1} for rain and 1 ms^{-1} for snow.

(ii) The terminal fall speed of the precipitation changes from that of snow to that of rain at the $0^{o}C$ level.

Also, with regard to the wind:

(iii) The variation of wind speed with height will be taken from the aerological profile at the nearest station to Durham at which the weather conditions are comparable. The surface wind speed will be taken as that at Durham, as this is most likely to be affected by local conditions.

(iv) A region of wind shear will be considered to be one where the wind speed changes with height (positive for an increase with increasing height). Changes in wind direction will not be considered; the aerological profiles show this to be a reasonable assumption, except occasionally in the first few hundred metres above the ground.

It is assumed that the precipitation is charged at a height H above the ground, and that the potential gradient at the ground is largely due to the space charge (of opposite sign) remaining in the cloud. Such a situation would result in the observed inverse relation at the ground, whereas if the ground potential gradient was due largely to the space charge of the falling precipitation, no inverse relation would result.

The mirror-image effect is taken as due to the passage of portions of cloud which are slightly more or less active electrically, but the difference not being sufficient to affect the presence of the overall inverse relation. A column of slightly increased (or decreased) precipitation

current will fall from the region of cloud to the ground, being deflected by any wind shear. It is this deflection which will determine whether there is a time lag between the potential gradient and precipitation current at the ground; if there is no shear, there will be no lag, as then the region of enhanced cloud charge will be above an observer at the ground at the same time as the precipitation current from this region arrives.

A typical situation is shown in Fig. 8.7 where the behaviour of a precipitation particle during fall from charging at height $\bar{z} = 0$ is considered. The origin of the co-ordinate system is taken to be the point of charging P for convenience of calculation. The frame of reference moves with the charging level at the horizontal wind velocity V (note that positive $\bar{z}$ is downwards).

If the wind shear k is constant with altitude

$$k = -\frac{dv}{dz} = -\frac{(V_g - V)}{H} \qquad (8.21)$$

(taking k to be positive if the wind speed increases with height above the ground).

A precipitation particle charged at P will experience a horizontal acceleration $\frac{dv}{dt}$ due to the wind shear as it falls to the ground.

$$\text{Now} \quad \frac{dv}{dt} = \frac{dv}{dz} \cdot \frac{dz}{dt} = -kw \qquad (8.22)$$

where w is the fall velocity of the particle.

The horizontal distance x travelled at time t after charging will be

FIG. 8.7 Calculation of time lags in the mirror-image effect

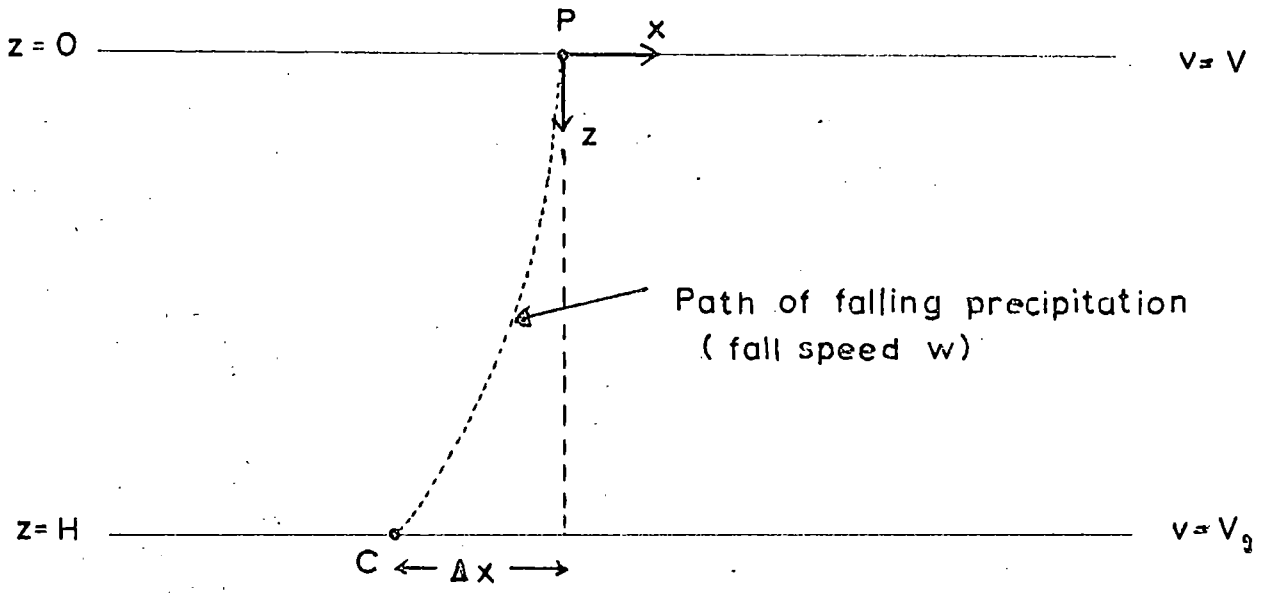

Precipitation collector is at point C

Co-ordinate system (origin at P) moves with the cloud at wind speed V.

Wind shear $k = \frac{V - V_g}{H}$

$$x = \frac{1}{2} \frac{dv}{dt} t^2 = -\frac{1}{2} kwt^2 \qquad (8.23)$$

But $t = \frac{z}{w}$

and so $x = -\frac{1}{2} \cdot \frac{kz^2}{w}$ (8.24)

Therefore, when the particle reaches the ground, the horizontal distance Δx travelled from the point of charging, P will be

$$\Delta x = -\frac{1}{2} \frac{kH^2}{w} \qquad (8.25)$$

The time difference Δt between the point P being directly above the precipitation collector and the precipitation arriving at the collector will be

$$\Delta t = \frac{\Delta x}{V} \qquad (8.26)$$

This will be the time lag of the mirror-image effect if the assumptions made earlier in this section are true.

Then $$\Delta t = -\frac{1}{2} \frac{kH^2}{Vw} \qquad (8.27)$$

This expression predicts a negative value of time lag Δt if the wind increases with height above the ground, a situation when the potential gradient would lead. This agrees with the arbitrary convention adopted earlier, of a negative value of time lag representing the potential gradient leading.

For zero wind shear, no time lag results if the precipitation always travels at the horizontal wind speed. This boundary condition is satisfied by Eq. 8.28, since $\Delta t = 0$ when $k = 0$.

This theory strictly applies only in the case of a strong inverse relation due to a single charging region above the ground, when the effects of the space charge of the falling precipitation can be neglected. The presence of more than one region of wind shear is allowed for by calculating the time lag due to each region, but in each case using the value of V for the uppermost region, since this will be the horizontal speed of the charging region. The resultant time lag at the ground is then

$$\Delta T = \sum_i \Delta t_i \qquad (8.28)$$

where t_i is the value of time lag for the ith region.

8.5.3 Calculation of time lags during quiet precipitation periods

The above method was used to calculate time lags for periods of quiet precipitation at Durham when both the inverse relation and mirror-image effect were prominent. The calculated values, assuming various charging heights, are given in Table 8.5, together with the actual measured values. The wind profiles were taken from the aerological records at either the Shanwell or Hemsby stations, dependent on which station had weather conditions most similar to Durham. Ground wind speeds were again taken as the average at Durham during the precipitation period, as these were the

TABLE 8.5 MEASURED AND CALCULATED TIME LAGS OF THE MIRROR-IMAGE EFFECT

RECORD			CROSS CORRELATION MAXIMUM		CALCULATED TIME LAG (MINUTES)			AEROLOGICAL DATA STATION AND TIME
NO	DATE		COEFFICIENT	TIME LAG (MIN)	FROM 0°C LEVEL	FROM -5°C LEVEL	FROM -15°C LEVEL	
1/1	7/8	JAN	-0.47	+5.5	-	+3.5	+3.5	HEMSBY 23Z
					-	-5.5	-1.5	SHANWELL 23Z
1/2	8/9		-0.58***	-0.5	-	+0.5	-1.5	HEMSBY 23Z
					-1.0	+0.5	+15.5	SHANWELL 23Z
1/3	11		-0.67**	-7.5	-6.5	-6.5	- 9.0	SHANWELL 11Z
2/1	1/2	FEB	-0.93**	+1.0	-	-7.0	+1.5	SHANWELL 23Z
2/5	15		-0.56*	-1.0	-	-0.5	+6.5	SHANWELL 11Z
3/1	1	MAR	-0.27	-2.5	-1.0	-1.0	0.0	HEMSBY 23Z (29th)
3/5	6		-0.80***	-3.5	-0.5	-1.5	-0.5	SHANWELL 23Z
3/7	8		-0.63*	-2.0	-1.0	-2.0	+4.0	SHANWELL 11Z

Notes on next page

(cont.)

TABLE 8.5 (Continued)

RECORD			CROSS CORRELATION MAXIMUM		CALCULATED TIME LAG (MINUTES)			AEROLOGICAL DATA STATION AND TIME
NO	DATE		COEFFICIENT	TIME LAG (MIN)	FROM 0°C LEVEL	FROM -5°C LEVEL	FROM -15°C LEVEL	
4/4	8		-0.85***	-4.0	-0.5	-2.5	+7.0	SHANWELL 23Z(7th)
4/5	8/9	APR	-0.48*	+1.5	-1.0	-1.0	+10.0	SHANWELL 23Z
4/7	26/27		-0.45	-4.0	-1.5	-2.5	-	HEMSBY 23Z
6/6	7	JUN	-0.70*	-2.0	-1.0	-1.5	-	SHANWELL 11Z
6/9	10/11		-0.32	-3.0	-1.5	-2.5	-	HEMSBY 23Z
					-	+1.5	-	SHANWELL 23Z
6/14	19		-0.62**	-4.0	-	-3.0	-	SHANWELL 11Z

Significance levels of correlation coefficient: * 95% ** 99% *** 99.9%

most likely to be affected by local conditions.

Considering the approximations involved in this method, the calculated values of time lag in Table 8.5 agree surprisingly well with the actual values, assuming charging at the -5°C level (typically about 1.5 km altitude). The large time lag for record 1/3 of 11 January is predicted, as is the near-zero lag of record 2/5 of 15 February. The calculated time lags assuming charging at the melting level are all too small, while charging at the -15°C level (about 3.5 km) would usually result in the precipitation current leading. This latter result is due to the effects of the region of negative wind shear usually present in or above the nimbrostratus cloud layer (see for instance Fig. 6.14). This region was particularly prominent for the sleet record 1/1 and the rain record 4/5, and so these periods were included in the calculations, although not showing the usual direction of time lag.

8.5.4 Conclusions from the calculated time lags

This method of calculating the time lag of the mirror-image effect suggests that when the main charging region is located approximately around the -5°C level the calculated time lags are in reasonable agreement with the actual values. Certainly, if these time lags are largely determined by the height of the charging region and the wind shear beneath, charging at altrostratus levels (about the -15°C level) appears to be inconsistent with the usual magnitude and direction of time lag.

It must be borne in mind that quite considerable

assumptions have been made in calculating these time lags. In particular, the rain below the melting level is unlikely to travel horizontally at the wind speed, although it will be influenced by it. ASPINALL (1970) has in fact deduced an expression relating the behaviour of the falling raindrops to the horizontal wind speed in this situation, but it involved an unconvincing solution to a complicated differential equation.

The wind profiles were taken on each occasion from a single set of aerological data at a station a considerable distance from Durham. Despite careful comparison of the weather conditions at the station with those at Durham, they may have been considerably different, and possibly unrepresentative of average conditions over the whole period of precipitation. However, this method does show that the observed time lags during the mirror-image effect can be explained in terms of a cloud charging process, probably above the melting region, and the effects of wind shear between the cloud and the ground.

8.6 General conclusions

This Chapter has shown that many of the periods of quiet precipitation observed at Durham had electrical behaviour typical of that found by previous investigations. Both the inverse relation and mirror-image effect during rain can be explained qualitatively by two charging processes, one charging solid precipitation negatively and the second charging the precipitation positively on melting. Both processes are assumed to leave an opposite charge in the appropriate charging region. Some degree of quantitative

explanation has also been given, in particular for the time lags associated with the mirror-image effect.

The upper charging process appears most likely to be located in the lower, nimbostratus, cloud layer surrounding approximately the -5°C level. Charging in the upper, alto-stratus, layer would be consistent with the inverse relation during rain, but would not produce the usual time lag in the mirror-image effect. This conclusion agrees with the aircraft observations of Imyanitov and Chubarina, reported in Chapter 2, who found most charging in the 0°C to - 10°C regions of the cloud.

The inverse relation during snow can be explained by the upper charging process alone, located in the nimbostratus cloud layer. The theory of the mirror-image effect does not, however, explain the usual direction of time lag unless the wind shear between the cloud and the ground is consistently different during snow from that during rain; there is no evidence that this is so.

In all these cases a "quasi-static" state has been assumed, such that the precipitation currents and space charge densities do not vary significantly with height outside the charging regions, and that there are no significant horizontal variations in current or charge. The mirror-image effect is considered to be due to cloud regions of slightly greater or lesser activity passing a stationary observer at the ground; these variations are superimposed on the overall inverse relation at the ground.

The observed connection between the degrees of electrical and meteorological activity (the latter represented by the rate of rainfall) is consistent with the assumption that precipitation charging is associated with its formation. In particular the variance of the electrical quantities was found to increase with rate of rainfall.

CHAPTER 9

Other Periods of Precipitation and Some Other Topics

9.1 Periods of quiet precipitation

Most periods of quiet precipitation were examined in the previous Chapter, where their behaviour was seen to be generally consistent with the theories of Chalmers regarding the charging of quiet precipitation. Some of the periods which did not behave in this manner will now be considered.

9.1.1 The mirror-image effect

Most of the exceptions to the general pattern of behaviour are apparent if the mirror-image effect is considered. If Table 7.2 is examined, it can be seen that these exceptions are of two types:

(i) Periods with a maximum of negative cross-correlation (and hence mirror-image effect) for the precipitation current leading. Some of the time lags are much greater than usual, but not all the correlations are significant.

(ii) Three periods with a maximum of positive cross-correlation (and so no mirror-image effect) for the precipitation current leading. Again the time lags are much greater than usual.

There is only one record, 6/5 of the 4 and 5 June, which

does not fit these classifications, nor that of Chapter 8. This shows negative correlation, but for the potential gradient leading by 61 minutes. The correlation coefficient is not statistically significant in this case and point discharge currents may have occurred during a short part of the record when the potential gradient was high, and so this record will not be considered further.

9.1.2 The mirror-image effect with the precipitation current leading

If the two periods of snow are included, six records come into this category. Period 4/5 of the 8 and 9 April could be explained by wind shear effects (see the previous Chapter), as on this occasion aerological profiles show a considerable vertical region of wind speed decreasing with increasing altitude, which would cause the falling precipitation to advance ahead of the cloud. The time lag (1.5 min) is much smaller than for the two other periods of rain (5/1 and 6/16), suggesting that there may have been different factors acting in this case than for the other two periods.

A common feature of the records 5/1 and 6/16 is the low surface wind speeds throughout the period of rain; Table 7.3 shows the mean wind speeds at Durham to be respectively 1.5 and 1.0 ms^{-1}. The appropriate aerological profile at Shanwell for the record 5/1, shows the wind speed to be low right up to the altostratus cloud level at 3 km altitude, with the wind not exceeding 5 ms^{-1} until 3.2 km (see Fig. 6.21), with similar conditions persisting

12 hours later. A similar period of quiet rain was also recorded on the 3 and 4 August 1971, before the data handling system was developed. Steady rain fell in low wind conditions for nearly 19 hours, with a statistically significant cross-correlation coefficient of - 0.48 for the precipitation current leading by 10.5 min. The surface wind speed at Durham averaged 1.5 ms^{-1}, and the aerological profiles at both Shanwell and Aughton again show wind speeds mostly less than 5 ms^{-1} at up to 3 km altitude (Fig. 9.1).

It will be recalled that Chalmers' explanation of the mirror-image effect also included the case of a stationary developing cloud, for which he predicted a maximum of negative cross-correlation for the precipitation current leading. This could explain the periods of precipitation mentioned above, as the wind speeds in two of the cases were low right up to the altostratus cloud level, so that the cloud system would have been particularly slow-moving.

The much longer time lags during these periods of rain may also be consistent with this explanation, for if the variation in the electrical quantities at the ground is due largely to variation in electrical activity in the cloud, then the time lag may be associated with the time of fall of the precipitation from the cloud. Precipitation falling from nimbostratus cloud at 2 km through a melting level at 1 km would have a time of fall of about 20 min, assuming fall speeds of 1 ms^{-1} for snow and 5 ms^{-1} for rain. The recorded time lags were respectively 22 and 20 min for records 5/1 and 6/16 and 10.5 min for the 3 and 4 August 1971,

FIG. 9.1 Wind profile at Aughton 23Z 3 August 1971

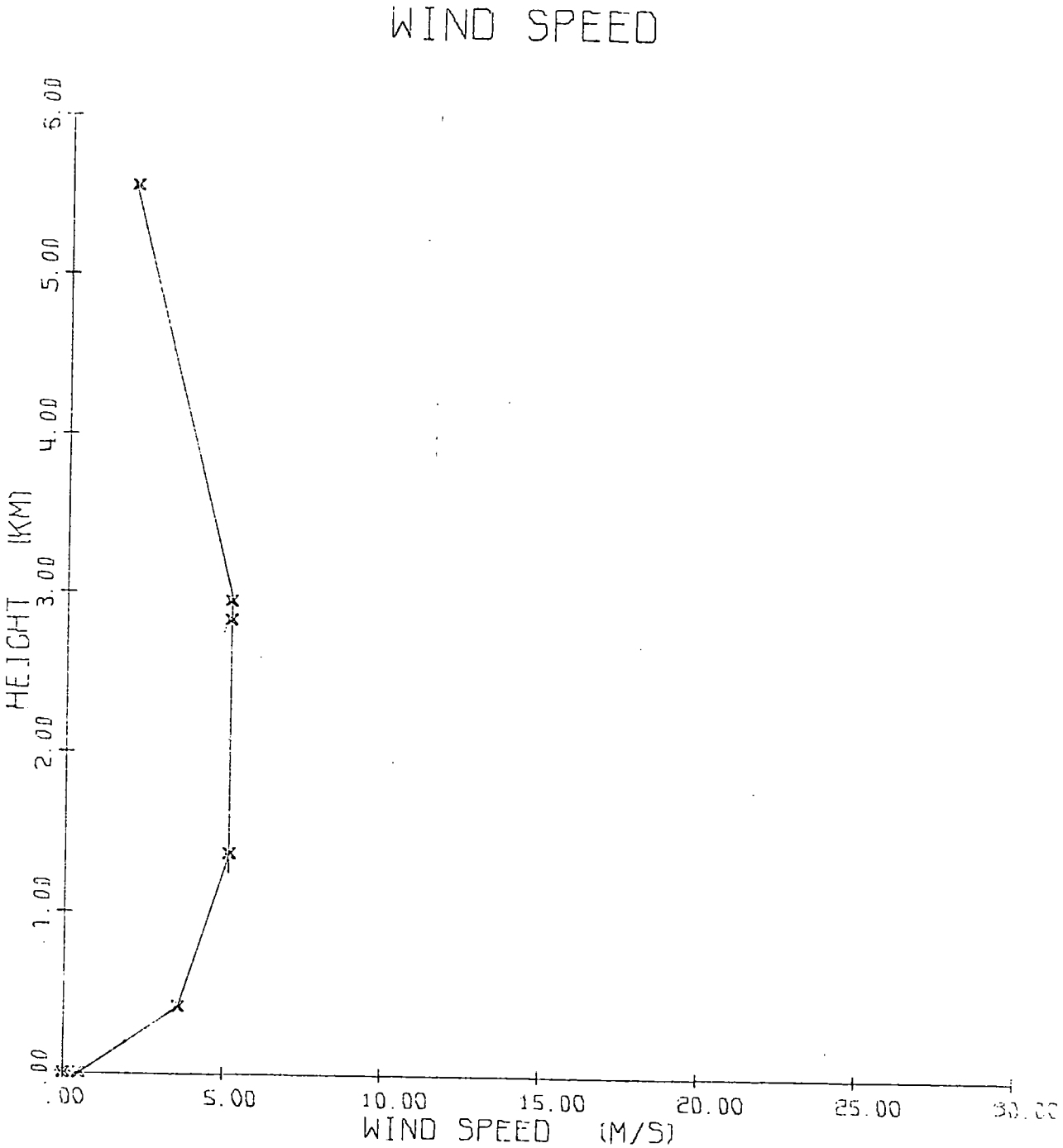

the melting level in fact being much higher in the latter case than in the other two cases.

While Chalmers' theory again may explain the behaviour of some of these periods of rain, there is still no explanation of the behaviour of the two periods of snow (and one of the periods of sleet). Conditions were not particularly quiet during these periods, although the electrical behaviour was similar to that in the periods mentioned above. The greater space charge of falling snow, due to its fall speed being less than rain, seems unlikely to be a factor, since the inverse relation is still present. Charging processes within the cloud, therefore, may not be sufficient to explain the electrical properties of quiet snow, and so possibly other effects may be responsible.

9.1.3 Other periods with the precipitation current leading

Two periods of rain (4/2 and 5/2) and one of sleet (2/5) show a statistically significant positive cross-correlation for the precipitation current leading. There are no common features of the three periods, however, which suggest possible reasons for this behaviour. Record 5/2 occurred during particularly quiet conditions when wind speeds were low, while record 2/5 was during particularly high wind speeds, with a mean of 9.5 ms^{-1} at Durham. Two of the records show minor peaks of negative correlation for the potential gradient leading, which is the usual behaviour of quiet rain, but this may be due to the periodicity of the electrical records producing a similar periodicity in the

cross-correlation function, as explained in Sect. 5.1.4. The inverse relation was present during all three records.

9.1.4 The inverse relation

Some periods of rain did not show an inverse relation, in which case both the potential gradient and precipitation current were negative. Referring to Table 7.1, these periods were 2/3, 3/10, 5/1, 6/7 and 6/13. In all but the last case the synoptic situation at the time, given in Table 7.3, was different from the usual one of a passing occluded or warm front. Thus for record 2/3 there was no evidence of any frontal feature, the precipitation at Durham being largely heavy drizzle, with the area of precipitation being confined to near the east coast of Northern England and Scotland. There was also no frontal feature which could account for period 3/10, but the high rate of rainfall (1.2 mm hr^{-1}) makes it unlikely to have been drizzle. Record 5/1 has already been examined in detail in Chapter 6, where it can be seen that the lack of any inverse relation is in fact confined to the first half of the record; the second half has different electrical properties, as examined in Sect 9.1.2. The usual frontal situation was again absent, except towards the end of the period when an occluded front had developed. (see Fig. 6.16).

Another aspect of the connection between the meteorological and electrical properties of quiet precipitation is thus suggested; that precipitation periods not showing an inverse relation tend to originate in different meteorological situations from those that do. More observations are

needed to clarify this relationship, and to suggest reasons for the different electrical behaviour.

Occasionally there was a period of rain with a mean positive potential gradient and a mean negative precipitation current; instances are records 6/11 and 6/16. The latter record showed the mirror-image effect, but with the precipitation current leading. In both cases the usual frontal feature was not evident, the latter record being rain associated with a cold front.

9.1.5 Summary

The conclusions of this section can be summarised as follows:

(i) Most of the meteorogically quietest periods of rain, i.e. when wind speeds were lowest, showed electrical behaviour different from that generally observed during quiet rain. This is particularly evident when the mirror-image effect is considered.

(ii) The electrical behaviour of these periods can be explained to some extent in terms of a predominantly stationary cloud in which the electrical activity is varying, as suggested by Chalmers. The presence of the inverse relation would suggest that the same charging processes are concerned as for the moving cloud situation.

(iii) The electrical behaviour of quiet snow is similar to very quiet rain, but the situation is not that of a stationary developing cloud.

(iv) Periods of quiet precipitation showing electrical behaviour different from that generally observed often originate in meteorological situations also different from usual.

The idea of a stationary, developing cloud sometimes being the origin of the electrical behaviour of quiet precipitation is supported by some observations of precipitation currents to horizontally separated receivers. CHALMERS (1967) reports simultaneous variations of current at distances up to 12 km apart, while more recently STRINGFELLOW (1969) found on several occasions significant correlation between simultaneous currents to receivers several kilometres apart. More often, of course, such measurements result in maximum correlation for a time difference approximately equal to the time of travel of the cloud from one receiver to the other (STRINGFELLOW, 1969; OWOLABI and CHALMERS, 1965). This finding is in accordance with the electrical behaviour of quiet precipitation being due to the movement of the cloud system past the observer on the ground.

9.2 Quiet and disturbed precipitation

While the present work is concerned with the electrical behaviour of quiet precipitation, the characteristics of a number of periods of disturbed precipitation will now be considered. It will be recalled that the term "disturbed" was proposed for periods which showed more violent electrical behaviour, and an example was given in Chapter 6. No common method of distinguishing quiet and disturbed precip-

itation has ever been given by workers investigating the subject; however the most usual method has been to describe as quiet those periods when the potential gradient does not exceed a certain magnitude, for instance 1000 Vm^{-1}; and all other periods would then presumably be classed as disturbed.

A similar approach has been taken initially in the present work, with $\pm$ 1500 Vm^{-1} being used as the limiting values of potential gradient (see Sect. 2.5.3). More detailed consideration of the electrical and meteorological conditions during some of the periods of disturbed precipitation at Durham suggest a more precise means of distinguishing quiet and disturbed precipitation.

9.2.1 Periods of disturbed precipitation

As the potential gradient and precipitation current were continuously recorded on chart whether or not precipitation was falling, records of many of the periods of disturbed precipitation at Durham were also obtained. Despite the chart records often being off-scale or changing rapidly, the frequency of sign reversals of the potential gradient and precipitation current could be obtained for all but the most disturbed periods. This frequency has already been seen to give a reasonable measure of the degree of electrical activity during quiet precipitation, and so should at least indicate whether the degree of activity during disturbed precipitation is considerably different.

Values of the frequency of sign reversals and details of the meteorological conditions during some of the periods

of disturbed precipitation recorded at Durham are given in Table 9.1. Both the meteorological and electrical quantities are generally greater than during quiet precipitation, with the frequency of sign reversals being mostly above 1.5 hr^{-1}, and precipitation rates as high as 2.6 mm hr^{-1}.

To compare periods of disturbed and quiet precipitation, the frequency of sign reversals of potential gradient and precipitation current are plotted against rate of rainfall in Figs. 9.2 and 9.3. Periods are classed as quiet from the criteria given previously in Sect. 2.5.3, and all others are considered to be disturbed. There is a clear transition from quiet to disturbed precipitation for a mean rate of rainfall of about 1.0 mm hr^{-1} and a frequency of sign reversals of about 2.0 hr^{-1} for both the potential gradient and the precipitation current.

9.2.2 The distinction between quiet and disturbed precipitation

The prominence of the transition from quiet to disturbed precipitation suggests that the frequency of sign reversals of either the potential gradient or the precipitation current could be used to distinguish the two types of precipitation, this quantity having the advantage of being readily obtainable from chart records. Figs. 9.2 and 9.3 suggest a value of 2.0 hr^{-1} as the transition point, although there is some overlap between the two types of precipitation. This value can be compared with that of 1.5 hr^{-1} given by REITER (1965) as the maximum frequency of potential gradient sign reversals in a stable 500 - 700 mb layer of the atmos-

TABLE 9.1 PROPERTIES OF SOME DISTURBED PRECIPITATION PERIODS AT DURHAM

DATE (1972)	START	FINISH	DURATION	MEAN RATE OF RAINFALL	FREQUENCY OF SIGN REVERSALS	
					POTENTIAL GRADIENT	PRECIPITATION CURRENT
	G.M.T.	G.M.T.	hr	mm hr^{-1}	hr^{-1}	hr^{-1}
26 JAN	13 00	23 30	10.5	2.3	9.5	4.9
3 FEB	16 30	22 30	6.0	2.3	4.3	3.7
3 MAR	14 45	18 45	4.0	2.0	11.1	4.0
4	18 15	20 50	2.6	1.4	9.2	5.0
7 APR	03 15	05 15	2.0	1.5	13.0	4.0
12 MAY	01 00	08 00	7.0	1.6	2.6	1.9
31	17 00	21 50	4.8	1.9	8.7	2.9
2	11 40	13 45	2.1	0.9	1.9	-
3/4 JUN	22 10	05 30	7.4	0.9	2.3	1.9
11	04 40	08 00	3.3	0.9	4.2	2.4
19	13 45	17 40	3.9	0.8	5.5	1.9

FIG. 9.2 Frequency of potential gradient sign reversals against mean rate of rainfall.
(Disturbed and quiet precipitation)

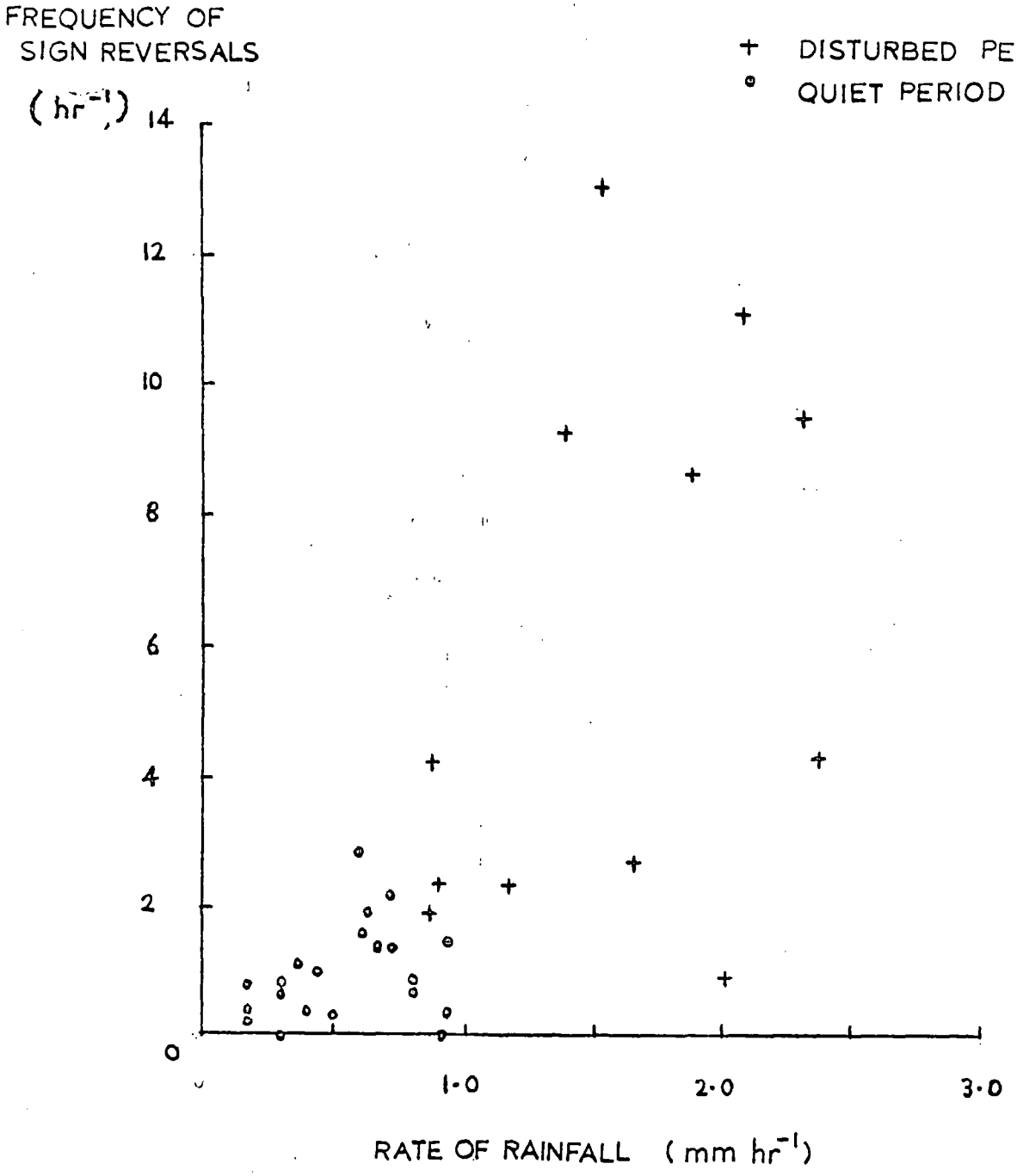

FIG. 9.3 Frequency of precipitation current sign reversals against mean rate of rainfall

(Disturbed and quiet precipitation)

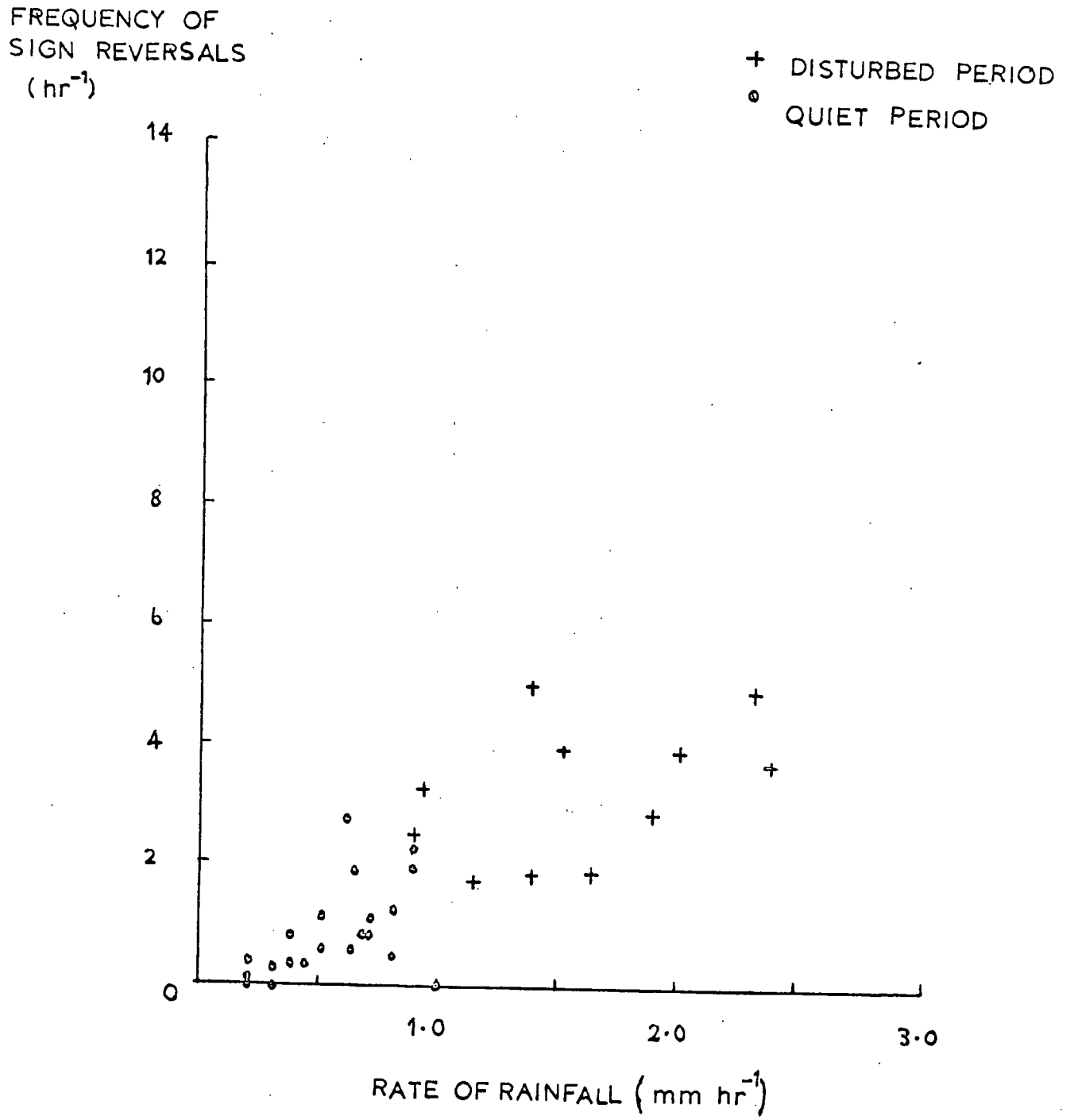

phere (see Sect. 2.2.1). If, as according to Reiter, this frequency reflects the transition in the cloud from stable to unstable conditions, it would appear that disturbed precipitation is associated with unstable conditions within the cloud, when the degree of atmospheric turbulence is much greater. Certainly, wind profiles during periods of disturbed precipitation, such as Fig. 6.27, generally show much greater wind speeds and wind shear within the cloud than usual during quiet precipitation.

The connection between the mean rate of rainfall and the degree of electrical activity is interesting, as all the periods of disturbed precipitation at Durham have a rate greater than about 0.8 mm hr^{-1} and all quiet periods have a rate less than about 1.2 mm hr^{-1}; indeed the mean rate of rainfall could also be used to distinguish the two types of precipitation. There is a definite trend for the electrical activity to increase with rate of rainfall, particularly when the precipitation current is considered.

The sudden transition from quiet to disturbed precipitation at about 1.0 mm hr^{-1} rainfall rate could be due to the potential gradient then reaching values high enough to generate significant point discharge currents, with consequent ion capture by the falling precipitation. While this would explain the sudden transition, clearly meteorological factors are also involved in the light of Reiters' conclusions as to the degree of atmospheric stability during the two types of precipitation.

9.2.3 Criteria for quiet precipitation

In view of the above conclusions, the following criteria for classifying steady precipitation as quiet are proposed:

(i) The potential gradient does not exceed 1500 Vm^{-1} in magnitude for a significant period of the record (say more than 10% of its duration).

(ii) The frequency of sign reversals of potential gradient or precipitation current does not exceed about 2.0 hr^{-1} when averaged over the record.

(iii) The mean rate of rainfall during the record does not exceed about 1.0 mm hr^{-1}.

(iv) To exclude showers and other short periods of rain, and to provide a sufficiently long averaging time for conditions (ii) and (iii), the duration of the precipitation period is at least 2 hours.

The conditions (ii) and (iii) are more or less equivalent, and if more records had been considered and the mean rates of rainfall known with more accuracy, it might have been possible to give more precise values to the transition points. In many cases conditions (ii) and (iv) alone will be sufficient; had they been used in the present work, condition (i) would nearly always have been satisfied.

There will always be some periods, of course, which for various reasons are difficult to classify. In particular there will be periods which are partly quiet and partly disturbed, in which case it is probably better to consider them as disturbed, unless the different parts of

the record can be easily distinguished. Periods of snow may prove difficult to classify as there is evidence that, in even a moderate wind, blowing snow may become considerably charged, possibly due to collision of the snowflakes. Such periods are characterised by high potential gradients although the precipitation rate is low. Such a period was observed at Durham on 18 January 1972, when light snowfall in a blustery wind resulted in a negative potential gradient often greater than the - 1500 Vm^{-1} limit for quiet precipitation.

9.3 Further work of Reiter

Since Chapter 8 was written, a recent paper of REITER (1972) has come to the authors' attention. In this paper are quoted more results of electrical measurements during quiet precipitation, based on eight years of observations at the same mountain stations as described previously. Reiter also briefly discusses possible charging processes which could account for the observed electrical behaviour.

9.3.1 The electrical observations

Reiter again finds the inverse relation and mirror-image effect to be prominent during quiet precipitation, as well as the reversal of precipitation charge on the melting of snow to rain. The relationship between the precipitation current and potential gradient is found to be little affected by altitude or precipitation rate, although the precipitation current density shows a tendency to increase

with rate of rainfall. This latter finding was suggested in the present work (see Fig. 8.1) although a more prominent relationship was found between potential gradient and precipitation rate.

9.3.2 Charge separation processes

The relationship between potential gradient and precipitation current density is considered by Reiter to be best explained by a charge separation process acting during the fall of the precipitation, rather than by an ion-capture process whereby the falling precipitation captures point-discharge ions of opposite charge. The main evidence against the ion-capture theory is:

(i) The charge per unit volume brought down by precipitation is inconsistent with values likely from ion-capture.

(ii) The potential gradient must be sufficiently high immediately before a period of precipitation for the ion-capture process to operate at the start of precipitation, or else the inverse relation would not immediately apply. An initially high potential gradient is not usually seen in Reiters' observations (or in those of the present work).

Reiter concludes that the charge separation process consists of the separation of oppositely charged, minute snow particles or rain droplets during the fall of precipitation. This results in negatively charged snow falling in a positive space charge, producing a positive potential gradient at the ground. A similar situation would apply

during rain, but with the signs reversed. Two features of quiet precipitation are quoted as particularly supporting this view:

(i) Just before precipitation reaches the ground, the potential gradient often becomes (in the case of snow) negative, returning to positive when the snow arrives. This could be due to the effect of the negative charge of the falling snow nearest to the ground, which is subsequently replaced by the effect of the positive space charge of the small ice particles when the snow has reached the ground.

(ii) After precipitation has ceased, the potential gradient takes about 15 to 30 minutes to recover to its normal, fair-weather value, which could be due to the time taken for the minute snow particles (or rain droplets) to disperse or to be dissipated by conduction.

This explanation of the origin of the electrical behaviour differs from that proposed by Chalmers in one important aspect: Reiter locates the charging in the falling precipitation, while Chalmers locates it within the cloud. Both agree in considering a second charging process to be associated with the melting of snow to rain.

One feature of the electrical behaviour which neither theory adequately explains is why the time lag of the mirror-image effect is different during snow, when the precipitation current leads, from that during rain, when

the potential gradient leads. While Reiter does not consider time lags, it seems reasonable to expect the precipitation current to lead in a stationary, developing cloud situation, since the space charge generated by the falling precipitation will need some time to build up following an increase in precipitation current. In the moving, quasi-static cloud situation, however, time lags would presumably be controlled by the same processes as in the Chalmers' theory, i.e. wind shear.

It is difficult to decide which theory offers a better explanation of quiet precipitation electrification. Chalmers' theory offers a reasonable explanation of the electrical behaviour, and experimental work of Imyanitov and Chubarina has been quoted as supporting the view of charging located primarily within the cloud. Reiter's theory may still offer an explanation of the behaviour of snow, since there is considerable evidence for charging effects associated with the collision and break up of snow particles (see Chapter 1).

9.3.3 Atmospheric turbulence and the degree of electrical activity

Reiter also elaborates his previous conclusions on this subject and expresses the frequency of sign reversals of the potential gradient as a function of the "vertical exchange coefficient" in the cloud layer between 1.8 km and 3.0 km altitude. This coefficient represents the degree of turbulence in this layer, and his summary of results is given in Fig. 9.4. The transition from stable

FIG. 9.4 Frequency of potential gradient sign reversals F_p against the vertical exchange coefficient A. From REITER (1972)

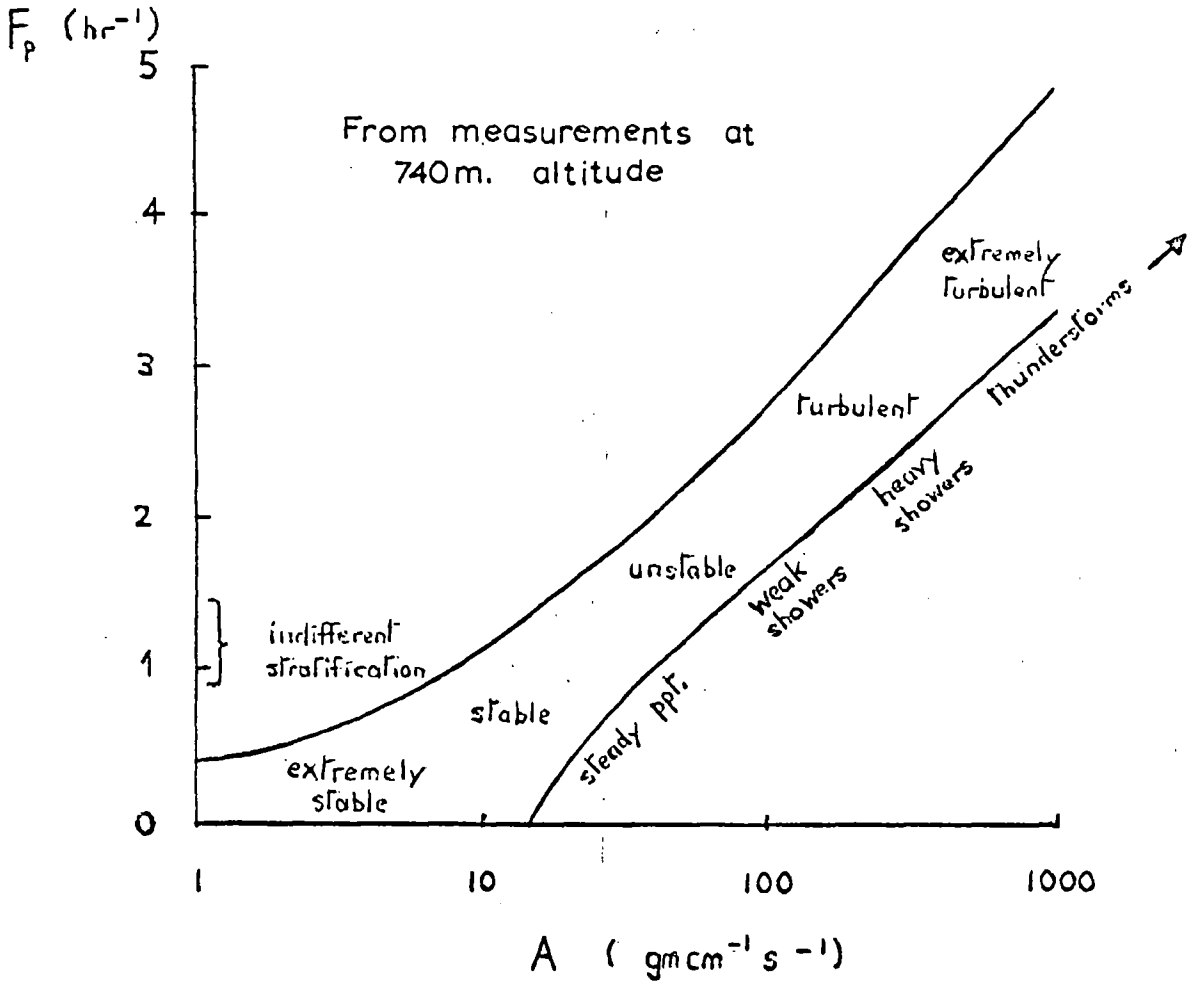

to unstable stratification is again given at about 1.5 reversals per hour, with rates of 4.0 and above representing extremely turbulent conditions. These results are interesting, as they suggest that it is possible to draw conclusions about the weather conditions, since heavy rain or even thunderstorms may be likely if the frequency of sign reversals is high. Conversely, a low frequency (or absence) of sign reversals indicates stable cloud conditions and heavy precipitation to be unlikely.

These conclusions have been seen to be supported by the observations at Durham, except that a transition frequency of 2 sign reversals per hour is more appropriate. This may be due to the different type of site at Durham from the mountain stations where Reiter made his observations. The increase in the frequency of sign reversals of both potential gradient and precipitation current with precipitation rate found at Durham (see Figs. 9.2 and 9.3) was not found by Reiter, although he included shower observations when the frequency will often be high and difficult to assess. The clearer relationship found at Durham between the standard deviation (and hence variance) of the electrical quantities and the rate of rainfall suggests that the frequency of sign reversals is in fact an approximate expression of the degree of variation of the electrical quantities, which is better expressed by the standard deviation or variance.

CHAPTER 10

General Conclusions and Recommendations for Further Work

10.1 The quiet precipitation results

Observation of nearly all periods of quiet precipitation at Durham between January and June 1972 show that both the inverse relation and mirror-image effect are usually present, and during such periods of rain the precipitation current is positive and the potential gradient negative, while during snow these signs are reversed. While the snow results are based on only two long periods of snow, they agree with the observations of earlier workers such as REITER (1965, 1968) and MAGONO and ORIKASA (1966).

The electrical properties of quiet precipitation have been specified in this work by:

(i) The mean values of potential gradient and precipitation current density during the period of precipitation. If these are of opposite sign then the inverse relation applies.

(ii) The cross-correlation coefficient between the potential gradient and precipitation current. If this is negative and statistically significant, then the mirror-image effect applies.

(iii) The time lag between the two electrical records for which the above cross-correlation is a maximum. This time lag will be of the order of a few minutes, with the potential gradient leading during rain, and

the precipitation current during snow.

It is considered that this method of statistically expressing the electrical properties of quiet precipitation corresponds to closely the methods of previous workers, who either by visually examining a chart record or by using graphical methods, determined whether the inverse relation and mirror-image effect were present. In addition it provides a quantitative method for describing the degree to which these effects are present during a period of precipitation.

It has also been seen that some periods of quiet rain show different electrical behaviour from the majority of periods, with for instance the potential gradient and precipitation current both being negative, the cross-correlation coefficient being positive, or the time lag being different in either magnitude or direction. While such periods are less common, they are certainly not isolated occurrences, and so any theory accounting for quiet precipitation electrification must also be capable of explaining how these less common periods arise.

10.2 Theories of quiet precipitation electrification

The theories of Chalmers concerning quiet precipitation electrification have been quoted in various chapters, and some theoretical work based on these theories was presented in Chapter 8 to test his conclusions in a more quantitative manner.

To summarise, Chalmers considers two main charging processes to account for both snow and rain electrification. The first process, operating at temperatures below 0°C, charges solid precipitation negatively while at the same time leaving a positive space charge within the charging region. If the falling

precipitation subsequently melts before reaching the ground, a second process changes the sign of the precipitation charge to positive, leaving behind a negative charge in this second charging region. The most likely location of this second process is within the melting region and there is strong experimental evidence that this is so.

The theoretical work in Chapter 8 attempted to find if these two charging processes can indeed account for the inverse relation at the ground, given the observed magnitudes of potential gradient and precipitation current density, the likely dimensions of the cloud system, and for rain typical heights of the melting level. Assuming that there are no significant horizontal variations in the cloud system (and hence in the degree of electrical activity), then Chalmers' theories were seen to be quite adequate during both rain and snow. The most likely location of the upper charging process was within the cloud up to roughly the $-10^{o}C$ level, with the lower process assumed to be at the melting region.

Chalmers' work can also be extended to explain the mirror-image effect and the time lags between the electrical variations. In the case of a moving cloud where the electrical activity is effectively constant, his prediction of a mirror-image effect with the potential gradient leading is borne out by the observations at Durham. Also, it has proved possible to calculate likely values of time lag assuming that the lag is due solely to wind shear between the cloud and the ground. The calculated values agree surprisingly well in direction and magnitude with those observed, for charging again within the regions of the cloud up to about the $-10^{o}C$ level.

This latter result should perhaps be treated with some caution for several reasons:

(i) The wind profiles used to calculate the wind shear, and hence time lag, were from stations a considerable distance from Durham (up to 150 km) where conditions could have been significantly different. Also, conditions will have changed with time, particularly for the longer records.

(ii) The behaviour of falling precipitation is uncertain, and is unlikely to be controlled entirely by the wind. During snow, when this assumption is most likely to be true, the actual time lags were of opposite direction to those calculated.

(iii) The calculation of time lags during rain in effect assumed that melting electrification resulted only in the change in the precipitation charge and potential gradient signs: the effect on any time lag immediately before this charging process was considered to be negligible. Nevertheless the magnitude of the time lags observed at the ground was too large to be explained solely by wind shear between the melting level and the ground, suggesting that the initial charging was at a higher level.

More support for Chalmers' theory is, however, given by the behaviour of a few of the precipitation periods where conditions were particularly quiet both meteorologically and electrically, and where the precipitation current was leading the potential gradient. Wind profiles showed the cloud system to be particularly slow-moving, with the electrical situation being that

predicted by Chalmers for a stationary cloud where the effects of electrical development are predominant. Different behaviour of the time lag might also be expected, as on these occasions there was little or no wind shear.

One feature of quiet precipitation which Chalmers' theory does not explain is the electrical behaviour of snow, when the precipitation current leads the potential gradient. The situation is certainly not that of a stationary, developing cloud, and evidently some other explanation is needed in this case.

In Chapter 9 some suggestions of Reiter as to possible charging processes were noted, whereby he proposed charging to be due to the breaking off of minute rain droplets or snow particles from the falling precipitation. If these droplets or particles carried an opposite charge to the precipitation then an inverse relation would arise. Reiter does not consider possible time lags in the mirror-image effect, and so in this respect it is difficult to compare this theory directly with that of Chalmers. The breaking process during snowfall seems more possible, as strong electrification of snow in high winds, due to the collision of snow flakes or ice particles, has been observed. Such a process during rain seems less likely, with the results of SMITH (1955) being mentioned in Chapter 2, which showed that even the impact of rain drops on the ground during quiet precipitation did not produce significant electrification. Reiter's theory may offer an explanation of the electrical behaviour of snow, therefore, and could be worth considering in any future investigation of the subject.

10.3 Possible charging processes

A number of charging processes which could be responsible for quiet precipitation electrification were outlined in Chapter 1, and these will now be reconsidered in the light of the results of the present work.

Charge separation on melting is almost certainly the explanation of the reversal of charge between snow and rain, and an estimate of the likely magnitude of this process can be obtained from Table 7.4, which lists the average values of precipitation charge per unit mass for the periods of precipitation at Durham. While individual values vary widely, a figure of + 20 pC gm^{-1} is typical for rain, with the two snow periods having values of - 17 and - 31 pC gm^{-1}. These figures suggest about 40 pC gm^{-1} as the charge separation on melting: however, allowing for the collection efficiency of the precipitation collector (it has been estimated at about 50%), a figure closer to 80 or 100 pC gm^{-1} might be more appropriate.

Measurements of the charge separation during melting have been made by several workers. The earliest investigation, that of DINGER and GUNN (1946), found a charge separation in ice samples of about 1 e.s.u. gm^{-1} (just over 300 pC gm^{-1}), but later work showed the experimental conditions to be unrealistic. More recently, ice samples melted in a controlled air stream have been found to produce charge of around 100 pC gm^{-1} by KIKUCHI (1965) and over 300 pC gm^{-1} by DRAKE (1968). The charge separation was found, however, to be very dependent on such factors as impurity concentrations and air bubble structure.

The amounts of charge separated are nevertheless sufficiently close to those suggested by the quiet precipitation observations to enable charge separation in melting snow to account for the charge reversal between snow and rain.

The charging process acting on solid precipitation is still uncertain, but several clues as to its behaviour are available from the quiet precipitation results. Again assuming 50% collector efficiency, a charge per unit mass of around 40 pC gm^{-1} is suggested. Its most likely location has been seen to be in the cloud between the 0°C level and approximately the - 10°C level. This is the region where both ice and supercooled water droplets are most likely to coexist, with the Bergeron process (see Sec. 2.1.7) being the likely origin of the precipitation. The charging process is also apparently affected by the degree of atmospheric stability and hence turbulence in the cloud region, and so mechanical effects may be involved.

These factors suggest ice impact processes (as proposed by CHALMERS, 1967) or, since supercooled water droplets are almost certainly present, riming processes. LATHAM and MASON (1961) have shown that a hail pellet can become negatively charged by the impaction and freezing of large supercooled cloud droplets, but these conditions are more relevant to shower or thunder clouds than to quiet precipitation clouds. Charging was found to be greatest in the - 6 °C to - 17°C region, moreover, which is somewhat higher than the region for quiet precipitation charging suggested above. There are other possible theories, for instance that of WORKMAN and REYNOLDS (1950), concerned with charge separation at an ice-liquid interface during freezing, although later workers have doubted its effectiveness.

The problem of snow charging has been investigated by MAGONO and ORIKASA (1966), who suggested that, in the quietest snowfall, Wilson's induction mechanism was responsible for charging. This seems unlikely, however, since it does not explain why the precipitation current leads the potential gradient during quiet snow. More importantly, they found that predominantly non-rimed crystals fell in these periods of snow, which thus excludes riming electrification as a charging process. In heavier snowfall, for example, at a rate of 1.7 mm hr^{-1} when the electrical record was disturbed, rimed crystals were observed, but often with a positive charge. This means that riming electrification may indeed only be effective in more showery, unstable conditions, as suggested above.

Ice impact or friction processes are still a possibility, since aggregation of ice particles to form snowflakes must occur, and Magono and Orikasa often observed occasional positively charged snow crystals in a snowfall of overall negative charge. This latter observation could be consistent with random collisions or frictional effects during the formation or fall of the snow.

Clearly the precise charging mechanism producing the observed electrical properties of quiet snow has yet to be identified, although it does appear to be a process which is predominant only in the quietest conditions.

10.4 The relationship between meteorological and electrical activity

The other important conclusions of this work concern the connection between the meteorological and electrical conditions during steady precipitation. While there is some evidence for

an increase of potential gradient and precipitation current density with rate of rainfall during quiet precipitation, the clearer relationship is between the degree of electrical activity (as expressed, for instance, by the standard deviation of the electrical quantities) and the rate of rainfall. Eventually this activity becomes so great that the precipitation becomes disturbed, with the electrical behaviour being completely different from that during quiet precipitation, similar in fact to that during showery precipitation. This transition from quiet to disturbed precipitation has been seen to be quite definite, with a rate of rainfall of 1.0 mm hr^{-1} and a frequency of electrical sign reversals of 2 hr^{-1} being suggested as the transition point between the two types of precipitation.

Since showery precipitation results from predominantly convective activity within the cloud, it could well be that this transition from quiet to disturbed precipitation reflects the transition from stable to unstable, convective, conditions whithin the cloud. This proposition is in effect made by REITER (1965, 1968), whose results concerning the relationship between the degree of stability in the 500 - 700 mb atmospheric layer and the rate of electrical sign reversals have been discussed in Chapters 2 and 9. The similarity between the values of 2 hr^{-1} from the present work and 1.5 hr^{-1} from Reiter for the frequency of electrical sign reversals just reflecting instability supports this view. This feature of precipitation also suggests that the electrical behaviour at the ground is controlled mainly by conditions within the cloud, rather than by purely local effects such as drop splashing or by the surface wind. However, in very heavy rain or high potential gradients, drop splashing at

the ground and point discharge currents might then have a significant effect on the electrical conditions.

These conclusions raise the possibility of using electrical measurements at the ground, in particular of potential gradient, for investigating conditions within the cloud, for instance in detecting convective or unstable conditions which could lead to heavy rain or thunder. One instance at Durham was a period of heavy drizzle and mist which showed a surprising degree of electrical activity more typical of disturbed precipitation; subsequently thundery showers occurred with several short periods of thunder and lightning.

The connection between meteorological and electrical conditions was also evident in some periods of quiet precipitation when the usual inverse relation or mirror-image effect were not present. A period of heavy drizzle in February 1972 at Durham is one instance, when both the potential gradient and precipitation current were negative. The drizzle was not originating in the usual frontal system, suggesting that coalescence processes could be responsible for its formation; in such a case different electrical behaviour might well be expected, since solid precipitation is not then involved.

10.5 Instrumentation for quiet precipitation measurements

Many of the problems of operating outdoor equipment for the measurement of atmospheric electrical parameters such as potential gradient, conductivity, space charge density and air - earth currents have been discussed by previous workers at Durham, for instance SHARPLESS (1968) and ASPINALL(1970). Consequently these problems will not be discussed at length here,

with only the following points being mentioned.

Regular inspection and maintenance of the equipment is considered to be of most importance, particularly for instruments such as the precipitation collector where very high electrical insulation must be maintained. When equipment is to be operated during the winter months, the effects of ice and frost must be considered, since it is under these conditions that any repair work is most difficult. For continuous measurement of precipitation periods, equipment such as field mills is best run continuously, so that only recording equipment need be switched on at the start of the period of precipitation.

The continual development of new electronic devices means that new techniques of measuring and amplifying the low currents and charges met with in atmospheric electricity are now available. In particular, future work could benefit from the use of integrated circuit amplifiers, which require much less power and space than conventional circuits and are less sensitive to the mechanical and thermal problems of outdoor instrumentation. Also logarithmic devices could be useful for the investigation of different scales of electrical behaviour, such as in the case of quiet and disturbed precipitation, ~~and so~~ avoiding duplication of instruments of different range or sensitivity.

Automatic recording of the potential gradient, precipitation current and any other quantities is considered essential in any systematic study of precipitation electricity. Periods of precipitation rarely arrive at convenient times, as can be seen from Table 7.1, and even with careful examination of current weather forecasts, periods can still arrive unexpectedly. If a tape recording system is used, as in the present work, some

method of automatic switching such as performed by the rain switch prevents precipitation periods being missed and minimises the amount of chart or tape to be examined.

The calculation of autocorrelation intervals in Chapter 7 provides some useful information concerning the frequency at which electrical measurements need to be made during quiet precipitation periods. The shortest autocorrelation interval was 4 minutes, while more usually being 10 to 15 minutes, so that measurements taken about every 5 minutes will usually be more than adequate to obtain statistically significant values of such quantities as means, variances and correlation coefficients. Only if time lags of the mirror-image effect are being considered need the electrical quantities be sampled more frequently: a sampling interval of 30 s, as chosen in the present work, will be quite satisfactory since most time lags were of the order of a few minutes.

An obvious need in the present work was for a better method of measuring the rate of rainfall than the standard rain gauge at Durham Observatory, which had a resolution of 0.04in(about 1 mm). Some work was done in designing such an instrument, which counted electronically the individual rain drops falling from a large funnel. Unfortunately time precluded completion of the instrument, the main problem being the determination of the optimum size of funnel for the range of rainfall rate being measured.

10.6 Recommendations for further work

The present work has clarified the electrical properties of quiet precipitation and suggested a definite transition point

in terms of either electrical activity or rate of rainfall above which the precipitation becomes disturbed. The most common type of electrical behaviour of quiet precipitation, when both the inverse relation and mirror-image effect is present, has been established, and so future work might consider the less common behaviour of certain periods, and the origin of these differences.

Explanation of the usual inverse relation and mirror-image effect in terms of cloud charging and melting electrification is adequate, with the main problem being the origin of the time lags in the mirror-image effect. Further investigation is clearly needed to find if the wind shear explanation can indeed explain the behaviour of rain, and to find an explanation for the behaviour of snow. In the latter case, the origin of the precipitation charge is still uncertain, partly because of the difficulty of explaining why the variations in precipitation current lead those of potential gradient.

Simultaneous aerological and electrical measurements at the same site would be helpful in investigating not only the effect of wind shear on the time lags in the mirror-image effect, but also the connection between the degrees of atmospheric stability and electrical activity. Such measurements may also be useful in determing whether on some occasions the electrical behaviour of quiet precipitation is due to slow-moving clouds where the effects of electrical development are being seen at the ground.

A network of measuring stations recording potential gradient

and precipitation current could be useful in deciding whether the electrical variations at the ground are due to the passage of regions of cloud with slightly different degrees of electrical activity, or to widespread development of activity within the cloud. Some attempts at such measurements, notably by STRINGFELLOW (1969) and OWOLABI and CHALMERS (1965), have been encouraging, but no systematic study has been made. Such a study would be useful in confirming the extent to which Chalmers' ideas as to the origin of the electrical behaviour of quiet precipitation are correct.

Previously the meteorological and electrical aspects of precipitation have often been treated as largely independent effects: many of the conclusions of this work have shown this not to be true and it is to be hoped that future work will establish fully the role that electrical charging plays in the physical processes of the atmosphere.

REFERENCES

ABBAS and LATHAM J.	1967	An experimental investigation of the selective ion-capture theory of cloud electrification. Quart. J.R. Met. Soc., 93, 474-482
ADKINS, C.J.	1959	The small-ion concentration and space charge near the ground. Quart. J.R. Met. Soc., 85, 237-252
ASPINALL, W.P.	1970	Atmospheric electric charge transfer in precipitation and associated synoptic conditions. Ph.D. Thesis, Durham University
ASPINALL, W.P.	1972	Mechanical-transfer currents of atmospheric electricity. J. Geophys. Res., 77, 3196-3205
ATLAS, D., TATEHIRA, R., SRIVASTAVA, R.C., MARKER, W. and CARBONE, R.E.	1969	Precipitation induced mesoscale perturbations in the melting layer. Quart. J.R. Met. Soc., 95, 544-560
AWE, O.	1964	Errors in the correlation between time series. J. Atmos. Terr. Phys., 26, 1239-1255
BENDAT, J.S. and PIERSOL, A.G.	1966	Measurement and analysis of random data. J. Wiley, New York.
BERGERON, T.	1935	On the physics of cloud and precipitation. Proc. 5th Assembly, U.G.G.I., Lisbon, 2, 156-170
BOWEN, E.G.	1951	Radar observations on rain and their relation to the mechanisms of rain formation. J. Atmos. Terr. Phys., 1, 125-131
BROWNING, K.A.	1971	Radar measurements of air motion near fronts Part 2. Weather, 26, 320-340

BROWNING, K.A., and HARROLD, T.W.	1969	Air motion and precipitation growth in a wave depression. Quart. J.R. Met. Soc., 95, 288-309.
CHALMERS, J.A.	1947	The capture of ions by ice particles. Quart. J.R. Met. Soc. 73, 324-334
CHALMERS, J.A.	1956	The vertical electric current during rain and snow. J. Atmos. Terr. Phys., 9, 311-321.
CHALMERS, J.A.	1958	The electricity of nimbo-stratus clouds. Recent Advances in Atmospheric Electricity. Pergamon Press, pp. 309-315
CHALMERS, J.A.	1965	The relation between precipitation current and potential gradient. J. Atmos. Terr. Phys., 27, 899-905.
CHALMERS, J.A.	1967	Atmospheric Electricity. 2nd edn., Pergamon Press, Oxford.
CHALMERS, J.A. and LITTLE, E.W.R.	1940	The electricity of continuous rain. Terr. Magn. Elect. 45, 451-458.
CHAPMAN, S.	1952	Thundercloud electrification studies. Cornell. Aero. Lab. Rep. VC. 603-P-1
COLLIN, H.L.	1969	An investigation of the atmospheric electrical phenomena within 22m of the ground in disturbed weather conditions Ph.D. Thesis, Durham University
DINGER, J.E. and GUNN, R.	1946	Electrical effects associated with a change in state of water. Terr. Magn. Atmos. Elect., 51, 477-494
DRAKE, J.C.	1968	Electrification accompanying the melting of ice particles. Quart. J.R. Met. Soc., 94, 176-188

ELSTER, J., and GEITEL, H.	1888	Uber eine Methode die Elektrische Natur der atmospharischen Niederschlage zu bestimmen. Met. Z., 5, 95-100
ELSTER, J, and GEITEL, H.	1913	Zur Influenztheorie der Niederschlagselektrizitat Phys. Z., 14, 1287-1292.
GROOM, K.N. and CHALMERS, J.A.	1967	The relation between rain current and potential gradient. J. Atmos. Terr. Phys., 29, 877-880
HARROLD, T.W. and BROWNING, K.A.	1967	Mesoscale wind fluctuations below 1500 metres. Met. Mag. 96, 367-376
IMYANITOV, J.M. and CHUBARINA, E.V.	1967	Electricity of the Free Atmosphere. Israel Program for Scientific Translation, Jerusalem. (Tr. from Russian: Gidrometeorologicheskoe Izdatelstvo, Leningrad, 1965)
IRIBARNE, J.V. and MASON, B.J.	1967	Electrification accompanying the bursting of bubbles in water and dilute aqueous solutions. Trans. Faraday Soc. 63, 2234-2245
KASEMIR, H.W.	1955	Measurement of the air-earth current density. Proc. Conf. Atmos. Electricity 1954, pp 91-95. Geophys. Res. Dir. AFCRA Bedford, Mass.
KIKUCHI, K.	1965	On the positive electrificatio of snow crystals during the process of their melting. Tokyo Conference on Cloud Physics, Tokyo and Sapporo
LANE-SMITH, D.R.	1967	A new design of sign discriminating field mill. J. Atmos. Terr. Phys. 29, 687-699
LANGLEBEN, M.P.	1954	The terminal velocity of snowflakes. Quart. J.R. Met. Soc., 80, 174-180

LANGLEBEN, M.P.	1956	The plan pattern of snow echoes at the generating level. J. Met., 13, 554-561
LATHAM, J.	1963	The electrification of frost deposits. Quart. J.R. Met. Soc. 90, 265-270
LATHAM J, and MASON, B.J.	1961	Generation of electric charge associated with the formation of soft hail in thunderstorms. Proc. Roy. Soc. A., 260, 537-549
LENARD, P.	1892	Uber die Elektrizitat der Wasserfalle. Ann. Phys. Lpz. 46, 584-636
MAGONO, C and KIKUCHI, K.	1963	On the positive electrification of snow crystals in the process of their melting. J. Met. Soc. Japan, 41, 270-277
MAGONO, C and KIKUCHI, K.	1965	On the positive electrification of snow crystals in the process of their melting. J. Met. Soc. Japan, 43, 331-342
MAGONO, C and ORIKASA, K.	1961	On the surface electric field caused by the space charge of charged raindrops. J. Met. Soc. Japan, 39, 1-11
MAGONO, C and ORIKASA, K.	1966	On the disturbance of surface electric field caused by snowfall. J. Met. Soc. Japan, 44, 260-279
MASON, B.J.	1952	The production of rain and drizzle by coalescence in stratiform clouds. Quart. J.R. Met. Soc., 78, 377-385
MASON, B.J.	1953	On the generation of charge associated with graupel formation in thunderstorms. Quart. J.R. Met. Soc., 79, 501-509

MASON, B.J.	1971	The Physics of Clouds (2nd Ed.) Oxford Univ. Press, London.
MATTHEWS, J.B. and MASON, B.J.	1964	Electrification produced by the rupture of large water drops in an electric field. Quart. J.R. Met. Soc., 90, 275-286
MOLYNEUX, J and DE'SA, P.	1962	A transistor voltage-to-frequency converter. Electronic Engineering, 34, 468-469
OWOLABI, J.E. and CHALMERS, J.A.	1965	Correlations of precipitation currents. J. Atmos. Terr. Phys., 27, 303-308
OWOLABI, J.E. and OLOAFE, G.O.	1969	The exposure factor of a cylindrical shield in the measurements of precipitation currents. J. Atmos. Terr. Phys., 31, 481-490
RAMSAY, M.W. and CHALMERS, J.A.	1960	Measurements on the electricity of precipitation. Quart. J.R. Met. Soc., 86, 530-539
REITER, R.	1965	Precipitation and cloud electricity. Quart. J.R. Met. Soc., 91, 60-72
REITER, R.	1968	A contribution to the atmospheric-electric phenomenology of non-thunderstorm clouds and precipitation. 4th Int. Conf. on the Universal Aspects of the Atmospheric Electricity, Tokyo.
REITER, R.	1972	Contribution to the problems of precipitation electricity. Arch. Met. Geoph. Biokl. A., 21, 247-272
SCRASE, F.J.	1938	Electricity on rain. A discussion of records at Kew Observatory 1935-6. Geophys. Mem., Met. Office London, No.75

SHARPLESS, G.T.	1968	An experimental study of the atmospheric electric elements at a rural site in conditions of low air pollution. Ph.D Thesis, Durham University
SIMPSON, G.C.	1909	On the electricity of rain and its origin in thunderstorms. Phil. Trans. R. Soc. A, 209, 379-413
SIMPSON, G.C.	1919	Atmospheric electricity. British Antarctic Expedition 1910-13. Meteorology, Vol.1 302-312. Thacker, Spark & Co. Calcutta.
SIMPSON, G.C.	1949	Atmospheric electricity during disturbed weather. Geophys. Mem., Met. Office, London, No.84.
SIMPSON, G.C. and SCRASE, F.J.	1937	Distribution of electricity in thunderclouds. Proc. Roy. Soc. A, 161, 309-352
SMITH, L.G.	1955	The electric charge of raindrops. Quart. J.R. Met. Soc., 81, 23-47
STEWART, J.B.	1964	Precipitation from layer cloud Quart. J.R. Met. Soc. 90, 287-303
STRINGFELLOW, M.F.	1969	The electrical structure of nimbrostratus clouds. Ph.D. Thesis, Durham University
WHIPPLE, F.J.W. and CHALMERS, J.A.	1944	On Wilson's theory of the collection of charge by falling drops. Quart. J.R. Met. Soc., 70, 103-120.
WILSON, C.T.R.	1916	On some determinations of the sign and magnitude of electric discharges in lightning flashes. Proc. Roy. Soc. A. 92, 555-574
WILSON, C.T.R.	1929	Some thunderstorm problems. J. Franklin Inst. 208, 1-12

WORKMAN, E.J. and REYNOLDS, S.E.	1950	Electrical phenomena occurring during the freezing of dilute aqueous solutions and their possible relationship to thunderstorm electricity. Phys. Rev., 78, 254-259
WORMELL, T.W.	1930	Vertical electric currents below thunderstorms and showers. Proc. Roy. Soc. A, 115, 443-455.

ACKNOWLEDGEMENTS

The author is indebted to Dr.W.C.A.Hutchinson for his supervision throughout this project,and to Professor G.D. Rochester,Head of the Physics Department,for providing the facilities at Durham University.

The author wishes to express his thanks to fellow members of the Atmospheric Physics Research Group for their useful help and comments at various stages of the work; in particular Mr.P.F.Martin and Mr.C.D.Jones must be mentioned. Mr.Jack Moralee must be thanked for constructing much of the apparatus,and Mr.Eric Lincoln for his advice on the design of the electronic circuits.

The staff of the Computing Unit at Durham University provided much advice on the computer programming aspects of this work,and the author is particularly grateful to the Punching Staff for processing the considerable quantity of data.

In the production of this thesis,Mrs.E.Lincoln is thanked for typing this thesis so patiently and competently, and Mr.Michael Lee for the photographic work.Finally,Mr. and Mrs.J.Warner are thanked for their help at Durham Observatory in providing much of the meteorological information.

The author was supported for this work by a Research Studentship awarded by the Natural Environment Research Council.